Novel proapoptotic p63 isoforms are driven by an endogenous retrovirus in the male germline of humans and great apes, likely increasing genome stability

Dissertation

To achieve the doctoral degree of

"**Doctor rerum naturalium**"

of the

Georg August University Göttingen

submitted by

Ulrike Beyer

born in

Magdeburg, Germany

Göttingen 2010

First referee: Prof. Ralf Ficner

Second referee: Prof. Tomas Pieler

Date of oral exam: 29.10.2010

Table of contents

1. Abstract

TAp63, a homolog of the tumor suppressor p53, has the capability to protect the female germ line by eliminating oocytes that suffered severe DNA damage upon irradiation. Though expression of TAp63 in male germ cells has been suggested, it is currently not clear whether TAp63 also functions as the guardian of the male germ line.

Here, we identify hitherto unknown human p63 transcripts with novel 5'-ends derived from incorporated exons, that are located upstream of the known TP63 exon 1. Expression analysis in a variety of human tissues revealed that these unique TAp63 transcripts are predominantly expressed in human testis. Interestingly, their most upstream region corresponds to a long terminal repeat (LTR) of the human endogenous retrovirus 9 (ERV9). Since the insertion of the ERV9 LTR upstream of the TP63 locus is unique to humans and great apes (*Hominidae*), we suggest that this retroviral integration event occurred very recently in evolution, around 15 million years ago. A corresponding p63 protein is the sole p63 species in healthy human testicular lysate and was detected in different male germ cells by immunohistochemistry. While this human p63 protein was absent in mature spermatozoa, spermatogonia were strongly p63-positive. In contrast, mouse testicular germ cells, lacking ERV9 sequences upstream of Trp63, show a lower relative abundance of p63 in murine sperm precursors as compared to human testis. Functional analyses indicate that the human male germ cell-encoded TAp63 protein (designated GTAp63) activates transcription mainly of proapoptotic target genes such as Puma and Noxa, partially associates with mitochondria, and augments apoptosis of human cells when cleaved by activated caspases near its carboxyterminal domain. A possible role of GTAp63 in testicular tumorigenesis is additionally supported by the notion that human testicular cancer tissues and cell lines largely lost p63 expression. Importantly, however, pharmacological inhibition of histone deacetylases completely restores p63 expression in testicular cancer cells, leading to a roughly 3000-fold increase in GTAp63 mRNA.

Our data provide evidence supporting the role of testis-specific GTAp63 in protecting the genomic integrity of the male germ line. Integration and selection of an endogenous retroviral LTR upstream of the TP63 locus may have greatly enhanced the guardian function of p63 in hominids. By providing increased germ line stability,

this event may have contributed to the evolution of humans and great apes and enabled their long reproductive periods.

2. Introduction

2.1 The p53 family of proteins

The family of p53 proteins consists of three members: p53, p63 and p73. They mainly function as transcription factors that regulate target genes involved in important cellular processes such as cell cycle progression, apoptosis and differentiation.

The first family member was discovered in 1979 in SV40-transformed cells. In these cells the oncogenic SV40 large T antigen was bound by a cellular protein, termed p53 (Lane and Crawford, 1979; Linzer and Levine, 1979; Melero *et al.*, 1979; Kress *et al.*, 1979). Structural analyses indicated that the p53 protein is composed of several conserved domains. The amino terminal transactivation domain (TA domain/TAD) is necessary for the interaction with transcriptional co-factors to activate or repress the transcription of target genes. Secondly, the central part of the p53 proteins is indispensable for the binding of p53 to specific response elements in the promoter regions of target genes. Therefore it is called the DNA-binding domain (DBD). The third domain is the oligomerization domain near the carboxy terminus, which allows the formation of p53 tetramers.
The p53 homologs p63 and p73 that were identified in 1997 and 1998 (Kaghad et al, 1997; Osada et al, 1998; Schmale & Bamberger, 1997; Yang et al, 1998), respectively, share the main structural features of the p53 protein; in particular, the DNA-binding domains are highly conserved between the family members. While the transactivation domain and oligomerization domain of p63/p73 show a lower degree of sequence similarity in comparison to corresponding domains of p53 (identities of approximately 25% or 35%, respectively), the amino acid sequence of the DBD is ~ 65% identical to that of p53 (Yang et al, 2002) (**figure 2.1**).
p63 and p73 are more closely related to each other than to p53. On one hand, both homologs share considerable higher sequence similarity with each other, reaching 85% amino acid identity in the DNA-binding and 40% or 60% in the transactivation or oligomerization domain, respectively. On the other hand, both p63 and p73 possess a longer carboxy terminus including additional conserved domains: The Sterile Alpha Motif is a protein-protein interaction domain, initially implicated in developmental processes (Arrowsmith, 1999; Ghioni et al, 2002). The Post-SAM domain is known to

be critical for the transactivation of target genes. This domain, which includes the transcription inhibitory domain (TID), is able to bind intramolecularly to residues in the TA domain which are necessary for the interaction of TAp63 with cofactors of the transcription machinery. Thus, by masking these residues in the transactivation domain, the TI domain interferes with the transactivation of target genes (Serber et al, 2002).

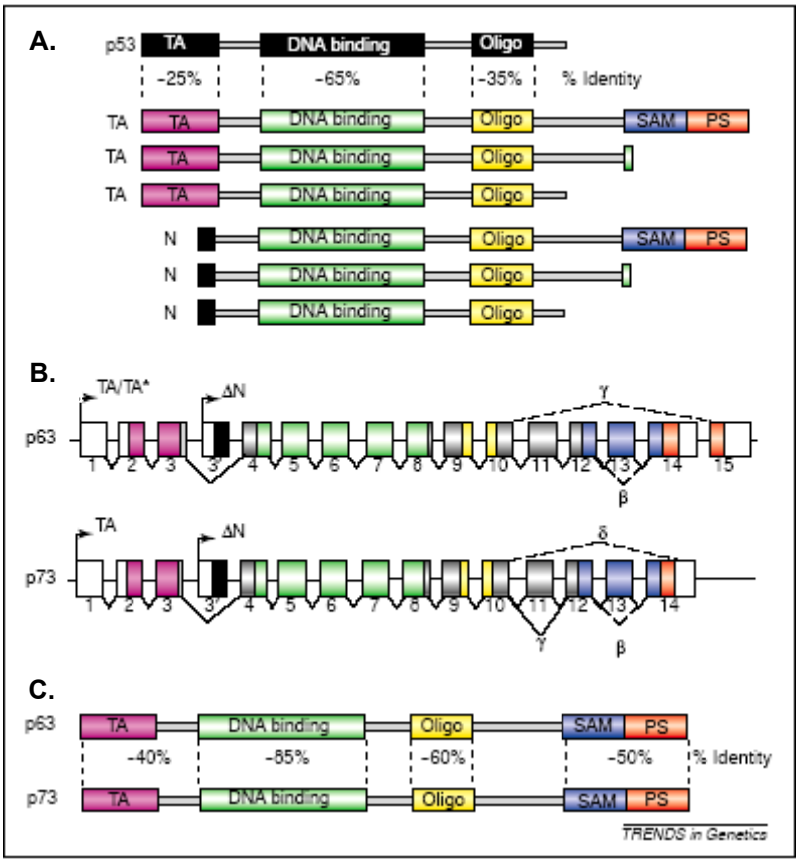

Figure 2.1: Members of the p53 protein family and their structure (Yang et al, 2002)

A. Domain structure of p53 and its homologues. p53/p63/p73 proteins possess similar conserved domains, however, p63 and p73 exist in different isoforms that differ in their amino terminal region and/or vary in the length of their carboxy terminus. The DNA-binding domain shows the highest degree of identity between the three members of the p53 family.

B. Gene structure of both p53 homologues. The loci of p63 and p73 show a very similar gene structure with two different promoters, TA and ΔN. In both cases alternative splicing of 3` exons gives rise to several distinct isoforms e.g. α, β and γ.

C. Sequence comparison of the different p63 and p73 domains reveales that p63 and p73 are more similar to each other than to p53.

TA, transactivation domain; DNA binding, DNA-bindung domain; Oligo, oligomerization domain; SAM, Sterile Alpha Motif; PS, Post-SAM domain

Moreover, the genomic architecture of the TP63 and TP73 genes differs from that of TP53 (**figure 2.1 B**). The loci of p63/p73 each contain two promoters. The TA promoter, which is located upstream of exon 1, gives rise to long isoforms that include the amino-terminal transactivation domain. Use of the second internal promoter, which is located in intron 3, generates shorter ΔN isoforms that lack the TA domain (Moll & Slade, 2004). However, ΔN isoforms were shown to possess a different transactivation domain (Dohn et al, 2001). More recently, an alternative promoter was also described for the TP53 gene (Bourdon et al., 2005). This internal promoter of TP53 is located in exon 4.

In addition, the complexity within the p53 family is increased by alternative splicing of exons (De Laurenzi et al, 1998; Moll & Slade, 2004; Yang et al, 1998). For p53 and p73 it has been shown that amino- as well as carboxy-terminal exons can be used alternatively, leading to the expression of several distinct isoforms (Murray-Zmijewski et al, 2006). In contrast, only carboxy-terminal exons of the TP63 gene were described to be spliced alternatively resulting in α, β and γ isoforms of p63.

In line with the described differences in the gene and protein structure of p53/p63/p73, distinct functions were assigned to the diverse members of the p53 protein family. While *in vitro* assays indicate that at least the transactivating isoforms of p63 and p73 are capable of transactivating a similar set of target genes as compared to p53, significant insight into the physiological functions of p53/p63/p73 was gained by studying several knockout mouse models or human diseases.
p53 was identified as an essential cellular tumor suppressor, since p53-deficient mice showed an increased susceptibility to cancer and more than 50% of human tumors contain a mutation in the TP53 gene (Levine, 1997). Moreover, tumors that retained wild-type p53 often have p53 protein which is functionally inactive due to the attenuated expression of p53 regulators such as Mdm2 or $p14^{ARF}$ (Danovi *et al.*, 2004; Kamijo *et al.*, 1998; Sherr und Weber, 2000). In non-transformed somatic cells, p53 is a key molecule to induce either cell cycle arrest or apoptosis upon DNA damage, oncogene expression or other cellular stress (Brooks & Gu, 2003). Therefore, p53 has been described as the guardian of the genome (Lane, 1992).

More recent studies have revealed that p53 might be additionally implicated in the regulation of glycolysis and autophagy, invasion and motility, angiogenesis, differentiation and bone remodeling (Vousden & Lane, 2007).
p53 does not solely function by transcriptional regulation of target genes. It has been shown that p53 contributes to the onset of apoptosis in two different ways. Besides the transactivation of proapoptotic target genes, e.g. PUMA and Noxa, cytoplasmic p53 protein is able to translocate to mitochondria to launch the intrinsic pathway of apoptosis. As a BCL2-homology domain-3 (BH3)-only protein p53 interacts with the anti-apoptotic BH3 proteins Bcl2 and BclXL, thereby facilitating the permeabilisation of the outer mitochondrial membrane and the release of cytochrome C (Mihara et al, 2003).
A similar transactivation-independent function has been assigned to the p73 protein (Sayan et al, 2008) but not yet to p63.

While p53 is primarily implicated in the prevention of tumor formation, its homologs p63 and p73 have crucial roles in developmental processes in mice and humans.
p63-null mice show severe defects in limb formation, absence of skin, and craniofacial malformations. They also fail to develop epithelial tissues, e.g. mammary glands, prostate and epidermal appendages like hair follicle and teeth, and die shortly after birth (Mills et al, 1999; Yang et al, 1999). In accordance, heterozygous point mutations in the TP63 gene are associated with autosomal dominant developmental disorders. Patients with mutated residues in the DNA-binding domain of p63 suffer from Ectrodactyly Ectodermal dysplasia Clefting (EEC), Split-Hand/Foot Malformations (SHFM) or the ADULT (Acro-Dermato- Ungual-Lacrimal-Tooth) syndrome, while point mutations in the SAM or Post-SAM domain result in ectodermal dysplasia syndromes without limb abnormalities (AEC and LMS syndromes) (Brunner et al, 2002; Celli et al, 1999; Duijf et al, 2002; McGrath et al, 2001). In adults p63 isoforms regulate the epidermal homeostasis. While ΔNp63α is predominantly expressed in basal keratinocyte stem cells maintaining their proliferation potential, transactivating TAp63 isoforms are involved in the terminal differentiation of committed epithelial cells (Koster & Roop, 2004; Pellegrini et al, 2001; Westfall & Pietenpol, 2004).

The third member of the p53 family, p73, also has distinct developmental roles. TP73 expression is strongly associated with proper neurogenesis (Moll & Slade, 2004). Mice deficient for p73 exhibit hippocampal dysgenesis, show malformations of the limbic telencephalon and have defects in pheromone signaling. Additionally, these mice suffer from chronic inflammations (Moll & Slade, 2004; Yang et al, 2000).
Besides its developmental functions, p73 has been shown to induce apoptosis independently of p53 upon ionizing irradiation and cisplatin treatment of cells (Gong et al, 1999; Melino et al, 2002).

Despite lots of studies on p63 and p73, their role in tumor suppression is still controversially discussed. Though only few human tumors harbor mutations in TP63 and TP73 (Irwin & Kaelin, 2001), certain tumor types, such as transitional cell carcinoma and squamous cell carcinoma, exhibit loss or reduced expression of p63 and/or p73 (Flores et al, 2005). Further evidence for a tumor suppressor function of the p53 homologs was provided by examining the long-term tumorigenic effects of p63 and p73 mutations. Flores *et al.* analyzed aging mice with mutations in all p53 family genes. They provide data that argue in favor of a tumor predisposition of mice harboring heterozygous mutations in p63 and p73. Compared to p53 +/- mice, double heterozygous mice (p53+/-; p63+/- or p53+/-; p73+/-) even displayed higher tumor burden and increased metastasis (Flores et al, 2005).

2.2 TAp63 – expression and function

This work aimed to investigate the expression pattern and physiological functions of the longer, transactivating p63 proteins, TAp63. These isoforms are transcribed from the TA promoter, located directly upstream of TP63 exon 1, and therefore include exons 1 to 3 (**figure 2.1**). Since the TP63 exons 2 and 3 encode for a TA domain that is homologous to the amino-terminal transactivation domain of p53, TAp63 proteins have been described as ‘p53-like’ isoforms (Candi et al, 2007), in contrast to the truncated ΔNp63 isoforms that are capable of antagonizing p53 functions (Yang et al, 1998).

As already described in chapter 2.1, three different carboxy-terminal variants (α, β and γ) are generated by alternative splicing. *In vitro* assays indicated that the shortest isoform TAp63γ is the most potent activator of p53 target genes. The longer TAp63α protein additionally contains the SAM domain and the transcription inhibitory domain, regulating p63 functions. The β isoforms of TAp63 lack the TID domain and therefore have higher transactivation potential as compared to α isoforms in transient transfection assays (Ghioni et al, 2002).

Though the *in vivo* functions of the diverse TAp63 proteins are still an ongoing debate, it is clear that they have a role in the development and maintenance of epithelial tissue. In embryonic development TAp63 initiates the onset of the epithelial stratification program. Within the developed epidermis TAp63 proteins are expressed in suprabasal cells. While ΔNp63α maintains keratinocytes in a proliferative state, TAp63 is implicated in terminal differentiation of committed epidermal cells (Nylander et al, 2002).

Besides its expression in epithelial tissue, TAp63 isoforms have been detected in several other human tissues, i.e. bone marrow, brain, colon, skeletal muscle, spleen and testis, and in germinal center B-cells of lymphoid tissue (Vincek et al, 2003). The expression of TAp63β and γ isoforms is associated with B-cell neoplasms.

Yang et al. postulated that in adult mice TAp63 mRNA is detectable in a variety of tissues including brain, heart and testis (Yang et al, 1998). In recent years, the expression pattern and functional consequences of p63 isoforms in reproductive tissues and germ cells has been under intense investigation by several groups (Gonfloni et al, 2009; Hayashi et al, 2004; Livera et al, 2008; Nakamuta & Kobayashi, 2003; Nakamuta & Kobayashi, 2004b; Nakamuta & Kobayashi, 2007; Pankow & Bamberger, 2007; Petre-Lazar et al, 2007; Suh et al, 2006). The role of TAp63 in female and male germ cells is described in more detail in chapter 2.3.

TAp63 proteins were shown to bind DNA through p53-responsive elements and to transactivate many different p53 target genes including cell cycle regulating genes, such as CDKN1A, as well as apoptotic targets, e.g. PUMA and Bax. Overexpression of TAp63 results in induction of apoptosis by transcriptional activation of death receptors and mitochondrial apoptosis effectors (Candi et al, 2007; Gressner et al,

2005). In hepatocellular carcinoma cells TAp63α is capable of triggering both the extrinsic apoptotic pathway by transactivation of the death receptor genes CD95, TNFRSF1A, TNFRSF10B, as well as the mitochondrial pathway through upregulation of the proapoptotic Bcl2 family members Bax and BCL2L11 and the expression of RAD9, DAP3 and APAF-1 (Gressner et al, 2005). The apoptotic pathways that are elicited by TAp63α are displayed in **figure 2.2**.

Further evidence for the pro-apoptotic function of TAp63 was provided by Jacobs *et al.*, who observed that the γ isoform is an essential pro-apoptotic protein during neuronal development of the sympathetic nervous system (Jacobs et al, 2005). In this context p63-mediated Bax induction is required for the apoptotic signaling.

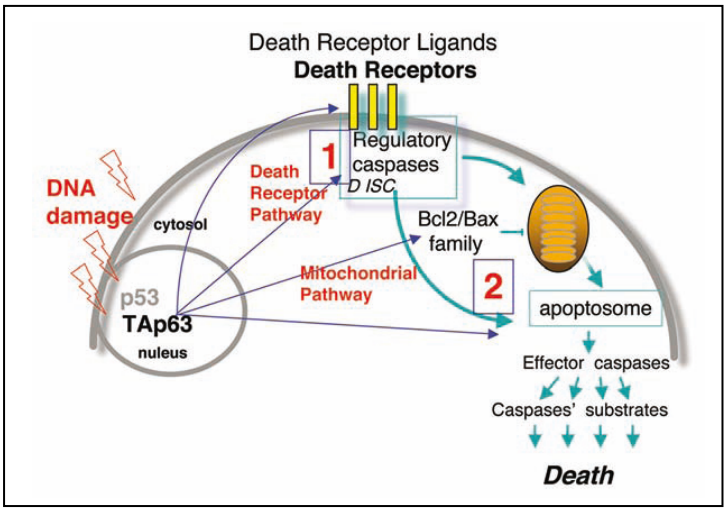

Figure 2.2: TAp63 induces apoptotic pathways (Candi et al, 2007)
Both pathways of apoptosis are triggered by overexpression of TAp63 in hepatoma cells. The extrinsic pathway is elicited by transactivation of death receptors such as CD95, TNFR1 and TRAILR1/2 (1). Moreover, TAp63 facilitates the intrinsic mitochondria-mediated apoptosis (2) by upregulation of proapoptotic members of the BCL2 gene family e.g. PUMA and Bax. In addition, TAp63 also targets APAF-1 and caspases to enhance apoptosis.

Dohn *et al.* used an inducible expression system in H1299 lung carcinoma cells to compare the activities of TAp63α *vs.* ΔNp63α. They found that p63α forms are potent inducers of apoptosis and lead to a reduction of the mitochondrial membrane potential comparable to p53. However, target genes were differentially activated by

TA or ΔNp63α. For example, the redox-related p53-inducible genes (PIGs) 3 and 8 were only induced by the tranactivating isoform (Dohn et al, 2001).

The capability of TAp63α to launch apoptosis of tumor cell lines led to the speculation that this protein might contribute to chemosensitivity of human cancers. Indeed, treatment of hepatocarcinoma cells with different chemotherapeutic drugs stimulated the expression of TAp63α protein, which resulted in enhanced chemosensitivity. In addition, siRNA-mediated silencing of TAp63 conferred chemoresistence to the cells (Gressner et al, 2005). The authors also found that inhibitors of caspases strongly reduced the TAp63α-mediated apoptosis.

Interestingly, a report published two years later indicated that caspase activation is a prerequisite for apoptosis enhanced by TAp63α (Sayan et al, 2007). Since p63α contains the carboxy-terminal transcription inhibitory domain, which renders the protein transcriptionally inactive, pre-activated caspases are needed to cleave off this inhibitory domain. After the preinitiation of apoptosis by UV-B radiation or cisplatin treatment, p63α is cleaved at the caspase cleavage site (aspartate residue at position 458) resulting in a cleaved p63 fragment that then efficiently increases apoptosis. Thus, TAp63 cleavage sensitizes cancer cells towards apoptosis (Sayan et al, 2007).

The understanding of the role of p63 in tumor formation is still preliminary. Though p63 is rarely mutated in human cancers (Hagiwara et al, 1999), some studies implicate TAp63 in tumorigenesis. There is evidence that TAp63 downregulation might contribute to formation of laryngeal squamous cell carcinoma (Pruneri et al, 2002) and malignant progression of bladder carcinoma (Park et al, 2000). Primary human bladder carcinoma show abnormally reduced levels of TAp63 mRNA. This reduction is correlated with the tumor stage and grade, since less than one third of superficial tumors have low TAp63 mRNA levels, while in more than 80% of invasive tumors TAp63 is hardly if at all detectable. The authors suggest that TAp63 expression is inhibited by promoter hypermethylation (Park et al, 2000).

Moreover, some p63 mouse models also provide data arguing for a tumor suppressor function of p63. Heterozygous mutations in p63 and p73 result in cancer prone mice (Flores et al, 2005). A recent study using a TAp63-specific conditional mouse model indicates that TAp63 is capable of halting tumorigenesis by the

induction of senescence through p53-independent pathways (Guo et al, 2009). This led to the speculation that TAp63 might be a potential target of anti-cancer therapy for human malignancies with compromised p53.

2.3 Germ cells and TAp63

As mentioned in the previous chapter, recently published data have linked the expression of TAp63 proteins to the regulation of germ cell survival/apoptosis during development and in gonads of adult mammals (Gonfloni et al, 2009; Kurita et al, 2005; Livera et al, 2008; Nakamuta & Kobayashi, 2003; Nakamuta & Kobayashi, 2004a; Nakamuta & Kobayashi, 2004b; Nakamuta & Kobayashi, 2007; Petre-Lazar et al, 2007; Petre-Lazar et al, 2006; Suh et al, 2006).

Germ cell development is a very tightly controlled process, since the differentiated germ cells give rise to further generations. Moreover, germ cells have to face a critical balance between maintaining adequate genetic integrity at the individual level to produce viable offspring and sufficient mutagenesis to support genetic adaptation at the population level (Walter et al, 2003).
Germ cell development is initiated early in mammalian embryogenesis and continues throughout adulthood. A few totipotent cells of the epiblast differentiate into germ cell progenitors. These primordial germ cells (PGC) migrate to extraembryonic locations, where they start to proliferate after gastrulation. Mitosis still continues after the primordial germ cells have migrated through the developing embryo to the genital ridges, where formation of the fetal gonads is initiated. Signals from somatic cells of the emerging gonads then direct germ cell differentiation toward the female or male lineage (Öllinger et al, 2010) and PGCs differentiate into either oogonia or prospermatogonia. The various stages of gametogenesis are depicted in **figure 2.3**.
Oogonia progress through mitotic divisions, generating the final germ cell population that is available to the female for the remainder of her life-span (Walter et al, 2003), as oogonia cannot be replenished at any stage of development. In the fetal ovary, the period of proliferation and apoptosis is followed by the onset of meiosis. Meiotic cell divisions are unique, since one round of DNA replication is combined with two rounds of chromosome segregation and cell division (Page & Hawley, 2003), resulting in

haploid gametes. Primary oocytes progress through first steps of meiosis including meiotic recombination, which is important for the generation of genetic diversity in the gametes and, in addition, essential for the correct segregation of chromosomes (Öllinger et al, 2010). Primary oocytes are arrested in the diplotene stage of prophase I. After birth meiosis I is completed, mature oocytes become secondary oocytes that progress through meiosis just prior to ovulation until they stop in the metaphase of meiosis II. Finally, meiotic division is completed after fertilization, thereby generating the large ovum and the small polar bodies (Walter et al, 2003)(**figure 2.3**).

In contrast, spermatogenesis has some major differences in comparison to oogenesis. During spermatogenesis meiotic reductive divisions are inhibited before birth; instead, male germ cells undergo meiosis only after the prepubertal initiation of germ cell differentiation (Caires et al, 2010). During the period of quiescence prospermatogonia undergo chromatin remodeling, establishing paternal imprints and *de novo* DNA methylation marks (Öllinger et al, 2010). A second major difference is provided by the fact that spermatogonia can be replenished. After the quiescent period some prospermatogonia give rise to undifferentiated type A_{single} spermatogonia, which are known as the true spermatogonial stem cells (SSC) that have the capability of self-renewal, thus providing a continual supply of differentiating germ cells. In 1994, Brinster & Zimmermann demonstrated in mice that transplantation of spermatogonial stem cells results in donor-derived spermatogenesis (Brinster & Zimmermann, 1994). The stem cell population in mammalian testis is responsible for continual sperm production throughout the reproductive life-span of adult males (Caires et al, 2010).

Type A spermatogonia undergo some mitotic divisions and finally differentiate into type B spermatogonia that then give rise to preleptotene spermatocytes. But only a minority of differentiating spermatogonia enters meiosis as primary spermatocytes, since the majority of premeiotic spermatogonia are lost due to apoptosis. Primary spermatocytes progress through meiotic recombination in prophase I. Only spermatocytes with properly paired and aligned chromosomes complete meiosis I, producing secondary spermatocytes that undergo the second meiotic division to yield haploid round spermatids. These cells progress through substantial morphological changes in a process known as spermiogenesis, to become mature spermatozoa (Öllinger et al, 2010).

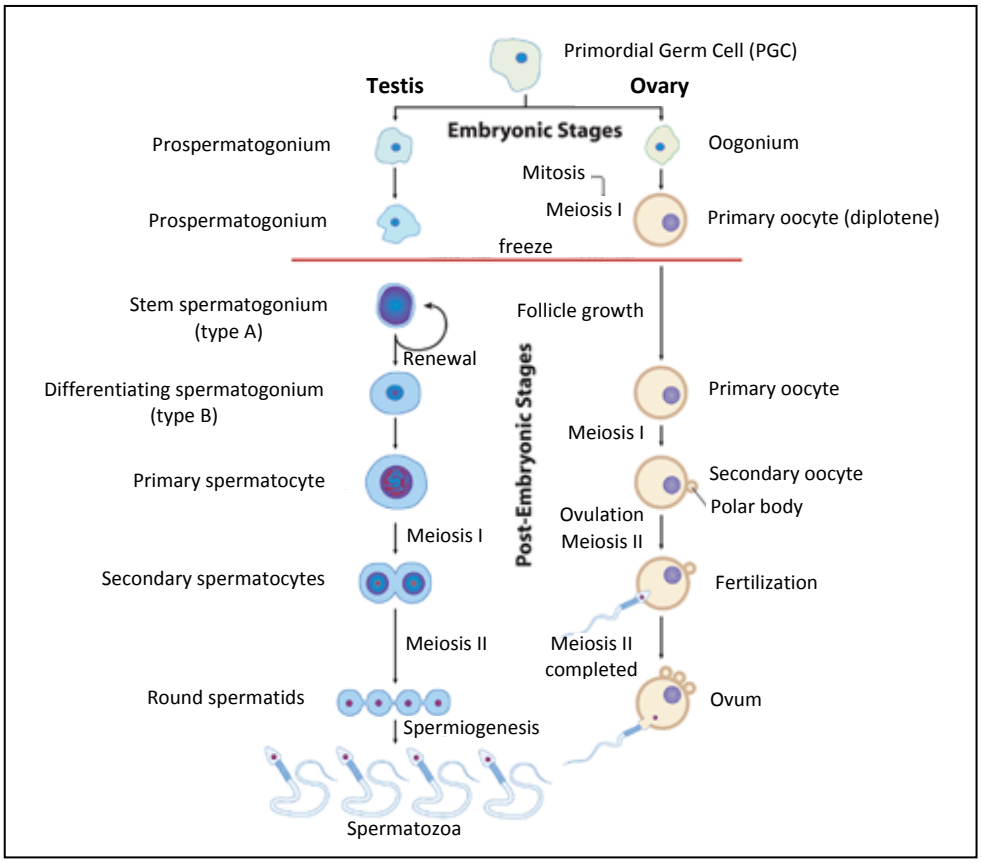

Figure 2.3: Stages of mammalian gametogenesis (Walter et al, 2003)
Gametogenesis is initiated early in embryonesis when primordial germ cells differentiate down the female or male pathway. Embryonic germ cells actively proliferate until mitosis ceases. Prospermatogonia then enter a quiescent period; in contrast, oogonia undergo meiosis I until they are frozen in diplotene of prophase I.
After birth oocytes grow, differentiate and continue meiosis just prior to ovulation, then enter a second freeze in metaphase II. Female gametogenesis is completed after fertilization of the mature egg.
In the male pathway there is a population of true germ stem cells (stem spermatogonia), which are capable of replenishing male germ cells. Type B spermatogonia differentiate into spermatocytes that continuously undergo both meiotic divisions, producing haploid round spermatids, which progress through spermiogenesis to give rise to the mature spermatozoa. Post-embryonic as well as embryonic stages of gametogenesis include waves of apoptosis, deleting germ cells with impaired genetic integrity, thereby enabling successful reproduction.

The spermatogenic epithelium of seminiferous tubules of the testis is not only composed of differentiating germ cells but also contains somatic sertoli cells that interact with the germ cells and function as nursing cells. In each seminiferous tubule, germ cells are present at various phases of differentiation (Caires et al, 2010). Near the basement membrane, the spermatogonial stem cells (SSCs) cells are

located. They replenish the germ cell population. As the diploid germ cells differentiate into mature haploid sperm, differentiated cells remain connected through cytoplasmatic bridges and move toward adluminal locations. Finally, the mature sperm is released into the lumen of seminiferous tubules (**figure 2.4**).

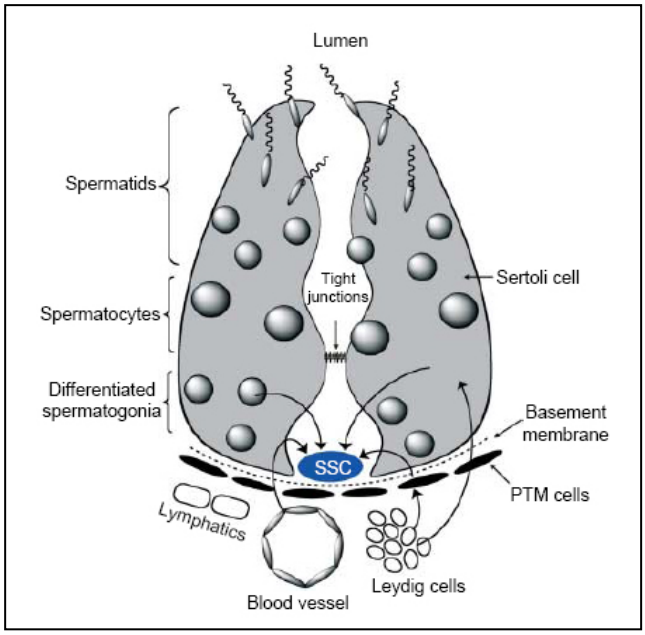

Figure 2.4: Structure of the spermatogenic epithelium (Caires et al, 2010)
Model of spermatogenesis inside seminiferous tubules of the testis. Basal spermatogonial stem cells (SSC) are potentially maintained through autocrine, paracrine mechanisms and signals that emanate from somatic cells (Sertoli, Leydig and peritubular myoid) or the micro-environment (indicated by arrows). Differentiation of spermatogonia into spermatocytes and then spermatids is accompanied by the movement of cells towards luminal locations. Sertoli cells provide a structural framework and nurse the germ cells.

The process of gametogenesis is associated with a high rate of cell turnover and differentiation. The DNA integrity of germ cells must be even more stringently guarded than in somatic cells, because successful reproduction is largely dependent on the genetic integrity of gametes (Walter et al, 2003). In addition, uncontrolled proliferation of germ cells might result in the formation of ovarian or testicular germ cell tumors. On the opposite, low levels of proliferation and differentiation may cause sterility (Petre-Lazar et al, 2007).

Several studies aimed to investigate the intracellular signaling pathways regulating gonocyte development. Since p53 is an essential regulator of cell cycle and apoptosis in somatic cells, it was suggested that p53 may also contribute to regulation of gametogenesis. Indeed, p53 was found to be expressed in primary spermatocytes. In mice, p53 protein level were shown to increase in spermatogonia and preleptotene spermatocytes upon irradiation (Beumer et al, 1998a). Beumer *et al.* studied the role of p53 in spermatogenesis using a p53 knockout mouse model. Their data indicate that p53 is important for the removal of lethally damaged spermatogonia upon irradiation, but also plays a role in the regulation of cell production during normal spermatogenesis (Beumer et al, 1998a).

Nevertheless, there is now clear evidence indicating an involvement of TAp63 isoforms in the development and stress-induced apoptosis of germ cells. Most of this evidence has been generated using mouse models. Importantly, proapoptotic p63 could be detected also in human testis (Vincek et al, 2003).

In mice, p63 expression was found in fetal germ cells of both genders (Guerquin et al, 2009), in postnatal oocytes of primordial and primary follicle (Gonfloni et al, 2009; Nakamuta & Kobayashi, 2007; Suh et al, 2006). In addition, p63 invalidation reduced the apoptosis of postnatal testicular germ cells, when testes were cultured *in vitro* (Petre-Lazar et al, 2007). Moreover, it has been suggested that p63 transcriptionally regulates genes required for the migration of primordial germ cells and the colonization of gonads (Kurita et al, 2005; Nakamuta & Kobayashi, 2004b).

Kurita et al. generated distinct p63 antibodies specific for TA or ΔN or p63α proteins to distinguish between different isoforms that are expressed in mouse ovary and testis (Kurita et al, 2005). They detected only TAp63 isoforms in ovary as well as in testis. While oocytes of primordial, primary and secondary follicles showed immunoreactivity with the TA and α-specific antibody in mouse and human, their immunostainings indicate that murine TAp63 γ-forms are presumably expressed in male germ cells. Furthermore, they saw strong p63 positivity only in the nuclei of spermatocytes and spermatids, whereas p63 staining was weak in spermatogonia and absent in mature sperm (**figure 2.5**).

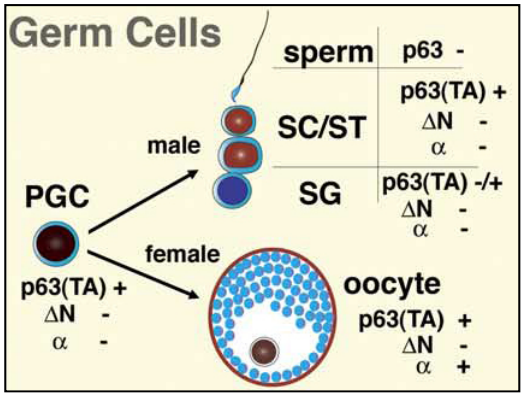

Figure 2.5: Expression of p63 isoforms in murine germ cells (Kurita et al, 2005)
Transactivating p63 is already expressed in primordial germ cells (PGC). Female germ cells maintain p63 expression, but the isoform is shifted from γ to α. In adult murine testis TAp63 is mainly detected in the nuclei of spermatocytes (SC) and spermatids (ST), while a subset of spermatogonia show faint immunoreactivity for p63 and haploid sperm does not express any p63.

In agreement with these results, other authors suggested that p63 expression is developmentally regulated and changes with the apoptotic/mitotic activities of testicular gonocytes (Petre-Lazar et al, 2007). In periods, when germ cells undergo intense mitosis and apoptosis, only the α-isoforms were detectable; in contrast, mitotic arrest was associated with downregulation of α-forms and upregulation of TAp63 γ-forms. Additionally, increased numbers of apoptotic gonocytes upon irradiation of fetal testis correspond to TAp63α upregulation (Petre-Lazar et al, 2006). Since p63 was able to trigger apoptosis of damaged spermatogenic cells, the authors concluded that 'p63 may play an important role in preventing testicular lesions, as apoptosis provides a mechanism for removing incorrectly differentiated gonocytes, which are thought to give rise to germ cell tumors (Petre-Lazar et al, 2007).

Interestingly, p63 invalidation in mouse models did not result in a failure of normal gonad formation and animals are fertile (Livera et al, 2008; Suh et al, 2006). Thus, TAp63 may only trigger apoptosis of germ cells when activated by initial DNA damage signaling, for example upon irradiation.

Indeed, TAp63α has been shown to be essential for radiation-induced oocyte death (Livera et al, 2008; Suh et al, 2006). Upon irradiation TAp63 proteins become phosphorylated and then bind to p53 cognate DNA sites to transactivate distinct target genes, e.g. proapoptotic genes, thereby promoting oocyte death. This

indicates that, at least, in the female germ line p63 may function as a guardian of the germline fidelity (Suh et al, 2006).

Notably, three years later, one group could show that murine TAp63α is activated to induce apoptosis of postnatal oocytes after treatment of mice with chemotherapeutic drugs (Gonfloni et al, 2009). The authors provided evidence connecting the tyrosine kinase c-Abl with the activation of TAp63α. They suggest a model whereby cisplatin-induced DNA double strand breaks lead to a nuclear accumulation and activation of c-Abl, which in turn phosphorylates TAp63, presumably on tyrosine residue Y149, resulting in enhanced apoptosis due to transactivation of apoptotic genes such as PUMA and Noxa. In consistence with their model, treatment with the c-Abl-inhibitor imatinib counteracts the cisplatin-induced depletion of the ovarian follicle reserve (Gonfloni et al, 2009).

In summary, all the provided data suggest an involvement of TAp63 in the regulation of mammalian germline apoptosis. This role of p63 proteins is supported by the notion that p63 analogs expressed in invertebrates may function in a similar fashion.

In the sea anemone *Nematostella vectensis* there are three different p53-like proteins: nvp63, nvpEC53 (ecdysozoan-like p53 homolog), and nvpVS53 (very short p53 homolog). Of those three p53 homologs, the nvp63 was found to be strongly expressed in the germ cell compartment, localized in early gametes (Pankow & Bamberger, 2007). Upon UV radiation these gametes undergo damage-induced cell death. Notably, execution of apoptosis in early gametes was prevented by siRNA-mediated knockdown of nvp63.

In the classical invertebrate model organisms *Caenorhabditis elegans* and *Drosophila melanogaster* only a single p53-like gene exists (Derry et al, 2001; Jin et al, 2000). The p53-like protein in *C. elegans*, termed CEP-1, has been shown to transcriptionally regulate a set of genes, which overlap with paralogs regulated by human p63 and p53 (Derry et al, 2007). Moreover, sequence comparison revealed that CEP-1 is more identical to human p63 than to p53 (Suh et al, 2006). These facts might imply a role of CEP-1 in germ line apoptosis in *C. elegans*. Findings of Derry *et al.* support this idea, since CEP-1 was shown to activate PHG-1, a negative regulator of cell proliferation in the germ line, in response to genotoxic stress, thus contributing to the activation of germ cell apoptosis (Derry et al, 2007).

Altogether, the DNA integrity of germ cells has to be stringently controlled. Vertebrate TAp63 proteins or TAp63α-like proteins in invertebrates are a crucial player to deplete germ cells with severely damage DNA during normal development and upon genotoxic stress. It has been proven that TAp63 is essential to maintain the female germline fidelity, while its function in adult male germ cells is less clear.

2.4 Germ cells and endogenous retroviruses

Mammalian genomes contain mobile genetic elements that use RNA intermediates to amplify and move through genomes. There are three main classes of these so-called retrotransposons: LINES (long interspersed elements) are ancient retrotransposons that encode two proteins to mediate retrotransposition; short interspersed elements (SINES) are derived from small cellular RNAs and are dependent on LINE-encoded proteins for transposition; and endogenous retroviruses that share several features with exogenous retroviruses (Öllinger et al, 2010).

Human endogenous retroviruses (HERVs) are the remnants of exogenous retroviruses that infected the genome of human ancestors several million years ago. Once integrated into the host genome, repeated amplification and transposition events resulted in huge numbers of provirus copies that were dispersed throughout the whole genome (Nelson et al, 2003). At present, retroviral sequences and sequences of retrotransposon origin constitute 7-8% of the human genome (Jern & Coffin, 2008).

Like their exogenous counterparts, HERVs consist of retroviral *gag* (group-associated antigen), *prot* (protease), *pol* (polymerase) and *env* (envelope) genes, flanked by long terminal repeat (LTR) regions, which are roughly 1 kb in size (Buzdin, 2007). LTRs are generated during reverse transcription of the viral genomic RNA and are essential for the integration of the provirus into host DNA. Each LTR is composed of three different regions: U3, R and U5 (Temin, 1981), which have important functions in promoting and enhancing proviral transcription. In addition, the R-region contains a polyadenylation signal that is used to terminate viral transcripts.

In contrast to exogenous retroviruses, e.g. HIV and HTLV, that have the capability to spread horizontally by generating infectious retroviral particles that, upon release

from the host cell, re-infect other host cells, endogenous retroviruses are transmitted vertically through the germline as Mendelian genes (Casau et al, 1999). The expression of HERVs in germ cells is critical for their survival, allowing re-integration events to be propagated through subsequent generations (Öllinger et al, 2010).

Once integrated into host genomes several million years ago, ERVs underwent subsequent selection processes removing viruses that were deleterious for host gene expression and retaining such ERVs that were even beneficial. In accordance, today most retrotransposons exist as solitary LTRs, arisen by recombination of the 5` and 3` LTR of full-length elements (Cohen et al, 2009). Since long terminal repeats possess functional enhancers, promoters, polyadenylation signals and splice sites, integration of such elements into the vicinity of cellular genes can influence host gene expression in various ways. It has been suggested that LTRs are involved in five pathways regulating the transcription of human cellular genes (Buzdin, 2007).
First, LTRs act as enhancers, changing transcription profiles of neighboring genes. As an example, an ERV9 LTR, integrated into the genomes of higher primates at least 15 mio years ago, was shown to initiate transcription in the upstream β-globin locus control region (LCR), thereby modulating the expression of β-globin genes in embryonic and hematopoietic cells (Ling et al, 2002; Long et al, 1998).
Secondly, LTRs may provide new promoters of nearby cellular genes. This is discussed in more detail below.
Third, since the R-region of any LTR contains a polyadenylation signal, LTR polyadenylation may cause abnormal termination of cellular transcripts.
In addition, LTRs may affect gene expression by providing alternative or aberrant splice sites. For example, a second variant of the leptin obesity hormone receptor is generated due to splicing into a HERV-K LTR (Jern & Coffin, 2008).
Finally, LTRs are thought to regulate host gene expression through RNA interference. Intronic LTRs are biased to promote transcription in the antisense direction, thus interfering with the transcription of the host gene in sense direction (Buzdin, 2007; Jern & Coffin, 2008). 15 of 28 identified intronic human LTRs were found to be active in germline cells (Buzdin, 2007).

As already mentioned many human LTRs function as promoters of nearby cellular genes. Cohen *et al.* reviewed well-studied examples of LTRs serving as promoters

for human genes (Cohen et al, 2009). They generated diverse models for the evolution of LTRs as promoters of neighboring genes (**figure 2.6**). LTRs contain functional transcription factor binding sites (TFBSs) that either were maintained during evolution (a) or evolved over time due to acquired mutations (b). Model (c) shows the exaptation phenomenon, meaning that a retroviral LTR promoter might become the primary promoter of a cellular gene in the case that it promotes a beneficial transcriptional pattern. Furthermore, LTRs can contribute to core promoter activity by providing upstream TFBSs that might confer a tissue-specific expression of the host gene (d).

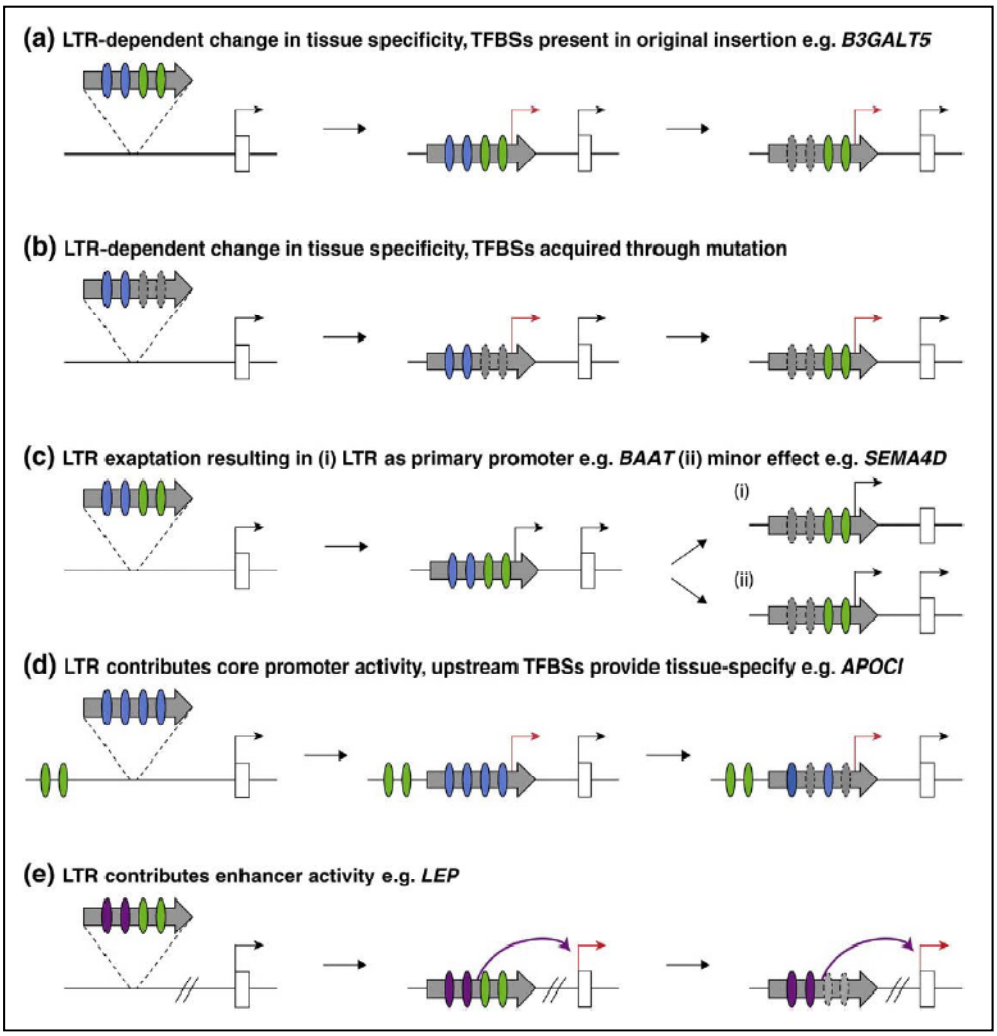

Figure 2.6: Retroviral LTRs as promoter of human genes (Cohen et al, 2009)
The scheme depicts different evolutionary models of the establishment of retroviral long terminal repeats (LTRs) as promoters (a-d) or enhancers (e) of adjacent cellular host genes.
LTRs, indicated by the thick grey arrow, contain diverse transcription factor binding sites (TFBSs; green, blue and purple ovals), recruiting cellular transcription factors that act in cis on cellular genes. Examples of human genes, regulated by specific LTRs, are displayed.

Though in most cases human LTR promoters have relatively subtle effects on cellular gene expression (Cohen et al, 2009), deviations from this trend do exist.

There is an intriguing example where retroviral integration contributed to species evolution. Integration of a gibbon ape leukemia virus/MLV-related provirus upstream of a duplicated pancreatic amylase gene in the common progenitor of great apes and Old World monkeys led to the expression of amylase in the parotic gland of descendants, thereby maybe influencing the dietary preferences of apes (Coffin et al, 1997).

Moreover, it is well-known that LTRs confer tissue specific expression of human genes. In placenta the expression of several genes, e.g. CYP19A1, IL2RB, NOS3 and PTN, is solely due to the presence of the LTR promoter (Cohen et al, 2009). In addition, retroviral genes have been shown to play important physiological roles in placental development. For example, the human syncytin-1, which is a HERV-W *env* gene product, is expressed in the trophoblast and mediates syncytium formation (Jern & Coffin, 2008).

Besides the high activity of LTRs in placenta, many ERV species are highly transcribed in germline cells and testis.

Several studies suggest that retroviral elements are especially active in testicular tissues. One group investigated the genomic distribution and expression of ERV9 elements, which belong to the HERV-R family (Svensson et al, 2001). They found 120 ERV9 loci distributed on most chromosomes. Interestingly, northern blot analysis revealed low ERV9 expression in a variety of tissues, but strong expression in human testis, which might be due to testosterone-driven activation of the LTR-dependent transcription.

In agreement with this finding, Crowell and Kiessling detected human retroviruses of the ERV9, HERV-E and HERV-K families in testis and epididymis (Crowell & Kiessling, 2007). However, Pi *et al.* did not detect activity of the ERV9 LTR enhancer in spermatozoa, but in oocytes and adult stem/progenitor cells (Pi et al, 2004).

In 2006, a comprehensive study of the expression of human-specific LTRs *in vivo* in testicular parenchyma and in seminoma was performed. A total of 60 new human-specific promoters were identified and shown to activate the transcription of host DNA to levels ranging from ~ 0.001 to 3 % of β-actin transcript levels (Buzdin, 2007).

Furthermore, an active HERV-K LTR was found to be preferentially expressed in more undifferentiated spermatocytes of adult testis (Casau et al, 1999). High

expression levels of HERV-K elements in testicular germ cell tumors and testicular teratocarcinoma cells correlates with the differentiation status, since the differentiation of a germ cell tumor (GCT) resulted in a dramatic decrease in HERV-K LTR expression. The limited expression of this LTR in adult testis was also shown in a transgenic mouse model (Casau et al, 1999).

The question remains why endogenous retroviruses are more active in placenta and reproductive tissues. There are two theories regarding this issue. First, retroviruses are more likely able to infect germ cells, thus ensuring HERV survival. In favor of this hypothesis, retroviral elements harbor binding sites for transcription factors that are specific for reproductive tissue. Secondly, ERV LTRs might be more active in the germline due to the reduced methylation status of germ cells (Cohen et al, 2009).
Soon after colonizing the gonads germ cells undergo widespread DNA demethylation. Subsequent *de novo* methylation occurs at different times in male and female germ cells. Full methylation in the male germline is achieved in quiescent prospermatogonia, while the DNA of growing oocytes is methylated only after birth (Öllinger et al, 2010). Since retrotransposon activity is associated with high mutagenic potential, developing germ cells, at least in mice, possess mechanisms to limit retroviral expression. Silencing of retrotransposons is achieved by DNA methylation, piRNA silencing and also host restriction factors such as APOBEC proteins and TRIM5α (Cohen et al, 2009; Öllinger et al, 2010). There is a correlation between defective retrotransposon silencing and aberrant progression through meiosis in mouse mutants. Silencing might be important to prevent retrotransposons from interfering with chromosome pairing during the meiotic prophase. Increased retrotransposition may cause DNA damage in meiotic germ cells, thus activating meiotic checkpoints and disrupting meiotic recombination. Alternatively, retrovirus-encoded proteins could interact with germ cell proteins, inducing cytotoxic effects in the germline cells (Öllinger et al, 2010).

In summary, germ cells have to limit the expression of endogenous retroviral elements to be able to progress through meiosis, allowing successful reproduction. However, retroviral integration events in germ cells can also positively influence host genomes of next generations, providing selective advantages of individuals with an

altered genome. Thus, transcription of ERVs in the germline contributes to shaping of the host genome and in this way might even affect evolution of species.

2.5 Aim of the work

The transcription factor p63 is a homolog of p53, which protects the genome integrity of somatic cells. Transactivating p63 isoforms, transcribed from the upstream promoter of the TP63 gene, have the capability of transactivating p53-responsive targets such as apoptotic genes (Candi et al, 2007). More recently, evidence indicated that TAp63 eliminates oocytes of primordial and primary follicles that have suffered severe DNA damage upon genotoxic stress (Gonfloni et al, 2009; Livera et al, 2008; Suh et al, 2006). Thus, TAp63 may function as the guardian of the female germ line. Importantly, however, the contribution of TAp63 to the genome fidelity of male germline cells is currently not clear.

This work aimed to define the expression pattern of p63 isoforms in human tissues, and to establish mechanisms that allow p63 to induce cell death.

Finally, analyses of the expression pattern of p63 in testicular germ cell neoplasms aimed to address the role of p63 as a tumor suppressor in testicular tissue and to find ways of restoring p63 expression in testicular cancer.

3. Materials

3.1 Cells

3.1.1 Bacteria strains

DH10B ElektroMAX:	Electric kompetent *Escherichia coli*

3.1.2 Eukaryotic cells

GH:	Testicular teratocarcinoma cell line
H1299:	Lung carcinoma cell line
HCT116 wt:	Colon carcinoma cell line
NCCIT:	Testicular teratocarcinoma cell line
Tera-2:	Testicular teratocarcinoma cell line
U2OS:	Osteosarcoma cell line

Testicular tumor cell lines were obtained from Roswitha Löwer, Paul-Ehrlich-Institut Erlangen/Frankfurt, Germany.

3.2 Culture media

3.2.1 Media for bacteria

Agar	Sigma-Aldrich
Ampicillin	Sigma-Aldrich

2YT-Medium:	1.6% (w/v)	Trypton
	1% (w/v)	Yeast extract
	0.5% (w/v)	NaCl
	dissolved in dH_2O	

LB medium:	1% (w/v)	Trypton
	1% (w/v)	Yeast extract
	0.5% (w/v)	NaCl
	dissolved in H_2O	

LB agar:	15% (w/v)	Bacto agar in LB medium
	1% (w/v)	Yeast extract
	0.5% (w/v)	NaCl
	dissolved in H_2O	

3.2.2 Media for eukaryotic cells

Dulbecco`s Modified Eagle Medium (DMEM), powder	GIBCO, Invitrogen
Ciprofloxacin (Ciprobay)	Bayer
Fetal bovine serum (FBS)	GIBCO, Invitrogen
Geneticin, 50 mg/ml Lösung	GIBCO, Invitrogen
L-glutamine	GIBCO, Invitrogen
Penicillin/Streptomycin	GIBCO, Invitrogen
Tetracycline	GIBCO, Invitrogen
Trypsin/EDTA	GIBCO, Invitrogen

Dulbecco's Modified Eagle's Medium:

10 g	DMEM powder
3,7 g	$NaHCO_3$
5,96 g	HEPES
	Ad 1 l H_2O

DMEM without additives was sterile filtered and afterwards stored at 4°C.

DMEM complete:	10 µg/ml	Ciprobay
	50 U/ml	Penicillin
	50 µg/ml	Streptomycin
	2 µg/ml	Tetracycline
	10%	FBS
	200 µM	L-glutamine
		dissolved in DMEM

DMEM -tet -cip: DMEM complete without the addition of Ciprobay and tetracycline

DMEM + geneticin: DMEM complete with 800 µg/ml geneticin

PBS buffer:
PBS for cell culture was prepared using PBS tablets (18912-014; GIBCO, Invitrogen) according to manufacturer's instructions and then autoclaved.

3.3 Mice

We used the mouse strain SV129. All mice were bred at the animal facility of the ENI institute in Göttingen. Mice were held in accordance to the restrictions of the German law regarding animal experiments.

3.4 Nucleic acids

3.4.1 Oligonucleotides

All primers were ordered from Metabion, Martinsried. Lyophilized oligos were dissolved in sterile water achieving primer stock solutions with a concentration of 100 µM.
The sequence of each oligonucleotide is given in 5'→ 3' orientation.

3.4.1.1 Oligonucleotides for PCR

Table 3.1: Oligonucleotides PCR

Name of oligonucleotide	Sequence
36B4_forward **36B4_reverse**	gattggctacccaactgttg caggggcagcagccacaaa
BBC3_forward **BBC3_reverse**	gccagatttgtgagacaagagg caggcacctaattgggctc
CDKN1A forward **CDKN1A reverse**	gaagaccatgtggacctgtc aagtggggaggaggaagtag
Downstream LTR_reverse	cttactcttaatgcatggtcc
GADD45A_forward **GADD45A_reverse**	ccatgcaggaaggaaaactatg ccaaactatggctgcacact
GAPDH_forward **GAPDH_reverse**	gaaggtcggagtcaacggatttg cagagatgatgacccttttggctc
LTR_forward **LTR_reverse**	agcgagaccacgaacccac aaggtttccccrcctttgtg
p63 exon 1_forward **p63 exon 2_forward** **p63 exon U1_forward** **p63 exon 2_reverse** **p63 exon 3_reverse**	tgtgccaccctacagtactgc gttattaccgatccaccatgtcc attccggacaccctatcagag cccagatatgctggaaaacct gcggatacagtccatgctaatc
p73 exon 2_forward **p73 exon 3_reverse**	caccacgtttgagcacctctg gatgtagtcatgccctccagg
PMAIP1_forward **PMAIP1_reverse**	ggactgttcgtgttcagctcgc gccggaagttcagtttgtctcc
TNF6SF6_forward **TNF6SF6_reverse**	tgttaatgcccaagtgactg acttggtattctgggtccg
Upstream LTR_forward	ttgggcatatccaggactag

3.4.1.2 Oligonucleotides for RACE experiments

Table 3.2: Oligonucleotides 5`RACE

Name of oligonucleotide	Sequence
5`RACE first primer	cctgcatgcggatacagtccatgctaatctc
5`RACE nested primer	tcccagatatgctggaaaacctctggactgagg

3.4.1.3 Oligonucleotides for cloning and mutagenesis

Table 3.3: Oligonucleotides cloning and mutagenesis

Name of Oligonucleotide	Sequence
Exon U1_BamHI_forward	tatatggatccggcaacccgctggggtc
Exon 3_NheI_reverse	agtcagagctagcctcaatcttgtttgtcgcac
pcDNA-TAp63fl_BamHI_forward	gatctcgacccacggatccgcccggctttatatctatatatac
pcDNA-TAp63fl_NheI_forward	gtgcgacaaacaagattgaggctagcatggactgtatccgcatg
Exon U1 mutATG_forward	ggacaccctatcagagattttgtcgact**ctg**aagtgctgggaacagagag
Exon U1 mutATG_reverse	ctctctgttcccagcacttcagagtcgacaaaatctctgatagggtgtcc
Exon 2 mutATG_forward	ggaaagaaagttattaccggtcgaccctgtcccagagcacacagac
Exon 2 mutATG_reverse	gtctgtgtgctctgggacagggtcgaccggtaataactttctttcc
GTAp63 C306R_forward	gaggcccggatccgtgcttgcccag
GTAp63 C306R_reverse	ctgggcaagcacggatccgggcctc
GTAp63 D497A_BvelI_forward	cactcctacaaccatacctgctggcatgggcgccaac
GTAp63 D497A_BvelI_reverse	gttggcgcccatgccagcaggtatggttgtaggagtg
GTAp63 stop498_NheI_forward	cgcaacgccctcactcctacaaccattcctgattagctagcagccaacattcccatga
GTAp63 stop498_NheI_reverse	tcatgggaatgttggctgctagctaatcaggaatggttgtaagtgagggcgttgcg

3.4.2 Silencing RNAs (siRNAs)

All siRNAs that were used in this work were synthesized by Qiagen. Lyophilized RNAs were dissolved in siRNA suspension buffer (Qiagen) to achieve stock solutions of 20 µM.

The sequence of the RNA molecules is shown in 5'→ 3' orientation.

Table 3.4: siRNAs

Name of siRNA	Sequence	Reference
Allstars negative		Qiagen GmbH
p63_1	aaccatgagctgagccgtgaa	Lee *et al.*, 2006
p63_3	aacagccatgcccagtatgta	Carroll *et al.*, 2006

3.4.3 Plasmids

pcDNA3 empty vector	Invitrogen, Karlsruhe; Expression vector for exogenous expression of proteins of interest under the control of the CMV promoter in eukaryotic cells; the vector contains an ampicillin resistence gene for selection of bacteria
pcDNA3 – EGFP	Expression vector for green fluorescent protein ; co-transfected as transfection control
pcDNA3 – TAp63α fl	Cloned by Michael Schümann ; Human full length TAp63α including the 3`UTR
pcDNA3 – TAp63γ	Human TAp63γ in the pcDNA3 backbone
pcDNA3 – p51A	Osada et al., 1998 Human TAp63γ without untranslated regions
pcDNA3 – p51B	Osada et al., 1998; Human TAp63α without untranslated regions
pIRES neo	Vector backbone from Clontech; the internal ribosomal entry site (IRES) results in bicistronic transcripts from the CMV promoter when expressed in eukaryotic cells; the vector was used for generation of cell lines stably expressing proteins of interest; Neomycin resistence

3.4 Proteins

3.5.1 Antibodies

Table 3.5: Primäry antibodies

Name	Dilution	Species	Provider
anti-β-actin	1:100000	monoclonal mouse	Abcam ab6225
anti-Cox IV	1:600	polyclonal rabbit	Abcam ab16056
anti-GFP	1:800	monoclonal rabbit	Invitrogen A11122
Anti-Lamin B1	1:1000	monoclonal mouse	Zymed 33-2000
anti-p63 4A4	1:1000	monoclonal mouse	Santa Cruz sc-8431

Table 3.6: Secondary antibody

Name	Dilution	Provider
donkey anti-mouse IgG (F_{ab}-fragment), HRP- conjugated	1:10000	Jackson ImmunoResearch
donkey anti-rabbit IgG (F_{ab}-fragment), HRP- conjugated	1:10000	Jackson ImmunoResearch
sheep anti-mouse IgG (F_{ab}-fragment), biotinylated	1:400	GE Healthcare

3.5.2 Enzymes

Table 3.7: Enzymes

Name	Order number	Provider
25 mM $MgCl_2$	R0971	Fermentas
Advantage2 PCR	639207	Clontech
dNTP-Mix, 25 µM each dNTP	U1420	Promega
M-MuLV reverse transcriptase	M0253	NEB
NEBuffer for M-MuLV, 10x	B0253	NEB

Pfu turbo DNA polymerase	600252	Fermentas
Restriction endonucleases, diverse	diverse	Fermentas
RNase inhibitor, recombinant	M0307	NEB
Taq DNA polymerase	EP0402	Fermentas
Taq buffer with KCl, 10x	B38	Fermentas

3.5.3 Human protein lysates

Protein lysates from human normal tissues were bought from Imgenex, San Diego, USA. These ready-to-use lysates had a concentration of 1 mg/ml and were stored at - 80°C until use.

Normal liver tissue lysate	40145
Normal ovary tissue lysate	40151
Normal testis tissue lysate	40150

3.5 Kits

Name	Order number	Provider
Big Dye Terminator Kit		AB/Ambion, USA
BCA™ proteine assay	23227	Thermo Scientific
Gel extraction kit	28706	Qiagen
Immobilon Western Chemiluminescence-HRP-substrate	WBKLS0500	Millipore
In situ cell death detection kit, POD	11684817910	Roche
Invisorb® plasmide miniprep kit spin two	10101404	InVITek
PCR Purification kit	28106	Qiagen
PureYield™ plasmide midiprep	A2492	Promega
QuikChange MultiSite-directed mutagenesis	200514	Stratagene
SMART™ RACE cDNA amplification kit	634914	Clontech

SuperSignal West Femto Maximum	34095	Pierce
TOPO-TA-cloning kit including the pCR®4-TOPO®-Vektor for sequencing	45-0030	Invitrogen

3.6 Chemicals

Adevodur developer for X-ray films	OMNILAB GmbH & Co. KG
Adevodur fixation reagent for X-ray films	OMNILAB GmbH & Co. KG
Agarose	Carl Roth GmbH + Co. KG
Ammonium persulfate (APS)	Carl Roth GmbH + Co. KG
Ampicillin sodium salt	Carl Roth GmbH + Co. KG
ATP	Carl Roth GmbH + Co. KG
Bacto-agar	Sigma-Aldrich GmbH
β-Mercaptoethanol	Sigma-Aldrich
Bovine serum albumine (BSA)	Carl Roth GmbH + Co. KG
Bromphenolblue	Sigma-Aldrich
Calcium chloride ($CaCl_2$)	Merck
Cisplatin (cDDP), powder	Sigma-Aldrich
Citrate monohydrate	Carl Roth GmbH + Co. KG
Chloroform	Carl Roth GmbH + Co. KG
Cycloheximide (Chx)	Sigma-Aldrich GmbH
3,3`-Diaminobenzidin-tetrahydrochloride (DAB)	Carl Roth GmbH + Co. KG
Di-potassium hydrogenphoshate (K_2HPO_4)	Carl Roth GmbH + Co. KG
Dimethyl sulfoxide (DMSO)	AppliChem GmbH
Di-sodium hydrogenphosphate di-hydrate (Na_2HPO_4 x 2 H_2O)	Carl Roth GmbH + Co. KG
1,4-Dithiothreitol (DTT)	Carl Roth GmbH + Co. KG
DNA-standard 1kb ladder	Fermentas
EGTA	Carl Roth GmbH + Co. KG
Eosin G	Carl Roth GmbH + Co. KG

Ethanol, >99,9%	Merck
Ethidium bromide	Sigma-Aldrich
Ethylenediamine-tetraacetate (EDTA)	Carl Roth GmbH + Co. KG
Formaldehyde, 37% solution	Carl Roth GmbH + Co. KG
Glycerin for microscopy	Carl Roth GmbH + Co. KG
Glycerol	Carl Roth GmbH + Co. KG
Glycine	Carl Roth GmbH + Co. KG
Glycogen Glyco blue	Ambion
H_2O, RNase-free	Ambion
HEPES	Carl Roth GmbH + Co. KG
HI-Di Formamide	Applied Biosystems
Hydrochloride acid (HCl)	Carl Roth GmbH + Co. KG
Hydrogen peroxide solution (H_2O_2), 30%	Carl Roth GmbH + Co. KG
Isoamylalcohol	Bio-Rad Laboratories GmbH
Isopropanol	Chemie-Vertrieb Hannover
Lipofectamine™2000	Invitrogen
Magnesium chloride ($MgCl_2$)	Carl Roth GmbH + Co. KG
Mannitol	Sigma-Aldrich
Mayer`s hematoxylin solution	Merck
Methanol, >99%	Carl Roth GmbH + Co. KG
Milk powder	Carl Roth GmbH + Co. KG
N,N,N´,N´-Tetramethylendiamine (TEMED)	Carl Roth GmbH + Co. KG
pH solution 4.01	Carl Roth GmbH + Co. KG
pH solution 7.01	Carl Roth GmbH + Co. KG
pH solution 10.01	Carl Roth GmbH + Co. KG
Ponceau S	Carl Roth GmbH + Co. KG
Potassium chloride (KCl)	Carl Roth GmbH + Co. KG
Potassium di-hydrogenphosphate (KH_2PO_4)	Carl Roth GmbH + Co. KG
Potassium hydroxide	Sigma-Aldrich
Protease inhibitor tablets, EDTA-free	Roche Diagnostics GmbH

Proteine standard prestained ladder	Fermentas
RNase inhibitor	Fermentas
ROTI®-Phenol	Carl Roth GmbH + Co. KG
Sodium acetate	Carl Roth GmbH + Co. KG
Sodium chloride (NaCl)	AppliChem
Sodium dodecylsulfate (SDS)	Carl Roth GmbH + Co. KG
Sodium hydrogenphosphate ($NaHPO_4$)	Carl Roth GmbH + Co. KG
Sodium hydroxide (NaOH)	Sigma-Aldrich GmbH
Sucrose, >99,5%	Sigma-Aldrich GmbH
SYBR Green	Stratagene GmbH
Trasylol (Aprotinin 500.000 KIE)	Bayer
Trehalose	USB Corp., USA
Trichostatin A (TSA)	Sigma-Aldrich
Tris base (tris(hydroxymethyl)aminomethane)	Carl Roth GmbH + Co. KG
Triton X-100	AppliChem
Trizol	Invitrogen
Tween-20	Serva
Xylol, >98%	Carl Roth GmbH + Co. KG

3.7 Buffers

CaRSB buffer:	10 mM	NaCl
	1.5 mM	$CaCl_2$
	10 mM	Tris-HCl pH 7.5
6x DNA sample buffer:	0.25%	Bromphenol blue
	40%	Sucrose
	10%	Glycerin
EB buffer:	10 mM	Tris (pH 8.5)

MS buffer:	210 mM	Mannitol
	70 mM	Sucrose
	5 mM	EDTA
	5 mM	Tris-HCl pH 7.6
6x Laemmli buffer:	0.35 M	Tris pH 6.8
	30%	Glycerin (v/v)
	10%	SDS (w/v)
	9.3%	Dithiotreitol (w/v)
	0.02%	Bromphenolblue (w/v)
10x running buffer for protein gels:	0.10%	SDS
	25 mM	Tris
	192 mM	Glycin
10x buffer for restriction enzymes:	Fermentas	
PBS (phosphate buffered saline):	236.9 mM	NaCl
	2.7 mM	KCl
	8.1 mM	Na_2HPO_4
	1.1 mM	$MgCl_2$
	1.5 mM	KH_2PO_4
	1.2 mM	$CaCl_2$
PBS/0.1% Tween:	0.1% (v/v)	Tween20
PBS ++:	137 mM	NaCl
	2.5 mM	KCl
	8.0 mM	Na_2HPO_4
	0.5 mM	$MgCl_2$
	1.5 mM	KH_2PO_4
	0.9 mM	$CaCl_2$
	pH was adjusted to 7.4	

Ponceau S solution:	0,5 g	Ponceau S
	1 ml	Pure acetic acid
	100ml	H_2O bidest
qPCR mastermix (2x):	75 mM	Tris-HCl, pH 8.8
	20 mM	$(NH_4)_2SO_4$
	3 mM	$MgCl_2$
	0.01%	Tween-20
		SYBR Green 1:80000
	200 µM	dNTPs
	0.25%	TritonX-100
	300 mM	Trehalose
	20 U/ml	Taq-Polymerase
RIPA buffer:	1%	Triton X-100 (v/v)
	1%	Desoxycholate (v/v)
	0.1%	SDS (w/v)
	20 mM	Tris-HCl, pH 7.5
	150 mM	NaCl
	10 mM	EDTA
		Trasylol (100000 KIE)
	Adjust pH with 1 M NaOH to 7.5	
Stripping buffer:	50 mM	Tris, pH 6.8
	2%	SDS
		β-Mercaptoethanol
	ad 100 ml	dH_2O
Sucrose buffer:	1/1.5 M	Sucrose
	2 mM	Dithiothreitol
	5 mM	EDTA
	10 mM	Tris, pH 7.6

50x TAE buffer:	2 M	Tris
	1 M	Natriumacetat
	0.1%	EDTA
	135 mM	NaCl
TD washing buffer:	5 mM	KCl
	25 mM	Tris, pH 7.6
Transfer buffer for wet blot:	100 ml	Western salts (10x)
	200 ml	Methanol
	700 ml	ddH_2O
10x Western salts:	60.55 g	Tris
	288.1 g	Glycine
	4 ml	10 % SDS (0.05 mM)
	ad 2 l	ddH_2O
	Adjust pH of the solution to 8.3	

3.8 Consumables

6-well/12-well cell culture plates	Greiner
96-well plates for qPCR	Sarstedt
96-well plates for luciferase assay Optiplate™ 96	Perkin Elmer
Cell culture flasks (25 cm^2, 75 cm^2, 175 cm^2)	Greiner
Cell culture petri dishes (d=8,5 cm)	Nunc
Cell scraper (16 mm/25 mm)	Sarstedt
Cover lids (24x40 mm)	Menzel GmbH
Cryo tubes Cryoline™	Nunc
Electroporation cuvettes Gene Pulser	Bio-Rad Laboratories GmbH
Fuji X-ray films Rx blue, 13x18 cm	Ernst Christiansen GmbH

Microtome blades Leica 819	Leica
Needles, different sizes	BD Microlance
PCR reaction tubes 0.2 ml	Sarstedt AG & Co
Pipette tips (2.5µl/2-200µl/1000µl)	Sarstedt
PP tubes (15 ml/50 ml)	Sarstedt
PROTRAN Nitrocellulose transfer membrane	Schleicher und Schuell
Reaction tubes (0.5 ml/1.5 ml/2ml)	Eppendorf
Sealing foil	Krups GmbH
Shandon Coverplates	Thermo Scientific
Shandon Coverplates cassettes	Thermo Scientific
Slides, 76x26 mm, cut	Knittel Gläser
Superfrost Plus coated slides	Thermo Scientific
Syringes, 1ml	B.Braun Petzold GmbH
Rotilabo® tissue cassettes	Roth
Ultrazentrifugation tubes Polyallomer, 14 ml	Beckman
Cover foils for qPCR plates	Sarstedt
Whatman 3MM blot paper	Whatman GmbH

3.9 Technical devices

Axio Scope.A1 microscope with AxioCam MRc and AxioVision 4.8 Software	Karl Zeiss MicroImaging GmbH
Bioruptor sonicator	Diagenode, Belgien
Centrifuge GMC-060	LMS Laboratory & Medical Supplies
Centro LB 960 luminometer	Berthold
Chromo4™ Realtime PCR machine	Bio-Rad Laboratories
Cooling table centrifuge Typ 5415R	Eppendorf
Cycler Biometra® T personal	Biometra

Electrophoration chamber, slides and combs for agarose gels	Harnischmacher Labortechnik
Eppendorf® Research Series 2100 pipettes (0.1-2.5µl; 0.5-10µl; 10-100µl; 100-1000 µl)	Eppendorf
Expert LE823S balance	Sartorius
Freezer -20° C	Liebherr
Freezer -80° C Hera freeze	Thermo Scientific
Gel iX Imager	Intas Science Imaging Instr. GmbH
Gene Pulser® II electroporator	Bio-Rad Laboratories GmbH
Glass cuvettes for histology	Omnilab
Glass dounce homogenisator, size A	Kontes Glass Inc.
Heating plate for slides	Thermo Scientific
HERAcell® incubator	Heraeus Instruments
Heraeus Megafuge 1.0R	ThermoElectron Corporation
Hettich MIKRO 22R mikrocentrifuge	Hettich GmbH & Co. KG
Incubator for bacteria	Memmert GmbH + Co. KG
InoLab® Serie 720 pH-meter	WTW GmbH
Intas Chemoluminescence Imaging	Intas Science Imaging Instr. GmbH
Liquide nitrogen tank LS4800	Labsystems Taylor Wharton
Magnet stirrer MR3001	Heidolph Instruments GmbH & Co. KG
Microm EC350 embedding station	Thermo Scientific
Microscope HBO 100	Karl Zeiss MicroImaging GmbH
Microtome Leica RM2235	Leica
Microwave MW 17705	Cinex
MiniVE Blotter western blot chamber	GE Healthcare
MiniVE SDS-PAGE chamber	GE Healthcare
NanoDrop® ND-100 spectrophotometer	Peqlab Biotechnologie
Neubauer chamber improved	Brand GmbH & Co. KG
Optimax X-ray film processor	Typon Röntgen-Film GmbH
Paraffin oven	Heraeus

PCR Cycler Advanced Primus25	Peqlab Biotechnologie GmbH
Pipet-Aid® portable XP	Drummond, USA
Shaker	Von Kreutz
Shaker Promax 2020	Heidolph
Shaker for bacteria cultures	New Brunswick Scientific GmbH
Table centrifuge typ MIKRO 22 R	Hettich Zentrifugen
Thermomixer comfort	Eppendorf AG
Ultracentrifuge, rotor with swinging buckets (Typ SW40)	Beckman
Vacupack 2 plus sealing machine	Krups GmbH
Vacusafe Comfort vacuum pump	IBS Integra Biosciences, Schweiz
Vortex mixer	VWR
Water bath HIR-3	Kunz Instruments
X-ray cassette, 13x18 cm	REGO X-Ray GmbH

4. Methods

4.1 Cellular biology

4.1.1 Working with bacteria

4.1.1.1 Transformation of chemical competent bacteria

For propagation of recombinant plasmids containing an antibiotic resistence gene plasmids were transformed into the *E.coli* bacterial strain DH10B^{TM}.
For this purpose bacteria were mixed with 100 ng DNA and incubated on ice for 30 min before warming at 37°C for 10 min. After cooling down for further 10 min on ice the transformed bacteria were plated on selective agar plates with 200 µg/ml ampicillin. They were then incubated overnight at 37°C, single cell clones were picked, inoculated in 2YT growth medium and plasmids were prepared using the plasmid midiprep system from Promega.

4.1.1.2 Electroporation of bacteria

Electroporation of bacteria was performed whenever high transformation efficiency was inevitable. Following QuikChange mutagenesis (see **4.3.3**) and ligation of DNA fragments DNA was transformed into bacteria by electroporation, which has a 100-fold higher efficiency compared to the chemical transformation.
7 µl of electro-competent *E.coli* ElektroMAX DH10B were mixed with 0.3 µl DNA. The whole reaction was pipetted into a pre-cooled electroporation cuvette (Biorad) without producing air bubbles between the plates and an electric field (1.7 kV, 200 Ω, 25 µF) was applied for 5 ms using the Genepulser Xcell (BioRad). 2YT bacterial medium was immediately added to the mixture and bacteria were afterwards incubated shaking at 37°C for 30-60 min, followed by plating bacteria on selective agar plates.

4.1.2 Working with eukaryotic cells

4.1.2.1 Cultivating, freezing and thawing eukaryotic cells

Cultivation of cells

Adherent cells were cultivated in coated petri dishes of different sizes (Greiner).

To avoid any contamination cells were passaged using a sterile laminar flow. All media and solutions were pre-warmed at 37°C.
Sub-cultivation of cells was performed when cells reached a confluency of approximately 80%. After discarding the growth media, cells were rinsed with PBS to remove any cell debris. Then cells were detached by incubating the cells with 0.5% trypsin/EDTA solution (30 µl/cm^2). The enzymatic reaction was stopped by adding the growth medium including 10% FCS. After resuspension cells were further diluted in the medium and seeded in clean Petri dishes or, alternatively, cells were counted using a Neubauer chamber and seeded for experiments at a special cell density. Incubation of cells was performed at 37°C under normal growth conditions of 5% CO_2 in a humidified incubator.
While for HCT116 cells McCoy`s medium was used, GH, H1299, NCCIT and U2OS cells were cultured in Dulbecco`s Modified Eagle medium containing different antibiotics. GH and NCCIT cells were grown in DMEM without tetracyclin and ciprofloxacin.

Freezing cells

For the long-term storage of cells in liquid nitrogen, low numbers of cell passages were used. Detachment of cells was followed by centrifugation for 5 min at 800 rpm. Afterwards cells were resuspended in pre-cooled freezing medium (10% DMSO, 20% FCS and 70% growth medium) and the cell suspension was aliquoted into cryo vials. After incubation for one night at -80°C the vials were transferred into liquid nitrogen the next day.

Thawing cells

Aliquots of frozen cells were removed from the liquid nitrogen. Cells were thawed as fast as possible in the hand; the cell suspension was then added to the pre-warmed growth medium. The next day, the medium was exchanged to remove the DMSO and all dead cells.

4.1.2.2 Transient transfection of eukaryotic cells

4.1.2.2.1 Transient transfection with plasmid DNA

To study the cellular function of proteins of interest they were transiently overexpressed in H1299 cells using Lipofectamin™ 2000 (Invitrogen) as transfection reagent. The day before transfection cells were seeded at a density of 1.2 x 10^5 in 12-wells or at a density of 2.5 x 10^5 in 6-well plates (see **4.1.2.1**).

According to the manufacturer`s instructions transfection reactions for one 12-well contained 1.2 µg plasmide DNA, 4 µl Lipofectamin and 200 µl DMEM without supplements. For transfections of cells in a 6-well format, twice the amount of all components was used. Following an incubation step at room temperature generated DNA-Lipofectamin complexes were carefully added to the cells.

To minimize the toxicity of the transfection reagent the medium was exchanged with fresh DMEM complete 4 h after transfection.

4.1.2.2.2 Transfection with siRNAs

For the knockdown of cellular proteins cells were tranfected with short interfering RNAs (siRNAs). 40 h prior to the transfection procedure 8 x 10^4 GH cells were seeded in 12-wells (see **4.1.2.1**). 50 pmol siRNA were mixed with 100 µl DMEM and 8 µl HiPerFect™ transfection reagent (Qiagen). After incubation for 10 min complexes were carefully pipetted onto the cells while slowly shaking the plate. Transfected cells were then incubated for 36h at 37°C in a humidified incubator prior to drug treatment (see **4.1.2.3**).

4.1.2.3 Treatment of cells with chemotherapeutic drugs

Cells were treated with different kinds of drugs such as the chemotherapeutic cisplatin (cDDP), the HDAC inhibitor trichostatin A (TSA) or the general inhibitor of translation cycloheximide (CHX).

The majority of drugs were bought as lyophilized powder and had to be dissolved in the organic solvent DMSO to achieve a stock solution at a specific concentration. These stock solutions were afterwards further diluted in the cells` growth medium

shortly before treatment of cells. Alternatively, aliquots of stocks were stored frozen at -20 °C or -80 °C and repeated cycles of freezing and thawing were avoided.

Whenever DMSO was used as solvent, we performed control treatment with DMSO alone.

4.1.2.4 Generation of stably transfected cells

The lung carcinoma cell line H1299 was used to generate cells consistently expressing a protein of interest to study long term effects of this protein regarding cellular proliferation or chemosensitivity of the cells.
For this purpose, cells were transfected with pIRES neo (Invitrogen) plasmids. Beforehand, proteins of interest were cloned into the internal ribosomal entry site (IRES) of the vector backbone, which additionally contains a neomycin resistance gene behind the CMV promoter (see **4.3.13.2**). Expression of pIRES plasmids in cells leads to generation of bicistronic transcripts allowing the expression of the protein of interest together with the antibiotic resistance. Following antibiotic selection of cells with neomycin surviving cell clones also contained the protein of interest.
In brief, H1299 cells were transfected using lipofectamine as described under **4.1.2.2.1**. 40 h after transfection cells were trypsinized and re-seeded in 10 cm Petri dishes, followed by addition of the antibiotic neomycin (final concentration: 800 µg/ml) the next day. Transfected cells were then selected for 10 days with a regular change of the neomycin-containing medium every 2 days. Afterwards, stable cell lines were either sub-cultivated and further used for experiments or grown cell colonies were fixed and stained with crystal violet to measure the number of clones.

4.1.2.5 Clonogenic assays

This assay was performed to analyze the long-term clonogenic survival of stable H1299 cells following the treatment of cells with the chemotherapeutic cisplatin.
One day after seeding cells in 12-wells the drug was added to the medium and the cells were incubated with cDDP for 24 h. Afterwards cells were washed, trypsinized and the cell number counted. For the DMSO-treated sample 5000 cells were re-seeded in a 100 mm dish. The same volume of cell suspension was used for seeding of the corresponding cisplatin-treated cell line. After 7-10 days of incubation grown

cell clones were fixed and stained with crystal violet. The Adobe Photoshop software was used to analyze the area of stained cells.

4.1.2.6 Flow cytometry

All flow cytometry analyses were performed using the Guava EasyCyte system (Millipore). This flow cytometer uses a micro capillary that sucks cells into the system and also contains the flow cell to analyze cellular parameters. The Guava EasyCyte was equipped with a standard laser with the wave length of 480 nm and three fluorescence channels for the detection of emitted light from analyzed cells.

4.1.2.6.1 Cell cycle analysis

To analyze cell cycle profiles upon drug treatment cells were stained with propidium iodide (PI). The intensity of the PI fluorescent signal correlates with the DNA content of cells. The sub G1 shoulder of the cell cycle profile is indicative for the dead fraction of cells, since those cells already have fragmented DNA.

Propidium iodide is a fluorescent dye that intercalates into nucleic acids. Because it cannot be taken up by healthy living cells, cells had to be fixed in 75 % of ethanol prior to their staining with PI.

Treated as well as untreated cells were harvested by trypsination. The cells, their medium and all used solutions were collected in Falcon tubes, followed by centrifugation of cells at 1800 rpm for 5 min. Afterwards cells were resuspended in PBS++ before three times the volume of 100 % ethanol was added very slowly in drops onto the cells to avoid cellular clumping. After fixation overnight at - 20°C cells were rehydrated in PBS and again pelleted at 1800 rpm. Then, cellular RNA was digested by incubating the cells with RNase A (Qiagen) at a final concentration of 1 mg/ml for 30 min at 37°C. Finally, cells were diluted in PBS. Directly before the measurement propidium iodide was added to the cells at a concentration of 30 µg/ml. For each sample 10000 single cells were analyzed with the Guava EasyCyte machine, measuring the size and the red fluorescent intensity for each single cell. The resulting raw data were further analyzed with the Modfit software tool to achieve percentages of cells in G1, G2/M or S-phase of the cell cycle or the percentage of apoptotic subG1- cells.

4.1.2.6.2 Guava caspase assay

This sensitive assay was performed to analyze drug induced cellular apoptosis more specifically, enabling to distinguish cells in different stages of apoptosis from dead cells.

The assay is based on the staining of living cells with specific caspase inhibitors coupled to fluorescent dies. In this work the Guava MultiCaspase assay from Millipore was used. It contains the pan-caspase inhibitor cVAD coupled to sulforhodamine. Cells possessing active effector caspases 3 and/or 7 stain positive in the yellow fluorescence channel. In addition, cells are counterstained with the intercalator 7-AAD, which cannot be taken up into healthy living cells. Therefore 7-AAD only stains cells with a leaky cell membrane. This signal is detected in the red fluorescence channel.

After drug treatment cells were trypsinized and immediately stained with the MultiCaspase reagent according to the manufacturer`s protocol for 1 h at 37°C, followed by several washing steps and counterstaining with 7-AAD. Cells were then directly analyzed with the Guava EasyCyte. Dot plots were generated, dividing cells into 4 different subpopulations of healthy/early apoptotic, mid-stage apoptotic, late-stage apoptotic and dead cells.

4.2 Working with mice

All mice work was performed according to the rules of the German law concerning animal experiments. Mice were held in the animal facility of the ENI institute (European Neuroscience Institute) in Göttingen.

For our experiments we used the mouse strain SV129.

4.2.1 Preparation of murine tissues

For the preparation of murine tissues for further analyses such as histology, immunohistochemistry and RNA isolation, mice were sacrificed by cervical dislocation. Tissues were carefully prepared with clean instruments and afterwards

washed in PBS, before the tissues were either fixed in 4 % phosphate-buffered paraformaldehyde or shock frozen in liquid nitrogen for RNA isolation.

4.3 Molecular biology

4.3.1 Preparation of plasmid DNA

Plasmid DNA was isolated from bacteria using the PureYield™ plasmid midiprep sytem (Promega).
The principle of the method is the alcalic lysis of bacteria. Centrifugation of neutralized lysed bacteria results in free DNA in the bacterial supernatant. Afterwards, DNA is purified by binding to silica columns. This is followed by elution of DNA from the columns with elution buffer (Tris buffer, pH 7.5).
Transformed bacteria were grown on selective agar plates. The day before the plasmid preparation, a single bacterial colony was picked from the agar plate and inoculated into 40 ml of bacterial culture medium containing ampicillin [200 µg/ml]. The culture was then incubated overnight at 37°C shaking at 200 rpm.

Upon modification of plasmids by QuikChange (see **4.3.3**) mutagenesis or ligation of plasmid fragments several bacterial clones from one plate were chosen, inoculated into each 2 ml of ampicillin-containing medium and grown overnight. In this case, DNA was then prepared on a small scale using the Invisorb® plasmide miniprep kit spin two (Invitek).

4.3.2 Determination of nucleic acid concentrations

The Nanodrop (Peqlab) was used to measure concentrations of nucleic acids by spectrophotometry. The absorption of DNA or RNA at a wave length of 260 nm was analyzed. Nucleic acid solutions were measured undiluted by adding 1 µl of the solution onto the instrument. Concentrations of solutions were calculated by multiplying the value for the measured absorption at 260 nm (A_{260}) with the specific nucleic acid factor (50 µg/ml for DNA and 40 µg/ml for RNA). The purity of nucleic acid solutions was assessed by looking at the ratios $A_{260} : A_{280}$ and $A_{260} : A_{230}$.

4.3.3 QuikChange™ mutagenesis

The QuikChange mutagenesis was performed to introduce point mutations into DNA. This method is based on a polymerase chain reaction (PCR) amplifying dsDNA in several cycles of denaturation, primer annealing and elongation of the DNA strand.
The QuikChange primers (**3.4.1.3**) introduce the desired mutations into the DNA template. Each primer binds complementary to one of the two strands of the plasmid template, mismatching nucleotides loop out. To still ensure proper binding of the oligonucleotides to the plasmid DNA, mutated nucleotides in primers are flanked by 10-15 unchanged nucleotides. QuikChange primers additionally contain a restriction site for endonucleases, allowing the identification of successfully mutated plasmids after digestion of plasmid DNA with corresponding enzymes.
The *Pfu* turbo polymerase was used in mutagenesis reactions because of its higher proof reading activity. This helps to avoid mutations in the DNA sequence where they are undesired.
Primers used for mutagenesis are listed in **table 3.3**.

PCR reaction:

Pfu turbo	1,0 µl
10x Pfu turbo Buffer	5,0 µl
dNTPs 20mM each	0,5 µl
Primer forward 5 µM	2,5 µl
Primer reverse 5 µM	2,5 µl
DNA 75 ng	x µl
ddH_2O	ad 50 µl
Final volume:	50 µl

All components were pipetted into PCR tubes on ice. The amplification of mutated DNA was performed in a PCR cycling machine (Peqlab) with the program below.

Cycling program:

No. of cycles	temperature	time
1	95°C	30 s
18	95°C	30 s
	55°C	1 min
	68°C	2min/kb of plasmid length
1	8°C	∞

Afterwards, the amplified DNA was digested with 1 µl of DpnI endonuclease [10 U/µl] for 2 hours at 37 °C. This special restriction enzyme only cuts fully methylated DNA, which is found after preparation of DNA from bacteria. Since the mutagenesis product is hemi-methylated or unmethylated, samples were enriched for the mutated plasmid by performing the incubation with DpnI. Following an ethanol precipitation of DNA (see **4.3.4**) the mutated plasmids were transformed into bacteria by electroporation (see **4.1.1.2**).

4.3.4 Purification of DNA

Mutated or amplified DNA has to be purified prior to the electroporation into bacteria. For this purpose ethanol precipitation of DNA was performed. First, 1/10 volume of the DNA solution sodium acetate (pH 5.5) was added to the sample, then, twice the sample volume of 100% ethanol followed. Finally, 1 µl of glycogen was added as a carrier molecule. The DNA precipitation was performed for at least 2 h at -20°C. After centrifugation at 13000 rpm at 4°C the precipitated DNA was washed with 70% ethanol, afterwards air dried for up to 10 minutes and then resuspended in 10 µl of sterile water.

The ethanol precipitation of DNA was also used to purify DNA prior to sequencing (see **4.3.8**).

4.3.5 Restriction of DNA with endonucleases

Following QuikChange mutagenesis reactions (see **4.3.3**) the mutated DNA was at first checked by digestion of the DNA with specific endonucleases. Restriction reactions had a total volume of 10 µl and contained the enzyme-specific 10 x buffer,

300 ng of plasmid DNA and 1 unit of enzyme. After mixing all components by vortexing, reactions were incubated at 37°C for 1 h. This was followed by electrophoretic separation of resulting DNA fragments in agarose gels (see **4.3.7**).
Restriction of DNA with endonucleases was also performed during cloning procedures (see **4.3.13**) to achieve blunted DNA or DNA fragments with specific overhangs. In that case restriction reactions were done on larger scale to get enough material for ligations.

4.3.6 Ligation of DNA fragments

For molecular cloning procedures purified DNA fragments with blunt or sticky ends, generated by restriction endonucleases (see **4.3.5**), were ligated using the T4 DNA ligase (Fermentas).
Dephosphorylated purified vector DNA was mixed with purified insert DNA in a molar ratio of roughly 1:3. In a total reaction volume of 5 µl each 0.5 µl of 100 µM ATP, 10x T4 DNA ligase buffer (Fermentas) and T4 DNA ligase HC (Fermentas) were added. Ligation of DNA was performed incubating the reaction overnight at room temperature.
0.3 µl of each reaction were directly used for electroporation of the ligated DNA into bacteria (see **4.1.1.2**).

4.3.7 Electrophoretic separation of DNA

Agarose gel electrophoresis is the method of choice to distinguish DNA molecules based on their size, as small DNA molecules move faster through the agarose polymer net than larger ones.
Samples to be analyzed were mixed with a corresponding amount of 6x DNA sample buffer including bromphenol blue. Depending on the size of DNA fragments, samples were loaded on agarose gels of lower percentage (~ 1%) or higher percentage (up to 2%). Before pouring gels ethidium bromide was added to the liquid agarose. To determine the size of DNA fragments a DNA standard (100 bp or 1 kb DNA ladder; Fermentas) was loaded next to the samples.
Gels were run at a constant voltage of 120 V and analyzed by UV illumination using the Intas GelDoc system.

4.3.8 Sequencing of DNA

DNA of generated QuikChange mutants, ligated DNA or PCR-amplified DNA fragments were controlled by sequencing, based on the method established by Sanger and Coulson (Sanger, 1977), using dideoxynucleotides for chain termination.

For this dideoxynucleotide sequencing method we performed a PCR using the BigDye® Terminator v3.1 Cycle Sequencing kit that consists of a 2x sequencing mix containing the polymerase, dNTPs and also fluorescence-labeled ddNTPs which result in termination of the nucleotide polymerization reaction.
For sequencing of plasmids 300 ng template were mixed with 8 pmol sequencing primer, 1.5 µl sequencing buffer and 1.5 µl sequencing mix in a total volume of 10 µl. The PCR was then performed as indicated in the following table.

cycles	temperature	time	step
1	96°C	2 min	initial denaturation
25	96°C	10 sec	denaturation
	55°C	15 sec	annealing
	60°C	4 min	elongation
	4°C	∞	cooling

After the cycling DNA was purified by ethanol precipitation and finally resuspended in 15 µl of HIDi™ formamide (Applied Biosysrems).

Analysis was performed using the ABI 3100 Automated Capillary Sequencer (Applied Biosystems). This sequencing machine consists of capillaries filled with a gel matrix, in which individual samples are injected. Nucleotides are then separated applying an electric field. During this process the machine detects the emission of the different fluorescent dyes in 4 detection channels. Finally, nucleotide sequences are generated by analyzing the resulting electropherograms.

4.3.9 Extraction of RNA using Trizol

For extraction of total cellular RNA the Trizol reagent (Invitrogen) was used.

Cells, cultured in a 6-well plate, were harvested by trypsination and afterwards carefully pelleted at 1800 rpm for 5 min. The medium was removed and cells were immediately lysed by thorough resuspension in 1 ml of Trizol reagent to achieve a homogeneous lysate. For complete dissociation of nucleoprotein complexes homogenates were incubated at room temperature for up to 10 min, prior to the addition of 200 µl chloroform to each sample. The mixture was vigorously shaken and incubated for 3 min to allow phase separation. After a centrifugation at 12000 x g for 15 min at 4°C total RNA was purified from the aqueous upper phase.
RNA purification was performed by using isopropanol for RNA precipitation. Afterwards, the precipitated RNA was washed twice with 75% ethanol. Finally, air-dried RNA was resuspended in 20 µl of sterile water.

4.3.10 Reverse transcription of RNA

Prior to gene expression analysis by quantitative PCR (see **4.3.10.2**) messenger RNAs were reverse transcribed following a do-it-yourself protocol. Within this protocol, Moloney murine leukemia virus-derived reverse transcriptase and RNase inhibitor from New England Biolabs were used.
In brief, for each RT reaction 1 µg of total RNA was pre-incubated with a mixture of oligo $dT_{23}VN$ and random nonamer primers and the deoxynucleotide mix (stock: 2.5 mM each dNTP; Promega) for 5 min at 70°C in a PCR cycler. Afterwards, samples were put on ice and a reaction mixture containing the RT enzyme (25 units), the RT buffer and 10 units RNase inhibitor was added to achieve a final volume of 20 µl each RT reaction. The polymerization reaction was performed for 1 h at 42°C. A following incubation step at 95°C for 5 min was necessary to inactivate the reverse transcriptase. Prior to PCR analyses cDNAs were diluted with ddH_2O to a final volume of 50 µl.
In addition to RT reactions the same RNAs were used in parallel in control -RT reactions, omitting the reverse transcriptase.

4.3.11 Polymerase chain reaction (PCR)

The Polymerase Chain Reaction (PCR) is the standard method to amplify dsDNA for various purposes. The method is based on three different steps that are repeated in various cycles. The first step of DNA denaturation is followed by annealing of primers

- short oligonucleotides of 18-25 bp length - to specific complementary sequences of the target DNA. During the third step these primers are extended by the DNA polymerase complementary to the parental DNA strand. The number of repetition steps depends on the PCR template and on the purpose of the PCR amplification.

4.3.11.1 PCR for amplification of DNA fragments

Conventional PCR was performed to amplify DNA fragments from genomic DNA of humans and primates that was already used in previous experiments by Ana Contente (Contente et al, 2003).
All components, including the *Taq* DNA polymerase (Fermentas), were pipetted into thin-wall PCR tubes, which were held on ice during the pipetting procedure.

	Final concentration	**1x**
10x *Taq* buffer	1x	4 µl
$MgCl_2$ stock (25mM)	3 mM	4.8 µl
dNTP mix (20 mM each)	200 µM each	0.4 µl
Primer for/rev (10 µM)	300 nM	1.2 µl
Taq DNA polymerase	1.25 units	0.25 µl
Water		28.7 µl
Genomic DNA (100 ng/µl)		0.6 µl
Total volume		40 µl

The cycling was performed in a PCR cycler (Peqlab) according to the following protocol.

cycles	**temperature**	**time**	**step**
1	95°C	3 min	initial denaturation
35	95°C	15 sec	denaturation
	58°C	15 sec	annealing
	72°C	15 sec	elongation
	4°C	∞	cooling

Resulting PCR products were analysed by agarose gel electrophoresis (see **4.3.6**).

4.3.11.2 Quantitative real-time PCR for amplification of cDNA

mRNA expression levels of diverse cellular genes were quantified by performing real-time PCR. For this purpose, 2 µl of cDNAs (see **4.3.9**) were used as PCR template in reactions with a final volume of 25 µl.

Our lab established a protocol for the preparation of a qPCR reaction mix used for realtime PCR. All components for the 2x mix (see tables below) were mixed on a larger scale, at least sufficient enough for all PCR reactions of one single experiment. The mix was aliquoted and afterwards shock frozen in liquid nitrogen. It was stored at -20°C until use.

10x qPCR buffer:

Component	stock concentration	final concentration
Tris-HCl (pH 8.8)	1.5M	750 mM
$(NH_4)_2SO_4$	1M	200 mM
Tween-20	10%	0.1%
ddH_2O		

2x reaction mix:

Component	stock concentration	final concentration
10x buffer	10 x	1x
MgCl	25 mM	3 mM
Sybr green	1:100	1:80 000
dNTPs	20mM	0.2 mM
Taq	5 U/µl	20 U/ml
Triton X100	10%	0.25%
Trehalose	1 M	300 mM

Cycling and sample analyses were performed with the Chromo4 Real-Time PCR system (BioRad). During the amplification of DNA fragments, which have a size of 150-300 bp, this system continuously measures the fluorescence of SybrGreen, which is incorporated into increasing amounts of dsDNA.

We used a two-step cycling protocol, followed by a stepwise increase of the incubation temperature to perform a melting curve analysis of the generated PCR product.

cycles	temperature	time	step
1	95°C	3 min	initial denaturation
40	95°C	15 sec	denaturation
	60°C	1 min	annealing + elongation
	plate read		
	60°C – 95°C; 0.5°C increment		Melting curve

Finally, relative mRNA levels were calculated by the $\Delta\Delta C_T$ method, assuming a PCR efficiency of 2. The expression of target mRNAs was normalized to the expression of GAPDH or 36B4 reference genes.

4.3.12 Rapid amplification of cDNA ends (RACE)

For the identification of novel TP63 exons we performed rapid amplification of 5`-cDNA ends (5`-RACE) using the SMART^{TM} RACE kit from Clontech.
The general strategy behind this RACE method is depicted in **figure 4.1**.
The SMART II A oligo (Clontech) binds to the dC-rich cDNA tail which was added to the 3`end of the cDNA by the PowerScript RT enzyme (Clontech) possessing terminal transferase activity. Template switching of the polymerase then generates a prolonged cDNA with the sequence of the SMART oligo at its 5`-end. In that way tailed cDNAs are amplified in a PCR reaction using a forward primer mix (UPM) that binds specifically to the tail, and a reverse primer, specific to known sequences of the gene of interest (SMART^{TM} RACE cDNA Amplification kit manual, Invitrogen).
Amplified RACE products are then characterized, cloned and sequenced.

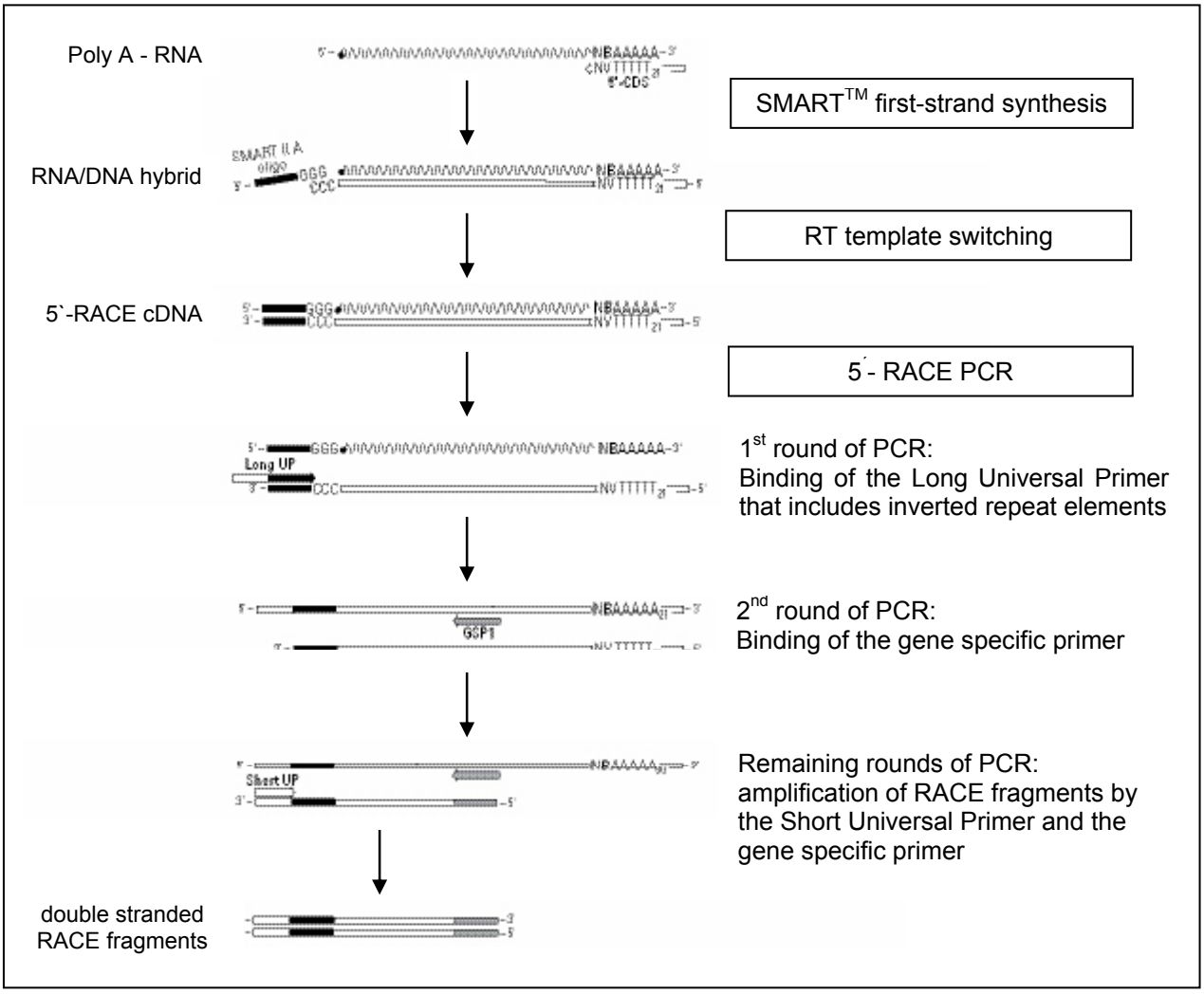

Figure 4.1: SMART™ RACE cDNA amplification (manual SMART™ RACE cDNA amplification kit, Invitrogen)
RNA is reverse transcribed by the PowerScript polymerase, which adds a dC-rich tail to the cDNA upon reaching the end of the RNA. The SMART II A oligo, which is included in the cDNA synthesis reaction, binds complementary to the dC-tail and is then used as template for the polymerase, resulting in cDNAs with 5`-tails. Theses tailed cDNAs are afterwards amplified in the 5`- RACE PCR reaction using the Universal Primer Mix (UPM) as forward primer and the gene-specific primer (GSP) as reverse primer. The UPM contains a Long Universal Primer that is used in the first round of PCR and binds specifically to the sequence of the tail adding more 5`-terminal nucleotides, and a Short Universal Primer that is used from the third round of PCR on. In the end, the RACE PCR generates double stranded fragments that contain all possible 5`- ends of a given gene of interest.

4.3.12.1 5`RACE for human TAp63

A 5`RACE experiment was performed from RNA, isolated from immortalized keratinocytes, to identify yet unknown 5`- termini of human TAp63. For this purpose, the gene-specific RACE PCR reverse primer was designed to bind specifically to the human TP63 exon 3.

Synthesis of RACE cDNA

All components, displayed below, were added into PCR tubes on ice.

	Volume per reaction
1 µg total RNA	1-3 µl
5`-CDS primer (12µM)	1 µl
SMART II A oligo (Clontech)	1 µl
sterile water	ad 5 µl

After proper mixing of components, samples were briefly centrifuged and afterwards incubated for 2 min at 70°C in the PCR cycler. Prior to the addition of following components, tubes were placed on ice for 2 min to allow for cooling of samples.

	Volume per reaction
5x First-Strand buffer	2 µl
DTT (20mM)	1 µl
dNTP mix (10mM)	1 µl
PowerScript Reverse Transcriptase	1 µl
Total volume	10 µl

The reverse transcription reaction was then performed by incubating the samples for 90 min at 42°C in the PCR cycling machine (Peqlab).

Prior to PCR reactions RACE cDNA samples had to be diluted in 100 µl Tricine-EDTA buffer (Clontech) and additionally heated for 7 min at 72°C.

RACE PCR

We prepared a PCR mastermix that was sufficient for all samples including one extra reaction.

	Volume per reaction
PCR water	34.5 µl
10x Advantage 2 PCR buffer	5 µl
50x dNTP mix (10mM)	1 µl
50x Advantage 2 polymerase mix	1 µl
Total volume	41.5 µl

Samples were mixed by vortexing. Afterwards, the RACE cDNA was mixed with primers, before the PCR mastermix was added to a final volume of 50 µl.
In addition, negative control reactions, either leaving out the UPM forward primer or the p63-specific reverse primer (GSP), were included in the PCR to control the specificity of the RACE amplification.

	5`RACE sample	**UPM only**	**GSP only**
RACE-ready cDNA	2.5 µl	2.5 µl	2.5 µl
10x Universal primer A	5.0 µl	5.0 µl	-
Gene specific primer (10µM)	1.0 µl	-	1.0 µl
water	-	1.0 µl	5.0 µl
Final volume	50 µl	50 µl	50 µl

For the cycling a touchdown PCR program was used to increase the specificity of the amplification of RACE cDNAs.

cycles	**temperature**	**time**
5	94°C	30 sec
	72°C	3 min
5	94°C	30 sec
	70°C	30 sec
	72°C	3 min
30	94°C	30 sec
	68°C	30 sec
	72°C	3 min

After the cycling 5 µl of each PCR reaction were loaded onto an agarose gel for analysis. To identify TAp63-specific RACE products primary PCR products were re-amplified in a second RACE PCR, this time using the nested p63-specific reverse primer. In the next step the RACE products were loaded onto a preparative agarose gel, cut out off the gel, extracted from the gel using the Gel Extraction kit (Qiagen) and eluted in 30 µl of EB buffer.
Prior to the cloning of RACE products into a TOPO TA cloning vector (Invitrogen), 3`-overhangs of adenosine nucleotides were added freshly to the eluted DNAs.

Generation of 3`- A overhangs

	Final concentration	Volume per reaction
Purified PCR fragment	-	28 µl
10x Taq buffer +KCl	1x	3.3 µl
25mM $MgCl_2$	1.5 mM	1.98 µl
20mM **dATP**	0.2 mM	0.33 µl
Taq DNA Pol (5u/µl)	0.5 units	0.1 µl
Final volume		34 µl

Samples were incubated for 20 min at 72°C and PCR fragments with 3`- overhangs were purified using the PCR Purification kit (Qiagen).

TOPO TA cloning

RACE DNA fragments were cloned into the pCR4 TOPO TA vector using the TOPO TA cloning kit for sequencing (Invitrogen)

	Volume per reaction
fresh PCR product	4 µl
diluted salt solution 1:4 in water (final salts: 50mM NaCl, 2.5mM $MgCl_2$)	1 µl
TOPO vector	1 µl
Total volume	6 µl

The reaction was gently mixed and incubated for 10 min at room temperature.
After the cloning reaction plasmids were transformed into One Shot TOP10 cells (Invitrogen) by electroporation according to the manufacturer`s instructions.
For each cloning reaction several bacterial clones were picked and grown, the DNA was extracted and finally sequenced.

4.3.13 Cloning of novel TAp63 isoforms

Novel TAp63 isoforms identified in the RACE experiment had to be cloned into expression vectors for eukaryotic cells: pcDNA3.1 (Invitrogen) was used for transient expression and pIRESneo (Clontech) for stable protein expression.

4.3.13.1 Cloning for transient expression

A pcDNA3 plasmid containing the full-length p63 (pcDNA-p63fl-myc) was used as template. In a first step this plasmid was mutated to introduce BamHI and NheI restriction sites in the p63 insert. Digestion of the mutated plasmid pcDNA-p63fl-BamHI/NheI results in the complete removal of p63 exons 1 and 2 and a partial removal of exon 3. The remaining vector fragment (~ 10 kb in size) was then dephosphorylized by incubation with CIAP (Calf Intestine Alkaline Phosphatase; Fermentas) for 30 min at 37°C, followed by gel extraction.

Inserts of the new amino termini of p63 isoforms were generated by PCR amplification from pCR4 TOPO vectors that contained the cloned RACE products. The PCR was performed using primer that introduce BamHI or NheI restriction sites at the ends of the PCR fragments (exon U1_BamHI_for and exon 3_NheI_rev) and the Phusion hot start DNA polymerase (Finnzymes) according to the manufacturer`s instructions.

cycling program:

cycles	temperature	time	step
1	98°C	30 sec	initial denaturation
5	98°C	20 sec	denaturation
	50°C	1 min	annealing
	72°C	2 min	extension
20	98°C	20 sec	denaturation
	60°C	1 min	annealing
	72°C	2 min	extension
1	72°C	10 min	final extension

Afterwards, the purified DNA fragments were also digested with BamHI and NheI for 2 h at 37°C.

Both, vector fragment and inserts were then purified by phenol-chlorophorm extraction. Inserts were ligated into the vector (see **4.3.6**) to achieve plasmids containing the newly identified p63 exons. Finally, the NheI restriction site was back-mutated to re-construct the correct open reading frame of TAp63.

4.3.13.2 Cloning for stable expression

To achieve stable expression of the novel p63 isoforms, the complete p63 insert was cut out from the pcDNA3-p63-exonU1 plasmid and cloned into the empty pIRES vector backbone by T/A cloning.

The insert was cut out using the restriction enzymes SalI and BamHI and further shortened by digestion with BamHI and XhoI to get rid of additional pcDNA3 sequences. The insert of roughly 5 kb in size was then blunted by incubation with 5 units Klenow (Fermentas) and dNTPs for 30 min at room temperature, followed by gel extraction (Qiagen kit).

The target pIRES plasmid was blunted by digestion with EcoRV, which cuts in the MCS in front of the IRES signal. Again, the digested vector was dephosphorylated by CIAP and phenol-chlorophorm extraction was applied.

In the next step, tailing reactions were performed generating a vector fragment with a dT-overhang and an insert with a dA-overhang. Therefore, insert or vector was incubated with the *Taq* polymerase in the presence of dATP or dTTP, respectively, for 20 min at 72°C. Finally, the tailed purified DNA fragments were ligated (see **4.3.6**).

The correct orientation of the insert was checked by digesting the resulting pIRES-U1p63 with BamHI and EcoRV.

4.4 Protein biology

4.4.1 Cell lysates for SDS-PAGE analysis

For the separation of proteins on the basis of their electrophoretic mobility in SDS-polyacrylamide gels, known as SDS-PAGE, cells had to be lysed under denaturing conditions.

Prior to harvest, transfected or treated cells were cultured in coated Petri dishes. Cells were then harvested by careful scraping. The procedure was performed on ice to minimize protein degradation. Complete cell suspensions were transferred into reaction tubes and cells were pelleted at 1800 rpm for 5 min. After washing of the cell pellet with PBS, cells were lysed by adding RIPA buffer containing a cocktail of protease inhibitors. Tubes were placed on ice. Lysates were then mixed with

Laemmli buffer, containing 2 % SDS and bromphenol blue, by vortexing thoroughly. Samples were additionally heated for 5 min at 95° while shaking at 1000 rpm. This step ensures complete denaturation of proteins by breaking protein disulfid bonds. It also leads to DNA shearing. Protein lysats were finally loaded on SDS gels (see **4.4.3**) or, alternatively, stored at -20°C.

4.4.2 Fractionation of mitochondria

Cell fractionation was performed to purify mitochondria and associated proteins. Mitochondria can be specifically enriched in a discontinuous sucrose gradient. We obtained the protocol for mitochondria isolation from cultured cells from the Moll lab, Stony Brook University, USA. It largely follows the method described by Bogenhagen and Clayton (Bogenhagen & Clayton, 1974).

Cultured adherent cells were detached by scraping, centrifuged for 5 min at 2000 x g and afterwards washed in TD buffer. Cells were then resuspended in CaRSB buffer containing 1.5 mM $CaCl_2$ that results in the swelling of cells. Then, cell lysis was performed by dounce homogenization, which was monitored under microscope. Lysis was stopped by adding 2.5 x MS buffer that contains EDTA, mannitol and sucrose. At this step an aliquot of the homogenate was taken to use it as the whole cell lysate control for Western blot analysis.

The rest of the homogenate was centrifuged twice to separate nuclei from the cytoplasmic cell fraction. The resulting supernatant was then very carefully loaded onto a discontinuous sucrose gradient, prepared by layering a 1 M sucrose buffer on top of a 1.5 M sucrose buffer. Upon ultracentrifugation for 35 min at 86,000 x g mitochondria appear as a white band at the 1-1.5 interphase of the gradient. They were carefully aspirated with a 18G needle using a 1 ml syringe. Washing of mitochondria in MS buffer was followed by pelleting at 16,000 x g for 15 min and resuspension in 1 x MS buffer. Purified mitochondria, together with control crude cell lysates, were subjected to SDS-PAGE and immunoblot analysis (see **4.4.3** and **4.4.4**).

4.4.3 Separation of proteins by SDS-PAGE

SDS polyacrylamide gel electrophoresis (SDS-PAGE) was used to separate proteins based on their size. In general, the anionic detergent SDS binds to proteins charging

them equally negatively. Upon application of an electric field the negative charged proteins move through the polyacrylamide gel in the direction of the anode. Dependent on their size proteins possess a different electrophoretic motility, moving faster or slower.

For this work, separating gels had a percentage of 8% or 10%, while stacking gels always reached 5%. Gels were poured as shown below.

Stacking gel:		
	6.8 ml	ddH_2O
	1.7 ml	30% Acrylamid solution
	1.25 ml	1 M Tris buffer, pH 6.8
	100 µl	10% SDS
	100 µl	10% Ammonium persulfate
	10 µl	TEMED

Separating gel:	8%	10%	
	9.3 ml	7.9 ml	ddH_2O
	5.3 ml	6.7 ml	30% Acrylamide solution
	5.0 ml	5.0 ml	1.5 M Tris buffer, pH 8.8
	200 µl	200 µl	10% SDS
	200 µl	200 µl	10% Ammonium persulfate
	12 µl	8 µl	TEMED

Polymerized gels were transfered into proper electrophoresis chambers filled with 1x SDS running buffer. Then, samples were loaded into gel pockets and current was applied. Gels were run at constant voltage of 130 V.

4.4.4 Immunoblot

After the separation of proteins in a polyacrylamide gel (see **4.4.3**), proteins were transferred on a nitrocellulose membrane to enable detection of proteins by immunostaining.

For the transfer of proteins we performed wet blots.

Blot construction:

cathode
sponge
3 Whatman papers
polyacrylamid gel
nitrocellulose membrane
3 Whatman papers
sponge
anode

Blots were run in corresponding blot chambers that were completely filled with the wet blot buffer containing 20% methanol. Protein transfer was then performed applying a constant voltage of 100 V for 90 min in the cold room.
Afterwards, the membrane was incubated in blocking solution (5% milk in PBS/0.1% Tween20) for at least 30 min on a shaker. This guarantees blocking of all free protein binding sites that would otherwise generate unspecific antibody binding.

For the following immunostainings both, primary and secondary antibodies were dissolved in the blocking solution. Incubation with primary antibodies was performed overnight at 4°C, while peroxidase-coupled secondary antibodies (Jackson) were applied to membranes for 1 h at room temperature. In between, blots were washed in PBS/0.1 % Tween20 several times.
Antibody-bound proteins were detected by Enhanced Chemiluminescence (ECL) using ECL kits from Pierce with differing sensitivities. Luminescent signals were analyzed by the Intas imager.

4.4.5 Immunohistochemistry

For the analyses of protein expression in tissues on the single cell level, proteins were detected by immunohistochemistry.
Prior to the immunostainings, formalin-fixed tissues were embedded in paraffin after a series of various incubation steps, including washing in PBS, dehydration in increasing concentrations of ethanol, penetration of the organic solvent xylol and at last of liquid paraffin.

Embedded tissues were cut into 5 µm thick sections using a microtome (Leica). Sections were applied onto Superfrost slides to ensure proper sticking of the tissue, and dried over night at 37°C.

Deparaffinization and hydration of sections via a descending alcohol series of xylol and isopropanol was followed by permeabilization of tissues, ensuring antigen retrieval. For this purpose, sections were microwave irradiated in 10 mM citrate buffer for 10 min. Blocking of endogenous peroxidase was then performed by incubation in 3% H_2O_2. Afterwards, slides were incubated with the p63 4A4 primary antibody, diluted 1:300 in 10 % FBS, overnight in the fridge. The secondary biotinylated anti-mouse antibody (GE Healthcare) was used at RT for 1h. Incubation of sections with streptavidin-peroxidase for 45 min at RT was followed by detection using DAB substrate. Cellular nuclei were weakly counterstained with hematoxylin. Finally, slides were dehydrated using an ascending alcohol series of ispropanol up to xylol and mounted in xylol-based mounting medium.

5. Results

5.1 Novel p63 isoforms are specifically expressed in testis

According to previous knowledge, the transcription factor p63 consists of 6 different isoforms that contain or lack the N-terminal transactivation domain due to alternative promoter usage. While the importance of deltaNp63 in epidermal homeostasis is known, the expression and physiological relevance of the transactivating TAp63 isoforms is not yet completely understood. In recent years TAp63 isoforms came into the focus of researchers, especially since Suh *et al.* could show that in mice TAp63 may act as the guardian of the female germline (Suh et al, 2006).
This work aimed to elucidate the expression pattern and function of human TAp63 in greater detail.

5.1.1 Novel TP63 transcripts contain hitherto unknown upstream exons

Primary RT-PCR analyses using distinct combinations of primers specific to TP63 exon 1, exon 2 or exon 3 showed that among different human cell lines there are major discrepancies in the expression level of p63 transcripts including or lacking exon 1. This result led us to the speculation that there are further, yet unknown TP63 exons upstream of exon 2. To characterize those exons rapid amplification of cDNA ends (5`RACE) was performed, the resulting RACE-PCR fragments were cloned and sequenced.
As suspected, we identified yet unknown TP63 exons. Blast analysis of the RACE products against the human genome showed that the three different novel exons are located upsteam of the TP63 exon1. These upsteam exons were designated exon U1, exon U2 and exon U3. The location of the exons in the human TP63 locus is depicted in **figure 5.1** (red boxes; known p63 exons are shown in black). Sequencing of the RACE products also revealed that the upstream exons U2 and U3 were used alternatively. Due to this alternative splicing three novel TP63 isoforms were generated that have either exon U1 alone, directly spliced onto exon 2 (red thick line) or additionally contain exon U2 or exon U3 in between exon U1 and exon 2 (red dotted lines). Importantly, all three novel isoforms omitted TP63 exon 1.

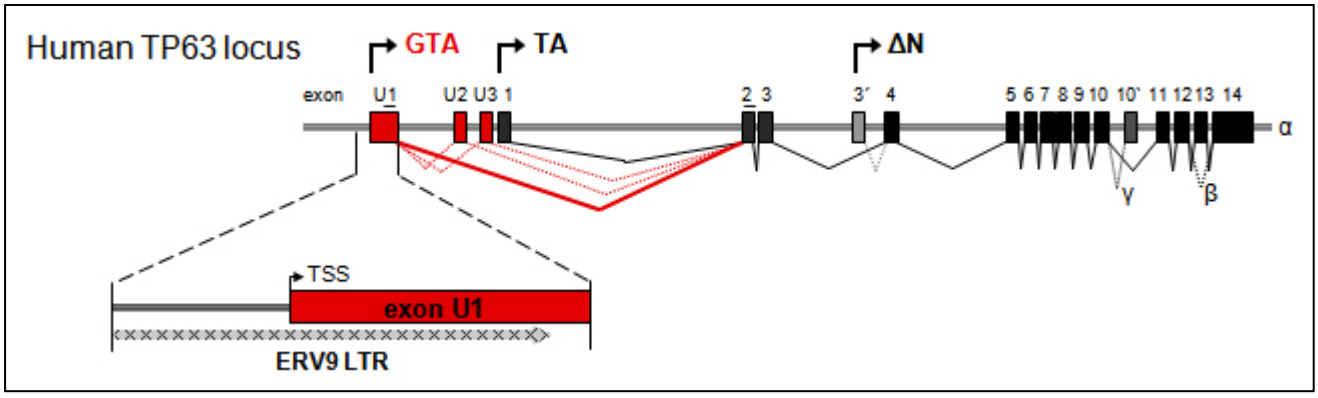

Figure 5.1: Genomic architecture of the human TP63 locus
By RACE experiments identified novel upstream exons U1, U2 and U3 which encode GTAp63 (germ-cell-encoded transactivating p63) are shown in red, while known exon of TP63 are shown in black. The solid red line indicates the predominant GTAp63 transcript where exon U1 is directly spliced onto exon 2, less abundant splice products are depicted by the dotted red lines. Above the exons there are the start sites of transcription (GTA, TA and ΔN). Alternative use of C-terminal exons generates α, β and γ isoforms.
The insert shows the genomic region of exon U1 with the transcriptional start site (TSS) enlarged. Of note, exon U1 overlaps with an endogenous retrovirus 9 long terminal repeat (ERV9 LTR).

From here on the novel TP63 transcripts were termed GTAp63, for 'germ-cell-encoded transactivating p63', because they could be readily detected in human testicular tissue.

The sequences of the identified upstream exons U1, U2 and U3 are displayed in **figure 5.2**. It mainly shows the major GTAp63 transcript with exon U1 being directly spliced onto exon 2. Other transcripts additionally contain the alternatively used exons U2 and U3, spliced in between exon U1 and exon 2. The figure also indicates binding sites of primers that were used for the amplification of the RACE cDNA and for following RT-PCR analyses.
Surprisingly, we found that the novel upstream exon U1 overlaps with the transcribed part of an endogenous retroviral LTR. This is described in more details in chapter 5.2.

Sequence GTAp63

ERV9 LTR

gccacccccctgctccacggcgcccagtcccatcgaccacccaagggctgaagagtgcaggcgcatggcgcgggactggca 80

ggcagctccatctgcagccccggtgggagatccactgggcgaagccagctggcctcctgagtctggtggggacgtggaga 160

atctttatgtctagctcagggattgtaaatacaccaatcagtgccctgtcaaaacagaccactcggctctaccaatcagc 240

exon U1

TATA box

aggaagtgggtggggccagataagagaataaaagcaggctgccccagccagcagtggcaacccgctggggtcaccttcca 320

cactgtggaagctttgttcttttgctctttgcagtaaatcttgctactgctcactctttgggtgcacactgcttttatga 400

gctgtaacactcaccgtgaaggtctgcagcttcactcctgaagccagcgagaccaggagtccactgggaggaacgaacaa 480

ctccagacgcaccgccttaagaacttcaacactcactgcgaaggtctgcagcttcactcctgagccagcgagaccacgaa 560

cccaccgtaaggaagaaactccgaacacatccgaacatcagaaggaacaaactccagacgcgccaccttaagagctgtaa 640

exon U1 forward primer

cactcaccgccagggtccgcggcttcattcttgaagtcagagagaccaagaacccaccaattccggacaccctatcagag 720

exon 2

attttgaaaactatgaagtgctgggaacagagagactggacagccttcacaaaggtggggaaaccttgtttcgtagaaac 800

cccagctcatttctcttggaaagaaagttattaccgatccaccatgtcccagagcacacagacaaatgaattcctcagtc 880

exon 2 reverse primer

exon 3

cagaggttttccagcatatctgggatttctggaacagcctatatgttcagttcagcccattgacttgaactttgtggat 960

5'RACE nested primer

gaaccatcagaagatggtgcgacaaacaagattgagattagcatggactgtatccgcatgcaggactcggacctgagtga 1040

5'RACE first primer

ccccatgtgg

Sequence exon U2

aaattgtggcttttatgacttcctgatgatcagtaccaaatcaacaaggcacaaatttgtgaatctatgtctgaaagaga 80

ggttcagcaacagctgtcttatgggctcaaactaaccaagggaag

Sequence exon U3

gcatccaatcacgacagagatcagaagttcagagatgcctccagctccaaattgccaacaacaagtgtggctactatacgt 80

caaggactctgaagccgtgagagagggggaagaacaacagtagagaggatgcccagctg

Figure 5.2: Sequences of novel TP63 upstream exons

The sequences of the newly identified exons U1, U2 and U3 are shown with the numbering of the nucleotides at the right side of the sequences. Exon boundaries and primer binding sites are indicated. The sequence corresponding to the ERV9 LTR is shown in red, the start codons (ATG) of GTAp63 are shown in blue. Grey bar, TATA box of the LTR promoter.

5.1.2 The predominant GTAp63 isoform contains exons U1 and 2

Having characterized the newly found exons we wondered if all three novel transcripts are equally expressed or if one of them is predominantly expressed.
RT-PCR analysis using a forward primer specific for exon U1 and a reverse primer specific for exon 2 (**figure 5.2**) resulted in two distinct PCR products of 205 or 344 bp in size, respectively. Control PCR reactions lacking the reverse transcriptase (-RT) or any template (H_2O) showed no product. Both PCR products were sequenced. The predominantly amplified product of 205 bp corresponds to the GTAp63 transcript where exon U1 is directly spliced onto exon 2 (**figure 5.3**; sequence in **figure 5.2**). The minor PCR product seen in **figure 5.3** also contained exon U2.

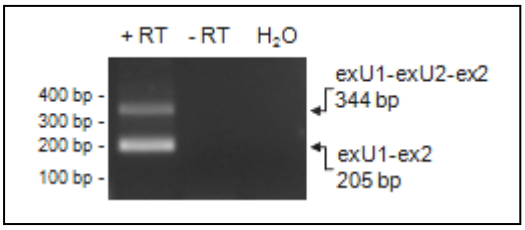

Figure 5.3: GTAp63 mRNA expression
RNA from human testicular tissue was reverse transcribed in two reactions with the reverse transcriptase (+RT) or without (-RT), followed by PCR amplification with the exon U1 forward primer and the exon 2 reverse primer. The major transcript corresponds to exon U1 fused to exon 2 but omitting exon U2.

Next, we addressed whether the predominant GTAp63 isoform also differs in the carboxyterminal protein sequence from the conventional TAp63. The predicted amino acid sequence of GTAp63 is shown in **figure 5.4**. It was compared to the long transactivating p63 isoform, termed TA* and starting from the methionin in exon 1, and to the shorter TAp63 that uses the start codon in exon 2. The alignment revealed that GTAp63 has a unique 19 amino acid long amino terminus (highlighted in blue letters) which is encoded by exon U1.
As highlighted in red in **figure 5.4** there are two possible translational start sites within the GTAp63 mRNA, the first one being in exon U1 and the second ATG lying in exon 2. So the question arose, which of these methionins is used as translational start codon.

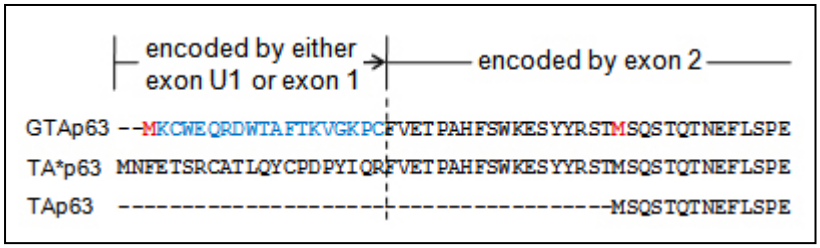

Figure 5.4: Protein sequences of the transactivating p63 isoforms
The predicted amino acid sequence of the major GTAp63 protein (in blue) is aligned to the sequence of the previously described TAp63 protein in which there are two possible translational start sites. GTAp63 differs from the long TA*p63 protein in the first 19 amino acids. The short TAp63 protein starts with the methionin in exon 2.

To answer the question, first full length GTAp63 mRNA including the known 5`and 3` untranslated regions were cloned into the pcDNA3 expression plasmid. Secondly, both possible GTAp63 start codons were mutated independently, where ATG was changed into CTG. The resulting mutant GTAp63 plasmids GTAp63mutATGexU1 or GTAp63mutATGex1 and the wild-type GTAp63α plasmid were overexpressed in H1299 lung carcinoma cells which are p53-null and do not express detectable p63. The cell lysates together with lysats from control empty vector-transfected cells were subjected to SDS-PAGE analysis. Expression of the empty vector served as control. Co-expression of a GFP expression vector and immunodetection of GFP were performed to control for equal transfection efficiencies. The result of the immunostaining is shown in **figure 5.5 A**.

Expression of GTAp63α construct gave rise to two distinct p63 protein bands specifically recognized by the p63 4A4 antibody. Importantly, the protein with higher molecular weight (~ 85 kDA) was expressed to higher levels than the protein with lower molecular weight (~ 80 kDa). While the mutation of the first ATG in exon U1 of GTAp63 resulted in the high abundancy of the lower molecular weight band corresponding to TAp63, GTAp63 was the only detected isoform when the second ATG of exon 2 was mutated. Overexpression of the conventional TAp63 plasmid as control generated also two distinct protein bands corresponding to TA*p63 and TAp63 protein.

The result of the experiment suggested that both ATGs can be used for initiation of translation, but the ATG in exon U1 is the predominantly used initiation codon. Translation from the second start codon in exon 2 may be controlled by the upstream ATG.

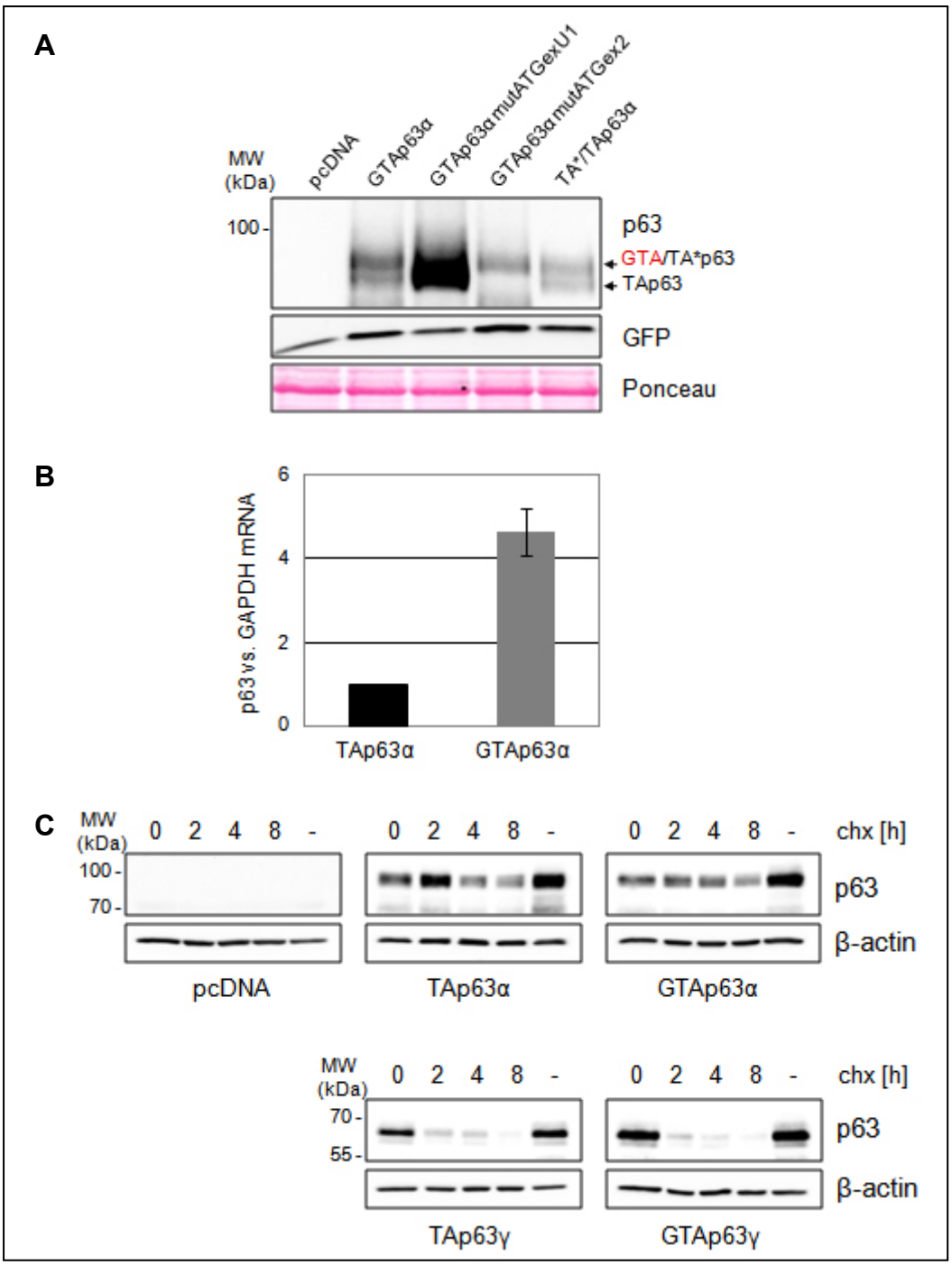

Figure 5.5: GTAp63 protein translation starts in exon U1

A. H1299 cells were transfected with pcDNA3 expression plasmids containing GTAp63 wt or mutant proteins in which the ATGs of exon U1 or exon 2 were mutated into CTG, or the conventional TAp63. Immunodetection of expressed p63 proteins transferred to a nitrocellulose membrane. The ATG of exon U1 is predominantly used as initiation codon generating the more abundant GTAp63 protein with higher molecular weight. The TAp63 protein was detected at lower molecular weight. Co-transfection of GFP as transfection control, Ponceau staining as loading control.

B. RT-PCR analysis from H1299 cells overexpressing GTAp63 or TAp63 under equal conditions. Levels of p63 mRNA were normalized to GAPDH. Mean values of p63 and standard errors from three independent experiments were shown. The normalized TAp63 mRNA was set to one.

C. H1299 cells were transfected as described above, followed by treatment with 100 µg/ml cycloheximide and the cell harvest at indicated times. SDS-PAGE analysis was performed. Detection of the p63 protein using the p63 4A4 mab resulted in no differences in protein stabilities. There was also no difference detectable in the stability of GTAp63 or TAp63 γ isoforms.

To note, when equal amounts of the plasmids containing either the full length GTAp63 or the full length TAp63 were transfected into H1299 cells, immunodetection of p63 showed that GTAp63 was expressed to much higher protein levels than TAp63 (data not shown). The difference in expression level could be due to increased transcription initiation or elongation, increased mRNA stability or increased protein stability of the GTAp63 isoform.
To investigate this further, we first determined the mRNA levels after the transfection of equal amounts of GTAp63 or TAp63 expression plasmids under the same conditions in H1299 cells. RNA was extracted and PCR amplification was performed with primers specific for exon 2 and 3. p63 mRNA was normalized to GAPDH mRNA. **Figure 5.5 B** shows the mean expression of p63 with standard errors from three independent experiments. GTAp63 mRNA was expressed to 5-fold higher levels than the conventional TAp63 suggesting higher mRNA stability of GTAp63.

Additionally, we also tested the protein stability of GTAp63 in comparison to TAp63. For this purpose the above mentioned expression plasmids were transfected into H1299 cells. To start from relatively equal levels of p63 protein the amount of transfected p63 plasmids was adjusted meaning that 4-fold more TAp63 DNA was used. 24 h after transfection cells were treated with a general inhibitor of translation, cycloheximide, at a final concentration of 100 µg/ml. Cells were harvested after 0, 2, 4 and 8 h and SDS-PAGE analysis was performed. Control cells were treated with the solvent DMSO for 8h.
This cycloheximide chase experiment did not result in any obvious difference in the protein stability of GTAp63α and TAp63α as roughly the same amount of protein could be detected even after 8 h of cycloheximide for both isoforms (**figure 5.5 C**). From this result it is hard to judge whether or not there is a difference in stability between GTAp63 and TAp63 in general since p63 α proteins are known to be very stable. So we repeated the whole experiment with the γ forms of p63 which do show a high protein turn over, probably making it possible to detect differences in GTAp63 and TAp63 protein stability. Both GTAp63γ and TAp63γ expression plasmids were transfected under equal conditions and cells were afterwards treated with cycloheximide as described above. Again, GTAp63γ did not show higher protein stability than the corresponding TA isoform.

Altogether, the data indicate that GTAp63 is expressed to higher levels in comparison to the conventional TAp63, at least partially due to increased mRNA amounts. But there might be some other contributing mechanisms, e.g. mechanisms that regulate translation initiation.

5.1.3 Expression of GTAp63 is predominantly found in testis

Next, we wanted to determine the expression of the newly identified GTAp63 across a variety of human tissues. Therefore, we used a panel of 20 human normal RNAs from Ambion to perform quantitative RT-PCR analysis.

Following the reverse transcription of 1 µg RNA per reaction cDNAs were amplified with primers detecting different portions of the p63 transcripts. GTAp63 was detected with the forward primer binding to exon U1 and the reverse primer binding to exon 2. The same reverse primer was also used for amplification of the conventional TAp63 but this time in combination with an exon 1 forward primer. The total amount of transactivating p63 mRNAs was analyzed with a primer pair corresponding to the exon 2 - exon 3 boundary. Normalized mRNA level were used to generate the graphs shown in **figure 5.6**.

While the conventional TAp63 isoform was detected in all included human tissues this was not true for GTAp63. Strikingly, only a few human tissues (cervix, lung, skeletal muscle, placenta, prostate, testis and trachea) showed detectable levels of this p63 mRNA. But only in the testis the GTAp63 form was highly abundant, meaning that it was ~ 500 - 1000-fold higher expressed than in the other, above mentioned tissues.

From this result we concluded that the GTAp63 expression is largely confined to testis in humans.

Of note, we were not able to detect GTAp63 in human ovarian tissue. This could be explained by two reasons. One reason might be the low amount of immature oocytes, which are thought to express TAp63, throughout the whole ovarian tissue. Secondly, the ovaries used for the generation of RNA sample of the panel, were from women in the age of 47 or 48, who probably do not possess a large number of immature follicle with oocytes anymore.

We then repeated the RT-PCR analysis additionally using RNA from young women (age of 23 and 27). Indeed, the sample of the 23 year-old woman showed detectable

GTAp63 (**figure 5.6**; ovary, age 23) but to a level which was still more than 600-fold lower as compared to testis.

This indicates that the GTAp63 expression in germ cells is restricted to the male gender.

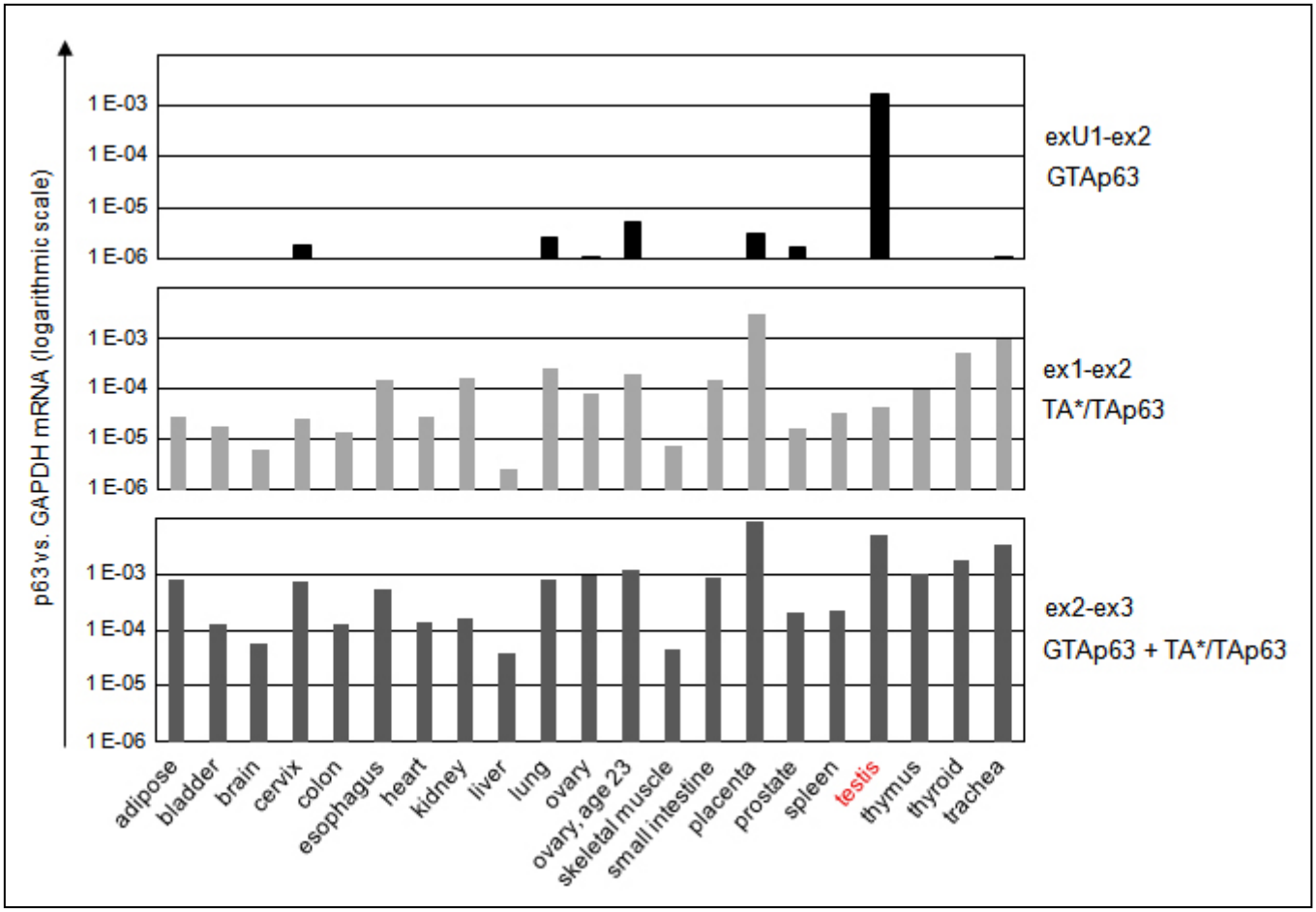

Figure 5.6: GTAp63 expression is largely confined to testis

Quantitative RT-PCR analysis performed from an array of normal human RNA. Primers were either specific for exon U1 – exon 2 (corresponding to GTAp63), for exon 1 – exon 2 (corresponding to conventional TAp63) or for exon 2 – exon 3 (both GTAp63 and TAp63). All p63 mRNA values were normalized to GAPDH. In testis (red label) GTAp63 was expressed up to ~1000-fold higher than in the tissues where it could be detected at all. Most human tissues showed no detectable GTAp63 mRNA but all expressed the conventional TAp63. The y-axis is shown in logarithmic scale.

5.2 GTAp63 is controlled by an endogenous retroviral LTR

5.2.1 TP63-associated LTR belongs to the ERV9 subfamily IX

Strikingly, the 5`portion of GTAp63 exon U1 corresponds to an endogenous retroviral long terminal repeat (LTR). The sequence of exon U1 was blasted against the human genome by using the BLAST N algorithm from the server of the National Center of Biomedicine Information (NCBI). We found that exon U1 is part of a solitary LTR of the endogenous retrovirus 9 (ERV9). The inset in **figure 5.1** shows the location of exon U1 in relation to the ERV9 LTR which is stably integrated in the human genome adjacent to the TP63 gene on the long arm of chromosome 3.

Retroviral LTRs are known to possess a promoter at the 3`end of the U3 region and the transcription initiation site at the 5` border of the R region 23-28 bp downstream of the TATA box (Temin, 1981) (**figure 5.7**). Indeed, sequence comparison revealed that transcription of exon U1 initiates 28 bp downstream of the TATA box of the ERV9 LTR U3 region (**figure 5.2**). This strongly suggests that the newly identified p63 isoforms are a result of ERV9 LTR-derived promoter activity.

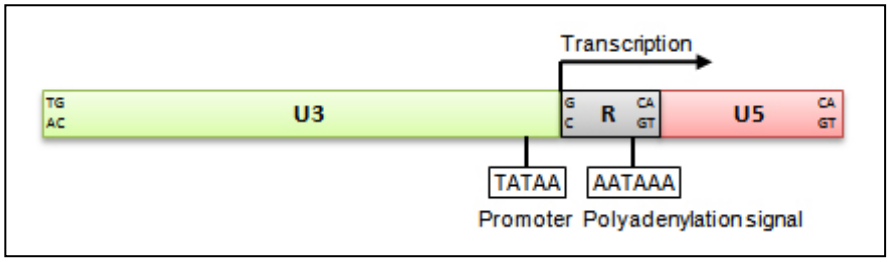

Figure 5.7: Structure of a retroviral Long Terminal Repeat (modified after Temin, 1981)
Any retroviral LTR consists of the unique regions U3 and U5 sandwiching the R region. The TATA box promoter in the U3 region initiates transcription directly at the border to the R region (black arrow), which contains a polyadenylation signal (AATAAA) 20 bp upstream of its 3`end. Conserved nucleotides in all three LTR regions are indicated.

The ERV9 family has been studied in the past by several groups. Importantly, previous paleogenomic analyses indicated that the integration of the ERV9 transposable elements into host genome happened relatively recently in primate evolution. Costas and Naveira established 14 subfamilies inside the ERV9 family of human endogenous retroviruses by performing multiple sequence alignment, followed by grouping of sequences according to shared nucleotide deletions and key

nucleotides in the most variable sites of alignment (Costas & Naveira, 2000). The ages of the subfamilies I – XIV were also estimated. The authors concluded that most of the subfamilies originated before gibbons separated from the higher apes, followed by the major expansion of ERV9 LTRs about 18 – 8 million years (MYr) ago until the split of gorillas, when it ceased down. The ERV9 stopped its spread through host genomes at the stage of the common ancestor of chimpanzees and humans about 6 MYr ago.

We tempted to investigate whether the integration of the ERV9 LTR into the vicinity of the TP63 gene was also a recent event in primate evolution. First, we compared the LTR sequence upstream of TP63 with the consensus sequences of the subfamilies I – XIV using the ClustalW algorithm (Thompson et al, 1994).

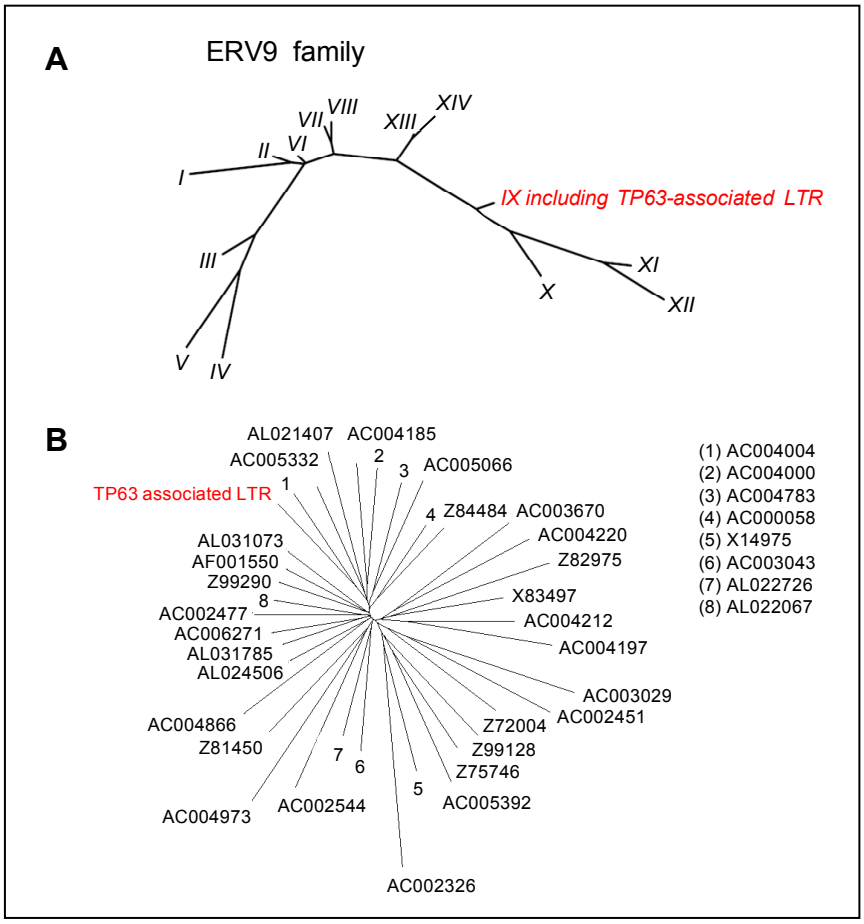

Figure 5.8: ERV9 LTR of TP63 belongs to ERV9 subfamily IX

A. The consensus sequences of ERV9 subfamilies I-XIV as described by Costas & Naveira were aligned using the Clustal W algorithm and a phylogenetic tree was generated (NJ method). Alignment of the TP63-associated LTR showed closest relation to subfamily IX (highlighted in red).

B. Phylogenetic reconstruction of the complete subfamily IX by the NJ method (ClustalW algorithm). The sequence of the TP63 ERV9 LTR is very similar to sequences of described subfamily members. Aligned sequences are designated by their GenBank accession numbers (Costas & Naveira, 2000).

The alignment revealed that the TP63-LTR belongs to the subfamily IX which also had been shown to be the predominant one among all subfamilies (Costas & Naveira, 2000). A phylogenetic tree generated with the neighbor joining (NJ) method and indicating the evolutionary distances between the ERV9 subfamilies is shown in **figure 5.8 A** (sequence alignment in **8.1**). Afterwards, all individual sequences inside the subfamily IX were retrieved by their GenBank accession number (depicted in **figure 5.8. B**). Multiple alignments of these sequences together with the sequence of the LTR upstream of TP63 (see appendix, **8.2**) generated a second phylogenetic tree (**figure 5.8 B**), where the phylogenetic distances between subfamily members are rather small.

We conclude that the TP63-associated ERV9 LTR is closely related to LTRs of the ERV9 subfamily IX.

5.2.2 Insertion of ERV9 LTR in the TP63 locus is specific to hominids

A previous study suggests that the ERV9 subfamily IX emerged around 18.7 million years ago and then underwent further spreading in host genomes until roughly 6 MYr ago (Costas & Naveira, 2000). This time period overlaps with a time in primate evolution when Old World monkeys had already branched off the New World monkeys and *Hylobatidae* began to diverge from higher apes until the common ancestor of chimpanzees and humans (Glazko & Nei, 2003).

We attempted to find out when the TP63-associated LTR had inserted into the TP63 locus. So we asked whether or not this LTR is also inserted upstream of TP63 in the genome of other primates. We used a PCR strategy to amplify different genomic regions of the ERV9 LTR and flanking sequences from an extended collection of genomic DNA from diverse primates. **Figure 5.9 A** represents a scheme of the human genomic region including TP63 exon U1 and the overlapping LTR. We performed 2 different PCRs. The first one amplified the LTR of exon U1 itself using primers that bind to the LTR (LTR forward) or to the 3`end of exon U1 (LTR reverse). The expected PCR fragment has a size of 215 bp. The result of this PCR is depicted in the upper panel of **figure 5.9 B**.

A PCR product of the expected size was detected in human (*Homo sapiens*), chimpanzee (*Pan troglodytes*), gorilla (*Gorilla gorilla*) and orangutan (*Pongo pygmaeus*) but neither in gibbon (Hylobates lar) nor in rhesus macaque (*Macaca*

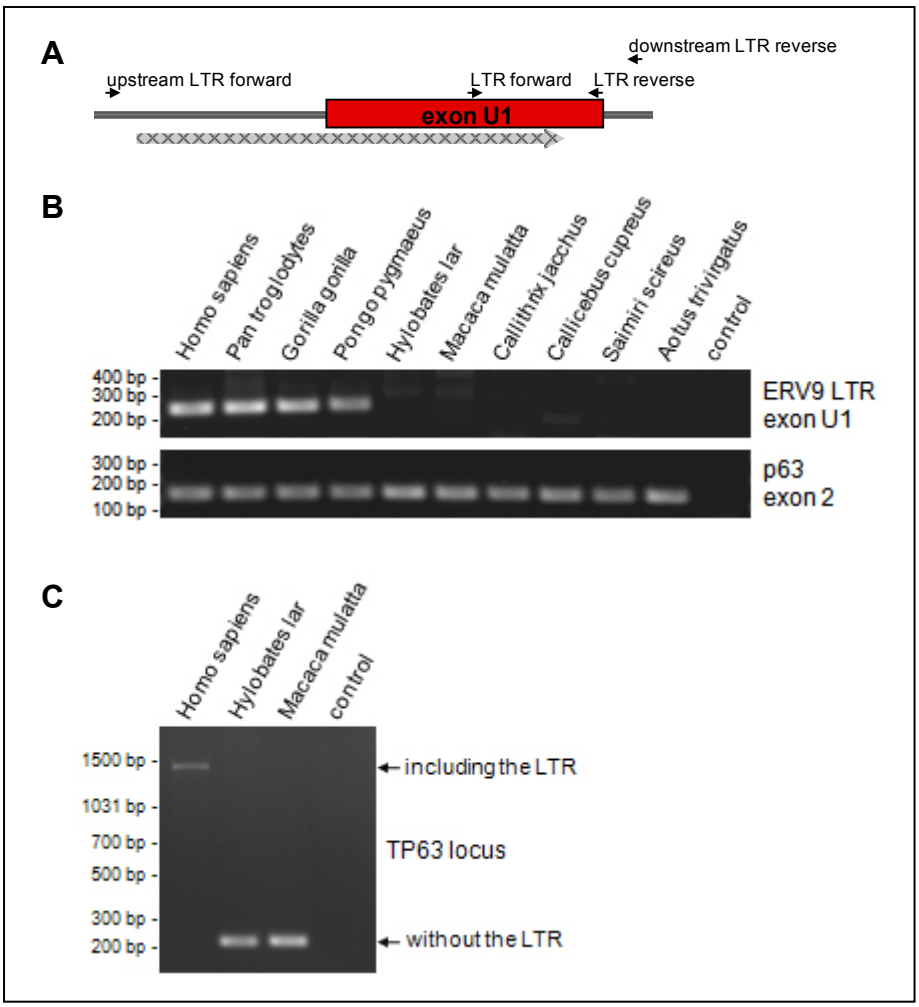

Figure 5.9: Insertion of ERV9 LTR into the TP63 locus in hominids

A. Schematic drawing of the human genomic region of chromosome 3 containg exon U1 of GTAp63 (red box) and the ERV9 LTR (grey arrow below). Indicated primers used to amplify genomic DNA from diverse primates either specifically bind to the LTR of exon U1 (LTR forward and reverse) or to sequences flanking the LTR.

B. PCR amplification of genomic DNA from diverse primates including humans, great apes and New World monkeys. PCR with primers binding to the LTR resulted in a specific product of 215 bp only in hominids (upper panel). Sequences of TP63 exon 2 were amplified in all tested species (lower panel). Control PCR reaction was performed without any template.

C. Amplification of genomic sequences spanning the LTR sequence at the TP63 locus using the upstream LTR forward and the downstream LTR reverse primer indicated in **A**. A long PCR product was generated from *Homo sapiens* indicative of the LTR integration into this part of genome. Amplification of genomic flanking sequences lacking the LTR sequence resulted in the short PCR product in *Hylobates lar* or *Macaca mulatta*. No product was observed in the water control.

mulatta) or all tested species of New World monkeys (*Callithrix jacchus*, *Callicebus cupreus*, *Saimiri scireus* and *Aotus trivirgatus*). The products of gorilla and orangutan were sequenced to confirm the specificity of the PCR also in these species. Control amplification of genomic sequences of TP63 exon 2 resulted in a specific PCR product of 123 bp in all tested species, only the water control generated no product at

all. This let us to the conclusion that the ERV9 LTR is integrated upstream of the p63 gene in the genome of higher primates from orangutan on. These primates including the humans belong to the family of hominids.

We also confirmed the latter result with a second PCR from genomic DNA of primates using a primer pair spanning the LTR at the TP63 locus. In order to design the primers we first compared the genomic sequence upstream of the human TP63 gene with the corresponding genomic sequence of the rhesus macaque (sequence was taken from the Ensembl genome browser website) and identified homologous sequences between the two species. Primers were then designed to bind specifically to the sequence upstream (forward PCR primer) or downstream of the LTR (reverse PCR primer) as shown in the schematic drawing in **figure 5.9 A**. The chosen PCR strategy should result in a long PCR product of ~1400 bp in humans and a short one of 215 bp in the macaque. Fortunately, PCR worked properly and we were able to detect the right fragments in *Homo sapiens* as well as in *Macaca mulatta*. As expected from the result in **figure 5.8 B** amplification of genomic DNA from *Hylobates* also generated the same small product as from *Macaca mulatta*, strongly indicating that the ERV9 LTR has not inserted into the region upstream of the gibbon`s TP63 gene.

Additionally, the PCR products from human, gibbon and macaque (**figure 5.9 B**) were sequenced. The alignment of the achieved sequences is depicted in **figure 5.10**. The numbering of aligned base pairs is shown on the right hand site of the figure. For space reasons nucleotides 121 – 1200 were removed which is indicated by the three vertical dotted lines. Highlighted in red letters is the sequence of the LTR that is inserted in humans. This LTR is flanked by CTAT sequences on both sites (**figure 5.10**). The gibbon sequence is homologous to the sequence of the macaque lacking the ERV9 LTR.

Moreover, available genome sequences further confirm that the LTR is unique to humans and great apes but absent in rhesus macaque and more distantly related mammals such as rodents (see appendix **8.3**).

Altogether, our obtained data suggest that the integration of the long terminal repeat of the endogenous retrovirus 9 upstream of the TP63 gene happened rather recently in primate evolution after gibbons had already branched off (~ 17 MYA) and before orangutans began to diverge. **Figure 5.11** summarizes this in an evolutionary tree.

Numbers in boxes indicate the estimated average times when species diverged from each other. A time scale is given at the bottom of the figure.

```
                    ....|....| ....|....| ....|....| ....|....| ....|....| ....|....|
Homo sapiens        TTGGGCATAT CCAGGACTAG AAATCCATAA GAAAACAGTA GATTGGAAAC TGAAAACACT 60
Hylobates lar       TTGGGCATAT CCAGGACTAG AAATCCGTAA GAAAACAGTA GATTGGAAAC TGAAAACACT
Macaca mulatta      TTGGGCATAT CCAGGACTAG AAATCCTTAA GAAAACAGTA GATTGGAAAC TGGAAACACT

Homo sapiens        ATTGAGAGGT GACAGCGTGC TGGCAGTCCT CACAGCCCTC GCTCGCTCTG GGCGCCTCCT 120
Hylobates lar       ---------- ---------- ---------- ---------- ---------- ----------
Macaca mulatta      ---------- ---------- ---------- ---------- ---------- ----------

        :                                       :                                   :

Homo sapiens        AGAGCTGTAA CACTCACCGC CAGGGTCCGC GGCTTCATTC TTGAAGTCAG AGAGACCAAG 1260
Hylobates lar       ---------- ---------- ---------- ---------- ---------- ----------
Macaca mulatta      ---------- ---------- ---------- ---------- ---------- ----------

Homo sapiens        AACCCACCAA TTCCGGACAC CCTATCAGAG ATTTTGAAAA CTATGAAGTG CTGGGAACAG 1320
Hylobates lar       ---------- ---------- ---ATCAGAG ATTTTAAAAA CTGTGAGGTG CTGGGAACAG
Macaca mulatta      ---------- ---------- ---GTCAGAG ATTTTAAAAA CTATGAAGTG CTAGAAACAG

Homo sapiens        AGAGACTGGA C---AGCCTT CACAAAGGTG GGGAAACCTT GGTAAGTACT CAG--TTTTC 1380
Hylobates lar       AGAGACTGGA GTTGAAGCTT CACAAAGGTG GGGAAACCTT GGTAAATACT CAGAGTTTTC
Macaca mulatta      AGAAATTGGA GTTGAAGCTT CACAAAGGCG GGGAAACCTT GGTAAATACT CAGAGTTTTC

Homo sapiens        AGTTGAAACC CAAGAAGATA AAAATCTAAA GGACCATGCA TTAAGAGTAA G
Hylobates lar       AGTTGAGATC CAAGAGGATA AAAATCTAAA GGACCATGCA TTAAGAGTAA G
Macaca mulatta      AGCTGAGACC CAAGAGGATA AAAATCTAAA GGACCATGCA TTAAGAGTAA G
```

Figure 5.10: LTR is missing in the TP63 locus of non-hominids

Genomic sequences of the TP63 locus from human and the non-hominid primates *Hylobates lar* and *Macaca mulatta* were aligned using the ClustalW algorithm (Thompson et al, 1994). The ERV9 LTR, shown in red, is not integrated in the primate`s genomes at the same position as it is in humans.

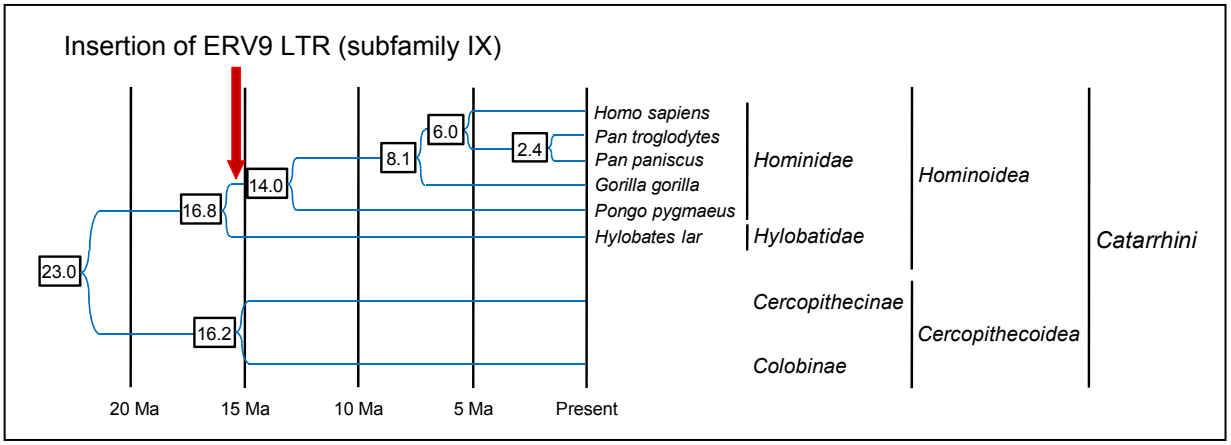

Figure 5.11: Insertion of ERV9 LTR into genomes of higher apes ~ 15 MYA

Evolutionary tree showing the timing of primate evolution and ERV9 LTR insertion adjacent to TP63 (red arrow). Numbers indicate the estimated averaged divergence times of lineages of primate species. Scheme was adapted from (Raaum et al, 2005).

From the obtained results we concluded that the TP63-associated LTR as a member of the ERV9 subfamily IX appeared in the genomes of higher primates around 15 million years ago. This retrotranspositional event is indicated in **figure 5.11** by the red arrow.

5.2.3 p63 is expressed to higher mRNA levels in humans

Next, we investigated whether the ERV9 LTR driven expression of p63 differs from the expression of p63 in species where the transcription of transactivating p63 isoforms is controlled by the TA-promoter upstream of TP63 exon 1.

Quantitative RT-PCR analysis was performed on testicular RNA originating from human, macaque or murine testicular tissue. Primers used for this analysis were degenerated to ensure proper binding also to the murine p63, and they amplify a product spanning the exon 2 - exon 3 boundary of p63 mRNAs. For normalization the PCR was also performed with degenerated primers for the housekeeping gene GAPDH. The normalized values of the mean p63 mRNA expression levels from three PCR reactions are shown in **figure 5.12**. Expression of testicular p63 mRNA is higher in humans than in mice or rhesus macaque.

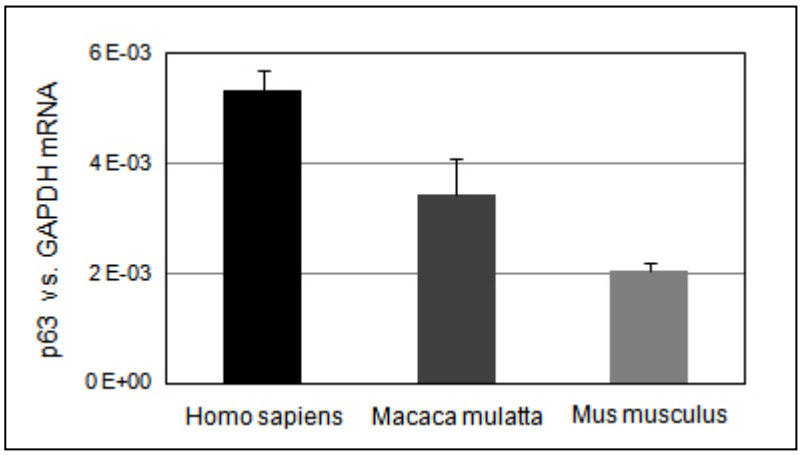

Figure 5.12: Increased expression of transactivating p63 in human testis
Quantitative RT-PCR analysis from the the testis of humans (*Homo sapiens*) and species of Old World monkeys (*Macaca mulatta*) or rodents (*Mus musculus*). Mean values of p63 mRNA normalized to the housekeeping gene GAPDH with standard error bars are shown. Triplicates were generated from one RNA sample each species.

In accordance with the unique expression of p63 under the ERV9 LTR promoter in humans, the higher expression of p63 in human testis suggests that the insertion of the ERV9 LTR upstream of TP63 enabled a more stringent surveillance of genomic stability, thus leading to a longer fertile life span of humans and great apes.

5.3 GTAp63 proteins is enriched in human spermatogonia

5.3.1 GTAp63 protein is detected in human testis tissue

Having found that the expression of GTAp63 transcripts is confined to testis we then addressed the protein expression of this newly identified p63 isoform in human testis. First, we performed SDS-PAGE analysis to detect endogenous GTAp63 protein in testicular tissue. Ready-to-use protein lysates from human normal tissues including liver, ovary and testis were bought from Amsbio. After blotting of proteins on a nitrocellulose membrane immunostaining of proteins with the monoclonal p63 4A4 antibody was done. The result of this staining is shown on the left side of **figure 5.13**. While we were not able to detect any p63 protein in liver and ovary, a single protein with a molecular weight around 85 kDa was detected in testis. The Ponceau staining of the nitrocellulose membrane that was performed prior to incubation with antibodies, indicated equal protein loading. Additionally, lysates of H1299 cells either transfected with GTAp63α or the empty pcDNA vector, were also subjected to SDS-PAGE, followed by detection of p63 protein with the 4A4 antibody. As it has been already described in chapter 5.1.2, the expression of the GTAp63α construct generated two distinct protein isoforms being GTAp63 and TAp63 (right side of **figure 5.13**). The detected endogenous testicular p63 protein corresponds to the one with higher molecular weight. Staining of control transfected H1299 cells resulted only in unspecific bands that are marked in the figure by an asterisk.

From the results of the experiment we concluded that the newly identified GTAp63 isoform is expressed to relatively high protein levels as the sole p63 species in human testis. As already mentioned above, there was no p63 protein at all detectable in the tested human ovary sample. But since we do not know the age of the woman donating this ovary tissue and since the mass of immature follicles compared to other cell types inside an ovary is reasonably small, we cannot exclude that GTAp63 protein might be also expressed in the female gonad.

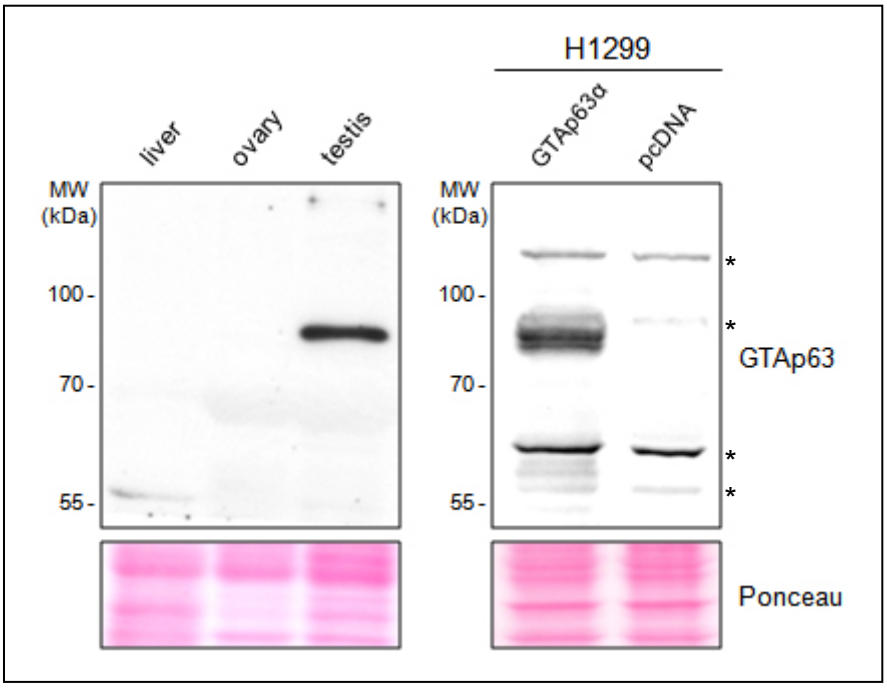

Figure 5.13: GTAp63 protein as the sole p63 species in human testis
Protein lysates from human tissues (liver, ovary and testis) were blotted on nitrocellulose and immunostained with the p63 4A4 mab (left side). The detected testicular p63 protein species was compared to GTAp63α exogenously expressed in H1299 cells (right side). pcDNA empty vector was expressed as control. The Ponceau staining indicates equal loading of proteins. Unspecific protein bands are marked by an asterisk.

5.3.2 p63 proteins are differentially distributed in testicular cells of human or mouse origin

In agreement with the testis-specific GTAp63 mRNA expression we showed the major expression of GTAp63 protein in human testicular tissue by immunoblot analysis.

In the following we determined the expression pattern of this novel p63 isoform throughout the spermatogenic epithelium lining the seminiferous tubules of testis. To delineate the specific testicular cell type expressing the GTAp63 protein, we performed immunohistochemistry analyses. All immunostainings of human testicular tissue sections were done in collaboration with the group of Ute Moll in Stonybrook, USA.

Sections of several paraformaldehyde-fixed human testicles were stained with various p63 antibodies and counterstained with hematoxylin. **Figure 5.14 A** shows the staining of a representative seminiferous tubule with the polyclonal p63 #9424

antibody as one example. p63 positivity is indicated by the brown nuclear staining of cells. Very interestingly, p63 protein was highly expressed in testicular precursor germ cells of the spermatogenic epithelium lining human seminiferous tubules. Specifically, basal diploid spermatogonia, which are designated in the figure by an arrowhead, exhibited the strongest staining. In addition p63 was also expressed in germ cells undergoing meiosis. Suprabasal spermatocytes, marked by a double arrow head, and round spermatids showed weak nuclear positivity for p63. In contrast, luminal haploid spermatozoa failed to stain positive. Hence, we observed a p63 gradient across the seminiferous epithelium. Cells loose p63 expression as they undergo maturation. This is compatible with a role of p63 in stem or precursor cells of the male germ line.

Th expression of p63 isoforms in murine testis has been controversely discussed. While some groups were able to detect p63 in the testis of rodents (Hayashi et al, 2004; Nakamuta & Kobayashi, 2004), Suh et al. suggested that TAp63 is not expressed in murine testis (Suh et al, 2006). For this reason we examined the expression of p63 protein across the epithelium of murine seminiferous tubules. A four month-old mouse of the SV129 background was sacrificed and its testicles prepared for immunohistochemistry. After fixation of the tissue in paraformaldehyde overnight it was cut into 5 µm thin sections. Multiple sections were immunostained with the p63 monoclonal 4A4 antibody. A representative staining of murine seminiferous tubules is depicted in **figure 5.14 B**.

We detected p63 protein also in the murine seminiferous epithelium. However, we revealed a difference in the distribution of p63 across the murine *vs.* human epithelium. While in humans p63 is predominantly detected in diploid basal spermatogonia, p63 staining showed maximum intensity in suprabasal meiotic spermatocytes (double arrowheads) in the murine seminiferous epithelium. Here, cells of the basal epithelial layer (arrowheads) mainly stained weakly if at all positive and elongating haploid spermatids (St) remained negative for p63. As a control a section from the same murine testis was additionally stained under the same conditions leaving out the primary antibody. We then observed no positive staining of testicular germ cells, proving that the positive staining of the germ cells was not due to cross reactivity of the secondary antibody with these cells (**figure 5.14 C**).

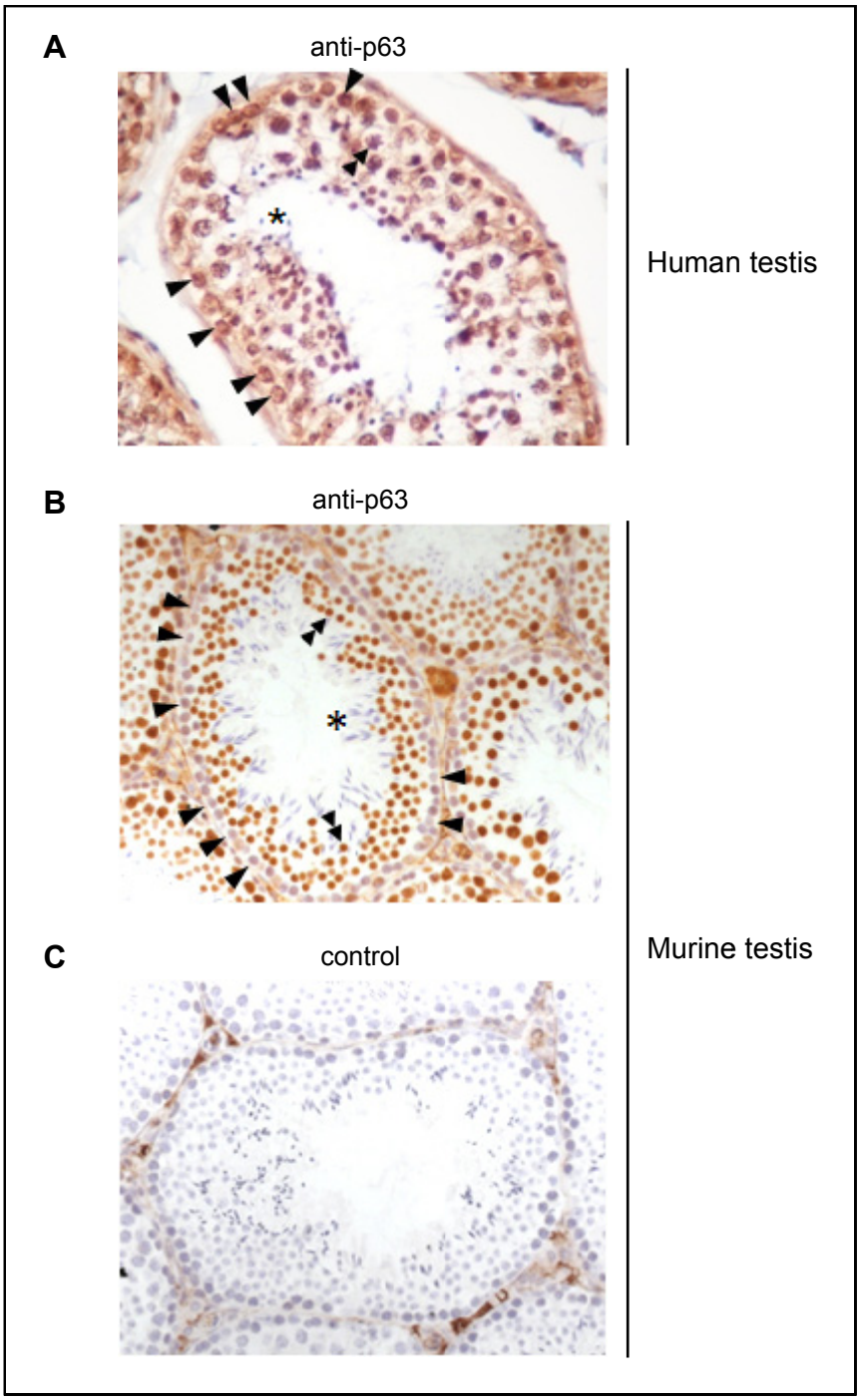

Figure 5.14: Distribution of p63 proteins in human and murine testicular tissue

A. Human testicular tissue from 39 year-old donor was immunostained with the polyclonal p63 #9424 antibody. Representative picture of diverse immunohistochemistry analyses from human normal tissue. Single arrowheads are indicative of diploid spermatogonia while primary spermatocytes undergoing meiosis are marked by double arrowheads. St, haploid spermatids.

B. Testicular tissue from a 4 month old SV129 mouse was fixed, sectioned and immunostained with the monoclonal p63 antibody 4A4. Here, basal spermatogonia revealed only a weak signal (single arrowheads), while the maximum of staining intensity was shifted to suprabasal spermatocytes (double arrowheads). Nuclei appeared blue after counterstaining with hematoxylin. St, spermatids.

C. The same testicular tissue that was used for p63 immunodetection (**B.**) was control stained under the same conditions but leaving out the primary antibody proving specificity of the p63 immunohistochemistry. Hematoxylin-counterstaining of tissue section.

Altogether, the findings from immunohistochemistry analyses indicate that the p63 protein is expressed both in human and murine testis but is differentially distributed in human *vs.* murine seminiferous epithelia. It is tempting to speculate that the ERV9 LTR insertion in hominids shifted p63 expression in favor of diploid spermatogonia being the true germ stem cells. Thereby, long term protection of the male germline could be ensured in long-lived species.

5.4 GTAp63 induces apoptosis upon genotoxic stress

Until now we identified a novel p63 isoform termed GTAp63 which is predominantly expressed in testis being mainly confined to the nuclei of basal diploid germ cells. This might suggest that GTAp63 might be a regulator of proliferation and survival of these male precursor germ cells.

The following chapter deals with the question whether GTAp63 functions in the regulation of cell proliferation, survival and/or apoptosis upon treatment of cells with genotoxic agents.

5.4.1 Long-term survival of stress induced cells is affected by GTAp63

The transactivating isoforms of p63 have been shown to induce apoptosis (Gressner et al, 2005; Helton et al, 2007). To address the capability of GTAp63 to induce apoptosis, we generated stable cells overexpressing GTAp63. For the generation of stable transfectants we chose the lung carcinoma cell line H1299, which is p53-null and easy to transfect. Cells were transfected with several GTAp63α constructs cloned right behind the internal ribosomal entry site (IRES) of the pIRES neo (Invitrogen) vector backbone. This strategy allowed simultaneous expression of GTAp63 proteins together with a neomycin resistence from bicistronic transcripts. Neomycin-selected cells also expressed the protein of interest. All experiments were additionally performed with H1299 cells being stably tranfected with the empty pIRES vector to control for side effects as a consequence of the stable transfection itself.

We also introduced different mutations into the wild-type GTAp63α isoform by QuikChange mutagenesis (**4.3.3**). **Figure 5.15** represents a schematic drawing of the GTAp63α protein with its distinct protein domains including the central DNA-binding

domain (DBD), the oligomerization domain (oligo) and the Sterile Alpha Motif (Schlereth et al). Introduced mutations are indicated by vertical red lines. The cystein at position 306 is located in the DNA-binding domain (DBD) and was identified to be one of the residues indispensable for binding of p63 to the DNA of its cognate target gene promoters (Celli et al, 1999). Thus, DNA-binding of GTAp63 is disrupted in the C306R mutant. Another introduced point mutations changed the aspartate at position 497 into an alanin residue, generating the D497A mutant. Recently it has been shown that upon DNA-damage induction p63 is cleaved by activated caspases at a specific caspase cleavage site resulting in a cleaved p63 fragment lacking the Sterile Alpha Motif and the Post-SAM domain. This aminoterminal p63 protein then functions in amplifying the damage-induced apoptosis (Sayan et al, 2007).

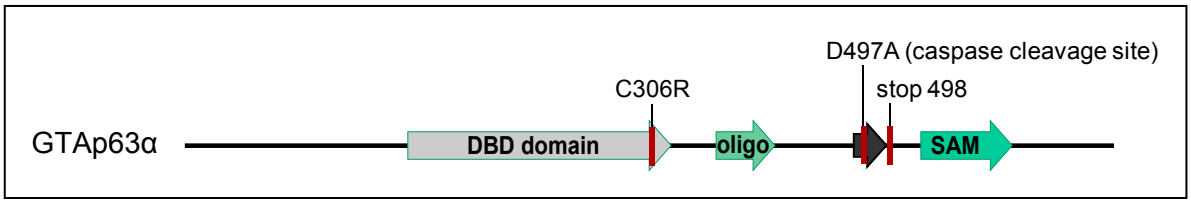

Figure 5.15: Mutant GTAp63 proteins
Schematic drawing of the GTAp63α domain structure including the DNA-binding domain (DBD), the oligomerization domain (oligo) and the Sterile Alpha Motif (Schlereth et al). Point mutation introduced into the GTAp63α construct for functional analyses are indicated by red lines. Numbering of the mutated positions refers to conventional TAp63 starting from the ATG in exon 2. Mutation of the DBD at position 306 disrupts DNA-binding of p63 and mutation of the aspartate at position 497 destroys the caspase cleavage site (dark grey arrow) whereas the introduced stop codon at position 498 results in a truncated aminoterminal GTAp63 protein.

We then generated stable transfectants of H1299 cells expressing either the GTAp63 wt protein or mutants described above or the empty vector. Since the obtained stable cell lines did not show any obvious differences in their ability to grow in culture, we assume that in the absence of any genotoxic stress, GTAp63 remains neutral.
Next, we addressed whether the expression of GTAp63α enhances apoptosis of cells upon induction with genotoxic stress. For this purpose the stable cells were treated with the chemotherapeutic agent cisplatin (cis-diaminodichloroplatin, cDDP). Following the cellular uptake of cisplatin, the chloride ions of the molecule are exchanged to hydroxy groups, generating reactive platins that cross-link DNA molecules (Alderden et al, 2006).

We determined the long-term survival of cDDP-treated stable transfectants by performing a clonogenicity assay (**figure 5.16**). In brief, 24 h after treatment of cells with 10 µM cisplatin the drug was removed and cells were incubated for further seven days. Afterwards we analyzed the area covered by the surviving cell clones upon either drug induction or control DMSO treament. For each stable cell line the percentage of confluence was generated by calculating the ratio between the covered area of the cisplatin-treated and the control treated sample (**figure 5.16 B**). The results of two independent experiments are shown as dual columns.

Importantly, only a few cells expressing GTAp63 wt survived the cisplatin treatment on long-term as indicated by the low percentage of confluence. This prominant decrease in the number of long-term survivors was not seen when either DNA-binding or caspase-cleavage of GTAp63 was abolished in the C306R or D497A mutant, respectively.

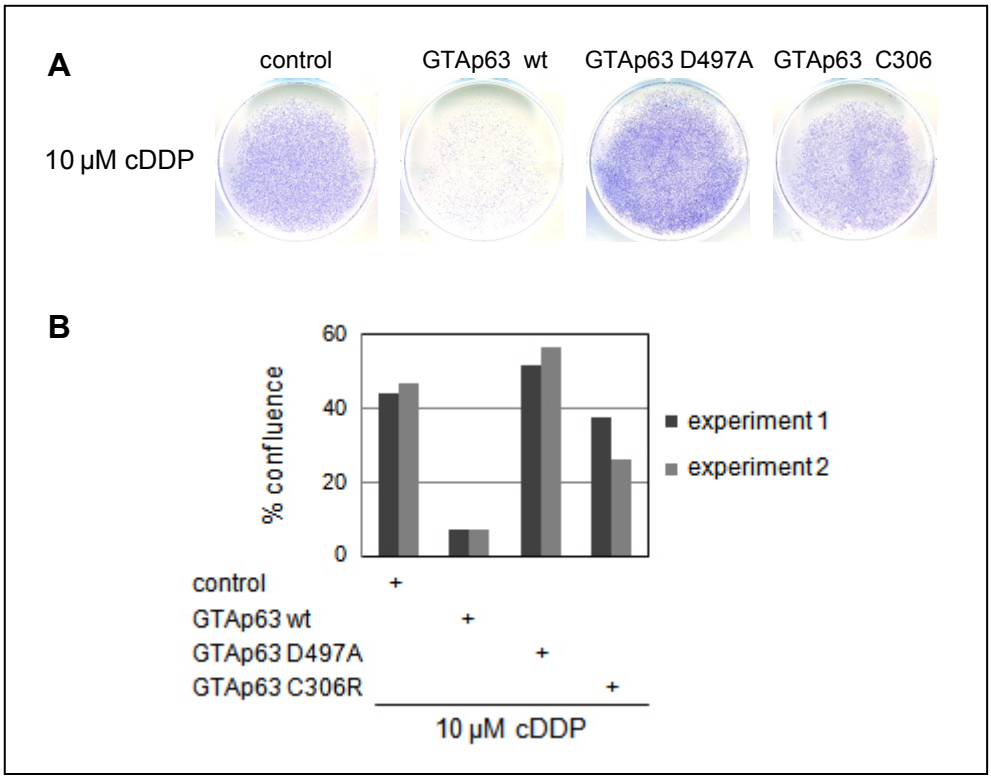

Figure 5.16: GTAp63 decreases long-term survival

A. H1299 cells stably expressing GTAp63 wt protein or its mutants D497A or C306R were treated with 10 µM cisplatin (cDDP) for 24h. After the drug removal cells were cultured for seven days before grown colonies were fixed and stained with crystal violet. Treatment of H1299 cells stably transfected with the empty pIRES neo vector served as control.

B. Quantification of areas covered by cell clones that survived the cisplatin treatment described in A. Percentages reflect the ratios of cDDP-treated *vs.* control treated cells. Results from two independent experiments are shown as dual columns.

The result let us to the assumption that GTAp63 is able to enhance the cisplatin-induced apoptosis.

Our result is in agreement with the published data from Sayan *et al.* (Sayan et al, 2007). They could show that upon DNA-damage signaling caspases become activated, which then cleave off the transcription-inhibitory domain of p63, generating an amino terminal p63 fragment with the ability to augment the damage-induced apoptosis.

In order to reproduce previous results, we treated cells stably overexpressing GTAp63 wt or mutants C306R and D497A or the empty vector with either 10 or 30 µM cisplatin for 24h. Control treatment was performed with the solvent DMSO. Cell lysates were loaded onto SDS gels and Western blot analysis was performed (**figure 5.17**). The full length GTAp63α protein was detected in all cells expressing wt or mutant p63. The immunodetection with the p63 4A4 monoclonal antibody revealed a second p63 protein with a molecular weight of around 60 kDa. This smaller p63 protein was only detected in cells expressing the GTAp63 wt protein or the DBD-mutant after treatment with cisplatin. Also, the higher dose of 30 µM cDDP let to increased levels of the lower p63 band that probably represents the caspase-cleaved aminoterminal p63 fragment. As expected, mutation of the caspase-cleavage site prevented the detection of this truncated p63 protein.

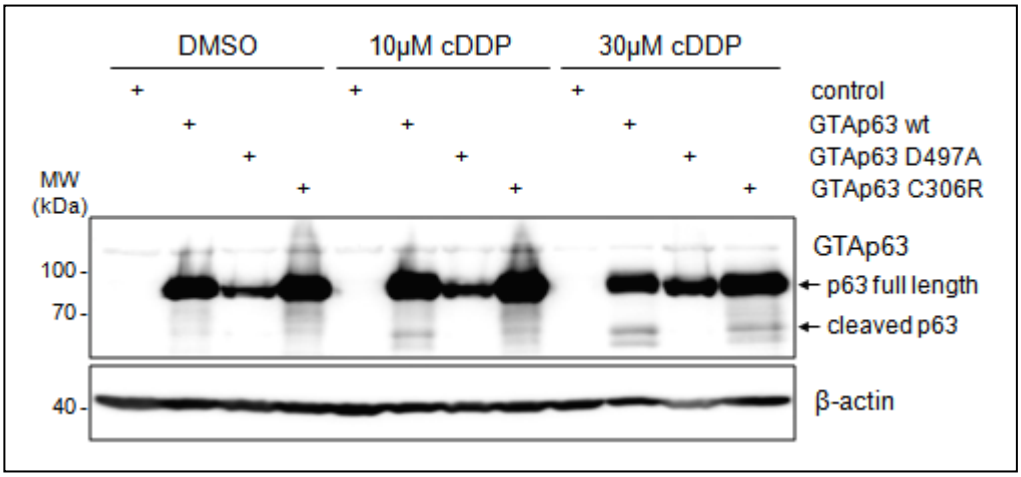

Figure 5.17: Cispaltin induces caspase-cleavage of GTAp63
Stable H1299 transfectants expressing either empty vector or GTAp63 wt or its mutant forms were treated with 10 or 30 µM cisplatin or the solvent DMSO for 24h. Protein lysates were subjected to SDS-PAGE analyses, followed by immunostaining of the nitrocellulose with the monoclonal p63 4A4 antibody. Besides the full length GTAp63 a smaller p63 protein was detected which corresponds in its size to the caspase-cleaved p63 fragment described by Sayan *et al.* The beta-actin staining indicates equal protein loading.

Taken together, the results strongly suggest that upon cisplatin-induced DNA damage GTAp63 is cleaved at its carboxy terminal region by activated caspases, resulting in a truncated amino terminal p63 protein. Further, we could also confirm that the aspartate residue at position 497 is at least necessary for the caspase-cleavage which also seems to be dose-dependent.

5.4.2 Caspase-cleaved GTAp63 amplifies apoptotic mechanisms

Next, we wanted to examine the effect of GTAp63 on short-term apoptosis of cells induced by genotoxic stress.

We used the same four stably transfected H1299 cell lines that were already described above. This time we performed flow cytometric analyses of the cells treated with DMSO or 10 µM cisplatin. After incubation of the four different cell lines with the chemotherapeutic for 24 h, cells were stained with sulforhodamine-labeled DEVD, a caspase inhibitor specifically binding to the active sites of effector caspases 3 and 7. Since the inhibitor peptide is covalently linked to the activated caspases by a fluoromethyl ketone group (Guava MultiCaspase reagent) this assay can be used to determine the number of activated caspase enzymes present in a cell. Cells were additionally counterstained with the cell-impermanent dye 7-amino actinomycin (7-AAD). Only cells that have lost their membrane integrity, i.e. cells in later stages of apoptosis and dead or necrotic cells, can be permeated by this dye.

After the measurement of fluorescence signals from the stress-induced stable cells by flow cytometry, dot plots were generated from the raw data (**figure 5.18 A**). Healthy and early apoptotic cells are shown in red. Cells that stained positive for activated caspases 3/7 are indicated by the blue and green color.

Those cells can be further subdivided into 7-AAD-negative mid-stage apoptotic and double positive late-stage apoptotic cells. The percentages of the last two cell populations are displayed in the dot plots.

As it can be seen in **figure 5.18**, GTAp63 wt cells had an increased amount of apoptotic cells after the initiation of apoptosis by cisplatin. While up to 40% of the cells expressing the GTAp63 wt protein were positive for active effector caspases, cells expressing mutants of GTAp63 or the empty vector showed in only up to 20% of apoptosis (**figure 5.18 B**). Without the addition of cisplatin we detected no obvious

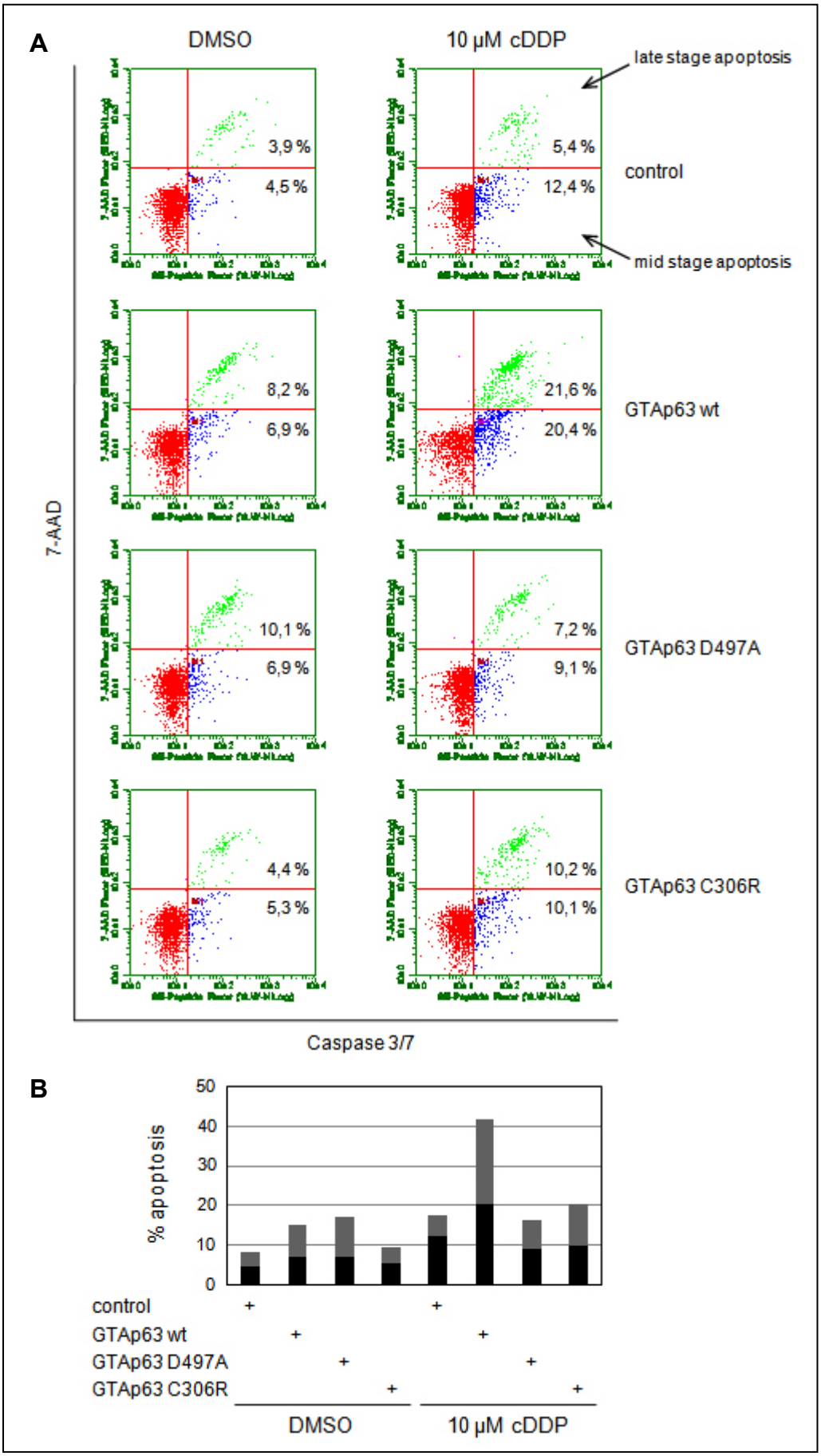

Figure 5.18: GTAp63 enhances DNA damage-induced apoptosis

differences in the apoptotic populations of the four cell lines, indicating that upon DNA damage induction GTAp63 enhances apoptosis after being cleaved by initially activated caspases.

To mimic the generation of the caspase-cleaved p63 we constructed a third GTAp63 mutant, termed GTAp63 stop498, where the introduction of a stop codon immediately after the aspartate residue used for enzymatic cleavage, results in the expression of an aminoterminal p63 fragment lacking the carboxyterminal SAM and Post-SAM domain (**figure 5.15**).

H1299 cells were transfected with pIRES plasmids containing GTAp63 wt, DBD-mutant C306R, caspase-cleavage mutant D497A or the new GTAp63 stop498 mutant. After selection of transfected cells with neomycin for seven days we stained cells with crystal violet to quantify the area that was covered by the grown cells. For statistics the experiment was performed three times in total. For each experiment we calculated the ratio of areas covered by each of the GTAp63-expressing cells *vs.* control cells transfected with the empty vector. The resulting mean values of these ratios and standard deviations from the three independent experiments are displayed in **figure 5.19**. This figure also includes one representative picture of scanned cell culture dishes for each transfection.

Figure 5.18: GTAp63 enhances DNA damage-induced apoptosis (continued)

A. H1299 cells stably transfected with GTAp63 wt or its mutants or empty vector as control, were treated with cDDP or DMSO for 24h. Fractions of apoptotic cells were determined by staining of activated caspases 3/7 with fluorescently labeled DEVD, followed by flow cytometric measurement. Counterstaining with 7-amino actinomycin (7-AAD) revealed membrane disintegration. Dot plots were generated by plotting the SR-fluorescence *vs.* 7-AAD fluorescence. Analyzed cells were divided into healthy/early apoptotic cells (lower left, red), mid-stage apoptotic cells (lower right, blue), late-stage apoptotic cells (upper right, green) and necrotic cells (upper left, pink). Percentages of caspase 3/7 positive cells (mid- and late-stage apoptotic cells) are shown.

B. Quantification of the fraction of apoptotic cells from figure A. The percentages of control, GTAp63 wt or mutant cells in mid-stage apoptosis are shown as black bars, while grey bars reflect the percentages of cells in the later stage of apoptosis staining also positive for 7-AAD.

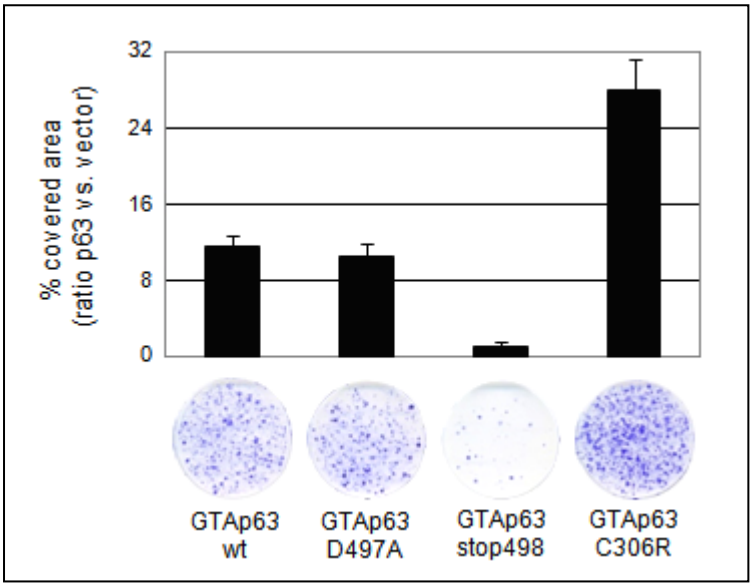

Figure 5.19: Expression of truncated GTAp63 suppresses clonogenic cell survival
Clonogenic assay of H1299 constitutively overexpressing GTAp63 wt protein or indicated mutants. The ratios of quantified areas covered by cells upon transfection of each GTAp63 expression plasmid *vs* empty vector is displayed as means and standard deviations from three independent experiments. *Bottom,* For each transfection one representative picture of stained cell clones is shown.

Indeed, constitutive overexpression of the truncated GTAp63 strongly suppressed clonogenic survival, as indicated by the very few grown cell clones covering less than 2% of the area covered by control cells. Of note, we were not able to culture the stable transfectants of GTAp63 stop498 on long-term as we did for all other transfectants, suggesting that the constitutive expression of the aminoterminal GTAp63 fragment is toxic to cells, probably leading to apoptosis.

5.4.3 Genotoxic stress induces proapoptotic p63 target genes

Having found that GTAp63 is able to amplify apoptotic signaling cascades initiated by genotoxic stress, we aimed to investigate the mechanisms by which GTAp63 enhances apoptosis.

Since p63 is a transcription factor with the ability to activate p53-responsive genes, we next assessed whether GTAp63 is capable of transactivating proapoptotic target genes upon initial cisplatin induction.

For this purpose, we again used the stable H1299 cells expressing either the empty vector as control or one of the three GTAp63 proteins (wt, D497A or C306R). After

treatment of cells with 10 µM cisplatin cells were harvested for RNA isolation, and quantitative RT-PCR analysis was performed to determine the level of known p53/p63-responsive genes. The results of at least three independent experiments are displayed as mean values and standard deviations in **figure 5.20**.

We quantified mRNA expression level of the apoptotic genes PUMA/BBC3, Noxa/PMAIP1 and CD95L/TNF6SF6 and of the cell cycle arrest genes p21/CDKN1A and GADD45A. The expression levels of all targets were normalized to mRNA level of the housekeeping gene GAPDH, and the values of DMSO treated control cells were set to one.

The overexpression of GTAp63 wt in cells treated with DMSO caused only little changes in the expression levels of p53 target genes. However, treatment of cells with cDDP let to a markedly increase in the expression of proapoptotic targets PUMA, Noxa and CD95L as a consequence of GTAp63 wt protein expression. Though we already detected slightly higher amounts of CD95L mRNA in normal growing GTAp63 expressing cells *vs.* control cells, CD95L mRNA level were further increased after cisplatin treatment. Upon the treatment we noticed a three-fold higher expression of CD95L mRNA in cells stably transfected with GTAp63 in comparison to control cells.

The ability to selectively transactivate proapoptotic target genes was only seen in cells expressing the wild-type GTAp63 protein. Specific loss-of-function point mutations within the DNA-binding domain (C306R) or the caspase-cleavage site (D497A) abolished this transactivation ability (**figure 5.20**). In contrast, upregulation of tested cell cycle regulating genes p21/CDKN1A and GADD45A upon cisplatin showed no dependency on GTAp63 since the p21 mRNA level of cDDP-treated cell expressing wild-type GTAp63 were only ~ 1.1-fold higher than the p21 mRNA level of treated control cells.

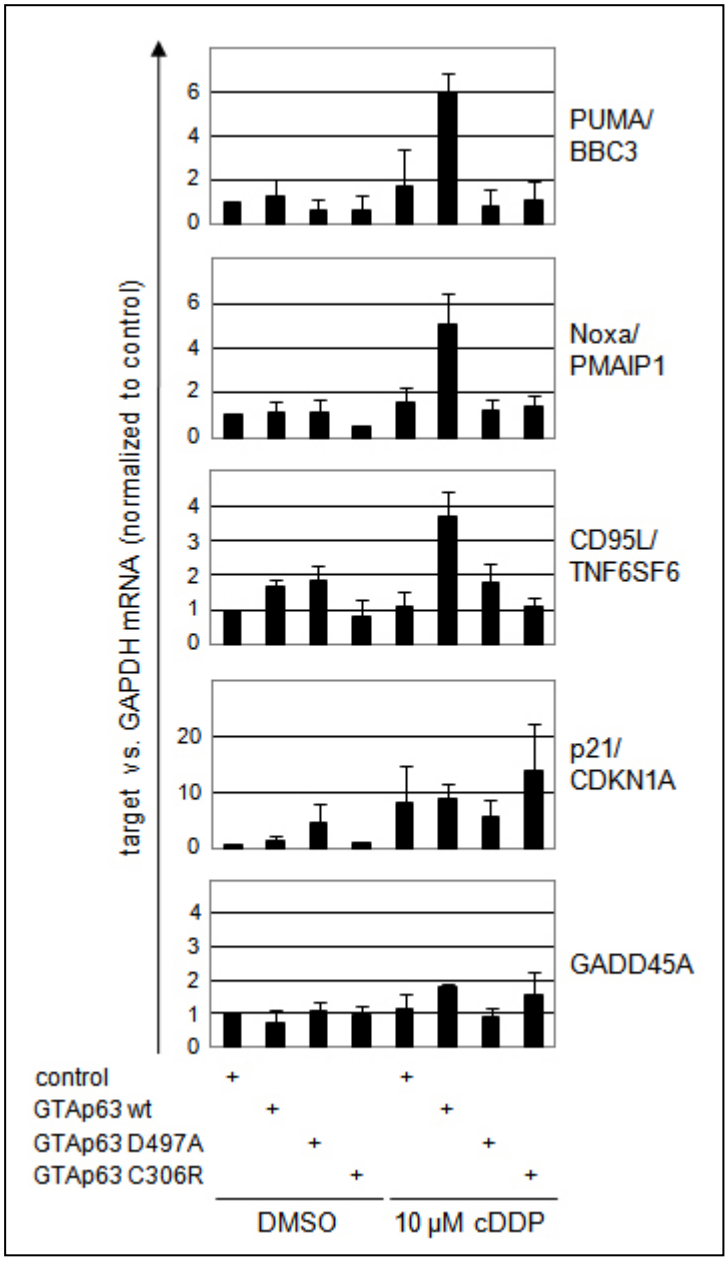

Figure 5.20: Transactivation of apoptotic target genes

H1299 cells stably transfected to express wild-type GTAp63 or mutants D497A or C306R were treated with 10 µM cDDP or DMSO for 24h. The expression of p53-responsive target genes was analyzed by RT-PCR. Only apoptotic target genes (PUMA, Noxa, CD95L) are activated in wild-type GTAp63- expressing cells, while GTAp63 had no effect on cell cycle regulating targets (p21 and GADD45A).

5.5 GTAp63 associates with mitochondria

5.5.1 GTAp63-enhanced apoptosis is partially transcription-independent

The p53 protein is able to induce apoptosis via transcriptional activation of proapoptotic target genes upon stress signals. However, p53 has been additionally shown to lead to apoptosis through direct protein-protein interaction at mitochondria (Dumont et al, 2003; Mihara et al, 2003).

Since it is not proven yet that p63 can act in a similar fashion, we first tested whether the germ cell-associated TAp63 is capable to augment stress-induced apoptosis even when transcription is blocked. Actinimycin D (act D), an inhibitor of *de-novo* RNA synthesis, was used at a final concentration of 4 µM to inhibit transcription.

Stable H1299 cells transfected to express wild-type GTAp63 or empty vector as control were treated with either 30 µM cisplatin or 4 µM actinomycin D alone, or with the combination of both drugs. As a control we also treated both cells with the solvent DMSO under the same conditions. Cell death was then assessed by staining cells with propidium iodide and measurement of the cellular DNA content by flow cytometry. We analyzed the percentage of cells with subG1 DNA content, which is indicative for dead cells.

Figure 5.21 displays the mean percentages of cells in subG1 and standard deviations from three independent experiments. The raw data from one of the three experiments are shown as histograms below the quantification; the percentages of subG1 shoulders, marked in blue, are indicated (**figure 5.21 B**).

We were able to confirm that pre-initiated apoptosis is augmented in the presence of wild-type GTAp63. In comparison to vector-transfected control cells the percentage of subG1 cells is roughly 14-fold higher in the GTAp63-expressing cells. When we additionally treated cells with the transcription inhibitor actinomycin D, as depicted in the last two columns in **figure 5.21**, we still could see a clear increase in the number of cells with subG1 DNA content in the samples where wild-type GTAp63 was stably expressed, as compared to control cells.

We concluded that indeed, GTAp63-mediated cell death can not solely rely on the transcriptional activation of proapoptotic genes.

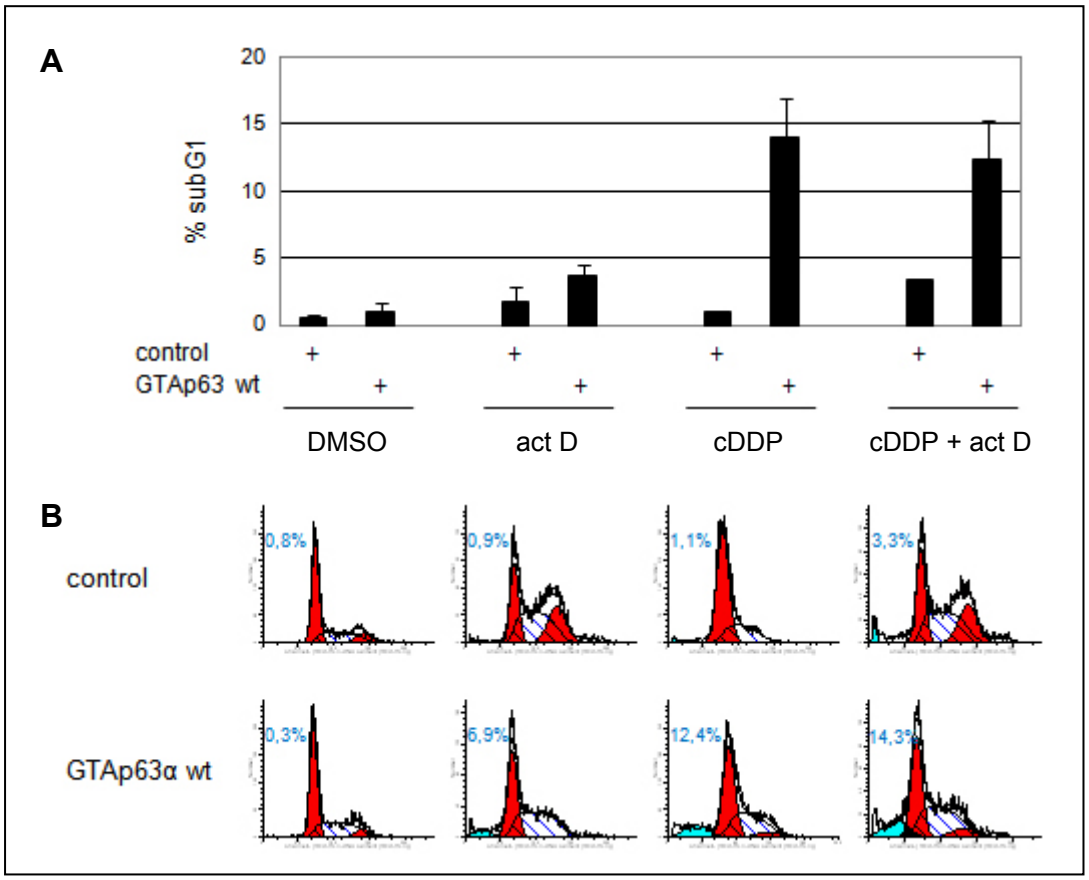

Figure 5.21: Transcription inhibition does not abolish GTAp63-enhanced apoptosis
A. H1299 cells stably expressing wild-type GTAp63 or the pIRES vector backbone (control) were treated with 30 µM cisplatin and/or the inhibitor of transcription actinomycin D (act D; 4 µM). Cell death was assayed by propidium iodide staining and flow cytometry analysis. The apoptotic cell population is represented by the subG1 shoulder of cell cycle profiles. Mean values and standard deviations from three independent experiments are displayed. The percentage of DMSO-treated control cells being in subG1 was set to one.
B. Raw data from one of the three experiments described in A. Histograms display cell cycle profiles of H1299 cells stably transfected with empty vector (control) or wild-type GTAp63, treated with the indicated drugs above. subG1 shoulders with corresponding percentages of dead cells are marked in blue.

5.5.2 Cleaved GTAp63 is enriched at mitochondria

The data from the last result suggest the existence of transcription-independent mechanisms contributing to the augmentation of apoptosis by GTAp63.

We speculated that, in analogy to p53, caspase-cleaved GTAp63 might locate to mitochondria to activate the intrinsic apoptotic pathway.

To test the hypothesis we performed cell fractionation experiments to purify mitochondria. First, H1299 cell stably transfected to express either wild-type GTAp63α or the DNA-binding mutant C306R were treated with 30 µM cisplatin or

DMSO alone for 24 h. Afterwards cells were harvested and lysed by dounce homogenization. Mitochondria were isolated using a sucrose gradient and ultracentrifugation. The highly purified mitochondria were then lysed and subjected to SDS-PAGE, followed by immunodetection of p63 using the monoclonal 4A4 antibody (**figure 5.22 A**). In addition to the mitochondria we also took control samples at each step of the purification procedure, which were also loaded onto SDS-PAGE. Immunodetection of proteins of crude lysates is depicted in **figure 5.22 A**; the blots from the nuclear and the cytosol fractions are not shown.

Upon cisplatin induction we repeatedly detected two different protein forms of GTAp63, the major one being the full length α-isoform with a molecular weight of ~ 85 kDA (see **figure 5.5**), and the other one being the aminoterminal p63 fragment that can be clearly seen in the longer exposures of p63 immunostaining (**figure 5.22 A**). Both p63 protein species were also detected in purified mitochondria of cells expressing the wild-type GTAp63 as well as the C306R mutant, although the cleaved fragment seemed to be enriched only at the mitochondria of wild-type cells.

Control immunostainings with antibodies specific for the nuclear protein lamin B1 and for Cox IX as a mitochondrial marker, indicated successful purification of mitochondria without any contamination from other cellular compartments (**figure 5.22 A** and data not shown).

Next, we quantified the signal intensities from the p63 immunoblot described above (**5.22 A**). The ratio of cleaved *vs*. full-length GTAp63 was calculated for total lysates and mitochondria of cells constantly expressing wild-type GTAp63 (**figure 5.22 B**). While it was hardly possible to detect any cleaved p63 in the cells treated with DMSO alone, upon treatment of cells with the chemotherapeutic cisplatin we saw a clear increase in the intensity of cleaved p63. The ratio was further shifted towards the cleaved p63 fragment in the purified mitochondria where we measured a 2-fold increase in caspase-cleaved *vs.* full-length GTAp63, as compared to the crude lysate.

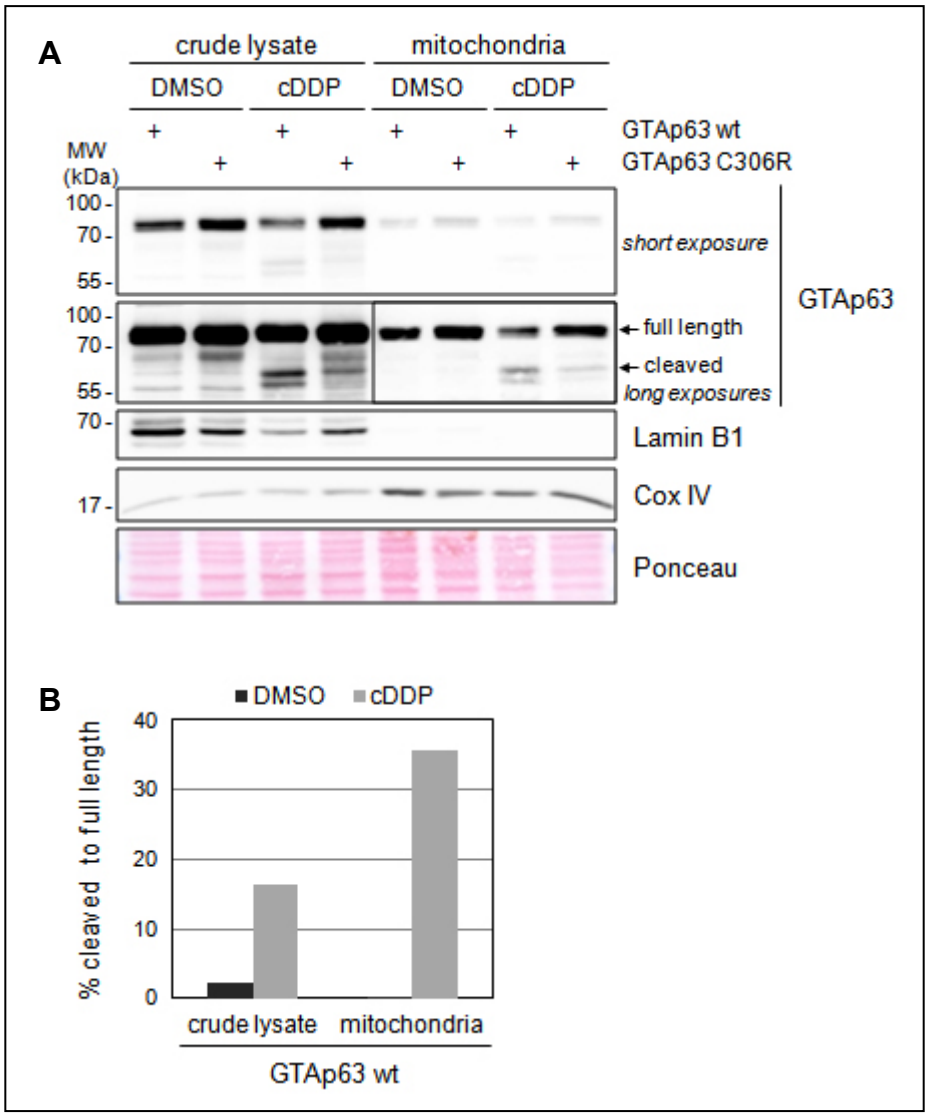

Figure 5.22: GTAp63 associates with mitochondria

A. Cell fractionation of stable H1299 cells expressing either wild-type GTAp63 or the mutant C306R after treatment with 30 µM cisplatin or DMSO alone for 24 h. Crude lysates and lysates of highly purified mitochondria were subjected to SDS-PAGE, followed by immunoblot analysis using antibodies specific for p63 (mab 4A4), for the nuclear protein lamin B1 or for cox IV as a marker of mitochondria. Immunodetection of p63 resulted in two distinct proteins, marked with full-length or cleaved GTAp63. The latter one could only be detected in longer exposures of the membrane. Ponceau staining indicates equal protein loading.

B. Quantification of signal intensities from the blot in A. Ratios of cleaved *vs.* full-length wild-type GTAp63 for total cell lysates and mitochondria were calculated. Black bars indicate treatment with DMSO alone, and grey bars depict ratios of cells treated with cisplatin.

Taken together, our data strongly suggest that caspase-cleaved GTAp63 protein not only augments stress-induced apoptosis through gene activation, but also directly activates the intrinsic apoptotic pathway at the mitochondria, providing a positive feedback for apoptosis upon DNA damage.

5.6 GTAp63 is a potential tumor suppressor in testicular cancers

5.6.1 GTAp63 expression is lost in testicular cancer cells

Though p63 is a homologue of the tumor suppressor p53, its function in suppressing human malignancies has been controversially discussed in recent years.

Since in male germline cells we saw high expression of GTAp63, shown to be able to enhance apoptosis upon activation by an initial DNA-damaging stimulus, we speculated that GTAp63 might act as a tumor suppressor guarding the germ line from accumulation of DNA damage, therefore also contributing to suppression of testicular malignancies. This implies the expectation that GTAp63 tends to be lost in testicular cancers.

To test our hypothesis we investigated the expression of GTAp63 in human malignancies from testicular tissue. All work with human tissues was performed in collaboration with the group of Ute Moll, Department of Pathology, Stonybrook University, USA. In total 60 cases of seminoma and 27 cases of embryonal carcinoma were analyzed by immunohistochemistry.

Figure 5.23 displays each one representative example of seminoma and embryonal carcinoma. Tissue sections were stained with hematoxylin and eosin (left side) or immunostained with a specific polyclonal p63 #9424 antibody recognizing a common region shared by all isoforms of human p63. p63 positivity is reflected by brown nuclear staining of cells.

Indeed, we were not able to detect p63 in the shown examples of seminoma or the embryonal carcinoma (**figure 5.23**). In contrast, a preinvasive tumor stage still expressed p63. Atypical cells of Germ Cell Intratubular Neoplasms (GCIN) stain positive for p63 (top panel of **figure 5.23**; arrowheads). We additionally assessed whether p63 is also lost in the female counterpart ovarian dysgerminoma. Indeed, three of five analyzed tumors lack p63 protein. An example where p63 was not detected in female cancer cells is depicted in the bottom part of **figure 5.23**.

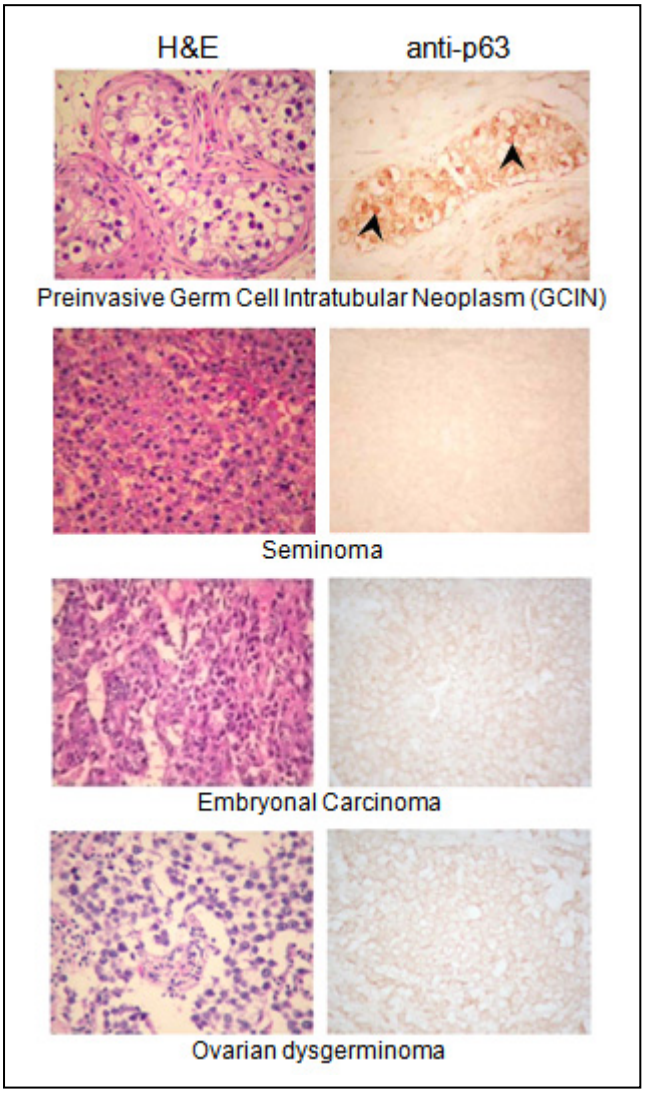

Figure 5.23: p63 expression is lost in invasive testicular cancers

Immunohistochemistry of diverse human tissues derived from testicular cancers. Representative examples of seminoma or embryonal carcinoma were either stained with hematoxylin and eosin (H&E) or immunostained with the polyclonal p63 antibody #9424.
*Top, S*taining of preinvasive Germ Cell Intratubular Neoplasm (GCIN) showing that p63 is still retained in atypical GCIN cells (arrowhead). Seminiferous tubules lack any sign of normal differentiation and spermatogenesis.
Bottom, H&E staining and immunohistochemistry of an example of ovarian dysgerminoma, also showing no detectable p63 protein.

A summary of immunohistochemistry results of all analyzed human tissues is given in **table 5.1**; total numbers of cases and numbers of cases positive or negative for p63, are shown. Of note, 100% of analyzed embryonal carcinoma lost p63 expression while in seminoma we were still able to detect p63 in some cases, as only 77% of seminomas (46 of 60 cases) were negative for the p63 protein. While also the majority of ovarian dysgerminoma did not show p63 expression, the pre-invasive stage of testicular cancer retained p63 positivity in 5 of 6 cases.

In sum, we conclude that the development of invasive testicular germ cell neoplasm correlates with the loss of GTAp63 expression. This is consistent with a role of GTAp63 as tumor suppressor.

Table 5.1: p63 detection in human testicular cancer and ovarian dysgerminoma

Tumor Type	No. of Cases	p63 negative	p63 positive	% p63 negative
Seminoma	60	46	14	**77%**
Embryonal Carcinoma	27	27	0	**100%**
Ovarian Dysgerminoma	5	3	2	**60%**
Germ Cell Intratubular Neoplasms (GCIN)	6	1	5	**17%**
TOTAL	**98**	**77**	**21**	**79%**

5.6.2 GTAp63 expression is transcriptionally silenced in testicular malignancies

Next, we determined mRNA level of GTAp63 in three randomly chosen testicular cancer cell lines. GH, NCCIT and Tera-2 were obtained from Roswitha Löwer, Paul-Ehrlich-Institut Erlangen (Lower et al, 1984).

RNA was isolated from the cell lines and together with RNA from normal human testis (RNA panel, Ambion) reverse transcribed with a mixture of oligo-(dT) and random primers. We then performed quantitative real-time PCR with three sets of primers specific for different p63 isoforms. GTAp63 mRNA was detected with primers binding to exon U1 and exon 2, while for quantification of mRNA level of the conventional TAp63 primers specific for exon 1 and 2 were used. The combination of p63 exon 2 forward and exon 3 reverse primers detected the sum of GTAp63 and conventional TAp63 forms. p63 mRNA level were normalized to GAPDH reference gene mRNA. The quantification results are shown in **figure 5.24**.

In comparison to the very high expression of GTAp63 in normal human testis, all three testicular cancer cell lines had dramatically reduced levels of GTAp63 mRNA. We detected a fold reduction on average of at least 3000 fold. This result is in agreement with the loss of p63 protein in malignant testicular tumors as compared to healthy tissue. Interestingly, mRNA level of conventional TAp63 forms (TA*p63/TAp63) were also decreased in the cancer cells, but not nearly to the extent of GTAp63 mRNA reduction. We only noticed a decrease of 10-100 fold. Quantitative

PCR with primers specific for exon 2 and exon 3 resulted also in reduced mRNA level of p63 in the tumor cells as compared to normal testis, since this primer pair detected the sum of transactivating p63 (GTAp63 + conventional TAp63) forms with the dominant expressed isoform being GTAp63.

We assumed from these data that expression of GTAp63 is transcriptionally silenced in cancers of testicular origin.

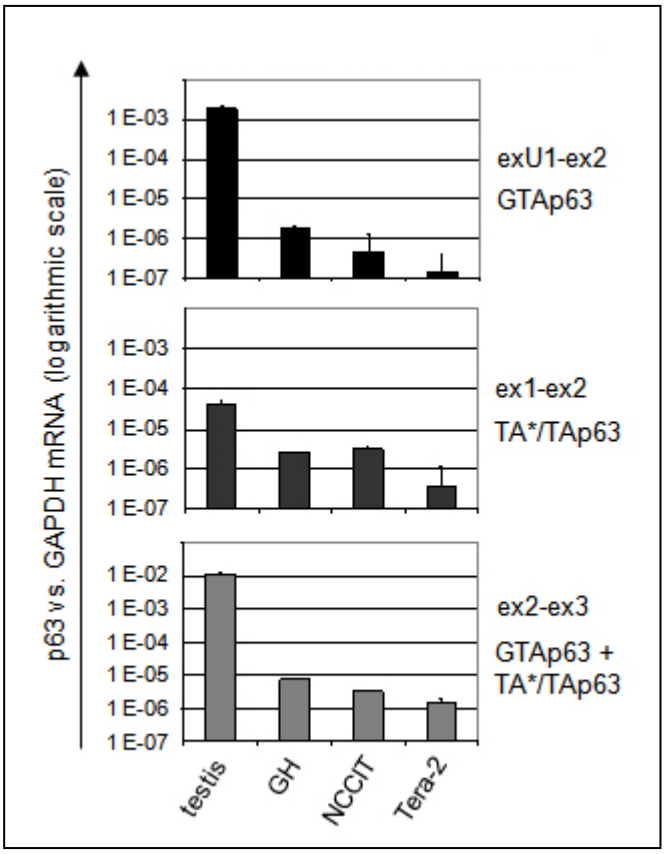

Figure 5.24: GTAp63 expression is lost in testicular cancer cells
RNA was isolated from 3 different testicular cancer cell lines (GH, NCCIT and Tera-2) and RT-PCR analysis was performed using primers specific for exon U1-2 (detection of GTAp63), exon 1-2 (detection of conventional TA*/TAp63) or exon 2-3 to detect the sum of all transactivating p63 isoforms. In contrast to the high expression of GTAp63 in normal testis tissue, its expression is strongly downregulated by ~3000 fold in the cancer cells. There was only little effect on the TA*/TAp63 mRNA level. The y-axis is shown in the logarithmic scale.

5.6.3 GTAp63 expression is rescued by HDAC inhibition

In an attempt to clarify the mechanistic basis for silencing of GTAp63 expression at the transcriptional level, we next examined the effect of HDAC inhibition on mRNA level of GTAp63 in testicular tumor cells. Therefore, we treated GH teratocarcinoma

cells with trichostatin A (TSA), a known inhibitor of histone deacetylases (HDACs), at concentrations of 250 or 500 nM. As control treatment with DMSO alone was performed in parallel. 16 h after treatment cells were harvested for RNA extraction. GTAp63 mRNA level were quantified by performing real-time RT-PCR analysis with primers binding to TP63 exon U1 and exon 2. GAPDH mRNA levels were used for normalization.

Interestingly, we detected a very strong increase in GTAp63 mRNA expression upon treatment of cells with trichostatin A (**figure 5.25**). Even the lower TSA concentration of 250 nM resulted in a ~ 3000-fold upregulation of GTAp63, which was further increased by the higher TSA dose of 500 nM.

In addition, we performed this RT-PCR experiment with the colon cancer cell line HCT116. Previously these cells were already shown to be responsive to trichostatin A regarding the upregulation of p63 (Sayan et al, 2007). We confirmed their result but, however, the effect of TSA was much weaker in the colon cancer cells than in testis-derived cells, proving that the restoration of GTAp63 mRNA expression upon HDAC inhibition is testis-specific.

To assure the specificity of HDAC inhibition by trichostatin A on the GTAp63 promoter we next analyzed expression of conventional TAp63 and TAp73, another homologue of the p53 family. As shown in **figure 5.25 B** the increase in TAp63 or TAp73 mRNA level was far less pronounced compared to that of GTAp63 mRNA. Quantitative RT-PCR analysis only resulted in 14- or 1.5-fold increase, respectively (**figure 5.25 B**).

In the following experiment we determined protein expression in testicular tumor cells treated with the HDAC inhibitor trichostatin A. The two different testicular cell lines GH and NCCIT, and the osteosarcoma cell line U2OS as control were incubated with 500 nM TSA. Cells were harvested after several time points ranging from 0 h to 24 h for Western blot analysis. The monoclonal p63 4A4 antibody was used to immunostain endogenous p63 protein. Directly after the treatment with TSA we did not detect a specific p63 band in any of the three tested cell lines (**figure 5.25 C**).

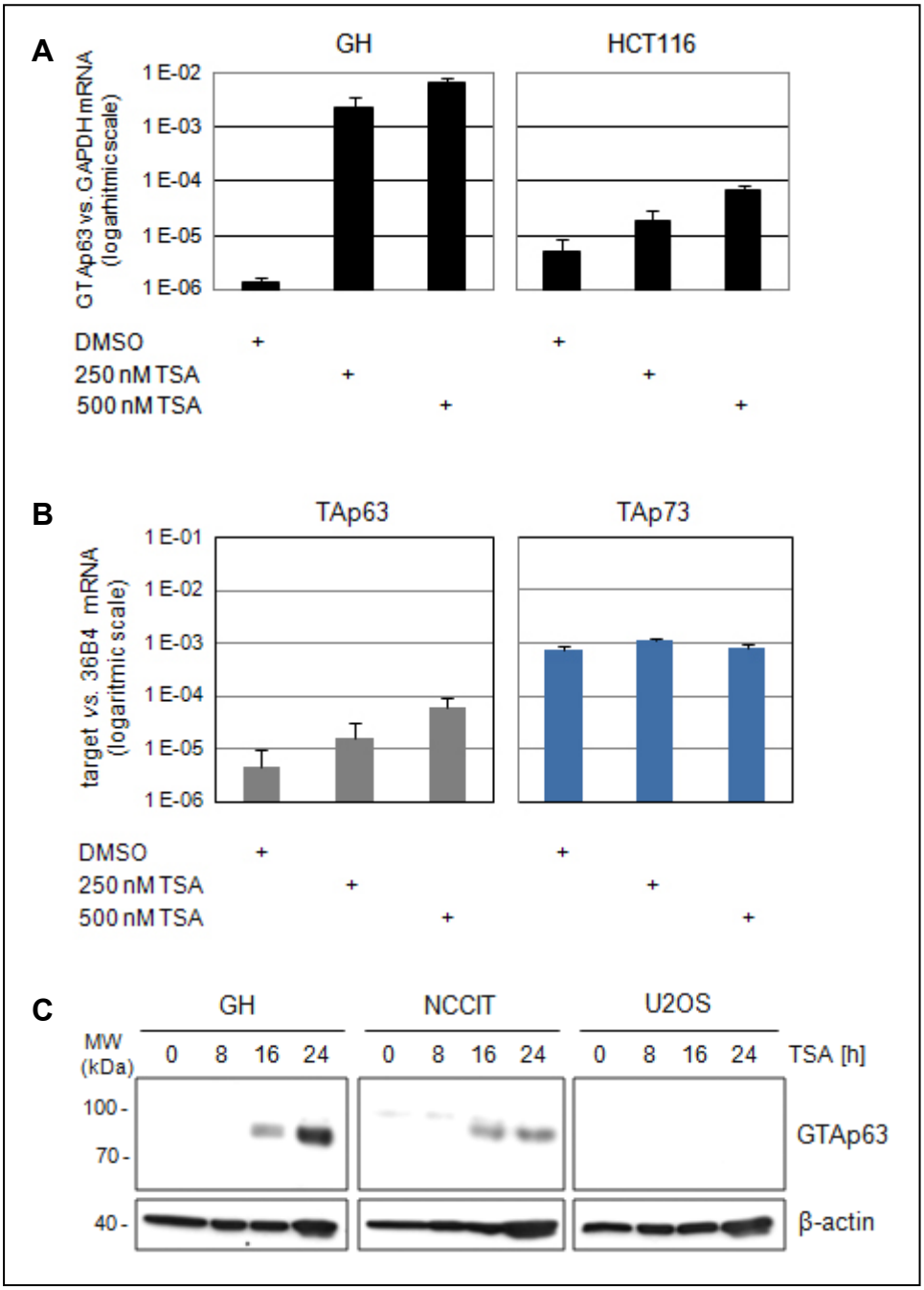

Figure 5.25: HDAC inhibition rescues GTAp63 expression

A. GH cells (teratocarcinoma) were treated with either DMSO alone or the HDAC inhibitor trichostatin A (TSA) at indicated concentrations for 16 h. GTAp63 mRNA level were analyzed by RT-PCR and normalized to GAPDH. Upon TSA treatment GTAp63 is upregulated up to ~3000 fold. This strong effect is specific for testicular cancer cells as HCT116 colon carcinoma cells showed only mild induction of the GTAp63 expression.

B. GH cells were treated with DMSO alone or two different concentrations of TSA, as described in figure A. Total cellular RNAs were reverse transcribed and then analyzed by real-time PCR. The levels of TAp63 or TAp73 mRNAs were quantified by normalization to expression levels of the reference gene 36B4. Note the logarithmic scale.

C. Testicular cancer cells GH and NCCIT or osteosarcoma cells U2OS were treated with 500 nM TSA for the indicated time. Proteins were subjected to SDS-PAGE, followed by immunostaining with the p63 4A4 mab. While there was no GTAp63 protein detectable in U2OS cells, both testicular cells showed restored GTAp63 protein expression upon HDAC inhibition. Beta actin staining served as loading control.

As expected, we noticed a restoration of GTAp63 protein in GH and NCCIT cells after 16 h of TSA, which was further increased after 24 h, especially in GH cells. In contrast, at each time of this experiment U2OS cells did not express any p63 protein, reflecting again the specific rescue of GTAp63 upon histone deacetylase inhibition through TSA in human testicular cancers.

To confirm that the TSA-restored protein really corresponds to GTAp63α, we performed two different experiments using GH teratocarcinoma cells (**figure 5.26**).
In the first experiment we specifically ablated expression of GTAp63 by siRNA mediated knockdown. GH cells were at first transfected with a control negative siRNA (lane 2) or a siRNA specific for a region of p63 that is included in all isoforms (see **3.4.2**) (lane 3). A third sample was mock transfected (lane 1). 36 h after the transfection trichostatin A at a final concentration of 500 nM was added to cell cultures, followed by incubation for 16 h. Afterwards cell lysates were subjected to SDS-PAGE and immunoblot analysis. Staining with the p63 4A4 antibody revealed the expression of GTAp63 protein that could be specifically and very efficiently silenced by using the siRNA against p63 (lane 3). The Ponceau staining showed equal loading of proteins in all samples.

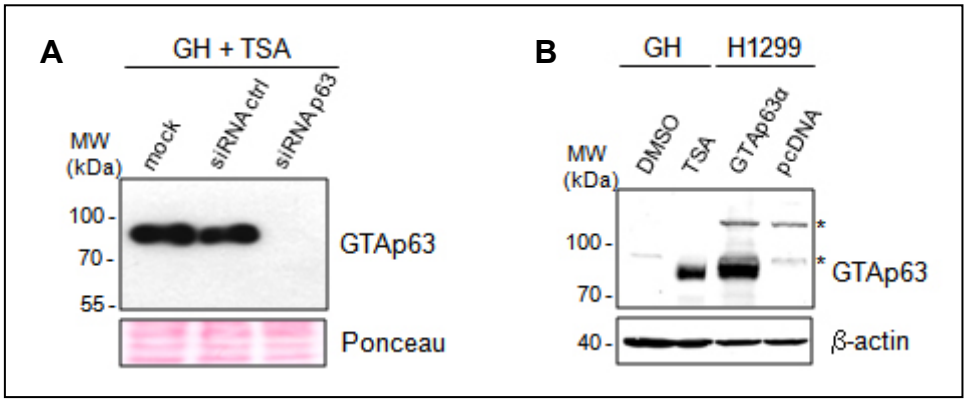

Figure 5.26: p63 knockdown ablates the restoration of GTAp63
A. Testicular tumor cells GH were transfected with siRNA specific for p63 or negative control siRNA or mock transfected. After 36h treatment of cells was performed with 500 nM trichostatin A (TSA) for 16h, proteins were loaded onto SDS-PAGE and afterwards analyzed by immunostaining with the p63 4A4 monoclonal antibody. Ponceau staining as loading control.
B. GH cells treated with 500 nM TSA or DMSO alone for 16 h were analyzed by SDS-PAGE and immunoblotting. The size of endogenous testicular p63 protein, as detected by the p63 4A4 mab, corresponds to GTAp63 expressed from a plasmid in transfected H1299 lung carcinoma cells. Control transfected H1299 cells showed only unspecific bands (*). Beta actin staining was performed as loading control.

Secondly, we compared the p63 protein rescued by TSA *vs.* exogenous GTAp63α transcribed from a plasmid transfected into lung carcinoma cells H1299 (**figure 5.26 B**). The electrophoretic motility of the endogenous GTAp63 in GH cells was identical to recombinant GTAp63α. We also detected additional bands in H1299 cells transfected with GTAp63 or the empty pcDNA3 vector using the p63 4A4 antibody (indicated by an asterisk next to the band). This might be due to cross-reactions of the antibody with other cellular proteins.

Taken together, we found that testicular tumor cells that have lost their GTAp63 could be potentially treated with the HDAC inhibitor trichostatin A to rescue GTAp63 expression.

Since inhibition of histone deacetylases is not the only mechanism to restore the expression of transcriptionally silenced genes, we then questioned how demethylation would affect GTAp63 protein level in GH cells. We chose 5`-azacytidine (5-aza) as demethylating agent and treated cells with two different doses of this drug (1 and 5 µM) for 24 h (**figure 5.27**, lanes 2 and 3). Control treatments with DMSO alone (lane 1) and 0,3 or 1 µM TSA (lanes 4 and 5) were performed under the same conditions. While we were able to detect GTAp63 protein after HDAC inhibition, GTAp63 remained lost after the treatment with 5`-azacytidine. This indicates that GTAp63 loss in testicular tumors does not happen on the basis of promoter methylation.

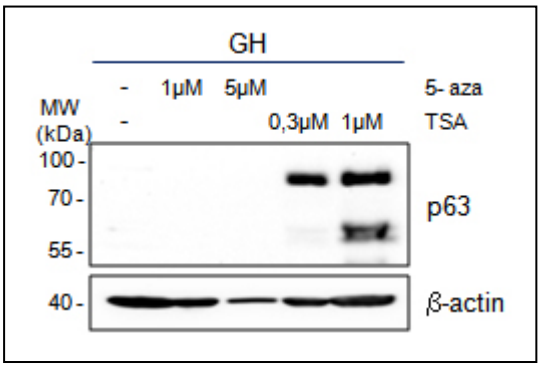

Figure 5.27: Demethylation has no effect on expression of GTAp63
GH cells (teratocarcinoma) were treated with the demethylating agent 5`-azacytidine (5-aza) or the HDAC inhibitor trichostatin A (TSA) at indicated concentrations; DMSO treatment was performed to control for unspecific side effects. On nitrocellulose blotted proteins were detected by immunostaining using p63 4A4 mab. Staining for beta actin is indicative for equal protein loading.

5.6.4 SAHA is a potential chemotherapeutic for testicular cancers

The complete rescue of GTAp63 expression in cancer cells of testicular origin upon HDAC inhibitor treatment let us to the assumption that these drugs might be used in chemotherapy to treat testicular cancers. Since trichostatin A is too toxic to be used in patients, we tested another HDAC inhibitor, suberoylanilide hydroxamic acid (SAHA) which is currently in clinical use for malignant lymphoma therapy (Marks & Xu, 2009).

Therefore, we decided to perform experiments, in which testicular tumor cells were induced with SAHA. We treated GH testicular cells with 5 and 10 µM SAHA or DMSO alone for 24 h. The same experiment was also performed in osteosarcoma cells U2OS as control. As shown in **figure 5.28**, indeed, GTAp63 expression was rescued even with the low concentration of SAHA. The effect was specific for testicular cells since no p63 protein at all was detected in cells of other origin.

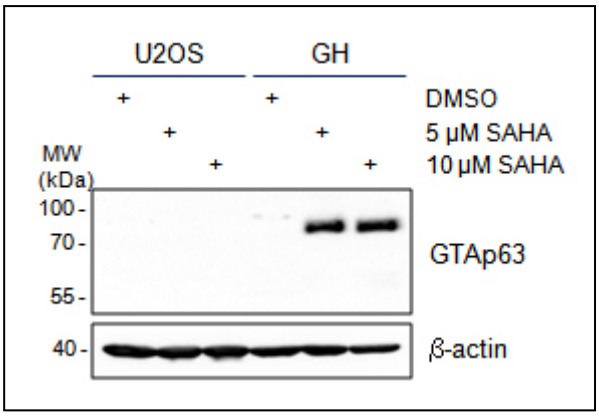

Figure 5.28: SAHA restores GTAp63 in testicular tumor cells
Western blot analysis of testicular tumor cell line GH treated with the clinically used HDAC inhibitor SAHA at indicated concentrations. Treatment with DMSO alone served as control. Nitrocellulose membrane was stained for p63 (4A4 mab) and beta actin as loading control. Re-expression of GTAp63 upon SAHA treatment was specific for GH cells since no such protein was detected in the osteosarcoma cell line U2OS.

Altogether, we conclude that in tumors of testicular origin GTAp63 is not genetically lost, but transcriptionally repressed by the action of HDACs and therefore in principal restorable. We found that HDAC inhibition indeed resulted in the rescue of GTAp63 expression in testicular cancers. The magnitude of this induction is to our knowledge

the most dramatic increase in gene expression reported so far for HDAC inhibition. Our findings could be beneficial for the therapy of testicular malignancies. In clinics SAHA might be used to treat patients suffering from testicular cancers, perhaps in combination with the conventional cisplatin therapy.

6. Discussion

The function and tissue specificity of the p53-homolog p63, especially of the transactivating TAp63 isoforms, was controversial in the literature, though diverse publications suggested a role of TAp63 during germ cell development and in the protection of the germ line fidelity upon genotoxic stress. While some researchers were able to detect TAp63 in human and murine male germ cells (Guerquin et al, 2009; Hayashi et al, 2004; Nakamuta & Kobayashi, 2003; Nakamuta & Kobayashi, 2004a; Petre-Lazar et al, 2007; Vincek et al, 2003), one widely acknowledged report indicates that TAp63 expression is biased towards the female germ line (Suh et al, 2006).

In this work we identify hitherto unknown transactivating p63 isoforms that are predominantly expressed in human adult testis. Since the novel p63 is specifically detected in spermatogonia and primary spermatocytes, we designated this novel isoform GTAp63, for germ-cell associated transactivating p63. Surprisingly, GTAp63 is transcribed from an unknown upstream promoter being part of an endogenous retrovirus long terminal repeat, integrated into host genomes of primate ancestors quite recently in primate evolution (~15 million years ago). Insertion of the retroviral LTR upstream of the TP63 in humans and also higher apes, hence in the common ancestor of hominids, possibly provides an example that a retroviral integration event has played a role in primate evolution. We suggest that LTR-driven expression of TAp63 may have facilitated the development of species with longer reproductive periods.

We further show that GTAp63 induces cell death upon DNA damage by transactivating the proapoptotic target genes PUMA and Noxa, as well as partial association with mitochondria to amplify the intrinsic apoptotic pathway. Because of these findings we suggest that GTAp63 may function in maintaining the integrity of the male germ line. Thus, insertion of a retrovirus nearby TP63 probably was of great benefit for hominids, promoting enhanced protection of the male germ line from deleterious DNA damage by GTAp63, thereby enabling successful reproduction during the long reproductive periods of humans and their closest relatives.

The role of GTAp63 in the regulation of germ cell apoptosis upon genotoxic stress led us to propose that GTAp63 might be a potential tumor suppressor in testicular tissue. This notion is supported by our finding that human germ cell cancers, derived

from testicular germ cells, frequently lost p63 expression epigenetically. Importantly, moreover, treatment with HDAC inhibitors restores GTAp63 expression in testicular cancer cells. Thus, we provide also evidence for a pharmacological rescue of GTAp63, maybe useful in clinics to cure testicular malignancies.

6.1 ERV9 LTR-driven p63 expression in germ cells

p63 is the evolutionarily most ancient member of the p53 family. Presumably, the most ancient gene of this family is most closely related to a p63/p73 hybrid gene being earliest expressed in primitive metazoa such as the sea anemone (*Nematostella vectensis*) (Belyi et al, 2009). In response to UV radiation nvp63 selectively causes apoptosis of hydra germ cells (Pankow & Bamberger, 2007). Furthermore, other primitive organisms such as flies, e.g. *D. melanogaster*, and roundworms, e.g. *C.elegans*, also express single p63-related proteins functioning in the germ line to initiate apoptosis in response to DNA damage. For example, the fly p63/p73 hybrid called dmp53 is activated during meiosis. Sustained dmp53 activation is achieved upon impaired resolvation of meiotic homologous recombination (Lu et al, 2010), requiring the action of Spo11 that is a topoisomerase generating DNA double strand breaks needed for strand exchange during the recombination process (McKim & Hayashi-Hagihara, 1998). In *C.elegans*, CEP-1 induces cell death in the germ line in response to DNA damage, hypoxia and starvation (Derry et al, 2001).
Importantly, though higher organisms evolved numerous p53/p63/p73 proteins with distinct physiological functions, p63 proteins are still employed for the surveillance of the genomic integrity of germ cells (Belyi et al, 2009).
Thus, the protective function of p63 in germline has persisted from metazoan until primates and humans, and therefore is conserved over one billion years of evolution (Belyi & Levine, 2009). Tumor suppressive functions inside the p53 family may have arosen from the primordial activity of maintaining germline fidelity (Lu et al, 2010).

In this work, we provide evidence arguing in favor of higher complexity of p63 gene regulation especially in the male germ line of humans and related hominids, generated by expression of a germ cell-associated p63 transcriptionally regulated by a retroviral ERV9 LTR. Human individuals produce roughly 50-200 million

spermatozoa per day. This means that male germ cells are extremely active in replication as compared to any other cell type. In conclusion, spermatogonia and spermatocytes must be equipped with even more stringent mechanisms protecting these cells from DNA damage.
Our results indicate that retroviral LTR-driven GTAp63 might fortify such protective mechanisms in testicular germ cells.

In mice, insertion of retroviruses or retroviral elements resulted in a number of germline mutations, e.g. proviral insertion caused recessive mutation of hairless, a potential zinc finger protein (Stoye et al, 1988).
Retroviral elements itself are potent agents of genomic instability either as a direct consequence of the transposition event or due to non-allelic recombinations involving transposon copies at distinct loci on the same or different chromosomes. Non-allelic recombination events during meiosis might interfere with the process of aligning homologous chromosomes during the zygotene-pachytene stages of meiotic division I (Öllinger et al, 2010), presumably resulting in impaired progression through meiosis. Thus germ cells must have evolved special mechanisms to repress retroviral activity protecting themselves from the dangerous effects of retroviruses.
We propose a model whereby impaired retroviral repression in the germ line might also lead to de-repression of the ERV9 LTR upstream of TP63, thus resulting in enhanced transcription of GTAp63 in germline cells. In turn, GTAp63 eliminates germ cells with impaired genome integrity by initiating apoptosis, thereby providing kind of feedback loop to minimize the danger of retroviral transposition.

ERV9 retroviral insertions have been reported throughout the whole human genome, including 50 copies of endogenous retrovirus and additionally 3000-4000 solo LTRs (Ling et al, 2002). Southern blot analyses with probes for ERV9 *gag*, *pol* and *env* sequences revealed that chromosome 3 contains several integrated ERV9 retroviral elements (Svensson et al, 2001). Furthermore, ERV9 LTR promoted mRNA expression was highest in human testicular tissue. This is in agreement with the predominant LTR-driven expression of GTAp63 mRNA in adult human testis, detected by the quantification of p63 transcript levels in a variety of human normal tissues (**figure 5.6**).

In addition, a recent report connects ERV9 LTR promoter activity with transcription in germ cells (Pi et al, 2004). Using a GFP reporter of the ERV9 LTR, originally described to enhance transcription in the human β-globin gene locus in hematopoietic and embryonic cells (Ling et al, 2002; Long et al, 1998), the autors studied the activity of this LTR in a transgenic zebrafish model and found high ERV9 LTR activity in the germ line of the transgenic zebrafish. The reporter was also active in human oocytes and stem/progenitor cells of diverse adult tissues (Pi et al, 2004), suggesting conserved mechanisms of LTR promoter regulation in germ cells. However, β-globin LTR-derived transcripts were not detected in male germ cells. This discrepancy in the germline expression of the β-globin ERV9 LTR, as compared to our GTAp63 expression data, could be explained by taking into account that, firstly, Pi et al. investigated the activity of an ERV9 LTR integrated into a different genomic context. Secondly, though known ERV9 LTRs are more than 90 % identical in their sequence, a few changes in polymorphic nucleotides might interfere with tissue specificity.

We also detected GTAp63 transcripts in ovarian RNA samples from young women. But in comparison to testicular samples, GTAp63 was ~ 600-fold lower in the tested ovaries. In contrast, we have evidence that expression levels of the conventional TAp63 are comparable between ovary and testis (**figure 5.6**). Altogether, this led us to the assumption that the insertion of the retroviral LTR element upstream of TP63 biased expression of GTAp63 towards the male germ line. Still, we cannot exclude that GTAp63 also plays a role in human female germ cells. Low levels of GTAp63 mRNA in ovarian samples might be due to the lower abandancy of oocytes throughout ovarian tissue. Further experiments will be necessary to clarify this issue. For this purpose, high amounts of human primordial oocytes sufficient for RNA analysis would have to be prepared, which is incompatible with ethical standards, thus making it a difficult task.

We found that in human testis the predominant p63 isoform is a GTAp63 form containing exon U1 directly spliced onto exon 2. This specific testicular isoforms is shown to be expressed to higher levels than the conventional TAp63 that has been recently implicated in the genomic fidelity of oocytes (Gonfloni et al, 2009; Livera et al, 2008; Suh et al, 2006). Exon U1 encodes for 19 amino acids that differ from the residues encoded by TP63 exon 1 (**figure 5.4**). We did not yet investigate how this

new amino terminus influences the function of the TAp63 protein in detail. However, it might have an impact on translational regulation of p63 expression, since disruption of the translational start codon in exon U1 results in markedly increased level of TAp63 protein starting from the methionin in exon 2 (**figure 5.5**).

In addition, we identified two other GTAp63 exons U2 and U3, alternatively spliced in between exon U1 and exon 2. It will be interesting to investigate under which circumstances GTAp63 transcripts including either exons U2 or U3 are expressed. Further experiments have to be performed to determine the physiological consequences of the expression of these novel GTAp63 isoforms. At least, exon U3 seems to be conserved in different species. Exon U3 is found in the mouse Trp63 locus (see appendix chapter 7).

In sum, our results strongly suggest that the activity of the ERV9 LTR promoter leading to GTAp63 expression is specific to male germ cells. However, the signals that enhance LTR promoter activity still have to be elucidated. ERV9 LTRs have been described to contain GATA, CCAAT and CCACC motifs which can bind human transcriptions factors in placental and hematopoietic tissues (Ling et al, 2002). Notably, we also found such motifs in the ERV9 LTR upstream of TP63. La Mantia *et al.* present data that a Sp1 binding site contributes to transcriptional activation of LTR-driven genes (La Mantia, 1992). Moreover, steroid hormones and growth factors can regulate the expression of some endogenous retroviruses. An ancient retroviral element inserted upstream of mouse sex-linked protein (*slp*) imposes androgen responsiveness on its neighboring genes (Coffin et al, 1997). A tissue-specific activation of the TP63-associated LTR promoter in testis might be achieved by testosterone.

In agreement, two recent genome-wide studies also show that LTRs impact tissue specificity (Conley, 2008; Faulkner, 2009). However, the use of LTR promoters is expected to result only in subtle changes of host gene expression since there is natural selection against LTRs leading to drastic changes in host gene expression. Rather LTR-driven transcription allows fine-tuning of host transcription, thereby also driving speciation (Cohen et al, 2009).

We detected p63 positivity in both, human and murine testis though the ERV9 LTR is integrated in humans but not in mice. This might indicate that insertion of the ERV9 LTR adjacent to TP63 also promoted fine-tuning of p63 expression in male germ

cells. Indeed, human p63 mRNA level in testis tissue were only roughly 3 times higher than in the corresponding murine tissue (**figure 5.12**). However, we realized a distinct distribution of the p63 protein expression within the seminiferous epithelia of the human *vs.* the murine testis (**figure 5.14**). We suggest that the ERV9 LTR promoter activity shifted p63 expression from a main location in murine spermatocytes towards strong expression in human spermatogonia which are the true germ stem cells. Here, fine-tuning may have enabled long term protection of the male germ line in long-lived species.

Interestingly, in Hodgkin's lymphoma derepression of an LTR from the endogenous retrovirus THE1B was recently shown to lead to expression of the proto-oncogene CSF1R, thereby contributing to the pathogenesis of lymphomas (Lamprecht et al, 2010). Conversely, the insertion of the ERV9 LTR upstream of TP63 represents to our knowledge the first example of an endogenous retrovirus-derived sequence that controls expression of a gene which functions in germ line protection and tumor suppression.

6.2 ERV9 LTR insertion – a role in primate evolution?

Endogenous retroviruses are integrated as proviruses into host genomes. Following the integration event viruses undergo subsequent selections for those insertions that are less harmful or even beneficial for the host. The selection process for HERVs has been going on for an estimated period of 100 million years (Jern & Coffin, 2008). Numbers of endogenous retroviruses peaked around 30-40 million years ago, when Old World and New World monkeys diverged. It has been suggested that this retroviral burst contributed to the evolution of early primate lineages, protecting early ancestors carrying stably integrated ERVs from infections with exogenous retroviruses (Sverdlov, 2000), thereby resembling kind of survival factor.
Today, the vast majority of retroviral sequences is considered neutral invader material without any utility to the host. Nevertheless, retroviral integration events in germ cells being further propagated to subsequent generations may influence gene expression in a specific way conferring evolutionary advantages to individuals that

carry the inserted retroviral element. Indeed, it has been suggested that retroviruses were significantly involved in the evolution of hominid primates (Sverdlov, 2000).
Here, we provide evidence further supporting this theory. Our findings indicate that a specific retroviral integration event in primate ancestors enabled human evolution by providing increased germline stability.
Previously, several examples were described that insertion of an endogenous retrovirus not only affected the expression of an adjacent host gene, but, moreover, had an important impact on primate evolution. One such example is given by the integration of a HERV-E element that led to a switch from pancreatic to parotic expression of amylase, resulting in a change of the dietary preferences of apes (Coffin et al, 1997).
The growth factor pleiotropin (PTN) is another example. Expression of the PTN gene perinatally in the central nervous system and in some adult tissues is evolutionary conserved in New World monkeys and higher apes. However, integration of a HERV element into the intron of the PTN gene between the 5`-untranslated region and the coding reagion gave rise to an alternative promoter which is found in humans and great apes, but not in rhesus monkey. This novel retroviral promoter led to expression of the human pleiotropin in the trophoblast early in embryonic development (Schulte et al, 1996). Assuming that the growth factor expression in the trophoblast was phylogenetically advantageous, one can speculate that trophoblastic ERVs played a role in the evolution and divergence of placental mammals, specifically in the evolution of *Hominoidea* (Sverdlov, 2000).

In this work, we identified a long terminal repeat of the endogenous retrovirus family 9 (ERV9) promoting the expression of a novel p63 isoform in testicular germline cells. Recently, also other human genes have been identified to be controlled by ERV9 LTR promoters and enhancers. Transcription of the human zinc-finger coding gene ZNF80, which is even located on the same chromosome as TP63, is driven by a solitary ERV9 LTR that is located directly upstream of the zinc finger-coding region (Di Cristofano et al, 1995a). The same authors additionally used a PCR strategy to narrow down the time period of primate evolution, when the LTR inserted into the ZNF80 locus (Di Cristofano et al, 1995b). In accordance, we amplified genomic regions of the ERV9 LTR and flanking sequences from an extended collection of genomic DNA from diverse primates. In contrast to the ZNF80-LTR integration,

	Species	Life span	Begin of fertility	ERV9 LTR upstream TP63	Primate family
	Human	~ 80 years	Female: 10-18 years Male: 12-20 years	**yes**	Hominidae
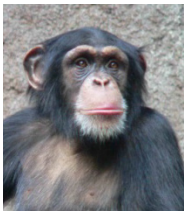	Chimpanzee	30-40 years	7 years	**yes**	Hominidae
	Gorilla	35-40 years	Female: 6-8 years Male: 10 years	**yes**	Hominidae
	Orangutan	50 years	Female: 7 years Male: 12-15 years	**yes**	Hominidae
	Gibbon	25 years	8-9 years	**no**	Hylobatidae
	Rhesus macaque	15-20 years	Female: 3-4 years Male: 6-7 years	**no**	Cercopithecinae

Figure 6.1: ERV9 LTR insertion into TP63 locus may have influenced reproductive periods of higher apes

The scheme depicts different primate species, from the family of *Cercopithecinae* on until the great apes and humans, representing the family of *Hominidae*. Living ages and the age of beginning fertility of the primate species are shown. Insertion of the ERV9 LTR upstream of the TP63 locus is only detected in hominids. Pictures of representative animals were taken from Wikipedia websites.

which happened after the split of orangutan from the other hominids, the LTR inserted in the TP63 locus was detected in all species of *Hominidae*, including great apes and humans (**figure 5.9**). In conclusion, integration of ERV9 upstream of TP63 must have occurred after the divergence of *Hylobatidae* from higher apes, around 15 million years ago. This time point of ERV9 integration adjacent to TP63 is supported by our results from phylogenetic sequence analyses, comparing the TP63-associated LTR sequence with sequences of recently identified members of the ERV9 family. The alignment (**figure 5.8**) indicated that the TP63-associated LTR belongs to the ERV9 subfamily, described to be highly active in retrotransposition during a time period starting around 18 MYA and going until 6 MYA (Costas & Naveira, 2000).

So, the ERV9 LTR inserted into the TP63 locus after the split of gibbons but before the divergence of orangutan. This is in agreement with recent results showing that other copies of the ERV9 LTR in the β-globin gene and in the axin gene are conserved in orangutan, gorilla, chimpanzee and humans (Ling et al, 2002).

Interestingly, separation of the *Hominidae* lineage, including human species, from other primates is associated with a boost in longevity and complexity, the latter being most obvious in cerebral development. Additionally, hominids have clearly longer phases of reproductivity than lower primates. While women and men are fertile for roughly 35-40 years and even up to 60 years, respectively, gibbons and lower apes only reach reproductive periods of less than 20 years (**figure 6.1**). For example, the rhesus macaque that belongs to Old World monkeys is reproductive for a period of 8 to 13 years. To note, increased time spans of primate reproductivity parallel ERV9 integration upstream of the TP63 gene. Therefore, we think that the retroviral integration contributed to the prolongation of reproductive phases in great apes and humans.

The 15 million years since the ERV9 insertion into the TP63 locus are in contrast to one billion years of p53 gene family evolution (Belyi & Levine, 2009). Notably, there is another, though less central, example of recent evolution of the p53 system. PIG3 (p53-induced gene 3) is a component of the DNA damage pathway (Lee et al, 2010) being involved in p53-mediated cell death. It has been shown that p53 mediates PIG3 induction by binding to a microsatellite sequence repeated within the PIG3 promoter (Contente et al, 2002). Though a small number of the satellite sequences are found in New World and Old World monkeys, p53 can only activate the PIG3 promoter in primate species of the *Hominoidea* superfamily including gibbons, great

apes and humans that all contain markedly higher numbers of the microsatellite (Contente et al, 2003). Thus, PIG3 responsivity to p53 was achieved during the evolution of higher primates. This example further stresses the necessity of more rigorous genomic surveillance mechanisms in higher primates and humans.
Altogether, we propose that insertion of the ERV9 LTR adjacent to TP63 conferred an evolutionary advantage to hominid species, providing them with increased levels of GTAp63 particularly in spermatogonia. This enabled the rigorous maintenance of the germ line over an expanded time of fertility.

6.3 GTAp63 as a potential testicular tumor suppressor

In normal human testis tissue p63 is strongly expressed in the germ cells, especially in the diploid spermatogonia and to a lesser extent in primary spermatocytes. In contrast, we found a very significant downregulation of p63 in testicular neoplasms. While p63 is still detected in the preinvasive tumor stage Germ Cell Intratubular Neolasms (GCNI), p63 expression is lost in malignant germ cell tumors with embryonal carcinoma being p63-negative in all analyzed cases and seminoma showing no p63-reactivity in 77% of cases. The loss of p63 expression was additionally confirmed in testicular tumor cell lines which in contrast to normal testis tissue do not contain detectable amounts of p63 mRNA or protein.
90 % of testicular tumors arise from germ cells. A major wave of testicular apoptosis occurs prepubertal when spermatogonic precursors undergo either mitotic divisions or apoptosis. In line with this fact, the incidence of testicular germ cell tumors (TGCT) increases shortly after the onset of puberty (Bahrami et al, 2007), implying that germ cell tumors may arise due to failures in apoptotic pathways of the testicular cells. The results presented in this work suggest that GTAp63 is at least one of the players involved in the regulation of male germ cell apoptosis.
Previous studies indicate that p53 contributes to testicular apoptosis during normal spermatogenesis and upon irradiation-induced DNAdamage (Beumer et al, 1998b). However, there is clear evidence arguing in favor of the existence of p53-independent apoptotic pathways in spermatogonia and the tumors derived thereof. Diverse TGCT cell lines have been shown to undergo apoptosis independently of p53 if induced upon chemotherapeutic drugs, ionizing radiation or Fas ligation

(Burger et al, 1999). Furthermore, irradiation-induced spermatogonial cell death still occurs in p53 knockout mice (Hamer et al, 2001), pointing in the same direction.
Though we do not have direct evidence that abrogation of p63 function is causal for the onset of germ cell tumors, the loss of p63 expression seems to be linked with invasive tumor stages, thus might allow testicular tumors to further progress.
This finding is in agreement with the work of Guo *et al.* that reported a role for TAp63 in preventing tumor formation as well as progression of already established tumors *in vivo* using mouse models (Guo et al, 2009).

We propose that, mechanistically, testicular tumors efficiently silence p63 gene expression by epigenetic gene silencing through the action of histone deacetylases (HDACs). Very importantly, we show complete restoration of p63 mRNA and protein level using distinct HDAC inhibitors such as trichostatin A (TSA) or suberoylanilide hydroxamic acid (SAHA). Recently, another group also reported increased p63 mRNA level upon treatment of tumor cells with TSA (Sayan et al, 2007). The magnitude of p63 induction in the colon carcinoma cells is much less prominent than in testicular cancer cells, where we detected a nearly 5000-fold induction of the TP63 gene as compared to a 16-fold induction of p63 mRNA in colon cancer cells.
HDACs are not only known to deacetylate histones, thereby leading to a closed chromatin structure and transcriptional repression, but also to target non-histone proteins such as transcriptional regulators, signal transduction mediators, DNA repair enzymes, nuclear import regulators, chaperone proteins and viral proteins (Marks & Xu, 2009). Our results do not exclude that de-repression of the TP63 gene upon HDAC-inhibitor treatment of testicular germ cells might also involve the acetylation of certain non-histone proteins functioning as regulators of the p63 gene expression, leading to the transactivation of the p63 gene upon HDAC inhibition.
Moreover, pharmacological HDAC inhibition has been shown to promote antiproliferative effects on cancer cells. Diverse HDAC inhibitors are in clinical trials as monotherapy or in combinations with other anti-cancer therapies. For example, SAHA (also known as Vorinostat) is already used to treat a subtype of T-cell lymphoma (Marks & Xu, 2009). Our data provide a rationale arguing in favour of HDAC inhibitors as useful adjuvant therapeutics in the treatment of testicular cancer.
Though testicular germ cell tumors are quite sensitive to platinum-based compounds like cisplatin, cisplatin is highly toxic to cells, leading to transcription inhibition, the

activation of multiple stress signaling pathways, but also to the generation of reactive oxygen species (ROS) (Tripathi et al, 2009). Taken the facts together, patients suffering TGCTs might benefit from a therapy using HDAC inhibitors in combination with the conventional therapy. Such an adjunct strategy possibly improves the anti-cancer effects and lowers the toxicity of germ cell cancer therapy.

We observed that germ cell associated GTAp63 enhances apoptosis in a tumor cell model. Recent data already show that TAp63 alpha is induced by diverse chemotherapeutics, leading to cell death in human cell lines and also in mouse oocytes (Gonfloni et al, 2009; Gressner et al, 2005). Apoptosis in male germ cells requires the action of anti- and proapoptotic members of the Bcl-2 family of proteins; additionally it involves Fas (CD95) and Fas ligand (CD95L) molecules (Tripathi et al, 2009). In line with this, GTAp63 enhanced cisplatin-induced cell death by transactivating the propaoptotic Bcl-2 proteins PUMA and Noxa as well as the induction of FasL (**figure 5.20**). In addition, GTAp63 also inhibits long-term cell survival in response to genotoxic stress.
Unfortunately, we could not prove that the inhibition of GTAp63 function can confer chemoresistence to testicular cells, as it has been shown for hepatocarcinoma cell lines (Gressner et al, 2005). We had to pretreat testicular cancer cells with HDAC inhibitors to restore p63 expression prior to the induction of p63 apoptotic function by cisplatin. HDAC inhibition as such already elicited apoptosis, making it difficult to detect significant changes in the apoptotic response after knockdown of p63.
To address the *in vivo* functions of GTAp63 one could isolate human germ cells to use them in primary cell cultures. Since these cells would then have to be transfected to silence p63, which is probably not easy to achieve, we have not yet made such attempts.

Previous evidence suggests that DNA damage-induced activation of kinases such as c-Abl or other imatinib-sensitive tyrosine kinases precedes the TAp63-dependent germ cell death (Gonfloni et al, 2009), whereas p63 is negatively regulated by germ cell-associated microRNAs (Scheel et al, 2009). Interestingly, activation of effector caspases upon an initial DNA damage stimulus is a prerequisite for GTAp63 to efficiently augment germ cell apoptosis. As has been described by Sayan *et al.* for TAp63-mediated apoptosis (Sayan et al, 2007), GTAp63 is similarly cleaved at its

carboxy terminus by pre-activated caspases, resulting in the release of a p63 fragment that can further amplify damage-induced cell death. Thus, this mechanism provides a positive feedback loop that ensures sufficient elimination of damaged germ cells.

Transactivating isoforms of p63 have been connected to the mitochondrial apoptosis pathway (Gressner et al, 2005). The homolog p53 has the capability to directly interact with mitochondria to enhance the intrinsic apoptotic pathway, resulting in cytochrome c release (Dumont et al, 2003; Mihara et al, 2003).
Here, we report for the first time an interaction of p63 with mitochondria. Caspase-cleaved p63 seems to be enriched at mitochondria (**figure 5.22**). Thus, stress-activated GTAp63 might augment apoptosis in germ cells in part by directly acting at mitochondria, additionally contributing to the feedback loop to proapoptotic stimuli.

The results that were obtained during this work are schematically summarized in **figure 6.2**.

The integration of an ERV9 retroviral LTR upstream of the TP63 gene of hominids roughly 15 million years ago led to the expression of a novel GTAp63 isoform which is associated with male germ cells. Upon genotoxic stress GTAp63 enhances apoptosis of spermatogenic cells. Activated caspases might further activate the apoptotic function of GTAp63 by cleavage of the GTAp63 protein. By the elimination of damaged germ cells GTAp63 plays a role in the male germ line surveillance. The potential contribution of GTAp63 to the suppression of testicular germ cell tumors is indicated by the silencing of the GTAp63 expression that was found in testicular cancers. Finally, inhibition of histone deacetylases results in the re-expression of the GTAp63 isoform.

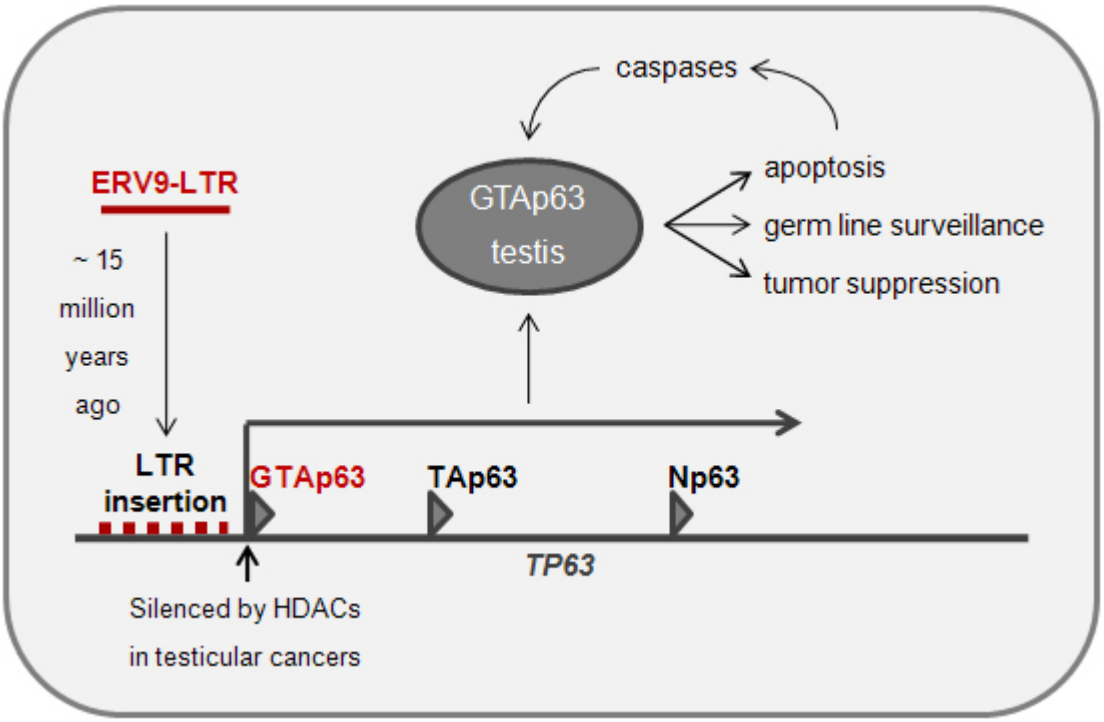

Figure 6.2: GTAp63 expression in hominid male germ cells
Insertion of the retroviral ERV9 LTR into the TP63 locus resulted in the expression of a novel GTAp63 isoform in hominid male germ cells. GTAp63 induces apoptosis upon genotoxic stress, thus contributes to germ line surveillance and suppression of testicular germ cell cancers which show silencing of GTAp63 expression by histone deacetylation.

In sum, we provide mechanisms that may exquisitely sensitize germ cells to DNA damage, which helps to prevent testicular cancers. Furthermore, and even more importantly, it ensures genetic fidelity of the male germline, thereby allowing successful reproduction.

7. Appendix A – murine GTAp63

7.1 Introduction

7.1.1 p63 isoforms in murine germ cells

Having investigated the expression and function of human transactivating p63 isoforms associated with male germ cells, we wondered if there exist similar p63 orthologs in male mice.

Human GTAp63 transcripts were found to contain hitherto unknown exons U1, U2 and U3 at their 5`-termini. Such exons have not yet been described in mice. However, some years ago, Bamberger and Schmale identified distinct p63 isoforms of the rat ortholog KET (keratinocyte transcription factor) by performing RACE experiments from rat tongue and placenta tissue. They designated the exons being located upstream of exon 2 exons 1, 1` and 1`` (Bamberger & Schmale, 2001). Sequence comparison of the three exons of the rat p63 gene with the human TAp63 exons reveals that rat exon 1 equals human exon U3, while exon 1` corresponds to human and murine exon 1, leading to TA*p63 isoforms.

The functions of TAp63 isoforms were already described in detail in this work in chapters 2.2 and 2.3. It has been controversially discussed whether murine TAp63 is expressed and functions in male germ cells.

Though some recent data argue against a role of murine TAp63 in the protection of the male germline fidelity (Suh et al, 2006), the results of several groups indicate that murine TAp63 induces apoptosis in germ cells having accumulated severe DNA damage, e.g. upon irradiation (Guerquin et al, 2009; Petre-Lazar et al, 2006). For example, Guerquin *et al.* showed increased germ cell survival in the fetal testis of p63 knockout mice after irradiation, as compared to wild-type mice (Guerquin et al, 2009).

We aimed to elucidate whether the adult male germ cells of irradiated mice that lack TAp63 show an impaired DNA damage response and fail to undergo apoptosis. Such a result would further argue in favor of TAp63 acting as a guardian of the male germ line fidelity.

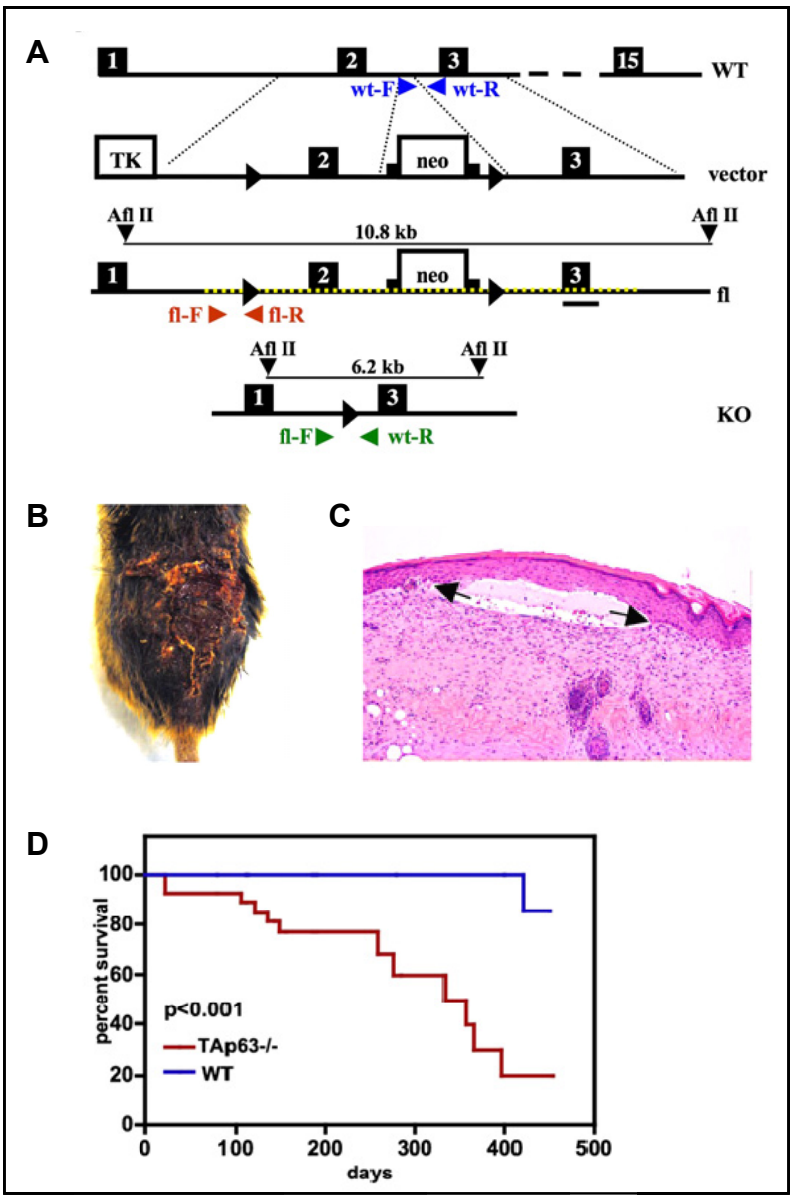

Figure 7.1: TAp63 knockout mouse (modified from (Su et al, 2009))

A. Generation of the TAp63 knockout mouse by targeted deletion of TP63 exon 2. The targeting vector contains exon 2 flanked by loxP sites (black arrowhead) and the neomycin resistance. Cre-mediated recombination leads to TAp63 ko mice lacking exon 2. Genotyping primers are indicated as colored arrowheads.

B. Ulcerated wounds of an 8 month-old TA knockout mouse are shown.

C. H&E stain of histological section from the skin of a TAp63 knockout mouse that developed a blister. Arrows indicate the split between epidermis and underlying dermal tissue.

D. Kaplan-Meier curve displays the decreased survival time of TAp63-/- mice (red line) in comparison to wild type control mice (blue line).

7.1.2 TAp63 knockout mouse model

There are distinct knockout mouse models in which the transactivating isoforms of p63 have been specifically ablated (Guo et al, 2009; Su et al, 2009; Suh et al, 2006).

Su *et al*. generated first a conditional TAp63 mouse that contains a TAp63 allel with a floxed exon 2. The resulting TAp63fl -/- mice were then crossed with germline-specific cre transgenic mice to achieve TAp63 knockout mice (Su et al, 2009) (**figure 7.1**). In comparison to wild-type control mice the TAp63 -/- mice exhibited shortened lifespan. The authors focused on the outcome of the TAp63 loss in the epidermis and found that knockout mice develop blisters and ulcerations, the latter resulting from impaired wound healing. From their results, the authors conclude that TAp63 is required for the maintenance of adult epidermal as well as dermal stem cells.
In our studies we used the TAp63 knockout mice generated by Su *et al.* to address whether specific ablation of TAp63 function results in changes in the morphology of the seminiferous epithelium consisting of the male germ cells. Moreover, we investigated the DNA damage response of the germ cells that lost TAp63 isoforms as compared to the response of wild-type cells.

7.2 Supplementary materials

7.2.1 Mice

For *in vivo* animal experiments we used a TAp63 knockout mouse that was established and already published by the group of Elsa Flores (Su et al, 2009).
The obtained mice were in a mixed background including C57/BL6 and SV129 mouse strains. Mice were crossed back into the SV129 background, but were still only in the second generation when used for experiments.
The SV129 wild-type mice that were used for the time course experiment were ordered from Charles River Laboratories International, Wilmington, USA.

7.2.2 Oligonucleotides

Name of primer	Sequence
murp63 exon U3_forward **mur p63 exon 2_reverse**	gatcagaagttcagagatgcctac tgttccagaaaatcccagatatgc
mur RACE first primer **mur RACE nested primer**	tgggcacccccctgtaaagctgttcttcc gccacagttttagagcccttgacgtagag

7.2.3 Antibodies

Name	Dilution	Provider
rabbit anti-cleaved caspase 3, 5A1E	1:200	Cell Signaling
donkey anti-rabbit IgG (F_{ab}-Fragment), biotinylated	1:200	GE Healthcare

7.2.4 Reagents

Name	Order number	Provider
In situ cell death detection kit, POD	11684817910	Roche

7.2.5 Consumables and technical devices

Wet chamber for slides	Weckert Labor
X-ray machine (RS225A)	Gulmay Medical

7.3 Supplementary methods

7.3.1 γ-irradiation of mice

Mice were irradiated at the University hospital, Department of Radiation therapy, Göttingen. Mice were subjected to a single whole body dose of γ-irradiation using the X-ray machine RS225A (Gulmay Medical). Mice were placed in a special container on top of a rotating plate, and a dose rate of 1 Gy per minute was applied for 30 sec to achieve a total dose of 0.5 Gy. Following irradiation the animals were incubated for different times.

7.3.2 TUNEL assay

Terminal dUTP Nick End Labeling (TUNEL) was performed to assay late stage apoptosis at the single cell level. Cleavage of genomic DNA during apoptosis results in free 3`-OH DNA ends. These DNA ends can be labeled by polymerization of

labeled nucleotides, which is catalyzed by the Terminal deoxynucleotidyl Transferase (TdT).

The In Situ Cell Death Detection kit from Roche was used to label fixed cells in paraffin-embedded tissue sections.

In brief, 5 µM tissue sections were pre-treated by heating in citrate buffer for 1 min to permeabilize fixed cells. Afterwards, sections were washed with PBS and incubated with the labeling reaction mix (Roche) in a wet chamber for 1 h at 37°C. Free cellular DNA ends in apoptotic cells are labeled with fluorescein due to incorporation of fluorescein-coupled dUTP during the tailing reaction. TUNEL positive cells were analyzed by fluorescence microscopy and pictures were taken.

7.4 Results

7.4.1 Novel TAp63 transcripts are expressed in murine testis

Having identified novel transactivating isoforms of the human TP63 gene, which are predominantly expressed in human male germ cells, we addressed whether there are similar, yet unidentified murine germ cell-associated TAp63 transcripts of the Trp63 gene.

Interestingly, sequence comparison of the human and the murine genomic region containing the p63 loci revealed that the novel human exon U3 might be conserved in mice. We performed 5`-RACE experiments using murine testicular RNA to confirm the existence of novel Trp63 exons that are included in testis-specific p63 transcripts.

PCR amplification of testicular RACE cDNA using a reverse primer which specifically binds to Trp63 exon 2 resulted in several distinct products. Subsequently, these products were re-amplified with nested primers and sequenced. Indeed, we obtained novel transcripts that contained a murine exon U3. In analogy to the genomic context of human exon U3 the mouse homologous exon is located upstream of Trp63 exon 1 on chromosome 16. Moreover, the Trp63 exon U3 is also directly spliced onto exon 2, omitting exon 1. However, we detected another TAp63 transcript variant, which additionally contains a part of exon 1. In this variant exon U3 is spliced to a splice acceptor site inside exon 1, giving rise to a transcript that consists of exon U3, part of exon 1 and exon 2 at its 5`-end. The genomic architecture of the Trp63 locus including the newly identified exon U3 - indicated in red color - is displayed in **figure**

7.2. In contrast to the human p63, we did not find other exons located even more upstream than exon U3 that are included in testicular TAp63 transcripts.

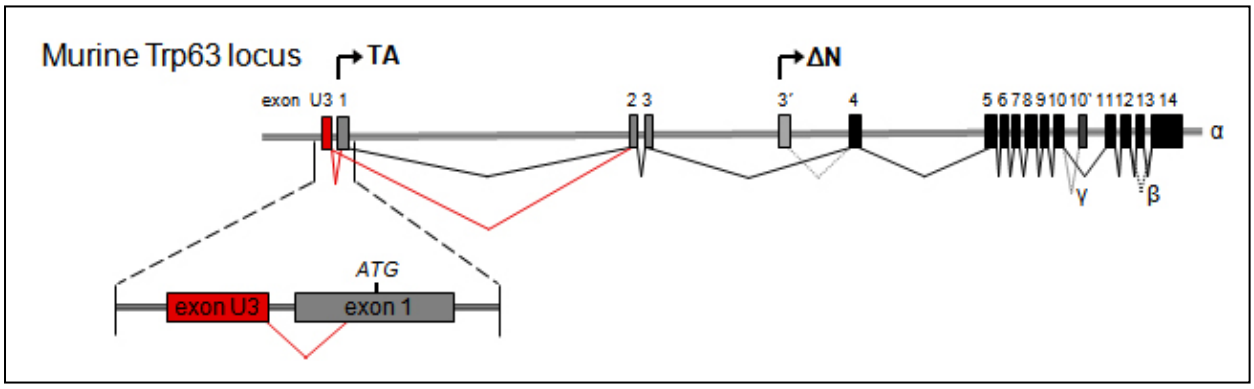

Figure 7.2: Structure of the murine Trp63 locus
Murine 5`RACE experiments identified a novel exon upstream of Trp63 exon 1. This exon was termed exon U3 because of its sequence homology to the novel human TP63 exon U3 (indicated by the red box). Known exons included in TAp63 transcripts are shown as grey boxes, while black boxes represent exons coding for the central DNA-binding domain and the carboxy-terminal part of Trp63. Red lines indicate splicing events that generate two novel Trp63 transcripts. A magnification of the genomic region that contains exon U3 and exon 1 is depicted in the insert. Alternative splicing at the 3` end of the Trp63 gene generates the distinct isoforms α, β and γ.

Next, we determined the expression of the newly identified GTAp63 isoforms in murine testicular tissue. GTAp63 mRNA level were determined by performing RT-PCR from total RNA that was isolated from mouse testes. The PCR primer were designed to bind specifically to exon U3 (mur p63 exon U3_forward primer) or exon 2 (mur p63 exon 2_reverse primer). Control PCR reactions contained either no template (water control) or non-transcribed RNA from a cDNA synthesis reaction without reverse transcriptase (-RT control). PCR products were loaded on an agarose gel, stained with ethidium bromide and visualized by UV illumination. The result is displayed in **figure 7.3**.

We detected two distinct PCR products at sizes of approximately 250 bp and 350 bp. The longer DNA fragment corresponds in size to the GTAp63 transcript that partially includes exon 1. The calculated length of this transcript was 344 bp. The PCR product with higher electrophoretic motility had a size of 241 bp and corresponds to the GTAp63 variant, in which exon U3 is directly fused to exon 2, omitting exon 1. The PCR amplification was specific since we did not observe any product in the control PCR reactions.

The result further indicates that, at least, in testicular tissue, both novel murine GTAp63 variants are expressed to equal mRNA levels (**figure 7.3**).

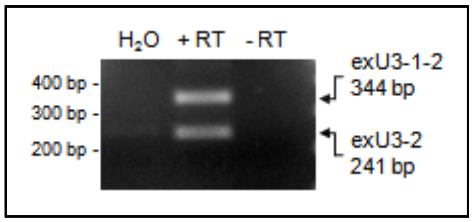

Figure 7.3: Novel TAp63 transcripts in murine testis
Murine testicular RNA was analyzed by RT-PCR using a primer pair that is specific for the Trp63 region from exon U3 to exon 2. Two products could be detected in the reaction with reverse transcriptase (+ RT), while no band was seen in control PCR reactions (- RT or water control). The detected PCR products correspond to Trp63 transcripts that have either exon U3 directly spliced onto exon 2, or additionally include part of exon 1.

7.4.2 TAp63 might affect testicular apoptosis upon irradiation of mice

The role of TAp63 in the induction of apoptotic pathways in murine male germ cells upon DNA damage has been controversially discussed.

While some published data argue against a function of TAp63 in the regulation of germ cell apoptosis in the testis (Suh et al, 2006), other authors suggested that TAp63 might be important for the onset of apoptosis in germ cells (Guerquin et al, 2009; Nakamuta & Kobayashi, 2003; Petre-Lazar et al, 2007; Petre-Lazar et al, 2006). p63 invalidation resulted in increased germ cell survival upon irradiation, at least in the fetal testis.

We aimed to investigate the implication of TAp63 in the apoptotic response of adult testicular germ cells upon irradiation. We hypothesized that a specific knockout of TAp63 isoforms might lead to a reduction in the sensitivity of adult germ cells towards γ-irradiation in male mice.

Before we started to irradiate TAp63 knockout mice, we performed irradiation experiments with wild-type SV129 mice. This mouse strain was chosen for initial irradiation experiments because the TAp63 knockout mice that we obtained from the lab of Elsa Flores, University of Texas MD Anderson Cancer Center, Houston, USA (Su et al, 2009), were back-crossed into the SV129 background.

Adult males at the age of 6-8 weeks were γ-irradiated with a single whole body dose of either 0.5 or 5 Gy. Mice were sacrificed at several times after the irradiation, ranging from 0h up to 6d post irradiation. Apoptosis of cells in the seminiferous epithelium was assayed at the single cell level using two different methods: immunostaining of cleaved caspase 3, which is indicative for activated caspase 3, and TUNEL labeling of DNA strand breaks that are a consequence of genomic DNA cleavage in late stage-apoptotic cells. For each sample and staining method 3 slides with each three tissue sections were analyzed and the percentage of the seminiferous tubules with at least three positive cells was calculated for each tissue section. Mean values and standard deviations were used to generate the graphs shown in **figure 7.4**.

We noticed a significant increase in the number of apoptotic cells that are located in basal regions of the seminiferous epithelium upon irradiation of adult mice. The percentage of seminiferous tubules that contained at least three apoptotic cells peaked at 24 h after irradiation and was decreased at later time points. Apoptosis was strongly reduced after 48 h and was back to the basal level 6 days post irradiation. As expected, the higher dose of 5 Gy elicited a stronger apoptotic response of germ cells, since the percentage of apoptotic tubules was increased to nearly 40% in comparison to less than 30% after 0.5 Gy. Moreover, upon irradiation with 5 Gy a marked increase in apoptosis was already detected at 12 h after irradiation.

Because the testicular germ cells of wild-type SV129 mice already showed a strong apoptotic response upon irradiation with 0.5 Gy, we decided to perform all other irradiation experiments with this lower dose. Tissues were then prepared 24 h after irradiation to analyse the apoptotic response of germ cells that either express or lack TAp63 proteins.

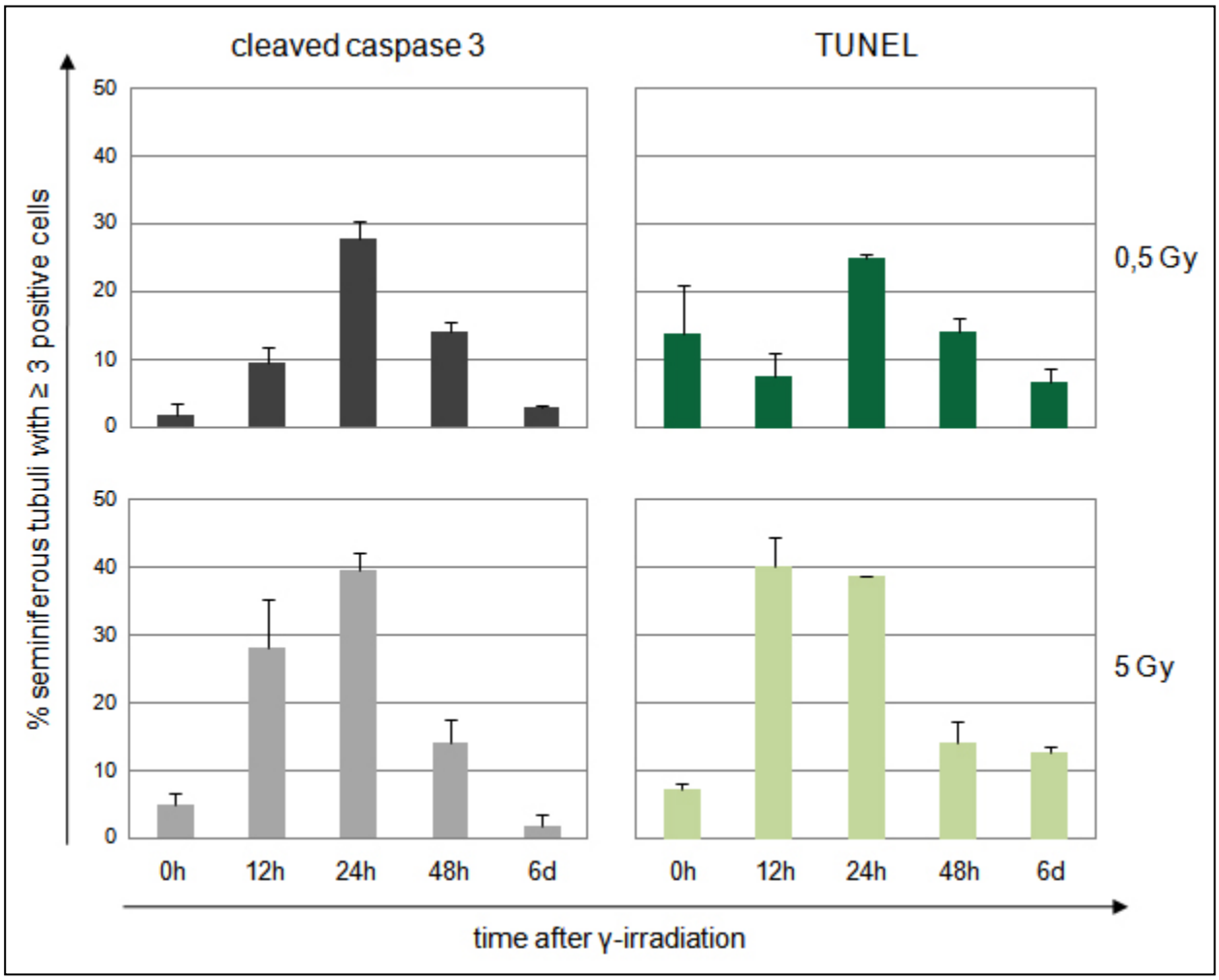

Figure 7.4: Apoptosis in the testes of irradiated mice
Analysis of apoptosis in testicular tissue of SV129 wt mice that were irradiated with a single dose of either 0.5 or 5 Gy. Murine testicles were isolated at indicated times after irradiation. Tissue sections were either immunostained with the cleaved caspase 3 antibody, or labeled with fluorescein-coupled dUTP in a TUNEL reaction. Apoptosis was determined by counting seminiferous tubules that contained at least three positive cells. Mean values and standard deviations from the staining of nine tissue sections for each sample are shown.

Next, we irradiated a 6 week-old TAp63 knockout mouse together with a wild-type littermate with a dose of 0.5 Gy. 24 h after the treatment mice tissues were prepared as already described above. Since liver cells are not very sensitive towards radiation-induced apoptosis, we also isolated and fixed liver tissue in addition to the testes of both mice. Apoptosis of adult testicular germ cells was again assessed by performing immunostaining of cleaved caspase 3 as well as TUNEL reactions, followed by calculation of the mean percentages of seminiferous tubules with ≥ three cleaved caspase 3 or TUNEL-positive germ cells (**figure 7.5**).

While roughly 20% of analyzed seminiferous tubules of the wild-type mouse contained three or more apoptotic cells upon irradiation, the TAp63 knockout showed less severe germ cell apoptosis. Ablation of TAp63 expression reduced the level of irradiation-induced testicular apoptosis by approximately 50 percent, as compared to irradiated wild-type testes (**figure 7.5 A**). The difference of apoptotic levels between wild-type and knockout testes was highly significant as shown by the p-values below 0.05 that were calculated by the Student`s t-test.
In addition, TAp63 knockout not only results in lower percentages of apoptotic tubules, but also dramatically decreased the total number of basal apoptotic cells lining the seminiferous tubules. Representative pictures from fluorescence microscopy are displayed in **figure 7.5 B**. While we even detected tubules with more than 20 TUNEL-positive cells in irradiated wild-type testis, we never saw tubules with such high numbers of late stage-apoptotic cells in irradiated TAp63 knockout testis.

In conclusion, our results argue in favor of a role of TAp63 in triggering apoptosis of male germ cells upon irradiation, thereby eliminating damaged germ cells.
These data must be further confirmed by repeated irradiation of adult male mice that do not express TAp63 isoforms.

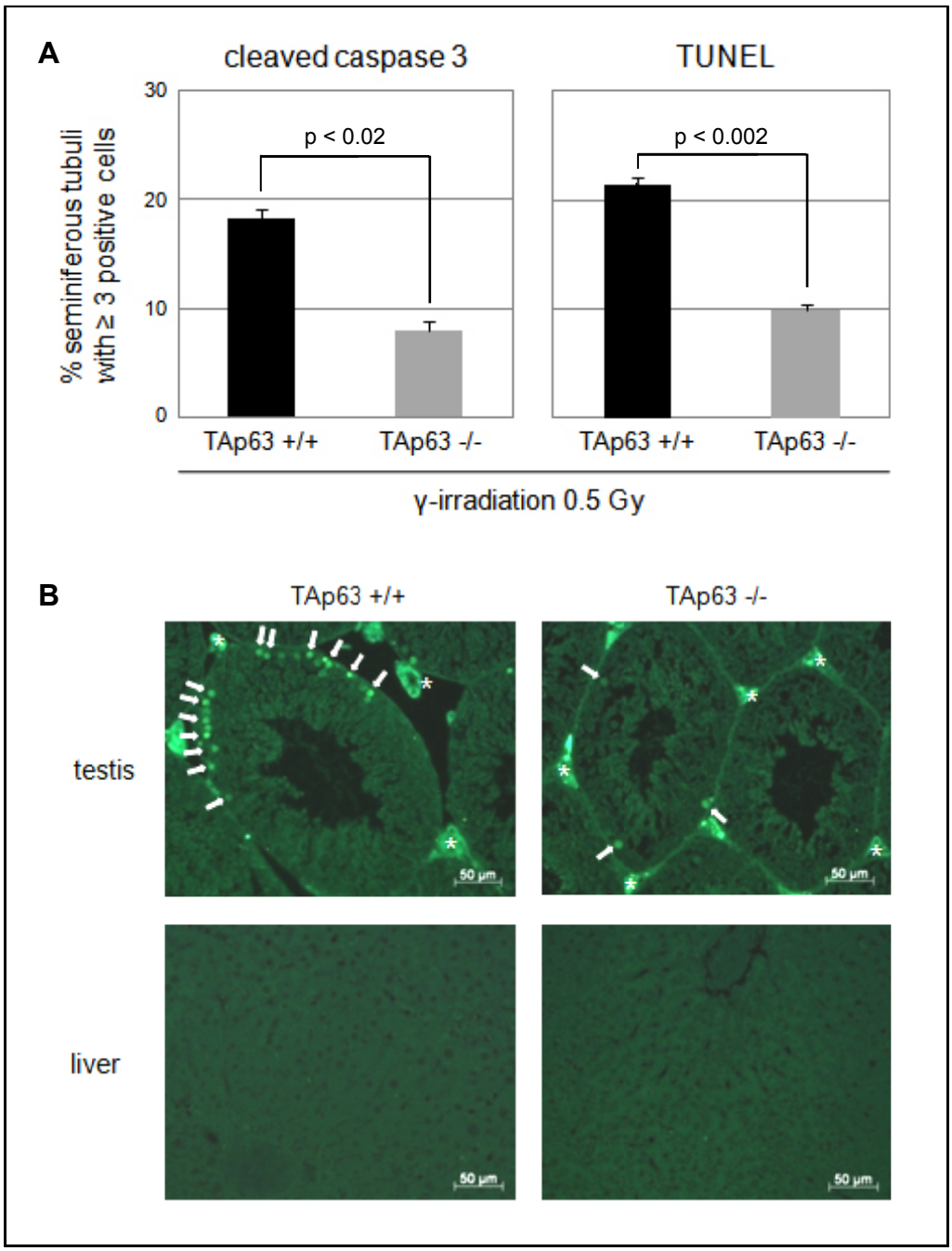

Figure 7.5: Apoptosis is decreased in TAp63 knockout mice upon γ-irradiation

A seven-week old TAp63 knockout mouse and its wild-type littermate were γ-irradiated with a single dose of 0.5 Gy. Testes of both mice were prepared 24 h after the irradiation. Paraffin-embedded tissue sections were either stained against cleaved caspase 3 or were used in a TUNEL reaction, which labels apoptotic cells containing fragmented DNA with fluorescein.

A. Apoptosis of irradiated testicular tissues was determined by counting seminiferous tubules that were positive for cleaved caspase 3 or TUNEL positive. Mean values of the percentages of the seminiferous tubules with ≥ three positive cells and standard error bars from nine analyzed sections from each mouse are shown. p-values calculated with the Student`s t-test indicate a significant difference between wild-type and knockout mice.

B. Representative pictures of the TUNEL staining of the testes isolated from the irradiated TAp63 knockout or wild-type mouse. TUNEL positive cells, indicated by white arrows, appear green due to incorporation of fluorescein-coupled dUTP during the labeling reaction. Unspecific TUNEL positivity is detected in Leydig cells in between the seminiferous tubules (asterisk). The lower panel show negative TUNEL staining of liver sections as control.

7.5 Discussion

In this part of the work we addressed two questions: First, does the mouse Trp63 locus contain hitherto unknown exons that are expressed in transactivating p63 transcripts associated with testicular tissue, as has been found in the human TP63 gene? Second, are TAp63 isoforms necessary to protect testicular germ cells by initiating apoptosis in response to severe DNA damage, thus ensuring genomic stability of male germ cells?

To answer the first question we performed RACE experiments from murine testicular tissue. Indeed, we found novel testicular Trp63 transcripts including the exon U3 that has been already identified in human GTAp63 transcripts (chapter 5.1). Our result from the murine RACE experiment is also in agreement with a previous study that described novel isoforms of the rat p63 ortholog KET (Bamberger & Schmale, 2001). The authors of this study found several tissue specific p63 transcripts with varying exons at their 5`- ends. One of the newly identified rat transcripts – termed TA1KET – corresponds to the murine transcript where exon U3 is directly spliced onto exon 2. Thus, we conclude that the human exon U3 is conserved throughout rodents. Bamberger and Schmale additionally detected another KET gene product, designated TA3KET, which is the major isoform in rat placenta, but is not expressed in human placenta. This indicates that different species possess a variety of TAp63 isoforms with diverse amino termini that are specifically expressed in distinct tissues. Our results further point in this direction since we observed a testicular splice variant of p63 including exon U3 and, in addition, a part of exon 1 that was neither amplified from human RNA (our data) nor detected in rat tissues (Bamberger & Schmale, 2001). The use of different amino termini in p63 isoforms might contribute to a fine-tuning of p63 function, leading to tissue-specific activities of p63 proteins. Further investigations have to be done to decipher the exact physiological consequences of the variety of p63 isoforms, especially in the context of germline fidelity and reproduction. Regarding this, it has to be addressed how the expression of different p63 gene products is achieved.

The second question dealt with the function of murine TAp63 isoforms as potentially important players in the protection of the male germline integrity upon severe DNA damage.

We provide evidence indicating that TAp63 contributes to the onset of apoptosis in adult murine germ cells that were exposed to γ-irradiation. Specific ablation of the TA forms of p63 in mice resulted in a markedly decreased apoptotic response of spermatogenic cells lining the seminiferous tubuli upon irradiation, as compared to wild-type littermates that retained TAp63 expression (**figure 7.5**). Since we only performed one experiment, we can only suggest that TAp63 is an essential apoptosis regulator of damaged germ cells. To statistically support our data we have to further irradiate several mice being homozygous for either the TAp63 wild-type or the knockout allel. In addition, treatment of TAp63 heterozygous mice could indicate whether there is a dose response effect of TAp63 ablation on the degree of testicular apoptosis.

Our observation correlates with the data presented by Guerquin *et al*. They recently showed that invalidation of the Trp63 gene in mice leads to increased germ cell survival upon γ-irradiation (Guerquin et al, 2009). However, loss of the homolog p53 had a similar effect on the apoptotic response of germ cells. In conclusion, p63 as well as p53 are implicated in the induction of apoptosis in severely damaged germ cells.

This redundancy in the function of p53 family proteins might also explain why we still detected some degree of apoptosis in irradiated mouse testes, even in the absence of TAp63.

In sum, we suggest that the function of TAp63 as a guardian of the male germ line, which has been already shown for primitive organisms such as the sea anemone *Nematostella vectensis* (Pankow & Bamberger, 2007), is also conserved in mice, leading to elimination of germ cells that evolved genomic instability.

8. Appendix B – supplementary tables

8.1 Consensus sequences of ERV9-subfamilies

```
I             TGAGAGGTGA CAGCGTGCTG GCAGCCCTCA CAGCCCTCGC TCGCTCTCGT CGCCTCCTCG GCCTCGGCGC CCATTCTGGC 80
II            TGAGAGGTGA CAGCATGCTG GCAGCCCTCG C--------- TCGCTCTCGG CGCCTCCTCG GCCTCGGCGC CCACTCTGGC
III           TGAGAGGTGA CAGCGTGCTG GCAGCCCTCG C--------- TCGCTCTCGG CGCCTCCTCG GCCTCGGCGC CCACTCTGGC
IV            TGAGAGGTGA CAACGTGCTA GCAGCCCTCG C--------- TCGCTCTCGG CGCCTCCTCG GCCTCGGCGT CCACTCTGGC
V             TGAGAGGTGA CAACGTGCTG GCAGCCCTCG C--------- TCGCTCTCGG CGCCTCCTCG GCCTCGGCGT CTGCTCTGGC
VI            TGAGAGGTGA CAGCGTGCTG GCAGCCCTCG CAGCCCTCGC TCGCTCTCGG CGCCTCCTCG GCCTCGGCGC CCACTCTGGC
VII           TGAGAGGTGA CAGCGTGCTG GCAGCCCTCA CAGCCCTCGC TCGCTCTCGG CGCCTCCTCG GCCTTGGCGC CCACTCTGGC
VIII          TGAGAGGTGA CAGCGTGCTG GCAGCCCTCG CAGCCCTCGC TCGCTCTCGG CGCCTCCTCG GCCTTGGCGC CCACTCTGGC
XIII          TGAGAGGTGA CAGCGTGCTG GCAGTCCTCA CAGCCCTCGC TCGCTCTCGG CGCCTCCTCT GCCTGGGCTC CCACTTTGGC
XIV           TGAGAGGTGA CAGCGTGCTG GCAGTCCTCA CAGCCCTCGC TCGCTCTCGG CGCCTCCTCT GCCTGGGCTC CCACTTTGGC
IX            TGAGAGGTGA CAGCGTGCTG GCAGTCCTCA CAGCCCTCGC TCGCTCTCGG CGCCTCCTCT GCCTGGGCTC CCACTTTGGC
GTAp63        TGAGAGGTGA CAGCGTGCTG GCAGTCCTCA CAGCCCTCGC TCGCTCTGGG CGCCTCCTCT GCCTGGGCTC CCACTTTGGT
X             TGAGAGGTGA CAGCGTGCTG GCAGTCCTCA CAGCCCTCGC TCGCTCTCGG CGCCTCCTCT GCCTGGGCTC CCACTTTGGC
XI            TGAGAGGTGA CAGCGTGCTG GCAGTCCTCA GAGCCCTCGC TTGCTCTCGG CACCTCCTCT GCCTGGGCTC CCACTTTGGC
XII           TGAGAGGTGA CAGCGTGCTG GCAGTCCTCA GAGCCCTCGC TTGCTCTCGG CACCTCCCCT GCCTGGGCTC CCACTTTGGT
Clustal Cons  ********** ** * ****  **** ****             * ***** *  * ***** *  **** ***   *   * ***

I             CGCGCTTGAG GAGCCCTTCA GCCCCCCGCT GCACTGTGGG AGCCCTTCTC TGGGCTGGCC GAGGCCGGAG CCGGCTCCCT 160
II            CGCGCTTGAG GAGCCCTTCA GCCCGCCGCT GCACTGTGGG AGCCCTTTCC TGGGCTGGCC GAGGCCGGAG CCGGCTCCCT
III           CGCGCTTGAG GAGCCCTTCA GCCCGCCGCT GCACTGTGGG AGCCCCTCTC TGGGCTGGCC GAGGCCGGAG CCGGCTCCCT
IV            CGCGCTTGAG GAGCCCTTCA GCCCGCCGCT GCACTGTGGG AGCCCCTCTC TGGGCTGGCC GAGGCCGGAG CCGGCTCCCT
V             CACGCTTGAG GAGCCCTTCA GCCCGCCGCT GCACTGTGGG AGCCCCTCTC TGGGCTGGCC GAGGCCGGAG CCGGCTCCCT
VI            CGCGCTTGAG GAGCCCTTCA GCCCGCCGCT GCACTGTGGG AGCCCCTTYC TGGGCTGGCC GAGGCCGGAG CCGGCTCCCT
VII           CGCGCTTGAG GAGCCCTTCA GCCCGCCGCT GCACTGTGGG AGCCCCTTTC TGGGCTGGCC AAGGCCGGAG CCGGCTCCCT
VIII          CGCGCTTGAG GAGCCCTTCA GCCCGCCGCT GCACTGTGGG AGCCCCTTTC TGGGCTGGCC AAGGCCGGAG CCGGCTCCCT
XIII          GGCACTTGAG GAGCCCTTCA GCCCGCCGCT GCACTGTGGG AGCCCCTTTC TGGGCTGGCC GAGGCCGGAG CCGGCTCCCT
XIV           GGCACTTGAG GAGCCCTTCA GCCCGCCGCT GCACTGTGGG AGCCCCTTTC TGGGCTGGCC AAGGCCGGAG CCGGCTCCCT
IX            GGCACTTGAG GAGCCCTTCA GCCCACCGCT GCACTGTGGG AGCCCCTTTC TGGGCTGGCC AAGGCCGGAG CCGGCTCCCT
GTAp63        GGCACTTGAG GAGCCCTTCA GCCCACTGCT GCACTGTGGG AGCCTCT-TC TGGGCTGGCC AAGGCCGGAG CCCGCTCCCT
X             GGCACTTGAG GAGCCCTTCA GCCCACCGCT GCACTGTGGG AGCCCCTTTC TGGGCTGGCC GAGGCCGGAG CCCACTCCCT
XI            GGCACTTGAG GAGCCCTTCA GCCCGCCGCT GCACTGTGGG AGCCCCTTTC TGGGCTGGCC GAGGCTGGAG CCCACTCCCT
XII           GGCATTTGAG GAGCCCTTCA GCCCCCCACT GCACTGTGGG AGCCCCTTTC TGGGCTGGCC GAGGCCGGAG CCCACTCCCT
Clustal Cons    *  ***** ********** **** *  ** ********** ****  *  * **********  **** **** **  ******

I             CRGCTTGCGG GGAGGTGTGG AGGGAGAGGC ACGGGCGGGA ACCGGGGCTG CGCGCGGCGC TTGCGGGCCA GCTAGAGTTC 240
II            CAGCTTGCGG GGAGGTGTGG AGGGAGAGGC GCGGGCGGGA ACCGGGGCTG CGCGCGGCGC TTGCGGGCCA GCGCGAGTTC
III           CTGCTTGCGG GGAGGTGTGG AGGGAGAGGC GCGGGCGGGA ACCGGGGCTG CGCGCGGCGC TCGCGGGCCA GCGCGAGTTC
IV            CTGCTTGCGG GGAGGTGTGG AGGGAGAGGC GCGGGCGGGA ACCGGGGCTG CGCGCGGCGC TCGCGGGCCA GCGCGAGTTC
V             CTGCTTGCGG GGAGGTGTGG AGGGAGAGGC GCGGGCGGGA ACCGGGGCTG CGCGCGGCGC TCGCGGGCCA GCGCGAGTTC
VI            CAGCTTGCGG GGAGGTGTGG AGGGAGAGGC GCGGGCGGGA ACCGGGGCTG CGCGCGGCGC TTGCGGGCCA GCGCGAGTTC
VII           CAGCTTGCGG GGAGGTGTGG AGGGAGAGGC GCGGGCGGGA ACCGGGGCTG CGCGCGGCGC TTGCGGGCCA GCGCGAGTTC
VIII          CAGCTTGCGG GGAGGTGTGG AGGGAGAGGC GCGGGCGGGA ACCGGGGCTG CGCGCGGCGC TTGCGGGCCA GCGCGAGTTC
XIII          CAGCTTGCGG GGAGGTGTGG AGGGAGAGGC GCGGGCGGGA ACCGGGGCTG CGCGCGGTGC TTGCGGGCCA GCGCGAGTTC
XIV           CAGCTTGCGG GGAGGTGTGG AGGGAGAGGC GCGGGCGGGA ACCGGGGCTG CGCGCGGTGC TTGCGGGCCA GCGCGAGTTC
IX            CAGCTTGCAG GGAGGTGTGG AGGGAGAGGC GCGAGCGGGA ACCGGGGCTG CGCGCGGCGC TTGCGGGCCA GCTGGAGTTC
GTAp63        CAGCTTGCAG GGAGGTGTGG AAAGAGAGGT GGGAGCGGGA ACTGGGGCTG CGCGCGGCGC TTCCGGGCCA GCTGGAGTTC
X             CAGCTTGCAG GGAGGTGTGG AGGGAGAGGC GCGAGCGGGA ACCGGGGCTG CGTGCGGCGC TTGCGGGCCA GCTGGAGTTC
XI            CAGCTTGCAG GGAGGTGTGG AGGGAGAGGC GCGAGCGGGA ACCGGGGCTG CGTGCGGCGC TTGCGGGCCA GCTGGAGTTC
XII           CAGCTTGCAG GGAGGTGTGG AGGGAGAGGC ACGAGCGGGA ACCGGGGCTG CGTGCGGCGC TTGCGGGCCA GCTGGAGTTC
Clustal Cons  * ****** * ********** *  ******    * ****** ** ******* ** **** ** *  ******* **  ******

I             CGGGTGGGCG TGRGCTTGGC GGGCCCCGCA CTCGGAGCGA CCGGCCGGCC CCGCCGGCCC CGGGCAGTGA GGGGCTTAGC 320
II            CGGGTGGGCG TGGGCTCGGC GGGCCCCGCA CTCGGAGCGG CCGGCCGGCC CCGCCGGCCC CGGGCAGTGA GGGGCTTAGC
III           CGGGTGGGCG TGGGCTCGGC GGGCCCCGCA CTCAGAGCGG CCGGCCGGCG CCGCCGGCCC CGGGCAGTGA GGGGCTTAGC
IV            CGGGTGGGCG CGGGCTCGGC GGGCCCCGCA CTCGGAGCGG CCGGCCGGCG CCGCCGGCCC CGGGCAGTGA GGGGCTTAGC
V             CGGGTGGGCG TGGGCTCGGC GGGCCCTGCA CTCGGAGCGG CCGGCCGGCG CCGCCGGCCC CGGGCAGTGA GGGGCTTAGC
VI            CGGGTGGGCG TGGGCTCGGC GGGCCCCGCA CTCGGAGCGG CCGGCCGGCC CCGCCGGCCC CGGGCAGTGA GGGGCTTAGC
VII           CGGGTGGGCG TGGGCTCGGC GGGCCCCGCA CTCGGAGCGG CCGGCCGGCC CCGCCGGCCC CGGGCAGTGA GGGGCTTAGC
VIII          CGGGTGGGCG TGGGCTCGGC GGGCCCCGCA CTCGGAGCGG CCGGCCGGCC CCGCAAGCCC CGGGCAGTGA GGGGCTTAGC
XIII          CGGGTGGGCG TGGGCTCGGC GGGCCCCGCA CTCGGAGCGG CCGGCCGGCC CCGCCGGCCC CGGGCAGTGA GGGGCTTAGC
XIV           CGGGTGGGCG TGGGCTCGGC GGACCCCGCA CTCGGAGCGG CCGGCCGGCC CCACCGGCCC CGGGCAGTGA GGGGCTTAGC
IX            CGGGTGGGCG TGGGCTTGGC GGGCCCCGCA CTCGGAGCGA CCGGCCGGCC CTGCCGGCCC CGGGCAATGA GGGGCTTAGC
GTAp63        CGGGTGGGCG TGGGCTTGGC GGGCTCTGCA CTCGGAACAG CCGGCCGGCC CCGCCGGCCC CAGGCAATGA GGGGCTTAGC
X             CGGGTGGGCG TGGGCTTGGC GGGCCCCGCA CTCGGAGCGA CCGGCCGGCC CTGCCGGCCC CGGGCAATGA GGGACTTAGC
XI            CGGGTGGGCG TGGGCTTGGC GGGCCCCGCA CTCGGAGCGA CCGGCCGACC CTGCTGGCCC CGGGCAATGA GGGACTTAGC
XII           CGGGTGGGCG TGGGCTTGGC GGGCCCCGCA CTCGGAGCGA CCGACCGACC CTGCTGGCCC CGGGCAATGG GGGACTTAGC
Clustal Cons  **********  * *** *** ** * * *** *** ** *   *** *** *  *  *  **** * **** **  *** ******
```

8.2 Sequences of members of the ERV9-subfamily IX

```
TP63-LTR       TGAGAGGTGA CAGCGTGCTG GCAGTCCTCA CAG-CCCTCG CTCGCTCTGG GCGCCTCCTC TGCCTGGGCT CCCACTTTGG 80
AC004004       TGAGAGGTGA CAGCGTGCTG GCAGTCCTCA CAG-CCCTCG CTTGCTCTCA GCGCCTCCTC TGCCTGGGCT CCCACTTTGG
AC005332a      TGAGAGGTGA CAGCGTGCTG GCAGTCCTCA CAG-CCCTCG CTCGCTCTCG GCGCCTCCTC TGCCTGGGCT CCCACTTTGG
AL021407b      TGAGAGGTGA CAGCGTGCTG GCAGTCCTCA CAG-CCCTCG CTCGCTCTCG GCGCCTCCTC TGCCTGGGCT CCCACTTTGG
AC004185       -GAGAGGTGA CAGCGTGCTG GCAGTCCTCA CAG-CCCTCG CTTGCTCTCC CCGCCTCCTC TGCCTGGGCT CCTACTTTGG
AC004000       TGAGAGGTGA CAGCGTGCTG GCAGTCCTCA CAG-CCCTCG CTCGCTCTCG GCGCCTCCTC TGCCTGGGCT CCCACTTTGG
AC000058       TGAGAGGTGA CAGTGTGCTG GCAGTCCTCA CAG-CTGTCG CTCGCTCTCG GCACCTCCTC TGCCTGGGCT CCCACTTTGG
Z84484         TGAGAGATGA CAGCGTGCTG GCAGTCCTCA CAG-CCCTCG CTCGCTCTCG GCACCTCCTC TGCCTGGGCT CCCACTTTGG
AC003670       TGAGAGGTGA CAGCGTGCTG GTAGTCCTCA CAG-CCCTCG CTCGCTCTCT GTGCCTCCTC TGCCTGGGCT ACCACTTTGG
AC004220       TGAGAGGTGA CAGCGTGCTG GCAGTCCTCA CAGGCCCTTG CTCTCTCTCG GCACCTCCTC TGCCTGGGCT CCCACTTCGG
AC003029       TGAGAGGTGA CAGTGTGCTG GCAGCCCTTG CAG-CCCTCG CTCACTCTTG GCGCCTCCTC TGCCTGGGCT CTCACTTTGG
AC002451       TGAAAGGTGA CAGCGTGCTG GCAGCCCTCA CAG-CCCTCG CTCACTCTCG GGGCCTCCTC TGCCTGGGCT CCCACTTTGG
AC003043       TGAGAGGTGA CACTGTGCTG GCAGTCCTCA CAG-CCCTCG CTCGCTCTCG GGGACTCCTC TGCCTGGGCT CCCACTTTGG
Z82975         TGAGAGGTGA CAGCGTGCTG GCAGTCCTCA CAG-CCCTCG CTCACTCTCG GCGCCTCCTC TGCCTGGGCT CCCACTTTGG
AL031785       TGAGAGGTGA CAGCGTGCTG GCAGTCCTCA CAG-CCCTCG CTCCCTCTCG GCGCCTCCTC TGCCTGGACT CCCACTTTGG
AC006271       TGAGAGGTTA CAGCGTGCTG GCAGTCCTCA CAG-CCCTCG CTCGCTCTCA GCGACTCCTC TGCCTGGGCT TCCACTTTGG
AC002544       TGAGAGGTGA CAGCGTGCTG GTAGTCCTCA CAG-CCCTCG TTCGCTCTTG GCGCCTCCTC TGCCTGGGCT CCCACTTTGG
Z81450         TGAGAGGTGA CAGCGTGCTG GCAGTCCTCA CAG-CCCTCG CTCGCTCTCA GCGCCTCCTC TGCCTGGGCT CTCACTTTGG
AC004973b      TCAGAGGTGA CAGCATGCTG GCAGTCCTCA CAG-CCCTCA TTCGCTCTTG GTGCCTCCTC TGCCTGGGCT CCCACTGTGG
AL022726a      TGAGAGGTGA CAGCGTGCTG GCAGTCCTCA CAG-CCCTCG CTCGCTCTCG GGACCTTCTC TGCCTGGGCT CCCACTTTGG
Z99290         TGAGAGGTGA CAGCGTGCTG GCAGTCCTCA CAG-CCCTCG TTCGCTCTGG GCGCCTCCTC TGCCTGGGCT CCCACTTTGG
AF001550       TGAGAGGTGA CAGCGTGCTG GCAGTCCTCA CAG-CCCTCG CTCGCTCTCG GCGCCTCCTC TGCCTGGGCT CCCACTTTGG
AC002477       TGAGAGGTGA CAGCGTGCTG GCAGTCCTCA CAG-CCCTCG CTCGCTCTCC GCGCCTCCTC TGCCTGGGCT CCCACTTCGG
AL031073       TGAGAGGTGA CAGCGTGCTG GCAGTCCTCA CAG-CCCTCG CTCTCTCTCT GCGCCTCCTC GGCCTGGGCT CCCACTTTGG
AC004783       TGAGAAGTGA CAGCGTGCTG GCAGTACTCA TAG-CCCTCC CTCGCTCTCG GCGCCTCCTC TGCCTGGGCT CCCACTTTGG
AC005066b      TGAGAGGTGA CAGCGTGCTG GCAGTCCTCA CAG-CCCTCG CTCGCTCTCG GCGCCTCCTC TGCATAGGCT CCCACTTTGG
AC004866       TGAGAGGTGA CAGCGTGCTG GCAGTCCTCA GAG-CCCTCG CTCGCTCTAG GTGCCTCCTC TGCCTGGGCT CCCACTTTGG
AL024506       TGAGAGGTGA CAGCGTGCTG GCAGTCCTCA CAG-CCCTAG CTCGCTCTCG GCGCCTCCTC TGCCTGGGCT CCCACTTTGG
X83497         TGAGAGGTGA CAGCGTGCTG GCAGTCCTCA CAG-CCCTCG CTCGCTCTCG GCGCCTCCTC TGCCTGGG-T CCCACTTTGG
AC004212a      TGAGAGGTGA CAGCCTGCTA GCAGTCCTCA CAG-CTCTCA CTCGCTCTGG GCGCCTCCTC TGCCTGGGCT CCCACTTTGG
AC004197a      TGAGAGGTGA CAGCGTGCTG GCAGTCCTCA GAG-CCCTCG CTTGCTCTCA GCACCTCCTC TGCCTGGGCT CCCACTTTGG
Z72004         TGAGAGGTGA CAGCATGCTG GCAGCCCTTA CAG-CCCTCG CTCGCTCTCC GCGCCTCCTC TGCCTGGGCT CCCACTTTGG
AL022067       TGAGAGGTGA CAGCGTGCTG GCAGTCCTCA CAG-CCCTTG CTCGCTCTCG GCGTCTCCTC TGCCTGGGCT CCTACTTTGG
Z99128         TGAGAGGTGA CAGCGTGCTG GCAGTCCTCA CAG-CCCTCG CTTGCTCTCG GCGCTTCCTC TGCCTGGGCT CCCATTTTGG
X14975         TGAGAGGTGA CAGCGTGCTG GC-GTCCTCA CAG-ACCTTG CTTGCTCTCG GTGCCTCCTC TGCCTGGGCT CCCACTTTGG
Z75746         TGAGAGGTGA CAGCGTGCTG GCAGTCCTCA CAG-CCCTCG CTTGCTCTCG GCGCCTCCTC TGCCTGGGCT CCCACTTTGG
AC005392       TGAGAGGTCA CAGCATGCTG GTAGTCCTCA CAG-CCCTCG CTCGCTCTCG GTGCCTCCTC TGCCTGGGCT CCCACTTTGG
AC002326b      ---------- -TGAGAGGTG ACAGCCCTCA CAG-CCCTCG CTTGCTGTCC ACGCCTCCTC TGCCTGGGCT CCCACTTTGG
Clustal Cons                     * *     *  **    **    *    *  ** *        * ***  ** * *  *    * *  **

TP63-LTR       TGGCACTTGA GGAGCCCTTC AGCCCACTGC TGCACTGTGG GAGCCTCTT- -CTGGGCTGG CCAAGGCCGG AGCCCGCTCC 160
AC004004       CGGCACTTGA GGAGCCCTTC AGCCCACCAC TGCACTGTGG GAGCCCCTT- TCTGGGCTGG CCAAGGCCGT AGCCCGCTCC
AC005332a      TGGCACTTGA G---CCCTTC AGCCCACCGC TGCACTGTAG GATCCCCTT- TCTAGGCTGG CCAAGGCGAG AGCCGGCTCC
AL021407b      TAGCACCTGA GAAGCTCTTC AGCCCACCAC CGCACTGTGG GAGCCCCTT- TCTGGGCAGG CCAAGGCCGG AGCCGGCTCC
AC004185       CGGCACTTGA GGAGCCCTTC AGCCCTCCGC TGCACTGTGG GAGCCCCTT- TCTGGGCTGG CCAAGGCCGG AGCCCTCTCC
AC004000       CGGCACTTGA GGAGCCCTTC AGCCCACCAC TGCATTGTGG GAGCCCCTT- TCTGGGCTGG CCAAGGGCAG AGCCGGCTCC
AC000058       CGGCACTTGA GGAGCCCTTC AGCCCACCGC TGCACTGTGG GAGCCCCTT- TCTGGGCTGG CCAAGGCCAG AGCCGGCTCC
Z84484         CGGCACTTGA GGAGCCCTTC ATCCCACCGC TGCACTGTGG GAGCCCCTT- TCTGGGCTGG CCAAGGCCAG AGCCGGCTCC
AC003670       CAGCACTTGA GGAGCCCTTC AGCCCACTGC TGCACTGTGG GAGCCCCTT- TCTGGGCTGG CCAAGGCCGG AGCCTGCTCT
AC004220       TGGCACTTGA GGAGCCCTTC AGCCCACCAC TGCACTGTGG GAGCCCCTT- TCTGGGCTGG CCAAGGCCGG AGCCAGCTCC
AC003029       TGGCACTTGA GGAGCCCTTC AGCCCACCAC TGCACTGTGG GAGCCCCTT- TCTGGGCTGG CCAAAGCCGG AGCTGGCTCC
AC002451       CAGCACTTGA GGAGCCCTTC AGCCCACCGC TGCACTGTGG GAGCCCTTT- TCTGGGCTGG CCAAGGCGGG AGCGGGCTCC
AC003043       CGGCACTTGA GAAGCCCTTC AGCCCACCGC TGCACTGTGG GAGCCCCTT- TCTGGGCTGG CCAAGACCGG AGCCAGCTCC
Z82975         CGGCACTTGA GGAGCCCTTC AGCCCGCCAC TGCACTGTGG GAGCCCCTT- CCTGGGCTGG CCGAGCCCAG AGC-------
AL031785       CGGCACTTGA GGAGCCCTTC AGCCCACCGC TGCACCCTGG GAGCCTCTT- TCTGGGCTGG CCAAGACCGG AGCCGGCTCC
AC006271       CGGCACTTGA GGAGCCCTTC AGCCCACCGC TGCACTGTGG GAGCCCCTT- TCTGGGCTGG CCAAGGCGGG AGCCGGCTCC
AC002544       CGGCATTTGA GGAGCCCTTC AGCCCACCAC TGCTCTGTGG GAGCCCCTT- TCTGGGCTGG CCAAGGCCGG AGCCAGCTGC
Z81450         TGGCACTTGA GGAGCCCTTC AGCCCACCAC TGCACTGTGG GAGCCCCTT- TCTGGGCTGG CCAAGGCCGG AGCCGGCTCC
AC004973b      CGGCACTTGA GGAGCCCTTG AGCCCACCAC TGCCCTGTGG GATCCCCTT- TCTGGGCTGG CCAAGGCCAG AGCCGGCT-C
AL022726a      CAGCACTTGA GGAGCCCTTA AGCCCACCGC TGCACTGTGG GAGCCCCTT- TCTGGGCTGG TCAAGGCCGG AGCCGGCTCC
Z99290         CGGCACTTCA GGAGCCCTTC AGCCCACCAC TGCACTGTGG GAGCCCCTT- TCTGGGCTGG CCAAGGCCAG AGCCGGCTCC
AF001550       CGGCACTTGA GGAGCCCTTC AGCCCACCGC TGCACTGTGA GAGCTCCTT- TCTGGGCTGG GCAAGGCCGA AGCCGGCTCC
AC002477       CGGCACTTGA GGAGGCCTTC AGCCCACCAC TGCACTGTGG GAGCCCCTT- TCTGGGCTGG CCAAGGCAGG AGCCGGCTCC
AL031073       CGGCACTTGA GGAGCCCTTC AGCCCACCGC TGCACTGTGG GAGCCGCTT- TCTGGGCTGG CGAAGGCCGG AGCCGGCTCC
AC004783       CGGCACTTGA G---CCCTTC AGCCCACCGC TGCTCTGTGG GAGCCCCTT- TCTGGGCTGG CCAAGGCCGG AGCCCACTCC
AC005066b      CGGCACTTGA GGAGCCCTTC AGCCCACCGC TGCGCTGTGG GAGCCCCTT- TGTGGGCTGG CCAAGGCCGG AGCCCACTCC
AC004866       CGGAAATTGA GGAGACCTTC AGCCCACCGC TGCACTGTGG GAGCCCCTT- TCTGGGCTGG CCAAGGCCGG AGCCCGCTCC
AL024506       CGGCACTTGA GGAGCCCTTC AGCCCACCGC TGCGCTGTGG GAGCCCCTT- TCTGGGCCGG CCAATACCGG AGCCGGCTCC
X83497         CGGCACTTGA GGAGCCCTTC AGCCCACTGC TGCACTGTGG GAGCCCTTTA CCTGGGCTGG CCAAGGCCGG AGCCGGCTCC
AC004212a      CGGCATTTGA GGAGCCCTTC AGCCCACCGC TGCACTATGG GAGCCCCTT- TCTGGGCTGG CCAAGGCCAG AGCCGGCTCC
AC004197a      CGGCACTTGA GGAGCCCTTC AGCCCACCGC TGCACTGTGG GAGTCCCTT- TCTGGGCTGG CCGAGGCCAG AGCCGGCTCC
Z72004         CAGCACTTGA GGAACCCTTC AGCCTGCCGC TGCACTGTGG GCGCCCCTT- TCTGGGCTGG CCAAGGCCAG AGCCGGCTCC
AL022067       GGGCACTTGA G---CCCTTC AGCCCACCGC TGCACTGTGG GAGCCCCTT- TCTGGGCTGG CCAAGGCTGG AGCCGGCTCC
Z99128         CGGCACTTGA GAAGCCCTTC AGCCCACCGC TGCACTGCGG GAGCCCCTT- TGTGGGCCGG CCAAGACCGG AGCCGGCTCC
X14975         CAGCACTTGA GAAGCCTTTC AGCCCGCCGC TGCACTGTAG GAGCCCCTT- TCTGGGCTGG CCAAGGCCGG AGCCGGCTCC
Z75746         CAGCACTTGA GGAGCCCTTC AGCCCACCGC TGCACTGTGG GAGCCCCTT- TCTGGGCTGG CCAAGGCCAG AGCCGGCTCC
AC005392       CAGCACTTGA GGAGCTCTTC AGCCCACCGC TGCACTGTGG GAGCCCCTT- TCTGGGCTGG CCAAGGCCAG AGCCAGCTCC
AC002326b      CAGCACTTGA GGAGCCCTTC AGCCCGTCTC TGCACTCTGG GAGCCCCTT- TCTGAGCTGG CCAAGGCCGG AGCCGGCTCC
Clustal Cons     * *  * * *      **  * **     *  **        *      **    *  ** **    *       ***
```

```
TP63-LTR       CTCAGCTTGC AGGGAGGTGT GGAAAGAGAG GTGGGAGCGG GAACTGGGGC TGCGCGCGGC GCTTCCGGGC CAGCTGGAGT 240
AC004004       CTCAGCTTGC AGGGAGGTGT GGAGGGAGAG GCGCGAGCGG GAACCGGGGC TGCGCGTGGC ACTTGCGGGC CAGCTGGAGT
AC005332a      CTCGGCTTGC AGGGAGGTGT GGAGGGAGAG GCGCGAGCGG GAACTGGGGC TGCGTGCTGC GCTTGTGGGC CAGCTGGAGT
AL021407b      CTCAGCTTGC AGGGAGGTGT GAAGGGAAAG GCGCGAGCGG GAACGGGGGC TGCGCGCGGC GATTGCGGGC CCGCTGGAGT
AC004185       TTCAGCTTGC GGGGAGGTGT GGAGGGAGAG GCGCGAGCGG GAACCGGGGC TGTGTGCCGC GCTTGCCGGC CAGCTGGAGT
AC004000       CTCAGCTTGC AGGGAGGTGT GGAGGGAGAG GCGCGAGCAG GAACCGGGGA TGCATGAGGC GCTTGCGGGC CAGCTGGAGT
AC000058       CTCAGCTTGC AGGGAGGTGT GGAGGGAGAG GCGCCAGCGG GAACCGGGGC TGCGCACGGC GCTTGCGGGC CAGCTGGAGT
Z84484         CTCAGCTTGA AGGGAGGTGT GGAGGGAGAG GCACGAGCGG GAACTGGGGC TGTGCGCGGC GCTTGCGGGC CAGCTGAACT
AC003670       CTCAGCTTGC AGGGAGGTGT GGAGGGAGAG ACGCCAGTGG GAACCGGGGC TGCGCGCCGC CCTTGCGGGC CAGCTGGAGT
AC004220       CTCAGCTTGC AGGGAGGTGT GGAGGGAGAG GCGTGAGAGG GAACTGGGGC TGCGCATGGC ACTTGAGGGC CAGTTGGAGT
AC003029       CTCAGCTTTC AGGGAGGTGT GGAGGGAGAG GCGCGAGCAG GAACCCGGGC TGCGCGCGGG GTTTGCGGGC CAGCTGGAGT
AC002451       CTCAGCTTGC AGGGAGGTGT GGAGGGAGAG GCGGGAGCGG GAACCGGGGC TGCGCGCTGC ATTTGCGGGC CAGCTGGAGT
AC003043       CTTAGCTTGC AGGGAGGTGT GGAGGGAGAG GCCCAAGCGG GAACCCGGGC TGCGCTCGCT GCTTGCGGGC CAGCTGGAGT
Z82975         --CGGCTTGC TGGGAGGTGT GGAGGGAGAG GTGCGAGCGG GAACCAGGGC TATGCGCGGC GCTTGCGGGC CAGCTGGAGT
AL031785       CTCAGCTTGC AGGGAGGTGT GGAGGGAGAG GCGCGAGCGG GAACCGGGGC TGCGCGCGGC GCTTGCGGGC CAGCTGGAGT
AC006271       CTCAGCTTGG TGGGAAGTGT GGAGGGAAAG GCGCGAGCGG GAACCGGGGC TGCGCGCGGC GCTTGCGGGC CCGCTGGAGT
AC002544       CTTAGCTTGC GGGGAGGTGT GGATGGAGAG GCACGAGTGG GAAGCGGGGC TGCGCGCGGC GCTTGCGGGC CAGCTGGAGG
Z81450         CTCAGCTTGC GGGGAGGTGT GGAGGGAGAG GCGCGAGCGG GAACCGCGGC TGCATGCG-- -CTTGCAGGC CAGCTGGAGT
AC004973b      CCCAACGTGG AAGGAGGTGT GGAGGGAGAG GCACCAGTGG GAACCGGGGC TGCACGCAGC GTTTGCAGGC CAGCTGGAGT
AL022726a      CTCAGCTGGC AAGGAGGTGT GGAGAGAGAG GCGCGAGCGG GAACCAGGGC TGCGCGCGGG GCTTGCAGGC CAGCTGGAGT
Z99290         CTCAGCTTGC AGGGAGGTGT GGAGAGAGAG GCGCGAGCGG GAACCGGGGC TGCGCAGGGC GCTTGCGGGC CAGCTGGAGT
AF001550       CTCAGCTTGC AGGCAGGTGT GGAGGGAGAG GCGCGAGCGG GAACCCGGGC TGCGCACGGC GCTTGCGGGC CAGCTGGAGT
AC002477       ---------- AGGGAGGTGT GGAGGGAGAG GCGCCAGCGG GAACCGGGGC TGCGCGCAGC GCTTGCGGGC CAGCTGGAGT
AL031073       CTCAGCTTGC AGGGAGGTGT GGAGGGAGAG GCGCTAGCGG GAACCGGGGC TGCACGCAGC GCTGGCGGGC CAGCTGGAGT
AC004783       CTCAGCTTAC AGGGAGGTGT GGAGGGAGAG GCGCCAGTGG GAACCGGGGC TGCGCCCGGC GCTTGCGGGC CAGCTGGAGT
AC005066b      CTCAGCTTGC AGGGAGGTGT GGAGGGAGAG GCGAGAGCGG GAACCAGGGC TGTGTGCGGC ACTTGCGGGC CAGCTGCAGT
AC004866       CTTAGCTTGC AGGGAGGTGT GGGGGGAGAG GCACGAGCGA GAACCAGGGC TGCGCGTGGC GCTTGCGGGC CAGCTGCAGC
AL024506       CTCAGCTTGC AGGGAGGCGT GGAGGGAGAG GCGCGAGCGG GAACCGGGGC TGCGCGCGGC TCTTGCGGGC CAGCTGGAGT
X83497         CTCAGCTTGC AGGGAGGTGT GGAGGGAGAG GAAAGAGCGG GAACCCGGGC TGCACGCGGC ACTTGCGGGC CAGTTGGAGT
AC004212a      CTCAGCTTGC AGGGAGGTGT GGAGGGAGAG GCGCGAGC-G GAACCGGGGC TGCGTGCAGT GCTTGCGGGC CAGCTGGAGT
AC004197a      CTCAGCTTGC AGGGAGGTGT GGAGGGAGAG GTGCGAGCAG GAACCGGGAC TGTGCGCGGC GCTTGCGGGC CAGCTGCAGT
Z72004         CTCAGCTTGC AGGGAGGTGT GGAGGGAGAG GCGCCAGCGG GAACCGGGGT TGCGTGCGGC GCTTGCGGGC CAGCTGGAGT
AL022067       CTCAGCATGC AGGGAGGTGT GGAGGGAGAG GCGCGAGCGG GAACCGGGGA TGTGCGCGGC GCTTGCGGGC CAGCTGGAGT
Z99128         CTCAGCTTGC AGGGAGGTGT GGAGGGAGAG GAGCGAGGGG GAACCGGGGC TGCACGCGGC GCTTTCGGGC CAGCTGGAGT
X14975         CTCAGCTTGC AGGGAGGTGT GGAGGGAGAG GCGCGAGCGG GAACCTGGGC TGCGGGCGGT TC-------- CAGCTGGAGT
Z75746         CTCAGCTTGC AGGAAGGTGT GGAGGGAGAG GCGCAAGTGG GAACGGGGGC TGGACGCGGC GCTTGCGGGC CAGCTGGAGT
AC005392       CTCAGCTTGC AGGGAGGTGT GGAGGGAGAG GCGCCAGC-G GAACCGGGGC TGCGCGTGGC GCTTGCGGGC CAGCTGGAGT
AC002326b      CTCAGCTTGA AGGGAGGTGT GGAGGGAGAG GCGCGAGTGG CAACCGAGGA TGCGCGAGGC GCTTGCGGGC CAGCTGGAGT
Clustal Cons                * * * ** *    ** **      **     **    *   *                     * * ** *

TP63-LTR       TCCGGGTGGG CGTGGGCTTG GCGGGCTCTG CACTCGGAAC AGCCGGCCGG CCCCGCCGGC CCC---AGGC AATGA---GG 320
AC004004       TCCGGGTCGG CGTGGGCTTG GCAGGCCCTG CACTTGGAAC AACTGACCGG CCATGCCGGC CCC---AGGC AATGA---GG
AC005332a      TCCGGGTGGG CGTGGGCTTG GCGGGCCCCG CACTCGGAGC AGCCAGCTGG CCCTGCGGGC CCC---GGGC AATGA---GG
AL021407b      TCCGGGTGGG CGTGGGCTTG GCGGGCCCCG CACTCTGAGG AGCCAGCCGG C--------- ---------- ----------
AC004185       TCCGGGTGGG CGTGGGCTTG GCGGGCCCCG CACTCGGAGC AGCCGGCCAG CCCTGCTGGC CCC---TGGC AATGA---GG
AC004000       TCCGGGTGGG CGTGGGCTTG GCGGGCCCCG CACTCGGAGC AGCCGGCCAG CCCTGCCGGC CCT---GGGG AATGA---GG
AC000058       TCCGGGTGGG CGTGGGCTTG GCGGGCCCCG CACTCGGAGC AGCCGGCCAG CCCTGCAGGC CCT---GGGC AATGA---GG
Z84484         TTCGGGTGAG CGTGGGCTTG GCGGGTCCCG CACTCGGAGC AGCCGGCCGG CCCTGCCAGC CCC---GGGC AATGA---GG
AC003670       TCCGGGTGGG CATGGGCTTG GCGGGCCCTG CACTCTGAGC AGCTGGCCGG CCCTGCCGGC CCC---GGGC AATGA---GG
AC004220       TCCGGGTGGG TGTGGGCTTG GTGGGCCCCA CACTCGGAGC AGCCGGCGGG CCCTACCAGC CCC---GGGC AATGA---GG
AC003029       TCCAGGTGGG CGTGGGCTTG GCAGTCCCCA CACTTGGAGT GGCCGGCCAG CCCTGCCGGC CCC----GGC AATGA---GG
AC002451       TCCGGGTGGG TGTGGGCTTG GCGGGCCCCA CACTCGGAGC GGCCGGCCGG CCAACCCTGC CCCCCGGGAC AATGA---GG
AC003043       TCCGGGTGGG CGTGGGCTTG GCGGGCCCCG CACTCGGAGC AGCCAGCCGG CCCTGCCGGC CCC---GGGC AATGA---GG
Z82975         TCTGGGTGGA CATGGGCTTG GCGG-CCCCG TACTTGGAGA GGCCCGCCGG CCCTGCCAGC CCC---GGGC AATGA---GG
AL031785       TCCGGGTGGG CGTGGGCTTG GCGGGCCCCG CACTCGGAGC AGCCGGCC-- --CTGCCGGC CCC---GGGC AATGA---GG
AC006271       TCCGGGTGGG CGTGGCCTTG GCGGGCCCCG CACTCGGAGC AGCAGGCCGG C-CTGCCGGC CCT---GGGC AATGA---GG
AC002544       TCCGAGTGGG CGTGGGCTTG GCGGGCCCTG CACTAGGAGC CACCAGCCGG CCCTGCCAGC CCC---GGGC AATGA---GA
Z81450         CCCGGGTGGG CGTGGGCTTG GTGGGCCCGG CACTCAGAGC AGCCGGCCAG CCCTGCCGGC CGC---GGGC AATGA---GG
AC004973b      TCCGGGTGGG CGTGGGCTTG GCGGGCCCCG CACTCGGAGC AGACGGCTGG CCCGGCCGGC CCC---GGGC AATGA---GG
AL022726a      TCCGCGTGGG CGTGGGCTTG GCGG-CCCCG CACTCGGAGC AACCGGCCGG CCCTGCCGGC CCC---GGGC AATGA---GG
Z99290         TCCGGGTGGG CGTGGGCTTG GCGGGCCCCG CACTCG-AGC AGCGGGCCGG CCCTGCCGGC CCC---GGGC AATGA---GG
AF001550       TCCGGGTGGG CGTGGGCTTG GCGGGCCCCG CACTGGGAGC AGCCAGCTGG CCCTGCCGGC CCC---GGGC AATGA---GG
AC002477       TCCGGGTGGG CGTGGGCTTG GCGGGCCCCG CACTCGGAGC AGCCGGCCGG CCCTGCCGGC CCC---GGGC AATGA---GG
AL031073       TCCGGGTGGA CGTGGGCTTG GCGGGCCCCG CACTCGGAGC AGCCGGCTGG CCCTGCCGGC CCC---GGGC AATGA---GG
AC004783       TCCGGGTGGG CGTGGGCTTG GCGG-CCCCG CACTCAGAGC AGCCGGCCGG CCCTGTCGGC CCC---AGGC AATGA---GG
AC005066b      TCCGGGTGGG CGTGGGCTTG GCGGGCCCCG CACTCGGAGC AGCCGGCTGG CCCTGCTGGC TCC---AGGC AATGA---GG
AC004866       TCCGGGTGGG CATGGGCTTG GCGG-CCACG CACTCGGAGC AGCCGGCCGG CCCTGCTGGC CCT---GGGC AGTGA---GG
AL024506       TCCGGGTGGG CGTGGGCTTG GCGGGCCCCG CACTCGGAGC AGCC---GGG CCCTG----- -------GGC AGTGA---GG
X83497         TCAGAGTGGG CATGGGCTTG GCGGGCCCCA CACTCGGAGC AGCC---CGG CCCTGCCGGC CCC---AGGC AATGA---GG
AC004212a      TCCGGGTGGG CGTGGGCTTG GCGGGCCCCG CACTCGGAGC AGCCGGCCGG CCCTGCCAGC CCC---AGGC AGTGA---GG
AC004197a      TCCAGGTAGG CGTGGGCTTG GCGG-CCCCG CACTCGAAGC AGCCAGCGGG CCCTGCAGGC CCC---GGGC AGTGA---GG
Z72004         TCCGGGTGGG CGTGGGCTTG GCGGGCCCCG CACTCTGAGC GGCCGGCTGG CCCTGCCG-C CCC---GGGC AATGA---GG
AL022067       TCCGGGTGGG TGTGGGCTTG GCGGACCCCG CACTCGGAGC AGCCGGCCGG CCCTGCCGGC CCC---GGGC AATGA---GG
Z99128         TCCAGGTGGG CGTGGGCTTG GCGGGCCCTG CACTCGGAGC AGCCAGCCGG CCCTGCTGGC CCC---GGAC AATGAGGAGG
X14975         GCAGGGTGGG CGTGGGCTTG GCGGGCC-TG CACTCGGAGC AGCCAGCCGG CCCTGCCGGC CCC---GAGC AATGA---GA
Z75746         TCCAGGTGGG CGTGGGCTTG GCAGGCCCCG CACTCAGAGC AGCCAGCTGG CCTTGCCGGC CCC---AGGC AATGA---GG
AC005392       TCCGGGTGGG CGTGGGCTTG GCAGGCCTCG CACTCGGAGC AGCCGGCTGG CCCTGCTGGC CCC---AGGC AATGA---GG
AC002326b      TCCGGGTGGG TGTGGGCTTG GCAGGCCCTG CACTCGGAGC GGCCGGCTGG CCCTGCCGGC CTC---AGGC AATGA---GA
Clustal Cons        **      *** **** *  *        ***   *
```

```
TP63-LTR       GGCTTAGCAC CCGGGCCAGC AGCTGTGGAG GG-TGTACTG GGTCCCCCAG CAGTGCCAGC CCACCAGCGC TGCGCTCG-- 400
AC004004       GGCTTAGCAC CTGGGCCAAC GGCTGAGGAG GG-TGTACTG GGTCTCCCAG CAGTGCCAGC CCATCGGCAC TGTGCTCG--
AC005332a      GGCTTAGAAC CCGGGCCAGC AGCTGCGGAG GG-TGTACTA GGTCCCTCAG CAGGGCCAGC CCACCAGCAC TGCACTCG--
AL021407b      -------AAC CCGGGCCAGC GGCTGCGGAG GG-TGTACTG GGTCCCCCAG CAGTGCCGGC CCACCGGCGC TGCGCTCGGT
AC004185       GACTTAGCAC CCGGGCCAGC AGCTGCGGAG GG-TGTACTG GGTCCCCCAG CAGTGCCAGC CCACCAGCGC TGCGCTCG--
AC004000       GACTTAGCAC CCGGGCCAGT GGCTGCGGAG AG-TGTACTG GGTCCCCCAG CAGTGCCGGC CCACCGGCAC TGCGCTCG--
AC000058       GGCTTAGCAC CCGGGCCAGC GGCTGCGGAG GG-TGTACTG GTTCCCCCAG CAGTGCCAGC CCACCGGCGC TGTGCTCG--
Z84484         GACTTAGCAC CCGGGCCAGC GGCTGCGGAG GG-TGTACTG GGTCCCCCAG CAGTGCCAGC CCACCGGCGC TGCGCTCG--
AC003670       GGCTTAGCAC CTGGGCCAGT GGCTGCGGAG GG-TGTACTG GGTCCCCCAG CAGTGCCAGC CCACCGGCGC TGCCCTCG--
AC004220       GGCTTAGCAC CCGGGCCAGC GGCTGCAGAG GG-TGTACTG GGTCCCACAG CAGTGCCAGC CCACCAGCAC TGCCCTCG--
AC003029       GGCTTAGCAC ACGGGCCAGT GGCTGCAGAG GG-TGTGTTG GGTCCCCCAG CAGTGCCGGC CCACCAGTGC TGTACTCG--
AC002451       GGCTTAGCAC CCAGGCCAGC GGCTGCGGAG GG-TGTACTG GGTCCCCCAG CAGTGCCGGC CCACCAGCAC TGTGCTGG--
AC003043       GGCTTAGCAC CCGGGCCAGC GGCTGCAGAG GG-CGTACTG GGTCCCCCAG CAGTGCCAGC CCACCA---- ----------
Z82975         GGCTTAGCAC CTGGGCCAGC GGCTGCGGAG GA-TGTGCTG GGTCCCCCAG CAGTGCTGGC CCACTGGCTC TGCGCTCC--
AL031785       GGCTTAGCAC CCGGGCCAGT GGCTGTGGAG GG-TGTACTG GGTCCCCCAG CAGTGCCAGC CCGCCGGCGC TGCTCTCG--
AC006271       GGCTTAGCAC CCGGGCCAGC GGCTGTGGAG GG-TGTACTG GGTCCCCCAG CAGTGCCAGC CCGCCGGCGC TGCGCTCG--
AC002544       GGCTTAGTAC CCGGGCCAGC AGCTGCGGAC GG-TGTACTG GGTCCCCCAG CAATGCCAGC CCACGGGCGC TGCTCTCG--
Z81450         GGCTTAGCAC CCGGGCCAGC GGCTGCGGAG GG-TGTGCTG GGTCCCCCGG CAGTGCCGGC CCACCGGAGC TGCGCTCA--
AC004973b      GGCTTAGCAC CTGGGCCAGC GGCTGGGGAG GG-TGTACTG GGGCCCCCAG CAGTGCCAGC CCACTGGCGC TGCGCTCA--
AL022726a      GGCTTAGCAC CCGGGCCAGC GGCTGAGGAG GG-TGTACTG GGTCCCCCAG CAGTGCCAGC CCACCGGTGC TGCGCTCG--
Z99290         GGCTTAGCAC CCAGGCCAGC GGCTGCGGAG AG-TGTACTG GGTCCCCCAG CAGTGCCAGC CCACCGGCGC TGCGCTCG--
AF001550       GGCTTAGCAC CCCGGCCAGC GGCTGCGGAG GG-TGTACTG GGTCCCCCAG CAGTGCTAGC CCACCGGCGC TGCGCTCC--
AC002477       GGTTTAGCAC CCGGGCCAGC GGCTGCGGAG AG-TGTACTG GGTCCCCCAG CAATGCCGGC CCACCGGCGC TGCGCTGG--
AL031073       TGCTTAGCAC CCGGGCCAGC GGCTGCAGAG GG-TGTACTG GGTCCCCCAG CAGTGCCAGC CCACCGGCGC TGCGCTCG--
AC004783       G-CTTAGCAC CCGGGCCAGC GGCTGCGGAG GA-TGTACTG GGTCCCCCAG CAGTGCCGGC CCACCGGCGC TGCGCTCT--
AC005066b      GACTTAGCAC CCGGGCCAGC GGCTGTGGAG GG-TGTACTG GGTCCCCCAG CAGTGCCAGC CCACCAGCGC TGTGCTCG--
AC004866       GGCTTAGC-C CCCGGCCAGC GGCTGCGGAG GG-TGTACTG GGTCCCCCAG CAGTGCCAGC CCACCGGCGC TGCGTTCG--
AL024506       GGATTAGCAC CCGGGCCAGC GGCTGCGGAG GG-TGTACTG GG-CCCCCAG CAGTGCCAGC CCACCGGCGC TGCGCTCG--
X83497         GGCTTAGCAC CCGGGCCAGC GGCTGCGGAG GG-TGTACTG GGTCCCCCAG CAGGGCCAGC CCACCGGCGC TGCACTCG--
AC004212a      GGCTTAGCAC CCGGGCCAGC GGCTGCGGAG GG-TGTACTA GGTCCCCCAG CAGTGCCGGC CCACCGGCGG TGCGCTCG--
AC004197a      GGCTTAGCAC CCGGGCCAGT GGCTGCGGAG GG-TGTACTA GGTCCCCCAG CAGTGCCGGC CCACTGGCGC TGCACTGG--
Z72004         AGCTTAGCAC CCGGGCCAGC GGCTGCGGAG GGGTGTGCTG GGTCCCCCAG CAGTGCCGGC CCACCGGCGC TGCGCTCG--
AL022067       GGCTTAGCAC CCGGGCCAGC GGCTGCGGAG GG-TGTACTG GGTCCCCCAG CAGTGACGGC CCACCGGCGC TGCACTCG--
Z99128         GGCTTAGCAC CCAGGCCAGC GGCTTCGGAG GG-TGTACTG GTTCCCCCAG CAGTGCCAGC CCGCCGGCGC TGTGCTCG--
X14975         GACTTAGCAC CCGGGCCAGC GGCTGCGGAG GG-TGTACTG GATCCCCCAG CAGTGCCAGC CCACCAGCGC TGTGCTTG--
Z75746         GGCTTAGCAC CCAGGCCAGT GGCTGCAGAG GG-TATACTG GGTCGCCCAG CAGTGCCAGC CCACCGGCGC TGCGCTCA--
AC005392       GGCTTAGCAC CCGAGCCAGC GGCTGCAGAG GG-TGTACTG GGTCCCCCAG CAGTGCCAGC CCACCGGCGC TGTGCTCG--
AC002326b      GGCTTAGCAC CCGGGCCAGC AGCTGCGGAG GG-TGTGCTG GGTCCTCCAG CAGTGCCAGC CCACTGGCGC TGCGCTGG--
Clustal Cons             *     ****    ***   **       *  *  *  *   * * **  *   ** **

TP63-LTR       ---------- ----ATTTCT CACCGGG-CC TTAGCTGCCT TCCCGTGGGG CAGGGCTCGG GACCTGCAGC CCGCCATGCC 480
AC004004       ---------- ----ATTTCT CACCGAG-CC TTAGCTGCCT TCCTGTGGGG CAGGGCTCGG GACCTGCAGC CCGCCATGCC
AC005332a      ---------- ----ATTTCT CACCGAG-CC TTAGCTGCCT TCCTGTGGGG CAGGGCTCGG GACCTGCAGC CCGCCATGCC
AL021407b      TTCTCACCGC TTAGATTTCT CACCGGG-CC TTAGCTGCCC TCCGGCGGGG CAGGGCTCGG GACCTGCAGG TCGCCATGCC
AC004185       ---------- ----ATTTCT CACCGAG-CC TTAGCTGCCT TCCCGCGGGG CAGGGCTGGG GACCTGCAGC CCGCCATGCC
AC004000       ---------- ----ATTTCT CACCGAG-CC TTAGCTGTCT TCCCGTAGGG CAGGGCTCGG GACCTGCAGC TCTCCATGCC
AC000058       ---------- ----ATTTCT CACCGGG-CC TTAGCTGCCT TCCCGCGGGG CAGGGCTGGG GACCTGCAGC CCGCCAAGCC
Z84484         ---------- ----ATTTCT CACCGGG-CC TTAGCTGCCT TCCTGCGGGG CAGGGCTGGG GACCTGCAGC CTGCCATGCC
AC003670       ---------- ----ATTTCT CACTGGG-CC TTAGCTGCC- ---CACGGGG CAGGGCTTGG GACCTGCAGG CTGCCATGCC
AC004220       ---------- ----ATTTCT CACTGGG-CC TTAGCTGCCT TCCCATTGGG CAGGGCTTGG GACCTGCAGC CCATCATGCC
AC003029       ---------- ----ATTTCT CGCCGGG-CC TTAGCTGCCT CCCGTCGGGG CAGGGCTCTG GACCTGCAGC CCCCCATGCC
AC002451       ---------- ----ATTTCT CGCTGGG-CC TTAGCTGCCT CCCGGCGGGG CAGGGCTCAG GACCGGCAGC CCGCCATGCC
AC003043       ---------- ---------- --CTGGG-CC TTAGCTGCCT TCCTGCAGGG CAGGGCTGGG GACCTGCAGC CCGCCATGCG
Z82975         ---------- ----ATTTCT CTCTGGG-CC TTAGCTGCCT CCCCGTGGGG CAGGGCTCGG GACCTGCAGC CCACCATGCC
AL031785       ---------- ----ATTTCT CACCGGG-CC TTAGCTGCCT TCCCGCGGGG CAGGATTCGG GAC-TGCAGC CCGCCATGCC
AC006271       ---------- ----ATTTCT CACCGGG-CC TTAGCTGCCT TCCCGCGGGG CAGGGCTCGG GACCTGCAGC CCGCCATGCC
AC002544       ---------- ----ATTTCT CACGGGG-TC TTAGCTGCCT TCCCGCCGGG CAGGGCTCCG GACCTGCAGC CCGCCATGCC
Z81450         ---------- ----ATTTCT CGCTGGG-TC TTAACTGCCT TCCTGCAGGG CAGGGCTCGG GAGCTGCAGC CCGCCATGCC
AC004973b      ---------- ----ATTTCT CACCAGG-GC TGAGCTGCCT TCCCGTGGGG CAGGGCTTGG GACCTGCAGC CCGCCGTGCC
AL022726a      ---------- ----ACTTCT CGCCGGG-TC TTAGCTGCCT TCCCGCGGGG CAGGGCTCGG GACCTGCAGC CCGCCATGCC
Z99290         ---------- ----ATTTCT CGCCGGG-CC TTAGCTGTCT TCCCGCGGGG CAGGGCTCAG GACCTGCAGC CCACCATGCC
AF001550       ---------- ----ATTTCT CACCGGG-CC TTAGCTGCCT TCCCGCGGGG CAGGGCTCGG GACTTGCAGC CCGCCATGCC
AC002477       ---------- ----ATTTCT CACTTGG-CC TTAGCTGCCT TCCCGCGGGG CAGGGCTCAC GACCTGCAAC TCGCCATGCC
AL031073       ---------- ----ATTTCT CACCGGG-CA TTAGCTGCCT TCCCGCGGGG CAGGGCTCGG GACCTGCAGC CCACCATGCC
AC004783       ---------- ----ATTTCT CGCGGGG-CC TTAGCTGCCT TCCTGCGGGG CAGGACTCGG GAC-TGCAGC CCGCCATGCC
AC005066b      ---------- ----ATTTCT CGCTGGG-CC TTAGCTGCCT TCCCGTGGGG CAGGGCTTGG GACCTGCAGC CCACCATGCC
AC004866       ---------- ----ATTTCT CGCCGGG-CC TTAGGTGCCT TCCGGCGGGG CAGGGTTAGG GACCTGCAGC CTGCCATGCC
AL024506       ---------- ----ATTTCT CGCCGGGGCC TTAGCCGCCT TCCCGTGGAG CAGGGCTCGG GACCTGCAGC CCGCCGTGCC
X83497         ---------- ----ATTTCT TGCTGGG-CC TTAGCTGCCT TCCCGTGGGG CAGGGCTCGG GACCTGCAGC CCGCCATGCC
AC004212a      ---------- ----ATTTCT CGCCAGG-CC TTAGCTGCCT TCGCACGGGG CAGGGCTCGG GACCTGCAGC CTGCCATGCC
AC004197a      ---------- ----ATTTCT CACTGGG-CC TTAGCTGCCT TCCCATGGGG CAGGGCTGGG GACCTGCAGC CCGCCATGCC
Z72004         ---------- ----ATTTCT CGCCGGG-CC TTAGCTGCCT TCCAGCGGGG CAGGGCTTAG GACCTGCAGC CCGCCATGCC
AL022067       ---------- ----ATTTCT CACCTGG-CC TTAGCTGCCT TCCCGCGGGG CAGGGCTCGG GACCTGCAGC CCGCCATGCC
Z99128         ---------- ----ATTTCT CACCATG-CC TTAGCTGTCT TCCTGCGGGG CAGGTCTCGG GACCAGCAGC CCGCCATGCC
X14975         ---------- ----ATTTCT CACCAGG-CC TTAGCTGCCT CCCCGTGGGG CAGGGCTCGG GACCTGCAGC CCGCCATGCC
Z75746         ---------- ----ATTTCT CACCAAG-CC TTAGCTGTCT TCCAGTGGGG CAGGGCTCAG GACCTGCAGT CCGCCATGCC
AC005392       ---------- ----ATTTCT CACCGGG-CC TTAGCTGCCT TCTGGCAGGG CAGGGCTCGG GACCAGCAGT CCGCCATGCC
AC002326b      ---------- ----ATTTCT GGCTGGG-CC TTAGCTGCCT CCCTGCGGGG CAGGGCTCGG GACCTGCCGC CCGCCATGGC
Clustal Cons                            *   *    * *   * *         * * ****  *    **   **        *  *
```

```
TP63-LTR       TGAGCCTCCC -ACCCGCTCT GTG------- --GGCTCCT- GTGTGGCCGG AGCCTCCTCG ACAAGCGC-- CACCCCCTGC 560
AC004004       TGAGCCTCCC -ACCCACTCT GTG------- --GGCTCCT- GTGCGGCCCA AGCCTCCTGG ACGAGCGC-- CACCCCCTGC
AC005332a      TGAGCCTCCC -ACCCCCTCC GTG------- --GGCTCCT- GTGCGGCCCG AGCCTCCT-- -CGAGCAC-- CACCCCCTGC
AL021407b      TGAGCCTCCC -ACCCGCTCC GTG------- --GGCTCCT- GTGCGGCCCG AGCCTCCCCC ACGAGCGC-- CATCCCCTAC
AC004185       TAAGCCTCCC -ACCCACTCC AAG------- --GGCTCCT- GTGCGGCCCG AGCCTCCTCG ACGAGCAC-- CACCCCCTGC
AC004000       TGAGCCTCCC -ACCCACTCC ATG------- --GGCTCCT- GTGCGGCCCA AGCCTCCCCA ACGAGCAC-- CACACCCTGC
AC000058       TGAGCCTCCC -ACCCGCTCC ATG------- --GGCTCCT- GTGCGGCCGG AGGTTCC-CG ACGACCGC-- CACCCCCTGC
Z84484         TGAGCCTCCC -ACCCGCTCC ATG------- --GGCTCCT- GTGCGGCCTG AGCCTCCCCG ACGAGCGC-- CACCCCCTGC
AC003670       TGAGCCTCCC -ACCTCCTCC ATG------- --GGCTCCC- GTGAGGCCCG AGCCTCCCCG ATGAGCGC-- TGCCCCCTGC
AC004220       TGAGCCTCCC -ACCCACTCC ATG------- --GGCTCCCC GTGCGGCCCA AGCCTCCCTG ATGAGCAC-- CGCCCCCTGC
AC003029       TGAACCTCCC --CCCACTCC CTG------- --GGCTCCT- GTGTGGCCCG AGCCTCCCCG ACGAGCAC-- CACCCCCTGC
AC002451       TGAGCCTCTC --CC--TTCC ATG------- --GGCTCCT- GTGTGGCAGG AGCCTCCCCG ACAAGCGC-- CGTCCCCTGC
AC003043       TGAGCCTCCC -ACCCACTCC ATG------- --GGCTCCT- GTGCGGCCCG AGCCTCCCGG ATGAGCGG-- CGCCCCCTGC
Z82975         TGAGCCTCCC --CCTCCGCC GTG------- --GGCTCCT- GTGCGGCCCA AGCCTCCCGG ATGAGCGCTC CGCCCCCTGC
AL031785       TGAGCCGCCC -ACCCCCTCC GTG------- --GGCTCCT- GTGC---CCG AGCCTCCCCG GTGAGCGC-- TGCCCCCTGC
AC006271       TGAGCCTCCC -ACCCACTCC ATG------- --GGCTCCT- GTGCGGCCGG AGCCTCCCCA ATGAGCGC-- TGTCCCCTGC
AC002544       TGAGCCTCCC -ACCCCCTCC ATG------- --GGCTCCT- GTGAGGCCGG AGTCTCCCCA G-GAGCAC-- TGTCCCCCGC
Z81450         TAAGCCCCCC -ACCCCCTCC GTG------- --GGCTCCT- GTGCGGACCG AGTCTCCCCG A-CGA----- ----------
AC004973b      TGAGCCTCCC -ACCCCCTCC GTG------- --GGCTCCT- GTGCAGCCCG AGCCTCCCCG ATGAGTGC-- TGTCCCCTGC
AL022726a      TGAGCCTCCC -ACCCGCTCC GTG------- --GGCTCCT- GTGCGGCCCG AGCCTTCCCG ATGAGCGC-- CGCCCCCTGC
Z99290         TGAGCCTCCC -ACCCACTCC GTG------- --GGCTCCT- ATGCGGCCCG AGCCTCCCAG ATGAGCGC-- CACCCCCTGC
AF001550       TGAGCCTCCC -ACCCCCTCC GTG------- --GGCTCCT- GTGCTGCCCG AGCCTCCCCG ACGAGCGC-- CACCCCTTGC
AC002477       TGAGCCTCCC -ACCCTCTCC GTG------- --GGCTCCT- GTGCGGCCCG AGCCTCTCCG ACGAGCGC-- CGCCCCCTGC
AL031073       TGAGCCTCCC -ACCCACTCT GTG------- --GGTTCCT- GTGCCGCCCC AGCCTCCCCG ACGAGCGC-- CACCCCCTGC
AC004783       TGAGCCTCCC -ACCCGCTCC GTG------- --GGCTCCT- GTGCCGCCCG AGCCTCCCCA ACGAGCAC-- CACCCCCTGC
AC005066b      TGAGCCTCCC -ACCCCCTCC TTG------- --GGCTCCT- GTGCCTCCGG AGCCTCCTCC ACGAGCGC-- CACCCCCTGC
AC004866       TGAGCCTCCC -ACCCTCTCC GTG------- --GGCTCCT- GTGCCGCCCG AGCCTCCCCG ATGAGTGC-- CGCCCCATGC
AL024506       TGAGCCTCCC -ACCCCCTCG GTG------- --GGCTCCT- GTGCGGCCCG AGCCTCCCCG ATGAGCGC-- CGCCCCCTGC
X83497         TGAGCCTCCA -ACCCCCTGG GTG------- --GGCTCCT- GTACGGCCCG ATCCTCCCCG ATGAGCGC-- CGCCCCCTGC
AC004212a      TGAGCCTCCC -ACCCCCTCC GTG------- --GGCTCCT- GTGCGGCCCA AGCCTCCCCG ACGAGCGC-- CGCCCCCTGC
AC004197a      TGAGCCTCCC -ACCCCCTCC ATG------- --GGCTTCT- GTGCGGCCGG AGCCTCCCCG ATGAGCAC-- CGCCCCCTGC
Z72004         TGAGCCTCCC -CCCGCCTCC GTG------- --GGCTCCT- GTGCAGACGG AGCCTCCCCG ACGAGCGC-- CGCCCCCTGC
AL022067       TGAGCCTCCC -ACCCCTTCC ATG------- --GGCTCCT- GTGC-GGCCA AGCCTCCCTG ACGAGTGC-- CGCCCTCTGC
Z99128         TGAGCCTCCC -ACCCCGTCC ATG------- --AGCTCCT- GTGCCGCCCG AGCCTCCCCG ATGAGTGC-- CGCCCCCTGC
X14975         TGAGACTCCC -ACCCCCTCC ATG------- --GGCTCCT- GTGCGGCCGG AGCCTCCCCG ATGAGCGC-- AGCCCCCTGC
Z75746         TGAGCCTCCC -ACCCCCTCC ATG------- --GGCTCCT- GTGCGGCCCG AGTCTCCCTG ACGAGCGC-- CACCCCCTGC
AC005392       TGAGCCTCCC -ACCCCCTCC ATGTGCGGCC CGAGCCTCCA GTGCGGGGGG AGCCTCCCTG AGGAGTGC-- CACCTCCTGC
AC002326b      TGAGCTTCCC CGCCCCCTCC ACG------- --GGCTCCT- GTGCGGCGGG AGCCTCCCTA ATGAGCGC-- CGCCCCCTGC
Clustal Cons   * *    *     **         *           *   *    *         *   *

TP63-LTR       TCCACGG-CG CCCAGTCCCA TCGACCACCC AAGGGCTGAA GAGTGCAGGC GCATGGCGC- GGGACTGGCA GGCAGCTCCA 640
AC004004       TCCACGG-CG CCCAGTCCCA TCGACCACCC AAGGGCTGAG GAGTGCGGGC GCACAGCGC- GGGACTGGCA GGCAGCTCCA
AC005332a      TCCACAG-CG CCCAGTCCCA TCGACCACCC AAAGGCTGAG GAGTGCAGGC GCAGGGCGC- GGGACTGGCA GGCAGCTCCA
AL021407b      TCCACAG-CG CCCAGTCCAA TCGACCACCC AAGGGCTGAG GAGTGTAAGT GCATGGCGC- GGGAGTGGCA GGCAGCTCCA
AC004185       TCCACGG-CG CCCAGTCCCA TCGACCACCC AAGGGCTGAG GAATGCAAGC GCACCGTGC- GGCACTGGTA GGCAGCTCCA
AC004000       TCCACGG-CG CCCAGTCCCA TCGACCACCC AAGGGCTGAG GACTGCGGGC GCACGGCGC- GGGACTGGCA GGCAGCTCCA
AC000058       TCCACGG-CG CCCAGTCCCA TCGACCACCC AAGGGCTGAG GAGTGCAGGC GCACGGCACC AGGACTGGCA GGCAGCTCCA
Z84484         TCCACAG-CG CCCAGTCCCA TCCACCACCC AAGGGCTGAG GAGTGCGGGC TCACGGCGC- CGGACTGGCA GGCAGCTCCA
AC003670       TCCATGG-CA CCCAGTCCCA TCGACCACCC AAAGGCTGAG GAGTGTGGGC ACACTGCAT- GGGACTGGCA GGCAGCTCCA
AC004220       TCCATGG-CA CCCAGTCCCA TCGACCACCC AAGGGCCGAG GAGTGCGGGC GCATGGCAA- GGGACTAGCA GGCAGCTCCA
AC003029       TCCACGG-CA CCCAGTCCCA TCAACCACCC AAGGGCTGAG GTGTGCGGGC GCACGGCAC- TGGACTGGCA AGCAGCTCCA
AC002451       TCCACCG-CG CCCAGTCCCA TCGACCACCC AAGGGCTGAG GAGAGCGGGC ACACGATGC- AGGACTGGCA GGCAGCTCCA
AC003043       TCCACGG-CG CCCAGTCCCA TCAACCACCC AAGGGCTGAG GAGTGTGGGC GCACGGTGC- GGGACTGGCA CGTAGCTCCA
Z82975         TCGACGG-CG CCCAGTCCCA TCGACCACCC AAGGGCTGAG GAGTGCGGGT GCACCGTGC- GGGACTGGCA GGCAGCTCCA
AL031785       TCCACGG-CG CCCAGTCCCG TCGACCACCC AAGGGCTGAG GAGTGGGGGC GCACGGCGC- GGGACCGGCA GGCAGCTCCA
AC006271       TCCACGG-CG CCCAGTCCCA TCGACCACCC AAGGGCTGAG GAGTGCGGGC GCACAGCGC- AGGACTGGCA GGCAGCTCCA
AC002544       TCCTCGG-CG CCCAGTCCCA TCGACCACCC AAGGGCTGAG GAGTGCAGGT AGACAGCGC- GGGACTGGCA GGTAGCTCCA
Z81450         ------G-CG CCCGGTCCCA TTGACCACCC AAGGGCTGAG GAGTGCGGGC GCACGGCAC- GGGACTGGCA GGCAGCTCCA
AC004973b      TCTACTG-CG GCCAGTCCCA TTGACCACCC AAGGGCTGAG GAGTGCGGGC GCATGGCGC- AGGACTGGCA TGCAGCTGCA
AL022726a      TGCACGG-CA CCCAGTCCCA TCCACCACCC AAGGGCTGAG GAGTGCCGGC GT-------- GAGAGTGGCA GGTAGCTCCG
Z99290         TCCACGG-TG CCCAGTCCCA TCGACCGCCC AAGGGCTGAG GAGTGCAGGC GCACTGCGC- GGGACTGGCA GGCAGCTCCA
AF001550       TCCACGG-CG CCCAGTCCCA CCGACCACCC AAGGGCTGAG GAGTGCGGGC CCACGGCGC- GGGACTGGCA GGCAGCTCCA
AC002477       TCCACGG-CG CTCAGTCCGA TCAACCACCC AAGGGCTGAG GAGTGCGGGC GCAC-GCGC- AGGACTGGCA GGCAGCTCCA
AL031073       TCCACGG-CG CCCAGTCCCA TCGACCTCCC AAGGGCTGAG GAGTGCGGGT GCACCGCAC- AGGACTGGCA GGCAGCTCCA
AC004783       TCCACGG-CG CCCAGTCTCA TCCACCACCC AAGGGCTGAG GAGTGCGGGC AGACGGCGC- AGGACTGACA GGCAGCTTCA
AC005066b      TCCACGG-CG CCCAGTCCCA TCTACCACCC AAGGGCTGAG GAGTGCAGGC GCACAGCAC- GGGACTGCCA GGCAGTTCCA
AC004866       TCCAGGG-CG CCCAGTCCCA TCGGCCACCC AAAGGCTGAG GAGTGCGGGC GCACAGCGC- AGGACTGGCA GGCAGCTCCA
AL024506       TCCATGG-CG CTCAGTCCCA TCGACCACCC AAGGGCTGAG GAGTGCCGGC GCACGGCGC- GGGACTGGCA GGCAGCTCCA
X83497         TCCA-GG-CA CCCAGTCCCA TCGACCACCC AAGGGCTGAG GAGTGCGGGT GCATGGGGC- AGGACTGGCA GGCAGCTCCA
AC004212a      TCCAGGG-CC CCCAGTCCCA TCGACCGCCC AAGGGCTAAG GAGTGTGAGC ACATGGCCC- AGGACTGGCA GGCAGCTCCA
AC004197a      TCCAGGG-CG CCCAGTCCCA CCGACCGCCC ACGGGCTGAG GACTGTGAGC GCATGGCGT- AGGACTGGCA GGCAGCTCCA
Z72004         TCCATGGGCG CCCAGTCCCA TCTACCACCA AAGGGCTGAG GAGTGTGGGC GCACAGCGC- CGGACTGGCA GGCAGCTCCA
AL022067       TCCACGG-CG CCCAGTCCCA TCGACCACCC AAGGGCTGAG GAGTGCGGG- GCACGGCGC- GGGACTGGCA GGCAGCTCCA
Z99128         TCCAGGG-CG CCCAGTCCCA TCGACCACCC AAGGGCTGAG GAGTGTGGGC ACACGGCAC- CAGACTGGCA GGCAGCTCCA
X14975         TCCACGG-CG CCCAGTCCCA TCAACCACCC AAGGGCTGAG GAGTGCGGGT TCACGGCGG- GGGACTGGCA GGCAGCTCCA
Z75746         TCCATGG-TG CCCAGTCCCA TCAACCACCC AAGGGCTGAG GAGTGCGGGC GCATGGCACC GGGACTAGCA GGCAGCTCCA
AC005392       TCCACAG-CA CCCAGTCCCA TCAACCACCC AAGGGCTGAG GAGCACGGGC ACATGGCGT- GGGACTGGCA GGCAACTCCA
AC002326b      TCCAAGG-CC CCCAGTCCCG TCAACCATGC AAGGGCTGAG GAGTGCAGGC GCAGGGCGT- GGGACTGGTG GGCAGCTCCA
Clustal Cons         *      * ***        **     *  ***  *  *       *                *        * *  * *
```

```
TP63-LTR       TCTGCAGCCC CGGTGGGAGA TCCACTGGGC GAAGCCAGCT GGCCTCCTGA GTCTGGTGGG GACGTGGAGA ATCTTTA-  718
AC004004       TCTGCAGCCC CGGTGCGGGA TCCACTGGGT GAAGCCAGCT GAGCTCCTGA GTCTGGTGGG -ACGTGGAGA ACCTTTA-
AC005332a      CCTGCAGCGC CGGTGCGGGA TCCACTGGGT GAAGCCAGCT GGGCTCCTGA GTCTGGTGGG GCCTTGGAGA ACCTTTA-
AL021407b      CCTGCAGCCC CTGTGCGGCA TCTACTGGGT GAAACCAGCT GGGCTCCTGA GTCTGGTGGG AACGTGGAGA ACCTTTA-
AC004185       CCTGCAGCCC CGGTGCGGGA TCCACTAAGT GAAGCCAGCT GGGCTCCTGA GTCTGGTGGG GACGTGGAGA GTCTTTA-
AC004000       CCTGCAGCCC CAGTGTGGGA TCCACTAGGT GAAACCAGTT GGGCTCCTGA GTCTGGTGGG GACGTCT--- --------
AC000058       CCTGCAGCTC TGGTGCGGGA TCCACTAGGT GAAGCCAGCT GGGCTCCTGA GTCTGGTGGG GACGTGGAGA ACCTTTG-
Z84484         CCTGCAGCCC CAGTGCAGGA TCCACTGGGT GAAGCCAGCT GGGCTCCTGA GTCTGGTGGG GAGGTGGAAA ACCTTTA-
AC003670       CCTCCAGTCC TGGTGAGGGA TCCACTGGGT GAAGCCAGCT GGGCACCTGA GTCTGGTGGG GACGTGGAGA ACCTTTA-
AC004220       CCTGCAGCCC CGGTGCGGGA TCCACTGGGT GAAGCCAGCT GGGCTCCTGA GTCTGGTGGA GACGTGGAGA ACCTTT--
AC003029       CCTGCGGCCC GGGTGCAGGA TCCACTGGGT GAAGCCAGCT GGGCTCCTGA CT--GGTGGG GACTTGGAGA ACCTTTA-
AC002451       CCTGCAGCCC CGGTGTGGGA TCCACTGGGT GAAGCCAGCT GGGTACCTGA CTCTGGTGGG GACTTGCAGA ACCTTTG-
AC003043       CCTGCAGCCC CTGTGCGGGA TCCACTGGGT GAAGCCAGCT GGGTTCCTGA GTCTGGTGGG GCCTTGGAGA ACCTTTA-
Z82975         CCTGCGGCCC CGGTGGGGGA TCCACTGGGT GAAGCTAGCT GGGCTCCTGA GTCTGGTGGG GACTTGGAGA ACCTTTA-
AL031785       CCTGCAGCCC CTGTGCGGAA TCCACTGGGT GAAGCCAGCT GGGCTCCTGA GTCTGGTGGG GACGTGGAGA ACCTTTA-
AC006271       CCTGCAGCCC CGGTGCAGGA TCCACTGGGT GAAGCCAGCT GGGCTCCTGA GTCTGGTGGG GACGTGGAGA ACCTCTAT
AC002544       CCTGCAGCCC CGGTGCGGGA TCCACTGGGT GAAGCCAGCT GGGCTCCTGA GTCTGGTGGG GACGTGGAGA ACCTTTA-
Z81450         CCTGCAACCC CGGTGCGGGA TCCACTGGGT GAAGCCAGCT GGGCTCCTGA TTCTGGTGGG GACGTGGAGA ACCTTTA-
AC004973b      CCTGCAGTCC CGGTGCAGAA TCCAGTGGGT GAAGCCAGCT GGGTTTCTGA GTCTGGTGGG GACGTGGAGA ACCTTTA-
AL022726a      CCTGCAGCCC CGGTGCGGGA TCCACTGGGT GAAGCCAGCT GGGCTCCTGA GTCTGGTGGG GACGTGGAGA ACCTTTA-
Z99290         CCTGCAGCCC CGGTGCGGGA TCCACTGGGT GAAGCCAGCT GGGCTCCCGA GTCTGGTGGG GACGTGGAGA ACCTTTA-
AF001550       CCTGCAGCCC CGGTGCAGGA GCCACTGGGT GAAGCCAGCT GGGCTCCTGA GTCTGATGGG GACGTGGAGA ACCTTTA-
AC002477       CCTGCAGCCC TGGTGTGGGA TCCACTGGGT GAAGCCAGCT GGGCTCCTGT GTCTGGTGGG GAGGTGGAGA ACCTTTA-
AL031073       CCTGCAGCCC CTGTGCGGGA TCCACTGGGT GAAGCCAGCT GGGCTCCTGA GTCTGGTGGG GACGTGGAGA ACCTTTA-
AC004783       CCTGCAGCCC CG-TGCGGGA TCCACTGGGT GAAGCCAGCT GGGCTCCTGA GTCTGGTGGG GCCTTGGAGA ATCTTTA-
AC005066b      CCTGCAGCCC CGGTGCAGGA TCCACTGGGT GAAGCCAGCT GGGCTCCTGA GTCTGGTGGG GCCTTGGAGA ACCTTTA-
AC004866       CCTGTAGCCC CAGTGCGGGA TCCACTGGGT GAAGCCAGCT GGGCTCCTGA GTCTGGTGGG GTCATGGAGA ACCTTTA-
AL024506       CCTGCAGCCC CCGTGCGGGA CCCACTGGGT GAAGCCAGCT GGGCTCCTGA GTCTGGTGGG GACGTGGAGA ACCTTTA-
X83497         CCTGCAGCCC CGGTGCGGGA TCCACTGGGT GAAGCCAGCT GGGCTTCTGA GTCTGGTGGG GACATGGAGA ACCTTTA-
AC004212a      CCTGCAGCCC CGGTGCTGGA TCCACTGGGT GAAGCCAGCT GGGCTCCTGA GTCTGGTGGG GACGTGGAGA GTCTTTA-
AC004197a      CCTGCGGCCC CGGGGCGGGA TCCACTGGGT GAAGCCAGCT GGGCTCCTGA GTCTGGTGAG GACGTGGAGA GTCTTTA-
Z72004         CCAGCAGCCC CAGTGCGAAA TCCACTGGGT GAAGCCAGCT GGGCTCCTGA CTCTGGTGGA GACTTGGAGA ACCTTTA-
AL022067       CCAGCAGCCC C--------- -------GGT GAAGCCAGCT GGGCTCCTGA GTCTGGTGGG GACGTGGAGA ACCTTTA-
Z99128         CCTGCAGCCC CAGTGCGGGA TCCACTGGGT GAAGCCAGCT GGGCTCCTGA GTCTGGTGGG GACGTGGAGA ATCT----
X14975         TCTGCAGCCC CAGTGCAGGA TCCACTAGGT GAAGCCAGCT GGGATCCTGA GTCTGGTGGG AACGTGGAGA ATCTTTA-
Z75746         CCTGCAGCCC CAGTGTGGGA TCCACTGGGT GAAGCCAGCT GGGTTCCTGA GTCTGGTGGG GATGTGGGGA ACCTTT--
AC005392       TCTGCAGCCC CAGTGTGGGA TCCACTGGGT GAAGCCAGCT GGGCTCCTGA GTCTGGTGGG GATGTGGA-- --------
AC002326b      TCTGCAGCCC CAGTGC-GGA TCCACTGGAT GAAGCCAGCT GGGCTCCTCA GTCTGGTGGG GACGTGGAGA ACCTTTA-
Clustal Cons    *       *                       *** * ** * *     *     *  * **       *
```

8.3 TP63 exon U1 in primates

```
Homo_sapiens        GGCAACCCGC TGGGGTCACC TTCCACACTG TGGAAGCTTT GTTCTTTTGC TCTTTGCAGT   60
Gorilla_gorilla     GGCAACCGGC TGGGGTCGCC TTCCACACCG TGGAAGCTTT GTTCTTTTGC TCTTTGCCGT
Pan_troglodytes     GGCAACCCGC TGGGGTCACC TTCCACACTG TGGAAGCTTT GTTCTTTTGC TCTTTGCAGT
Pongo_pygmaeus      GGCAACCCGC TCCGGTCCCC TTCTGCACTG TGGAAGCTTT GTTGTTC-GC TCTTTGCAAT
Macaca_mulatta      ---------- ---------- ---------- ---------- ---------- ----------
Clustal Consensus

Homo_sapiens        AAATCTTGCT ACTGCTCACT CTTTGGGTGC ACACTGCTTT TATGAGCTGT AACACTCA-C  120
Gorilla_gorilla     AAATCCTGCT ACTGCTCACT CGTTGGGTGC ACACTGCTTT TATGAGCTGT AACACTCC-C
Pan_troglodytes     AAATCTTGCT ACTGCTCACT CTTTGGGTGC ACACTGCTTT TATGAGCTGT AACACTCA-C
Pongo_pygmaeus      AAATCTTGCT ACTGCTCGCT CTTTGGGTCC GCACTGCTTT TATGAGCTGT AACACTCAAC
Macaca_mulatta      ---------- ---------- ---------- ---------- ---------- ----------
Clustal Consensus

Homo_sapiens        CGTGAAGGTC TGCAGCTTCA CTCCTGAAGC CAGCGAGACC AGGAGTCCAC TGGGAGGAAC  180
Gorilla_gorilla     CGCGAAGGTC TGCAGCTTCA CTCCTGAAGC CAGCGAGACC AGGAGTCCAC TGGGAGGAAC
Pan_troglodytes     CACGAAGGTC TGCAGCTTCA CTCCTGAAGC CAGCGAGACC AGGAGTCCAC TGGGAGGAGC
Pongo_pygmaeus      TGCAAAGGTC TGCAGCTTCA CTCCTGAAGC CAGCGAGACC AGGAGCCCAC TGGGAGGAAC
Macaca_mulatta      ---------- ---------- ---------- ---------- ---------- ----------
Clustal Consensus

Homo_sapiens        GAACAACTCC AGACGCACCG CCTTAAGAAC TTCAACACTC ACTGCGAAGG TCTGCAGCTT  240
Gorilla_gorilla     GAACAACTCC AGACGCACCG CCTTAAGAGC TGTAACACTC ACTGCAAAGG TCTGCAGCTT
Pan_troglodytes     AAACAACTCC AGACGTGCAG CCTTAAGAGC TGTAACACTC ACTGCGAAGG TCTGCAGCTT
Pongo_pygmaeus      GAACAACTCC AGACACACCG CCTTAAGAGC TGTAACACTC AACTCGAAGG TCTGCAGCTT
Macaca_mulatta      ---------- ---------- ---------- ---------- ---------- ----------
Clustal Consensus

Homo_sapiens        CACTCCTGAG CCAGCGAGAC CACGAACCCA CCGTAAGGAA GAAACTCCGA ACACATCCGA  300
Gorilla_gorilla     CACTCCTGAG CCAGCGAGAC CACGAACCCA CCATAAGGAA GAAACTCCGA ACACATCGGA
Pan_troglodytes     CGCTGCTGAG CCAGCGAGAC CACGAACCCA CCATAAGGAA GAAACTCCGA ACACACCCGA
Pongo_pygmaeus      CACTCCTGAG CCAGTGAGAC CACGAACCCA CCAGAAGGAA GAAACTCTCA ACACATCCGA
Macaca_mulatta      ---------- ---------- ---------- ---------- ---------- ----------
Clustal Consensus

Homo_sapiens        ACATCAGAAG GAACAAACTC CAGACGCGCC ACCTTAAGAG CTGTAACACT CACCGCCAGG  360
Gorilla_gorilla     ACATCAGAAG GAACAAACTC CAGACGCGCC ACCTTAAGAG CTGTAACACT CACCGCCAGG
Pan_troglodytes     ACATCAGAAG GAACAAACTC CAGACGCGCC ACCTTAAAAG CTGTAACACT CACCGCCAGG
Pongo_pygmaeus      ACATCAGAAG GAACAAACTC CAGACGCGCC ACCTTAAGAG CTGTAACACA CACCGCGAGG
Macaca_mulatta      ---------- ---------- ---------- ---------- ---------- ----------
Clustal Consensus

Homo_sapiens        GTCCGCGGCT TCATTCTTGA AGTCAGAGAG ACCAAGAACC CACCAATTCC GGACACCCTA  420
Gorilla_gorilla     GTCTGCGGCT TCATTCTTGA AGTCAGAGAG ACCAAGAACC CACCAATTCC GGACACCCTA
Pan_troglodytes     GTCCGTGGCT TCATTCTTGA AGTCAGAGAG ACCAAGAACC CACCAATTCC GGACACCCTA
Pongo_pygmaeus      GTCCGAGGCT TCATTCTTGA AGTCAATGAG ACCAAGAACC CACCAATTCC GGGCACACTG
Macaca_mulatta      ---------- ---------- ---------- ---------- ---------- ---------G
Clustal Consensus

Homo_sapiens        TCAGAGATTT TGAAAACTAT GAAGTGCTGG GAACAGAGAG ACTGGAC--- AGCCTTCACA  480
Gorilla_gorilla     TCAGAGATTT TGAAAACTGT GAAGTGCTGG GAACAGAGAG ACTGGAC--- AGC-TTCACA
Pan_troglodytes     TCAGAGATTT TGAAAACTAT GAAGTGCTGG GAACAGAGAG ACTGGAC--- AGC-TTCACA
Pongo_pygmaeus      TCAGAGATTT TAAAAACTAT GAAGTGCTGG GAACAGAAAG ACTGGAGTTG AAGCTTCACA
Macaca_mulatta      TCAGAGATTT TAAAAACTAT GAAGTGCTAG AAACAGAGAA ATTGGAGTTG AAGCTTCACA
Clustal Consensus   ********** * ****** * ******** *  ****** *  * ****     *   ******

Homo_sapiens        AAGGTGGGGA AACCTT
Gorilla_gorilla     AAGGTGGGGA AACCTT
Pan_troglodytes     AAGGTGGGGA AACCTT
Pongo_pygmaeus      AAGGTGGGGA AACCTT
Macaca_mulatta      AAGGCGGGGA AACCTT
Clustal Consensus   **** ***** ******
```

References

Alderden RA, Hall MD, Hambley TW (2006) The Discovery and Development of Cisplatin. *Journal of Chemical Education* **83**(5)**:** 728-null

Arrowsmith CH (1999) Structure and function in the p53 family. *Cell Death Differ* **6**(12)**:** 1169-1173.

Bahrami A, Ro JY, Ayala AG (2007) An Overview of Testicular Germ Cell Tumors. *Archives of Pathology & Laboratory Medicine* **131**(8)**:** 1267-1280

Bamberger C, Schmale H (2001) Identification and tissue distribution of novel KET/p63 splice variants. *FEBS Letters* **501**(2-3)**:** 121-126

Belyi VA, Ak P, Markert E, Wang H, Hu W, Puzio-Kuter A, Levine AJ (2009) The Origins and Evolution of the p53 Family of Genes. *Cold Spring Harbor Perspectives in Biology* **2**(6)**:** -

Belyi VA, Levine AJ (2009) One billion years of p53/p63/p73 evolution. *Proc Natl Acad Sci U S A* **106**(42)**:** 17609-17610

Beumer KJ, Pimpinelli S, Golic KG (1998a) Induced chromosomal exchange directs the segregation of recombinant chromatids in mitosis of Drosophila. *Genetics* **150**(1)**:** 173-188

Beumer TL, Roepers-Gajadien HL, Gademan IS, van Buul PP, Gil-Gomez G, Rutgers DH, de Rooij DG (1998b) The role of the tumor suppressor p53 in spermatogenesis. *Cell Death Differ* **5**(8)**:** 669-677

Bogenhagen D, Clayton DA (1974) The Number of Mitochondrial Deoxyribonucleic Acid Genomes in Mouse L and Human HeLa Cells. *Journal of Biological Chemistry* **249**(24)**:** 7991-7995

Brinster RL, Zimmermann JW (1994) Spermatogenesis following male germ-cell transplantation. *Proceedings of the National Academy of Sciences of the United States of America* **91**(24)**:** 11298-11302

Brooks CL, Gu W (2003) Ubiquitination, phosphorylation and acetylation: the molecular basis for p53 regulation. *Curr Opin Cell Biol* **15**(2)**:** 164-171

Brunner HG, Hamel BC, Bokhoven Hv H (2002) P63 gene mutations and human developmental syndromes. *Am J Med Genet* **112**(3)**:** 284-290

Burger H, Nooter K, Boersma AWM, Wingerden KEv, Looijenga LHJ, Jochemsen AG, Stoter G (1999) Distinct p53-independent apoptotic cell death signalling pathways in testicular germ cell tumour cell lines. *International Journal of Cancer* **81**(4)**:** 620-628

Buzdin A (2007) Human-Specific Endogenous Retroviruses. *TheScientificWorldJOURNAL* **7:** 1848-1868

Caires K, Broady J, McLean D (2010) Maintaining the male germline: regulation of spermatogonial stem cells. *J Endocrinol* **205**(2)**:** 133-145

Candi E, Dinsdale D, Rufini A, Salomoni P, Knight RA, Mueller M, Krammer PH, Melino G (2007) TAp63 and DeltaNp63 in cancer and epidermal development. *Cell Cycle* **6**(3)**:** 274-285

Casau AE, Vaughan JE, Lozano G, Levine AJ (1999) Germ Cell Expression of an Isolated Human Endogenous Retroviral Long Terminal Repeat of the HERV-K/HTDV Family in Transgenic Mice. *J Virol* **73**(12)**:** 9976-9983

Celli J, Duijf P, Hamel BC, Bamshad M, Kramer B, Smits AP, Newbury-Ecob R, Hennekam RC, Van Buggenhout G, van Haeringen A, Woods CG, van Essen AJ, de Waal R, Vriend G, Haber DA, Yang A, McKeon F, Brunner HG, van Bokhoven H (1999) Heterozygous germline mutations in the p53 homolog p63 are the cause of EEC syndrome. *Cell* **99**(2)**:** 143-153

Coffin JM, Hughes JF, Varmus. (1997) Retroviruses. Cold Spring Harbour Laboratoy Press.

Cohen CJ, Lock WM, Mager DL (2009) Endogenous retroviral LTRs as promoters for human genes: a critical assessment. *Gene* **448**(2)**:** 105-114

Contente A, Dittmer A, Koch MC, Roth J, Dobbelstein M (2002) A polymorphic microsatellite that mediates induction of PIG3 by p53. *Nat Genet* **30**(3)**:** 315-320

Contente A, Zischler H, Einspanier A, Dobbelstein M (2003) A promoter that acquired p53 responsiveness during primate evolution. *Cancer Res* **63**(8)**:** 1756-1758

Costas J, Naveira H (2000) Evolutionary history of the human endogenous retrovirus family ERV9. *Mol Biol Evol* **17**(2)**:** 320-330

Crowell RC, Kiessling AA (2007) Endogenous retrovirus expression in testis and epididymis. *Biochemical Society Transactions* **035**(3)**:** 629-633

De Laurenzi V, Costanzo A, Barcaroli D, Terrinoni A, Falco M, Annicchiarico-Petruzzelli M, Levrero M, Melino G (1998) Two new p73 splice variants, gamma and delta, with different transcriptional activity. *J Exp Med* **188**(9)**:** 1763-1768

Derry WB, Bierings R, van Iersel M, Satkunendran T, Reinke V, Rothman JH (2007) Regulation of developmental rate and germ cell proliferation in Caenorhabditis elegans by the p53 gene network. *Cell Death Differ* **14**(4)**:** 662-670

Derry WB, Putzke AP, Rothman JH (2001) Caenorhabditis elegans p53: Role in Apoptosis, Meiosis, and Stress Resistance. *Science* **294**(5542)**:** 591-595

Di Cristofano A, Strazzullo M, Longo L, La Mantia G (1995a) Characterization and genomic mapping of the ZNF80 locus: expression of this zinc-finger gene is

driven by a solitary LTR of ERV9 endogenous retroviral family. *Nucleic Acids Res* **23**(15)**:** 2823-2830

Di Cristofano A, Strazzullo M, Parisi T, La Mantia G (1995b) Mobilization of an ERV9 human endogenous retroviral element during primate evolution. *Virology* **213**(1)**:** 271-275

Dohn M, Zhang S, Chen X (2001) p63alpha and DeltaNp63alpha can induce cell cycle arrest and apoptosis and differentially regulate p53 target genes. *Oncogene* **20**(25)**:** 3193-3205

Duijf PH, Vanmolkot KR, Propping P, Friedl W, Krieger E, McKeon F, Dotsch V, Brunner HG, van Bokhoven H (2002) Gain-of-function mutation in ADULT syndrome reveals the presence of a second transactivation domain in p63. *Hum Mol Genet* **11**(7)**:** 799-804

Flores ER, Sengupta S, Miller JB, Newman JJ, Bronson R, Crowley D, Yang A, McKeon F, Jacks T (2005) Tumor predisposition in mice mutant for p63 and p73: Evidence for broader tumor suppressor functions for the p53 family. *Cancer Cell* **7**(4)**:** 363-373

Ghioni P, Bolognese F, Duijf PH, Van Bokhoven H, Mantovani R, Guerrini L (2002) Complex transcriptional effects of p63 isoforms: identification of novel activation and repression domains. *Mol Cell Biol* **22**(24)**:** 8659-8668

Gonfloni S, Di Tella L, Caldarola S, Cannata SM, Klinger FG, Di Bartolomeo C, Mattei M, Candi E, De Felici M, Melino G, Cesareni G (2009) Inhibition of the c-Abl-TAp63 pathway protects mouse oocytes from chemotherapy-induced death. *Nat Med* **15**(10)**:** 1179-1185

Gong JG, Costanzo A, Yang HQ, Melino G, Kaelin WG, Jr., Levrero M, Wang JY (1999) The tyrosine kinase c-Abl regulates p73 in apoptotic response to cisplatin-induced DNA damage. *Nature* **399**(6738)**:** 806-809

Gressner O, Schilling T, Lorenz K, Schulze Schleithoff E, Koch A, Schulze-Bergkamen H, Lena AM, Candi E, Terrinoni A, Catani MV, Oren M, Melino G, Krammer PH, Stremmel W, Muller M (2005) TAp63alpha induces apoptosis by activating signaling via death receptors and mitochondria. *Embo J* **24**(13)**:** 2458-2471

Guerquin MJ, Duquenne C, Coffigny H, Rouiller-Fabre V, Lambrot R, Bakalska M, Frydman R, Habert R, Livera G (2009) Sex-specific differences in fetal germ cell apoptosis induced by ionizing radiation. *Hum Reprod* **24**(3)**:** 670-678

Guo X, Keyes WM, Papazoglu C, Zuber J, Li W, Lowe SW, Vogel H, Mills AA (2009) TAp63 induces senescence and suppresses tumorigenesis in vivo. *Nat Cell Biol* **11**(12)**:** 1451-1457

Hagiwara K, McMenamin MG, Miura K, Harris CC (1999) Mutational analysis of the p63/p73L/p51/p40/CUSP/KET gene in human cancer cell lines using intronic primers. *Cancer Res* **59**(17)**:** 4165-4169.

Hamer G, Gademan IS, Kal HB, de Rooij DG (2001) Role for c-Abl and p73 in the radiation response of male germ cells. *Oncogene* **20**(32)**:** 4298-4304

Hayashi T, Yoshinaga A, Ohno R, Ishii N, Kamata S, Yamada T (2004) Expression of the p63 and Notch signaling systems in rat testes during postnatal development: comparison with their expression levels in the epididymis and vas deferens. *J Androl* **25**(5)**:** 692-698

Helton ES, Zhang J, Chen X (2007) The proline-rich domain in p63 is necessary for the transcriptional and apoptosis-inducing activities of TAp63. *Oncogene* **27**(20)**:** 2843-2850

Irwin MS, Kaelin WG, Jr. (2001) Role of the newer p53 family proteins in malignancy. *Apoptosis* **6**(1-2)**:** 17-29.

Jacobs WB, Govoni G, Ho D, Atwal JK, Barnabe-Heider F, Keyes WM, Mills AA, Miller FD, Kaplan DR (2005) P63 Is an Essential Proapoptotic Protein during Neural Development. *Neuron* **48**(5)**:** 743-756

Jern P, Coffin JM (2008) Effects of retroviruses on host genome function. *Annu Rev Genet* **42:** 709-732

Jin S, Martinek S, Joo WS, Wortman JR, Mirkovic N, Sali A, Yandell MD, Pavletich NP, Young MW, Levine AJ (2000) Identification and characterization of a p53 homologue in Drosophila melanogaster. *Proceedings of the National Academy of Sciences of the United States of America* **97**(13)**:** 7301-7306

Kaghad M, Bonnet H, Yang A, Creancier L, Biscan JC, Valent A, Minty A, Chalon P, Lelias JM, Dumont X, Ferrara P, McKeon F, Caput D (1997) Monoallelically expressed gene related to p53 at 1p36, a region frequently deleted in neuroblastoma and other human cancers. *Cell* **90**(4)**:** 809-819

Koster MI, Roop DR (2004) The role of p63 in development and differentiation of the epidermis. *J Dermatol Sci* **34**(1)**:** 3-9

Kurita T, Cunha GR, Robboy SJ, Mills AA, Medina RT (2005) Differential expression of p63 isoforms in female reproductive organs. *Mech Dev* **122**(9)**:** 1043-1055

Lamprecht B, Walter K, Kreher S, Kumar R, Hummel M, Lenze D, Kochert K, Bouhlel MA, Richter J, Soler E, Stadhouders R, Johrens K, Wurster KD, Callen DF, Harte MF, Giefing M, Barlow R, Stein H, Anagnostopoulos I, Janz M, Cockerill PN, Siebert R, Dorken B, Bonifer C, Mathas S (2010) Derepression of an endogenous long terminal repeat activates the CSF1R proto-oncogene in human lymphoma. *Nat Med*

Lane DP (1992) Cancer. p53, guardian of the genome. *Nature* **358**(6381)**:** 15-16

Lee JH, Kang Y, Khare V, Jin ZY, Kang MY, Yoon Y, Hyun JW, Chung MH, Cho SI, Jun JY, Chang IY, You HJ (2010) The p53-inducible gene 3 (PIG3) contributes to early cellular response to DNA damage. *Oncogene* **29**(10)**:** 1431-1450

Levine AJ (1997) p53, the Cellular Gatekeeper for Growth and Division. *Cell* **88**(3)**:** 323-331

Ling J, Pi W, Bollag R, Zeng S, Keskintepe M, Saliman H, Krantz S, Whitney B, Tuan D (2002) The Solitary Long Terminal Repeats of ERV-9 Endogenous Retrovirus Are Conserved during Primate Evolution and Possess Enhancer Activities in Embryonic and Hematopoietic Cells. *J Virol* **76**(5)**:** 2410-2423

Livera G, Petre-Lazar B, Guerquin MJ, Trautmann E, Coffigny H, Habert R (2008) p63 null mutation protects mouse oocytes from radio-induced apoptosis. *Reproduction* **135**(1)**:** 3-12

Long Q, Bengra C, Li C, Kutlar F, Tuan D (1998) A Long Terminal Repeat of the Human Endogenous Retrovirus ERV-9 Is Located in the 5' Boundary Area of the Human [beta]-Globin Locus Control Region. *Genomics* **54**(3)**:** 542-555

Lower R, Lower J, Frank H, Harzmann R, Kurth R (1984) Human Teratocarcinomas Cultured in vitro Produce Unique Retrovirus-like Viruses. *J Gen Virol* **65**(5)**:** 887-898

Lu W-J, Chapo J, Roig I, Abrams JM (2010) Meiotic Recombination Provokes Functional Activation of the p53 Regulatory Network. *Science* **328**(5983)**:** 1278-1281

Marks PA, Xu WS (2009) Histone deacetylase inhibitors: Potential in cancer therapy. *Journal of Cellular Biochemistry* **107**(4)**:** 600-608

McGrath JA, Duijf PH, Doetsch V, Irvine AD, de Waal R, Vanmolkot KR, Wessagowit V, Kelly A, Atherton DJ, Griffiths WA, Orlow SJ, van Haeringen A, Ausems MG, Yang A, McKeon F, Bamshad MA, Brunner HG, Hamel BC, van Bokhoven H (2001) Hay-Wells syndrome is caused by heterozygous missense mutations in the SAM domain of p63. *Hum Mol Genet* **10**(3)**:** 221-229

McKim KS, Hayashi-Hagihara A (1998) mei-W68 in Drosophila melanogaster encodes a Spo11 homolog: evidence that the mechanism for initiating meiotic recombination is conserved. *Genes Dev* **12**(18)**:** 2932-2942

Melino G, De Laurenzi V, Vousden KH (2002) p73: Friend or foe in tumorigenesis. *Nat Rev Cancer* **2**(8)**:** 605-615

Mihara M, Erster S, Zaika A, Petrenko O, Chittenden T, Pancoska P, Moll UM (2003) p53 has a direct apoptogenic role at the mitochondria. *Mol Cell* **11**(3)**:** 577-590

Mills AA, Zheng B, Wang XJ, Vogel H, Roop DR, Bradley A (1999) p63 is a p53 homologue required for limb and epidermal morphogenesis. *Nature* **398**(6729)**:** 708-713

Moll UM, Slade N (2004) p63 and p73: roles in development and tumor formation. *Mol Cancer Res* **2**(7)**:** 371-386

Nakamuta N, Kobayashi S (2003) Expression of p63 in the testis of mouse embryos. *J Vet Med Sci* **65**(8)**:** 853-856

Nakamuta N, Kobayashi S (2004a) Developmental expression of p63 in the mouse testis. *J Vet Med Sci* **66**(6)**:** 681-687

Nakamuta N, Kobayashi S (2004b) Expression of p63 in the mouse primordial germ cells. *J Vet Med Sci* **66**(11)**:** 1365-1370

Nakamuta N, Kobayashi S (2007) Expression of p63 in the mouse ovary. *J Reprod Dev* **53**(3)**:** 691-697

Nelson PN, Carnegie PR, Martin J, Davari Ejtehadi H, Hooley P, Roden D, Rowland-Jones S, Warren P, Astley J, Murray PG (2003) Demystified . . . Human endogenous retroviruses. *Molecular Pathology* **56::** 11-18

Nylander K, Vojtesek B, Nenutil R, Lindgren B, Roos G, Zhanxiang W, Sjöström B, Dahlqvist Å, Coates PJ (2002) Differential expression of p63 isoforms in normal tissues and neoplastic cells. *The Journal of Pathology* **198**(4)**:** 417-427

Öllinger R, Reichmann J, Adams IR (2010) Meiosis and retrotransposon silencing during germ cell development in mice. *Differentiation* **79**(3)**:** 147-158

Osada M, Ohba M, Kawahara C, Ishioka C, Kanamaru R, Katoh I, Ikawa Y, Nimura Y, Nakagawara A, Obinata M, Ikawa S (1998) Cloning and functional analysis of human p51, which structurally and functionally resembles p53. *Nat Med* **4**(7)**:** 839-843

Page SL, Hawley RS (2003) Chromosome Choreography: The Meiotic Ballet. *Science* **301**(5634)**:** 785-789

Pankow S, Bamberger C (2007) The p53 tumor suppressor-like protein nvp63 mediates selective germ cell death in the sea anemone Nematostella vectensis. *PLoS One* **2**(9)**:** e782

Park BJ, Lee SJ, Kim JI, Lee SJ, Lee CH, Chang SG, Park JH, Chi SG (2000) Frequent alteration of p63 expression in human primary bladder carcinomas. *Cancer Res* **60**(13)**:** 3370-3374

Pellegrini G, Dellambra E, Golisano O, Martinelli E, Fantozzi I, Bondanza S, Ponzin D, McKeon F, De Luca M (2001) p63 identifies keratinocyte stem cells. *Proc Natl Acad Sci U S A* **98**(6)**:** 3156-3161

Petre-Lazar B, Livera G, Moreno SG, Trautmann E, Duquenne C, Hanoux V, Habert R, Coffigny H (2007) The role of p63 in germ cell apoptosis in the developing testis. *J Cell Physiol* **210**(1)**:** 87-98

Petre-Lazar B, Moreno SG, Livera G, Duquenne C, Habert R, Coffigny H (2006) p63 expression pattern in foetal and neonatal gonocytes after irradiation and role in the resulting apoptosis by using p63 knockout mice. *Int J Radiat Biol* **82**(11)**:** 771-780

Pi W, Yang Z, Wang J, Ruan L, Yu X, Ling J, Krantz S, Isales C, Conway SJ, Lin S, Tuan D (2004) The LTR enhancer of ERV-9 human endogenous retrovirus is active in oocytes and progenitor cells in transgenic zebrafish and humans. *Proc Natl Acad Sci U S A* **101**(3)**:** 805-810

Pruneri G, Pignataro L, Manzotti M, Carboni N, Ronchetti D, Neri A, Cesana BM, Viale G (2002) p63 in laryngeal squamous cell carcinoma: evidence for a role of TA-p63 down-regulation in tumorigenesis and lack of prognostic implications of p63 immunoreactivity. *Lab Invest* **82**(10)**:** 1327-1334

Sanger F, Nicklen, S. and Coulson, A. R. (1977) DNA sequencing with chain terminating inhibitors. *Proc Natl Acad Sci USA* **74**

Sayan AE, Sayan BS, Gogvadze V, Dinsdale D, Nyman U, Hansen TM, Zhivotovsky B, Cohen GM, Knight RA, Melino G (2008) P73 and caspase-cleaved p73 fragments localize to mitochondria and augment TRAIL-induced apoptosis. *Oncogene* **27**(31)**:** 4363-4372

Sayan BS, Sayan AE, Yang AL, Aqeilan RI, Candi E, Cohen GM, Knight RA, Croce CM, Melino G (2007) Cleavage of the transactivation-inhibitory domain of p63 by caspases enhances apoptosis. *Proc Natl Acad Sci U S A* **104**(26)**:** 10871-10876

Scheel AH, Beyer U, Agami R, Dobbelstein M (2009) Immunofluorescence-based screening identifies germ cell associated microRNA 302 as an antagonist to p63 expression. *Cell Cycle* **8**(9)**:** 1426-1432

Schmale H, Bamberger C (1997) A novel protein with strong homology to the tumor suppressor p53. *Oncogene* **15**(11)**:** 1363-1367

Schulte AM, Lai S, Kurtz A, Czubayko F, Riegel AT, Wellstein A (1996) Human trophoblast and choriocarcinoma expression of the growth factor pleiotrophin attributable to germ-line insertion of an endogenous retrovirus. *Proceedings of the National Academy of Sciences of the United States of America* **93**(25)**:** 14759-14764

Serber Z, Lai HC, Yang A, Ou HD, Sigal MS, Kelly AE, Darimont BD, Duijf PH, Van Bokhoven H, McKeon F, Dotsch V (2002) A C-terminal inhibitory domain controls the activity of p63 by an intramolecular mechanism. *Mol Cell Biol* **22**(24)**:** 8601-8611

Stoye JP, Fenner S, Greenoak GE, Moran C, Coffin JM (1988) Role of endogenous retroviruses as mutagens: the hairless mutation of mice. *Cell* **54**(3)**:** 383-391

Su X, Paris M, Gi YJ, Tsai KY, Cho MS, Lin YL, Biernaskie JA, Sinha S, Prives C, Pevny LH, Miller FD, Flores ER (2009) TAp63 prevents premature aging by promoting adult stem cell maintenance. *Cell Stem Cell* **5**(1)**:** 64-75

Suh EK, Yang A, Kettenbach A, Bamberger C, Michaelis AH, Zhu Z, Elvin JA, Bronson RT, Crum CP, McKeon F (2006) p63 protects the female germ line during meiotic arrest. *Nature* **444**(7119)**:** 624-628

Svensson AC, Raudsepp T, Larsson C, Di Cristofano A, Chowdhary B, La Mantia G, Rask L, Andersson G (2001) Chromosomal distribution, localization and expression of the human endogenous retrovirus ERV9. *Cytogenet Cell Genet* **92**(1-2)**:** 89-96

Sverdlov ED (2000) Retroviruses and primate evolution. *BioEssays* **22**(2)**:** 161-171

Temin HM (1981) Structure, variation and synthesis of retrovirus long terminal repeat. *Cell* **27**(1, Part 2)**:** 1-3

Thompson JD, Higgins DG, Gibson TJ (1994) CLUSTAL W: improving the sensitivity of progressive multiple sequence alignment through sequence weighting, position-specific gap penalties and weight matrix choice. *Nucleic Acids Res* **22**(22)**:** 4673-4680

Tripathi R, Mishra DP, Shaha C (2009) Male germ cell development: turning on the apoptotic pathways. *Journal of Reproductive Immunology* **83**(1-2)**:** 31-35

Vincek V, Knowles J, Li J, Nassiri M (2003) Expression of p63 mRNA isoforms in normal human tissue. *Anticancer Res* **23**(5A)**:** 3945-3948

Vousden KH, Lane DP (2007) p53 in health and disease. *Nat Rev Mol Cell Biol* **8**(4)**:** 275-283

Walter CA, Walter RB, McCarrey JR (2003) Germline genomes--a biological fountain of youth? *Sci Aging Knowledge Environ* **2003**(8)**:** PE4

Westfall MD, Pietenpol JA (2004) p63: Molecular complexity in development and cancer. *Carcinogenesis* **25**(6)**:** 857-864

Yang A, Kaghad M, Caput D, McKeon F (2002) On the shoulders of giants: p63, p73 and the rise of p53. *Trends Genet* **18**(2)**:** 90-95

Yang A, Kaghad M, Wang Y, Gillett E, Fleming MD, Dotsch V, Andrews NC, Caput D, McKeon F (1998) p63, a p53 homolog at 3q27-29, encodes multiple products with transactivating, death-inducing, and dominant-negative activities. *Mol Cell* **2**(3)**:** 305-316

Yang A, Schweitzer R, Sun D, Kaghad M, Walker N, Bronson RT, Tabin C, Sharpe A, Caput D, Crum C, McKeon F (1999) p63 is essential for regenerative proliferation in limb, craniofacial and epithelial development. *Nature* **398**(6729)**:** 714-718

Yang A, Walker N, Bronson R, Kaghad M, Oosterwegel M, Bonnin J, Vagner C, Bonnet H, Dikkes P, Sharpe A, McKeon F, Caput D (2000) p73-deficient mice have neurological, pheromonal and inflammatory defects but lack spontaneous tumours. *Nature* **404**(6773)**:** 99-103

Abbreviations

7-AAD	7-amino actinomycin D
α	alpha, anti
ab	antibody
ADULT	Acro-dermato-ungual-lacrimal-tooth
AEC	Ankyloblepharon Ectodermal Dysplasia Clefting
amp	ampicillin
APS	ammonium persulfat
ATCC	American Type Culture Collection
ATP	adenosin tri-phosphat
β	beta
BSA	bovine serum albumin
°C	degree Celsius
cDNA	complementary DNA
cDDP	cis-Diammineplatinum(II) dichloride
CHX	cycloheximide
CMV	cytomegalie virus
CO_2	carbon dioxid
d	delta, desoxy
ddH_2O	double destilled water
Da	Dalton
DAB	3,3´-diamino benzidine
DBD	DNA-binding domain
Dept.	Department
DEVD	peptide that specifically inhibits caspase 3
DMEM	Dulbecco's modified Eagle medium
DMSO	dimethyl sulfoxid
DNA	desoxyribose nucleic acid
DNAse	desoxyribonuclease
ds	double strand
DSMZ	„Deutsche Sammlung von Mikroorganismen und Zellkulturen“
DTT	1,4-Dithiothreitol
E.coli	*Escherischia coli*

EB	elution buffer
EDTA	ethylendiamin tetraacetat
EEC	Ectrodactyly Ectodermal Dysplasia-Cleft lip/palate
ERV	endogenous retrovirus
et al.	*et altera*
FBS	fetale bovine serum
γ	gamma
g	gramm
GCIN	Germ Cell Intratubular Neoplasms
GTAp63	germ cell-associated transactivating p63
GZMB	Göttinger Zentrum für Molekulare Biowissenschaften
h	hour
H_2O	water
HDAC	histone deacetylase
H&E	hematoxylin-eosin stain
HERV	human endogenous retrovirus
IgG	immunoglobulin G
IHC	immunohistochemistry
k	kilo
L	liter
LB medium	Luria Bertani medium
LTR	long terminal repeat
m	milli
M	molar
min	minute
M-MuLV	Moloney Murine Leukemia Virus
mRNA	messenger RNA
µ	micro
n	nano
NCBI	National Center for Biotechnology Information
NTP	nucleoside triphosphate
OD	oligomerization domain
p	pico
P	phospho

PAGE	polyacrylamide gel electrophorese
PBS	phosphate buffered salt
PCR	polymerase chain reaction
Pfu	*Pyrococcus furiosus*
pH	negative decadic logarithm of the molar concentration of dissolved hydronium ions
PI	propidium iodide
qPCR	quantitative PCR
RACE	rapid amplification of cDNAs ends
RNA	ribose nucleic acid
RNAse	ribose nuclease
RT	reverse transcription, Reverse transcriptase
ss	single strand
SAHA	suberoylanilid hydroxamic acid
SAM	Sterile Alpha Motif
SDS	sodium dodecyl sulfate
sec, s	second
SHFM	Split-Hand/Foot Malformation
siRNA	small interfering RNA
TA	transactivating
TAD	transactivating domain
TAE	tris acetat EDTA
Taq	*Thermus aquaticus*
TEMED	N,N,N´,N´-Tetramethylen diamin
TSA	trichostatin A
Tris	tris hydroxymethyl amino methan
U	unit of enzyme activity
V	Volt
v/v	volume per volume
w/v	weight per volume
wt	wild type
Ω	Ohm

Acknowledgments

I would like to express my sincere gratitude to my supervisor Prof. Matthias Dobbelstein for the opportunity to work on this interesting PhD project and for the continuous strong support throughout the whole time. I greatly appreciated his guidance and encouragements and the instructive scientific discussions that have contributed to a nice and efficient working atmosphere.

Besides my supervisor, I would like to thank Prof. Ralf Ficner and Prof. Tomas Pieler for their support as members of my thesis committee.

Furthermore, I am very appreciative for the collaboration with the group of Ute Moll at Stony Brook University. I owe my thanks to Julian Moll-Rocek who provided valuable scientific data. I am very grateful for the great support of Prof. Ute Moll and the inspiring discussions that we had during her visits in Göttingen. I thank Lena Holembowski and Ramona Schulz for supporting me during the work with mice.
My gratitude is also dedicated to Margret Rave-Fränk who helped me with the irradiation of mice.

I specially thank all present and former members of the “Molecular Oncology“- group for their help and support and especially for the very nice working atmosphere. I am very grateful for the support of our two technicians Antje Dickmanns and Cathrin Hippel. Particularly, I am heartfully indebted to Isabella Drewelus, Cathrin Hippel, Karen Linnemannstönns and Tanja Prenzel who became real friends for me during the last years.

Special thanks go to my parents and my sister who supported me throughout the last years in various ways.

Curriculum vitae

Personal facts

Name	Ulrike Beyer
Address	Herrman-Rein-Str. 8A/App. 196, 37075 Göttingen
Date and place of birth	08.04.1979 in Magdeburg
Nationality	German
Marital status	single

Education

since 03/2006	Dissertation in Biology Dept. Molecular Oncology / GZMB Georg August University Göttingen
10/2000 – 01/2006	Study of Human biology Philipps University Marburg Qualifications: Diploma (degree: very good), Title of the work: Modification of p63 und p73 by the Inteferon-stimulated protein ISG15
1997 – 2000	Training as MTA (Medical Technical Assistent) Faculty of Medicine Otto-von-Guericke University Magdeburg Qualifications: Medical Technical Lab Assistent (degree: very good)
1991 – 1997	Grammar School in Magdeburg Qualifications: Abitur (degree: 2,0)
1989 – 1991	Secondary School in Magdeburg
1985 – 1989	Elementary School in Magdeburg

scientific work during study

05/2004 – 08/2004	Institute for Medical Mikrobiology Philipps-Universität Marburg DFG-Projekt: Role of T-cells for the pathogenesis of infections with H.pylorus
07/2003 – 10/2003	IMT (Institute of Molecular Biology and Tumor Research) Philipps-Universität Marburg Project: Identification of mRNA export factors associated with the RNA-binding protein Gbp2p
03/2003 – 05/2003	IMT (Institute of Molecular Biology and Tumor Research) Philipps-Universität Marburg Project: Identification of interaction partners of Gbp2p, Hrb1p und Nab2p

Publications

- Talos F, Wolff S, Beyer U, Dobbelstein M, Moll UM.:
  Brdm2 – an abberrant hypomorphic allele.
  Cell Death Differ. 2010 Jan; 17(1):184-186.

- Wolff S, Talos F, Palacios G, Beyer U, Dobbelstein M, Moll UM.:
  The alpha/beta carboxy-terminal domains of p63 are required for skin and limb development. New insights from the Brdm2 mouse which is not a complete p63 knockout but expresses p63 gamma-like proteins.
  Cell Death Differ. 2009 Aug; 16(8):1073-4.

- Scheel AH, Beyer U, Agami R, Dobbelstein M.:
  Immunofluorescence-based screening identifies germ cell associated microRNA 302 as an antagonist to p63 expression.
  Cell Cycle. 2009 May 1; 8(9):1426-32.

Göttingen, 20th October 2010

Ulrike Beyer